n° d'ordre : 2179

THESE

présentée à

L'UNIVERSITE DES SCIENCES ET TECHNOLOGIES DE LILLE

pour obtenir le titre de

DOCTEUR EN SPECTROCHIMIE

par

Ryuichiro IWAMOTO

ETUDE DE L'INFLUENCE DU PHOSPHORE SUR LES PROPRIETES DE CATALYSEURS D'HYDROTRAITEMENT A BASE DE Ni, Mo ET ALUMINE PREPARES PAR VOIE SOL-GEL.

Soutenue le 17 Décembre 1997 devant la Commission d'Examen

Membres du jury :

J.P.BONNELLE	Président du Jury
H. TOPSØE	Rapporteur
H.TOULHOAT	Rapporteur
J.C.DUCHET	Rapporteur
C.FERNANDEZ	Examinateur
J.GRIMBLOT	Examinateur

Ce travail a été effectué au Laboratoire de Catalyse Hétérogène et Homogène, U.R.A. C.N.R.S. n° 402, de l'Université des Sciences et Technologies de Lille (USTL).

Je remercie la Société IDEMITSU Kosan Co. Ltd., et le Japan Cooperation Center Petroleum (JCCP) pour leur appui financier qui a permis la réalisation de ce travail.

J'exprime ma profonde gratitude à Monsieur Jean-Pierre BONNELLE, Professeur à l'USTL, pour m'avoir accueilli dans son Laboratoire, et à Monsieur Gérard HECQUET son actuel directeur.

Je suis encore très reconnaissant envers Monsieur le Professeur Jean-Pierre BONNELLE qui a accepté de présider le Jury de cette thèse.

Monsieur le Dr. Henrik TOPSØE, (Haldor Topsøe A/S, Directeur de recherches en catalyse, Nymøllevej, Danemark), Monsieur le Dr. Hervé TOULHOAT, (IFP, Malmaison) et Monsieur le Professeur Jean-Claude DUCHET (I.S.M.R.A., Caen), m'ont fait l'honneur d'accepter d'examiner de façon approfondie ce travail. Je les en remercie sincèrement.

Je remercie chaleureusement Monsieur le Dr. Christian FERNANDEZ, USTL, qui m'a fait l'honneur de participer au jury de cette thèse.

Je suis particulièrement fier d'avoir eu la possibilité de travailler avec Monsieur Jean GRIMBLOT, Professeur à l'Ecole Nationale Supérieure de Chimie de Lille, qui a accepté de diriger ce travail, et surtout, de m'aider pendant ces deux dernières années. Je lui serai toujours reconnaissant pour ses nombreuses qualités humaines et sa grande disponibilité. Je le remercie sincèrement.

Je remercie Monsieur Léon GENGEMBRE et Mademoiselle Virginie MOINEAU qui m'ont permis un accès aisé aux analyses SPX. Mes remerciements vont également au Dr. Bertrand REVEL, au Dr. Pierre WATKIN, au Dr. Monique RIGOLE, au Professeur Michel GUELTON (USTL) et au Dr. Hartmut KRAUS (Swiss Federal Institue of Technology, Zurich) qui m'ont permis un accès aisé aux analyses RMN et 2D-RMN. Je remercie Monsieur Franck DUMEIGNIL qui m'a initié aux préparations de catalyseurs élaborés par voie Sol-Gel et tests catalytiques en HDS du thiophène, Monsieur Lionel Le BIHAN qui m'a donné des informations utiles sur la méthode Sol-Gel et Madame Mireille CHEVALIER pour l'aide précieuse qu'elle a apportée dans le tirage du manuscrit.

Enfin, je ne saurais oublier d'associer à ces remerciements tous les membres de ce laboratoire auprès desquels j'ai eu le bonheur de travailler durant ces deux ans.

INTRODUCTION GENERALE

Les procédés d'hydrotraitement constituent une technologie très importante dans le domaine du raffinage pétrolier pour améliorer la qualité des carburants et autres dérivés livrés sur le marché. Très schématiquement, les opérations d'hydrotraitement concernent principalement l'hydrodésulfuration (HDS), l'hydrodésazotation (HDN), l'hydrodémétallation (HDM), l'hydrogénation (HYD) et plus spécifiquement l'hydrodéaromatisation (HDA) et enfin l'hydrocraquage (HYC). Ces réactions sont conduites en présence d'hydrogène dont la pression est ajustée de 20 à 200 atmosphères selon le procédé et la nature de la charge à traiter (naphta, gazole, fioule ou résidu) et d'une charge catalytique dans un domaine de température variant de 200 à 450°C.

Le récent colloque sur l'hydrotraitement et l'hydrocraquage des fractions pétrolières (Ostende, février 1997) a montré que les conditions opératoires étaient fortement dépendantes de la situation du procédé dans le schéma de la raffinerie (1).

Les contraintes économiques actuelles qui nécessitent de fournir des carburants de plus en plus performants liées aux exigences sur la préservation de la qualité de l'environnement en évitant ou limitant les émissions de NO_x, SO_x, particules de suie et molécules aromatiques ont renforcé les recherches dans le domaine des hydrotraitements catalytiques; il s'agit « d'une vieille histoire avec de nouveaux challenges » (2). C'est ainsi que récemment, la qualité des carburants a du être constamment adaptée de par le monde pour résoudre les problèmes de pollution atmosphérique. Par exemple, la teneur en soufre des carburants diesel doit être réduite sous la limite de 0,05 % en poids et dans un proche avenir sous la limite de 0,02 % en poids. D'autre part, la demande en fractions légères (essences) tend à augmenter alors que l'approvisionnement en pétroles légers va en diminuant. Ceci implique la conversion (catalytique) de charges lourdes en fractions légères avec le même souci de qualité. Pour cet ensemble de raisons et de contraintes, l'amélioration des catalyseurs et des procédés s'avère inévitable.

Les formulations classiques des catalyseurs d'hydrotraitement consistent en une répartition d'oxydes de molybdène et de cobalt ou nickel à la surface d'une alumine de transition de grande aire spécifique et de porosité adaptée. Ces catalyseurs sont couramment préparés par imprégnation du support alumine. Une alternative intéressante consiste en l'utilisation de la méthode sol-gel (3) car elle permet d'obtenir des solides de très grande aire spécifique avec une quantité

importante d'éléments « déposés », tout en gardant une très bonne dispersion. D'autre part, l'addition de phosphore à la formulation catalytique s'est avérée très intéressante car certaines performances réactionnelles s'en sont trouvées améliorées (cet aspect sera repris dans la première partie de la thèse). Le phosphore est considéré comme un second promoteur et complète le rôle des promoteurs classiques Co ou Ni. En outre, la méthodologie sol-gel est parfaitement adaptée pour incorporer cet élément phosphore dans la formulation catalytique.

Cette étude présente donc l'influence que peut avoir le phosphore lorsqu'il est incorporé à la synthèse des catalyseurs conduisant respectivement à des solides notés Mo-P-alumine, Ni-P-alumine et Ni-Mo-P-alumine; l'ensemble de ces séries est préparé selon la méthodologie sol-gel déjà expérimentée au Laboratoire pour le système Mo-alumine. Seront systématiquement considérés les effets du P sur les propriétés texturales, structurales et catalytiques avec l'utilisation de tests sur molécules modèles.

Le mémoire est divisé en deux parties. La première constitue une revue bibliographique qui examine la chimie du phosphore en relation avec les hydrotraitements catalytiques ainsi que le rôle qu'il peut jouer. La deuxième partie présente l'essentiel des résultats expérimentaux obtenus sur les différentes séries de catalyseurs préparés. Après une courte introduction et un examen de la chimie afférente au processus sol-gel, les systèmes Mo-P, Ni-P et Ni-Mo-P seront successivement analysés et discutés. Le chapitre 2.2 est séparé en trois parties qui traitent de la genèse, de la caractérisation et des propriétés en HDS des catalyseurs (partie 2.2.1, publiée dans ***Studies in Surface Science and Catalysis***), des propriétés acides et hydrogénantes du même système (partie 2.2.2, sous presse à ***Journal of Catalysis***) et des caractérisations par RMN solide de ^{27}Al et ^{31}P (partie 2.2.3, soumise pour publication à ***Journal of Physical Chemistry***). Le chapitre 2.3 traite des solides Ni-P- alumine alors que le chapitre 2.4 est relatif aux catalyseurs Ni-Mo-P-alumine dont les caractéristiques seront comparées aux formulations précédentes plus simples. La sulfuration (partie 2.4.2) et les propriétés acides (partie2.4.3) sont examinées séparément car il s'agit de points clé pour élucider le rôle du P dans ces catalyseurs. Le mémoire présente enfin une conclusion générale et les perspectives à envisager.

Le document est essentiellement rédigé en anglais car une bonne partie des résultats obtenus est déjà publié dans divers ouvrages ou revues internationales ou est en passe d'être soumis pour publication. Selon le cas, une introduction, une conclusion ou un court résumé en français compléteront chaque chapitre.

Bibliographie

1. Voir les articles de F. Morel et al (p.1), J. Grootjans et al (p.17) et W.H.J. Stork (p.41) parus dans les ***Proceedings of the First International Symposium and Sixth European Workshop on Hydrotreatment and Hydrocracking of Oil Fractions, Studies in Surface Science and Catalysis,*** Vol. **106**, 1997.
2. Grange and X. Vanhaeren, ***Catal. Today*, 36**, 375, 1997.
3. Le Bihan, C. Mauchaussé, L. Duhamel, J.Grimblot and E. Payen, ***J. Sol-Gel Sci. Tech.*, 2**, 837, 1992.

PREMIERE PARTIE : Rôle du phosphore dans les catalyseurs d'hydrotraitement (Revue Bibliographique)

1.1. Introdution.

Les hydrotraitements des fraction pétrolières, et par extension, des liquéfiats de charbon ou de la biomasse, ont fait l'objet d'un nombre considérable d'études depuis les années 1940. Les progrès dans ce domaine ont été constamment mis en relief par de nombreux articles de revue qui ont traité, selon les cas:

- des caractérisations des fractions pétrolières et des familles de molécules à transformer,
- des principales réactions d'hydrotraitement,
- des procédés catalytiques,
- de la préparation des catalyseurs, de leur caractérisation et de leur activation,
- des phases actives et des effets promoteurs,
- des effets de supports, etc...

L'ouvrage présenté par H. Topsøe, B. S. Clausen et F. E. Massoth intitulé « Hydrotreating Catalysis, Science and Technology » (Springer-Verlag, Berlin Heidelberg, 1996) constitue sans aucun doute la revue récente la plus compléte. Ses 1514 références sont un outil très important pour toute personne intéressée par le sujet. Il apparaît cependant, que l'examen attentif de l'influence des éléments dénotés « additifs » ou « second promoteurs » (F, alcalins, P) est beaucoup moins traitée. En particulier, l'introduction du phosphore dans les formulations des catalyseurs d'hydrotraitement qui s'est avérée positive au cours des années 60, n'a fait l'objet, à notre connaissance, d'aucun article de revue. Il nous a donc semblé intéressant d'aborder ce mémoire par un examen bibliographique qui associe à la fois la chimie de base des molécules et composés phosphorés qui peuvent intervenir dans la catalyse des hydrotraitements et du rôle que cet élément induit à la fois dans la texture, la structure des catalyseurs et dans les performances pour les réactions d'hydrotraitement.

Cette revue sera soumise, dans son intégralité, pour publication. Elle comporte aussi quelques éléments qui seront largement détaillés dans la seconde partie.

List of abbreviations

pm	pico meter
PD	Pore Diameter
PV	Pore Volume
SSA	Specific Surface Area
IEP	Isoelectronic Point
CUS	Coordinatively Unsaturated Sites
HREM	High Resolution Electron Microscopy
EXAFS	Extended X-ray Absorption Fine Structure
NMR	Nuclear Magnetic Resonance
TPR	Temperature Programmed Reduction
TPS	Temperature Programmed Sulphidation
XRD	X-ray Diffraction
IR, FTIR	Infrared Spectroscopy or Fourier Transformed Infrared Spectroscopy
UV	Ultraviolet Spectroscopy
XPS	X-ray Photoelectron Spectroscopy
HDT	Hydrotreating
HDS	Hydrodesulphurization
HDN	Hydrodenitrogenation
HDM	Hydrodemetalization
HYD	Hydrogenation
ISOM	Isomerization
HYC	Hydrocracking
DBT	Dibenzothiophene
OPA	Ortho-propylaniline
DHQ	Decahydroquinoline
OPA	Ortho-propylaniline
VGO	Vacuum Gas Oil
LGO	Light Gas Oil
AHM	Ammonium Heptamolybdate

1.2 Rôle du phosphore dans les catalyseurs d'hydrotraitement (Role of phosphorus on the properties of alumina-based hydrotreating catalysts)

Content

1.2.1. Introduction

The removal of hetero atoms in petroleum fractions such as sulphur, nitrogen and metals (mainly V and Ni) has been becoming more and more an important subject to solve the environmental problems in these decades. Hydrotreating (HDT) of feedstock in the presence of catalysts is one of the most effective and practical methods to achieve this goal. Molybdenum or tungsten based catalysts promoted by cobalt or nickel have been widely used in commercial hydrotreating plants. Great attentions have been taken to get better understanding on the structure of active sites, reaction mechanism and effect of promotor to improve these catalysts. Especially, the role of Co and Ni and their location have been considerably studied because of their excellent and positive effects for major hydrotreating reactions. The nature and effect of the supports have been also examined such as Al_2O_3, SiO_2, Carbon, TiO_2, ZrO_2, Al_2O_3-SiO_2, Al_2O_3-TiO_2, Al_2O_3-ZrO_2 and so on. Many reports and reviews were already published for the above subjects (1-3).

Phosphorus has been also known as a second promotor to improve the Mo based hydrotreating catalysts. The positive effect of P has been first described in patent from the middle of the sixties or further earlier (4-5). However, a scientific approach of its role began just after the eighties, by reference to the available publications. Some researchers try to elucidate the role of P from the characterizations of catalysts. Others try to reveal it from the kinetic analysis of the reactions. In spite of great concerning on the effect of P, its role in the catalysts formulation is still a matter of debate. It is easy to understand the situation of phosphorus if one knows that P is described as so many words such as additive, second promotor, modifier etc. There is still less literature and no overall review about the effect of P comparing with those of Co and Ni in the author's knowledge. In this review, therefore, we tried to summarise the roles of P on preparation, physicochemical properties and catalytic performances of hydrotreating catalysts. The main concerning is to answer on the nature of P species present in catalysts and how it can affect the catalytic properties. We hope that this systematic overlooking will help a better understanding of P effects and further developments of P-containing hydrotreating catalysts.

Theories and principles of characterizations techniques are not described in the present review. For the convenience and to avoid confusion, all the catalysts ascribed in this review are referred in the same manner although the nomenclature of catalysts are sometimes different in the reference publications. Each catalyst component (element) divided by - indicate the sequence of its introduction into the catalyst formulation from right to left hand. Those divided by / between right and left belong to the support material and the loading elements,

respectively. For example, NiMo-P/Al means a catalyst prepared from which the P precursor is loaded on the alumina support at first, and then Ni and Mo are introduced simultaneously. CoMo/Al-P means that Co and Mo are introduced simultaneously on an alumina support doped with P oxo-species. Each element may represent its oxide or sulphided forms, even if it is written as an element. In all cases, Al refers to the alumina-based support or to its hydroxide precursor.

1.2.2. Basic properties of some P-based compounds related to the Co(Ni)-Mo-P-Al system

1.2.2.1 General description of phosphorus

The word « phosphorus » originally comes from "phosphoros" which means "light bearing planet Venus before sunrise" in ancient Greek (6) . The element P was first obtained from urine by Brand in 1669. It can be classified as a metalloid in the V^{th} group below nitrogen with an atomic number of 15 and an atomic weight of 30.973762. In the hydrotreating catalyst preparation and in the course of the different reactions on model molecules or on industrial feeds, P could form several types of compounds such as P oxo-compounds, aluminophosphates, molybdophosphate heteropoly compounds, organic P-containing compounds, reduced P-based species and so on. It is very important to keep in mind that handling of such P compounds sometimes needs special attention because some of them might be toxic, very corrosive or dangerous as spontaneous ignition in air may occur. In the present part, the properties and structures of various P compounds which are potentially related to the hydrotreating catalysts or reactions will be examined.

1.2.2.2 Elemental phosphorus

Elemental P can be classified into several allotropic forms such as white (or yellow), red, violet and black coloured compounds (6-9). White P is a water insoluble waxy compound consisting of tetrahedral P_4 molecules (P-P distance : 222 pm, bonding angle : 60°). White P takes α and β forms depending on the temperature and pressure. If white P is exposed to sunlight or heated with a trace of iodine, it transforms to a polymeric amorphous red P compound at low pressure. Violet P, which is comprised of mutually interconnected pentagonal channels, is stable at more higher temperature and pressure. Black P, which consisted of parallel double layers, is the most stable form from a thermodynamic point of view. The phase diagram of these elemental P compounds is shown in Fig. 1.

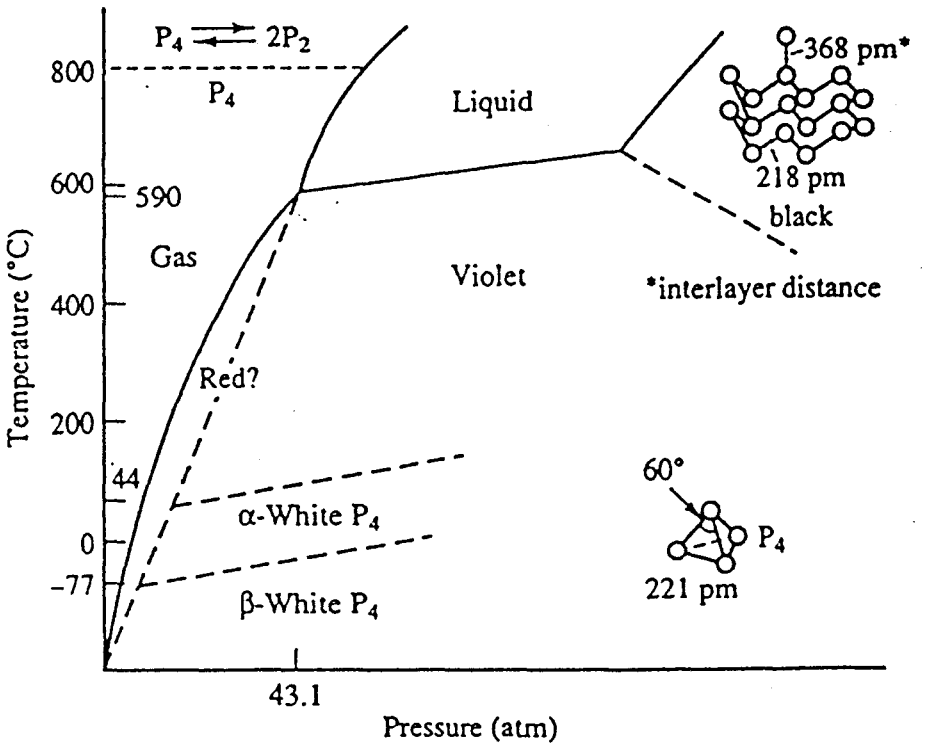

Figure 1. Phase diagram for elemental phosphorus (from ref. 8).

1.2.2.3. Phosphorus hydride (Phosphanes)

P forms many types of hydrides named phosphanes (7-9). The list of available phosphanes is shown in Table 1.

Table 1. List of known phosphane compounds (from ref. 8)

Phosphane series	Known compounds
P_nH_{n+2}	PH_3, P_2H_4, P_3H_5, P_4H_6, P_5H_7, P_6H_8, P_7H_9, P_8H_{10}, P_9H_{11}
P_nH_n	P_3H_3, P_4H_4, P_5H_5, P_6H_6, P_7H_7, P_8H_8, P_9H_9, $P_{10}H_{10}$
P_nH_{n-2}	P_4H_2, P_5H_3, P_6H_4, P_7H_5, P_8H_6, P_9H_7, $P_{10}H_8$, $P_{11}H_9$, $P_{12}H_{10}$
P_nH_{n-4}	P_5H, P_6H_2, P_7H_3, P_8H_4, P_9H_5, $P_{10}H_6$, $P_{11}H_7$, $P_{12}H_8$, $P_{13}H_9$
P_nH_{n-6}	P_7H, P_8H_2, P_9H_3, $P_{10}H_4$, $P_{11}H_5$, $P_{12}H_6$, $P_{13}H_7$, $P_{14}H_8$, $P_{15}H_9$
P_nH_{n-8}	$P_{10}H_2$, $P_{11}H_3$, $P_{12}H_4$, $P_{13}H_5$, $P_{14}H_6$, $P_{15}H_7$, $P_{16}H_8$, $P_{17}H_9$
P_nH_{n-10}	$P_{12}H_2$, $P_{13}H_3$, $P_{14}H_4$, $P_{15}H_5$, $P_{16}H_6$, $P_{17}H_7$, $P_{18}H_8$, $P_{19}H_9$, $P_{20}H_{10}$
P_nH_{n-12}	$P_{13}H$, $P_{14}H_2$, $P_{15}H_3$, $P_{16}H_4$, $P_{17}H_5$, $P_{18}H_6$, $P_{19}H_7$, $P_{20}H_8$
P_nH_{n-14}	$P_{15}H$, $P_{16}H_2$, $P_{17}H_3$, $P_{18}H_4$, $P_{19}H_5$, $P_{20}H_6$, $P_{21}H_7$
P_nH_{n-16}	$P_{17}H$, $P_{19}H_3$, $P_{20}H_4$, $P_{21}H_5$, $P_{22}H_6$
P_nH_{n-18}	$P_{19}H$, $P_{20}H_2$, $P_{21}H_3$, $P_{22}H_4$

1.2.2.4 Phosphides

The strong chemical reactivity of P induces also formation of a lot of single and mixed phosphides with several metals (7-10). Phosphides which are relevant to hydrotreating catalyst formulation are listed in Table 2.

Table 2 List of phosphide relevant to hydrotreating catalyst formulations (adapted from ref. 8)

Metal	Single phosphides	Mixed phosphides
Mo, W	MoP MoP_2, WP_2 W_2P MoP_4, WP_4 Mo_3P, W_4P Mo_8P_5 Mo_4P_3	Mo_2Ni_3P $Mo_2Ni_6P_3$ $NiMoP$ $NiWP$ $CoMoP$ $CoWP$ $NiMoP_2$
Ni, Co	NiP, CoP Ni_2P, Co_2P Ni_3P NiP_3, CoP_3 Ni_5P_2, Ni_5P_4 Ni_8P_3, $Ni_{12}P_5$ $NiCo_9P_5$	$CoWP_2$ $NiWP_2$ $CoMoP_2$ $NiMo_2P_3$ WNi_4P_{16} $NiMoP_8$ $NiWP_8$
Al	AlP	-

1.2.2.5 Phosphorus Oxides

When P reacts with molecular oxygen, it forms many types of phosphorus oxides with different oxidation states (7-9). Under low partial pressure of oxygen, P forms predominantly P_4O_6. P_4O_6 is a colourless waxy compound in which the six P-P bonds of P_4 tetrahedra (Fig. 1) are replaced by P-O-P bridges (P-O distance : 162 pm). This compound is stable at 25°C in air but easily transformed to H_3PO_3 in the presence of water according to the following reaction :

$$P_4O_6 + 6\,H_2O \rightarrow 4\,H_3PO_3 \qquad \text{Eq. (2.1)}$$

P_4O_{10}, the dimeric structure of P_2O_5, is a colourless crystal made with four bridged P tetrahedra through oxygen atom (see Fig. 2). Hydrolysis of P_4O_{10} finally leads to H_3PO_4 according to the following sequence :

$$P_4O_{10} \xrightarrow{+2H_2O} H_4P_4O_{12} \xrightarrow{+2H_2O} 2H_4P_2O_7 \xrightarrow{+2H_2O} 4H_3PO_4 \quad \text{Eq. (2.2)}$$

In addition to P_4O_6 and P_4O_{10} which have formal P^{III} and P^{V} oxidation states, other P oxide compounds such as P_4O_7, P_4O_8 and P_4O_9 also exist. Their structure are shown in Fig. 2.

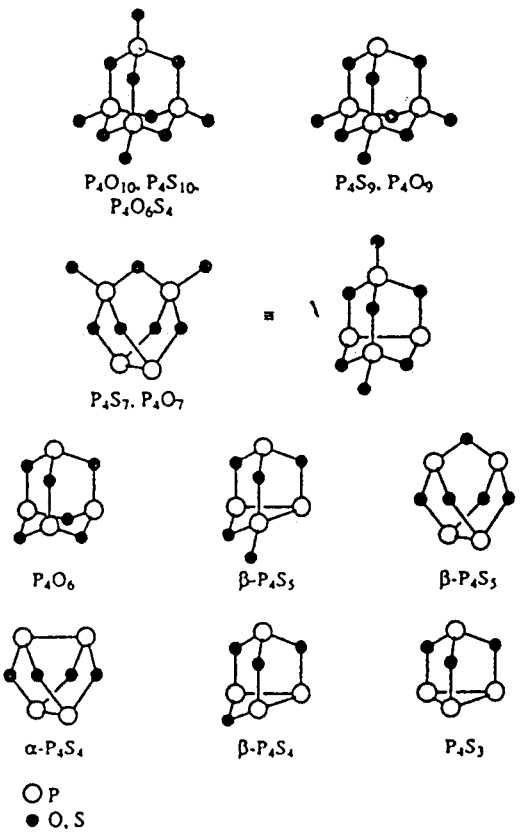

Figure 2. Structure of phosphorus oxides, sulphide and oxosulphide (from ref. 8).

Furthermore, the strong chemical reactivity of P_2O_5 allows to prepare a lot of organic P oxo-complexes with alcoholic solvents (10,11). For example, with butanol (But-OH), the following reactions are suggested :

$P_2O_5 + 2\ But\text{-}OH + H_2O \rightarrow 2\ PO(OH)_2(OBut)$ Eq. (2.3)

$P_2O_5 + 4\ But\text{-}OH \rightarrow 2\ PO(OH)(OBut)_2 + H_2O$ Eq. (2.4)

$P_2O_5 + 6\ But\text{-}OH \rightarrow 2\ PO(OBut)_3 + 3H_2O$ Eq. (2.5)

1.2.2.6 Phosphorus oxysulphides and sulphides

Since hydrotreating catalysts are almost always under sulphiding conditions during their activation and use (presence of H_2, H_2S and thio-organic molecules etc.), phosphorus sulphide or oxysulphide compounds may play an important role as long as the reactions proceed including the activation step. Many kinds of P sulphide compounds such as P_4S_3, P_4S_4, P_4S_5, P_4S_7, P_4S_9 and P_4S_{10} can be formed depending on the P/S atomic ratio effectively measured in the catalysts (7-10,12). The structures of P sulphides are basically analogous to those of P oxides as shown in Fig. 2. For example, P_4S_{10} has a structure similar to that of P_4O_{10} (P-S distance : 209 pm). The structure of P_4S_9 is also similar to that of P_4S_{10} but one terminal S atom is lacking. These « P-S » compounds are rather thermally stable heterocycles but they are chemically reactive : for example, they spontaneously ignite in air or they are hydrolyzed to H_3PO_4 and H_2S in the presence of water (moisture).

1.2.2.7 Oxy-acid of phosphorus and their derivatives

The oxy-acids of phosphorus and their derivatives are defined as compounds which contain both P-OH and P=O groups (7-9,12). Orthophosphoric acid, phosphorous acid and hypophosphorous acid are well known as the oxy-acid compounds which contain three, two and one OH groups associated with the P atom, respectively. The schematic structures are shown below :

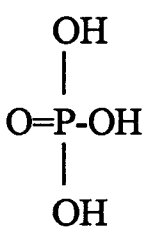

Orthophosphoric acid (H_3PO_4)

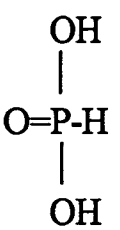

Phosphorous acid (H_3PO_3)

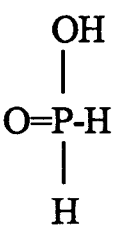

Hypophosphorous acid (H_3PO_2)

Since P-OH bonds dissociates into $P\text{-}O^-$ and H^+ in the presence of water, they usually give some acid property. The acidity of the oxy-acid of phosphorus decreases with increasing the number of P-H bonds because P-H bond does not

dissociate in water.

The orthophosphoric acid is a water soluble triprotic acid which has medium acid strength (pK_A=2.1, 7.2, 12 as H_3PO_4, $H_2PO_4^-$ and HPO_4^{2-}, respectively). Its Hammet acidity Ho is lower than that of H_2SO_4, HCl and HNO_3 (Fig. 3)(13). Anhydrous H_3PO_4 is a colourless molecular structure consisted of PO_4^{III} layers in which P has a tetrahedral symmetry.

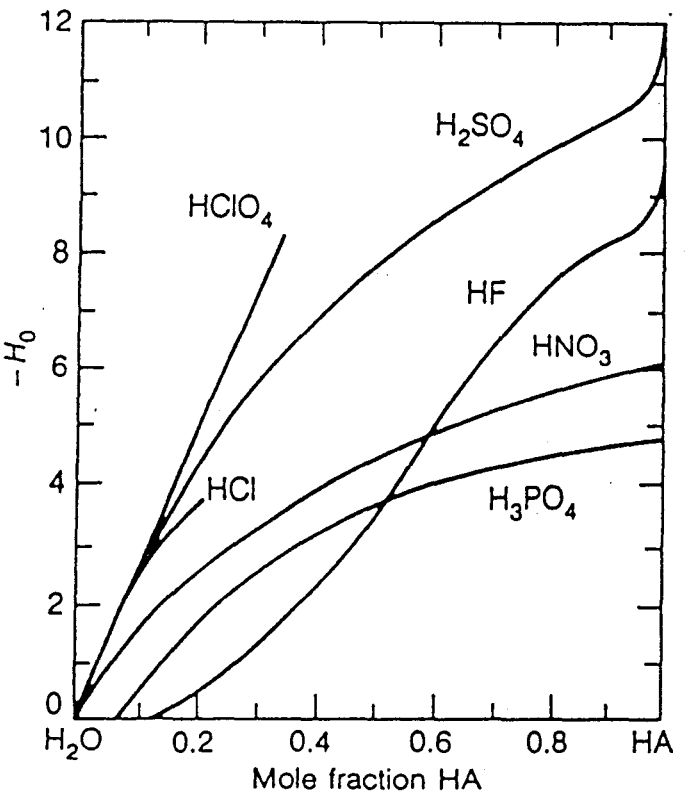

Figure 3. Comparison of the Hammet acidity function H_0 of H_3PO_4 with some other mineral acids (from ref. 13).

Step wise dehydration of phosphoric acid or phosphorous acid favors formation of polymeric P-O-P bonds. Condensation of phosphates leads to form several types of poly oxo-P compounds such as straight chained phosphates, cyclic metaposphates and cross linking ultraphosphates.

In relation to these oxy-acids, phosphorus thioxy acids and thio acids in which some or all of the oxygen atoms in the P oxy-acids are replaced by sulphur

atoms respectively, are also known. Their general description can be found in ref. (8). The general physicochemical properties found in the literature of selected phosphorus compounds described above are shown in Table 3.

Table 3 Physical constants of selected phosphorus compounds (adapted from ref.7)

compound		density	melting point (°C)	boiling point (°C)	molecular weight
P_4 (white)		1.82	44.1	280	123.89
(red)		2.34	590		
(violet)		2.36	590		
(black)		2.7			
PH_3			-133	-87.7	34
$P_2O_5(P_4O_{10})$		2.39	580		141.94
$P_2O_4(P_2O_8)$		2.54	>100	180(vac.)	125.95
$P_2O_3(P_4O_6)$		2.16	23.8	175.4	109.95
$P_4O_6S_4$			102	295	348.15
$P_2S_5(P_4S_{10})$		2.09	290	514	444.54
P_4S_7		2.19	310	523	348.34
P_4S_3		2.03	174	408	222.09
H_3PO_2	hypophosphorus acid	1.49	26.5	130(d)	66
H_3PO_3	orthophosphorous acid	1.65	73.6	200(d)	82
$H_4P_2O_5$	pyrophosphorous acid		38	120(d)	145.98
H_3PO_4	orthophosphoric acid	1.7	40	213	98

(a) vac.: under vacuum. d: decomposition before boiling

1.2.2.8 Aluminium orthophosphates

The content of P in hydrotreating catalysts is typically less than 10 wt% by reference to the aluminium framework. However, aluminium orthophosphates, which contain stoichiometrically ~25.4 wt% of P, is one of the most well known P compounds whose presence is commonly reported in P-containing hydrotreating catalysts. Therefore, a rather detailed examination of aluminium orthophosphate structure deserves interest in this review. Crystalline aluminium orthophosphates (Al_2O_5-P_2O_5-H_2O ternary compounds) have analogous structures to all the SiO_2 modifications such as quartz, crystobalite, trydimite and so on. In principle, the aluminium orthophosphate are classified into basic (Al:P >1), neutral (Al:P=1) and acid phases (Al:P<1). Table 4 shows the list of crystalline aluminium orthophoshpate reported in the literature (14).

Table 4. List of orthophosphates in the ternary system Al_2O_3-P_2O_5-H_2O. (adapted from ref. 14)

No.	Composition	Mineral name / Polymorphism	Crystal system
Basic (Al : P > 1)			
1	$Al_4(OH)_3(PO_4)_3$	Trolleite	Monoclinic
2	$Al_2(OH)_3(PO_4)$	Augelite	Monoclinic
3	$Al_2(OH)_3(PO_4)\cdot H_2O$	Senegalite	Orthorhombic
4	$Al_3(OH)_3(PO_4)_2\cdot 5H_2O$	Wavellite	Orthorhombic
5	$Al_4(OH)_3(PO_4)_3\cdot 11H_2O$	Vashegyite	Orthorhombic
6	$Al_3(OH)_3(PO_4)_2\cdot 9H_2O$	Kingite	Triclinic
7	$Al_2(OH)_3(PO_4)\cdot 4.75H_2O$	Bolivarite	(amorphous to X-ray)
8	$Al_3(OH)_6(PO_4)\cdot 6H_2O$	Evansite	(amorphous to X-ray, opalescent glass)
Neutral (Al : P = 1)			
9	$AlPO_4\cdot 2H_2O$	Variscite-Lucine (VL)	Orthorhombic
		Variscite-Messbach(VM)	Orthorhombic
		Metavariscite(MV)	Monoclinic
Acid (Al : P < 1)			
10	$Al(H_2PO_4)_3$	A	Trigonal
		B	
		C	Rhomboedral
11	$Al(H_2PO_4)(HPO_4)\cdot H_2O$		Monoclinic
12	$H_3O[Al_3(H_2PO_4)_6(HPO_4)_2]\cdot 4H_2O$		Monoclinic
13	$Al_2(HPO_4)_3\cdot 3.5H_2O$		
14	$Al_2(HPO_4)_3\cdot 4H_2O$		
15	$Al(H_2PO_4)(HPO_4)\cdot 2.5H_2O$		
16	$Al_2(H_{2-x}PO_4)_3(H_{3x}PO_4]\cdot 6H_2O$	$(0 \le x \le 1)$	Trigonal
17	$Al_2(HPO_4)_3\cdot 6.5H_2O$		
18	$Al_2(HPO_4)_3\cdot 8H_2O$		

The structure of basic aluminium orthophosphate such as Trolleite, Augelite, Senegalite and Wavellite are shown in Fig. 4. Trolleite and Augelite have dimeric and tetrameric units, respectively. Senegalite and Wavellite have chain-like structure units. The structure of Vashegyite and Kingite are not defined yet while they might have a layered structure. Bolivarite and Evansite are amorphous by XRD.

Neutral aluminium orthophosphate compounds such as Variscite-Lucine (VL) and Metavariscite (MV) have 3-dimensional structure consisted of $Al(O_p)_4(O_{H2O})_2$ octahedra and PO_4 tetrahedra as shown in Fig. 5 (where O_p and O_{H2O} mean oxygen atoms belonging to phosphate and water, respectively). The structure of Variscite-Messbach (VM) has not been identified yet.

Five crystalline structures have been found for acid aluminium orthophosphate. Among them, $Al(H_2PO_4)_3$-A and $Al(H_2PO_4)_3$-C are built by $Al(O_p)_6$ octahedra and $PO_2(O_H)_2$ tetrahedra with one dimensional and three dimensional linkage, respectively as shown in Fig. 6 (where O_H means oxygen atoms belonging to P-OH group).

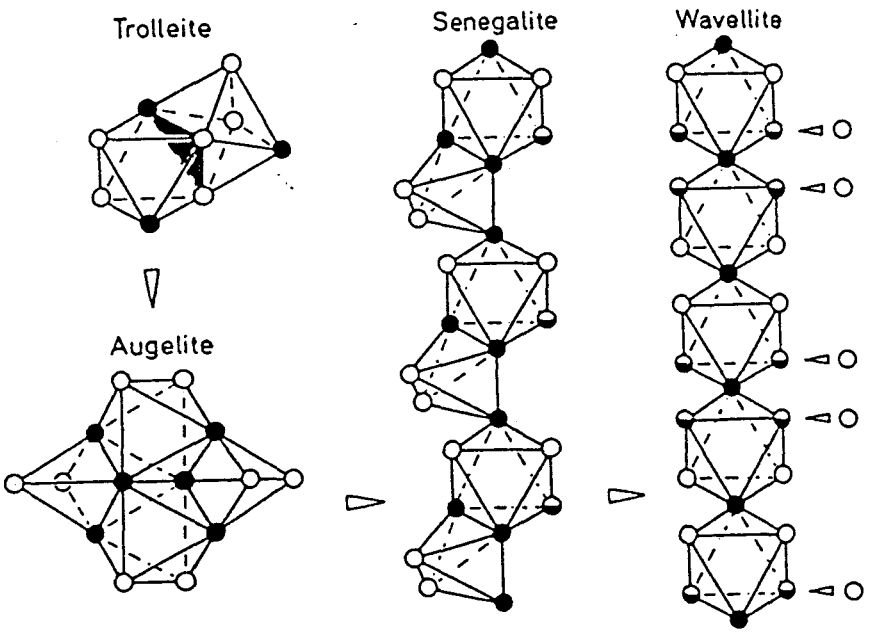

Figure 4. Structure of basic aluminium orthophosphates. The schemes show only position of oxygen atoms: oxygen atoms of hydroxide ions (O_{OH}) [closed circle], oxygen atoms of phosphate ions (O_p) [open circle], oxygen atoms of H_2O molecules (O_{H2O}) [half open circle] (from ref. 14).

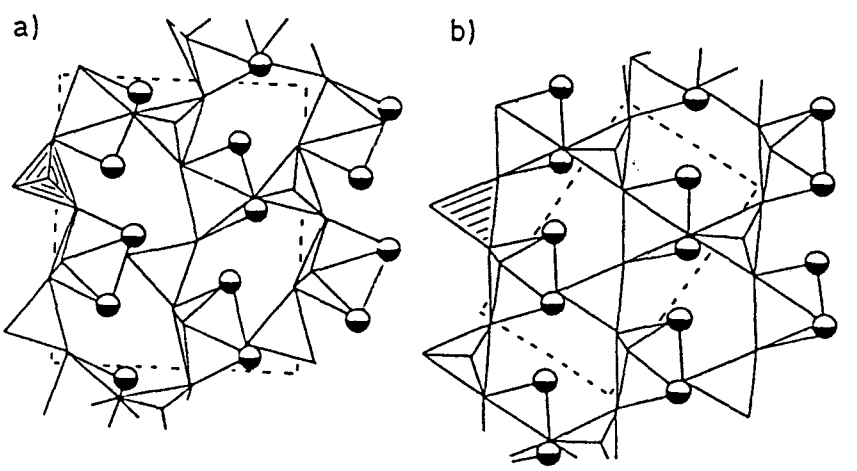

Figure 5. Part of the crystal structures of neutral aluminium phosphates.
(a) Variscite-Lucine (VL) and (b) Metavariscite (polyhedral representation). The shaded tetrahedra serves to emphasize the difference in the otherwise identical connectivities (from ref. 14).

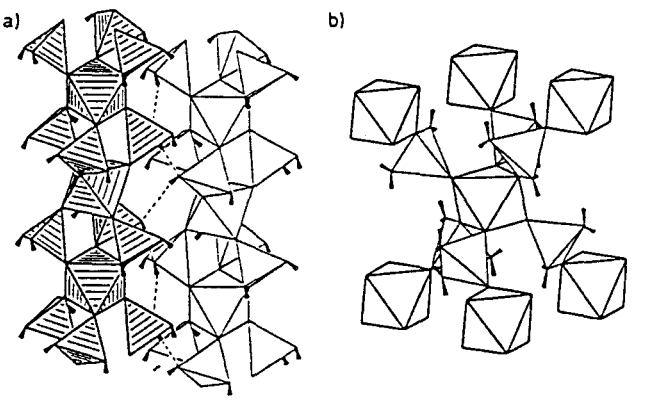

Figure 6. Part of the crystal structures of acid aluminium orthophosphates (polyhedral representation). (a) $Al(H_2PO_4)_3$-C and (b) $Al(H_2PO_4)_3$-A. One structural unit of $Al(H_2PO_4)_3$-C is indicated by shading. The hydrogen atom position are shown by wedges (from ref. 14).

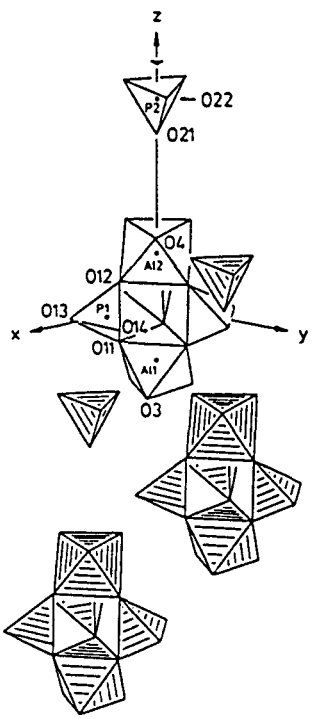

Figure 7. Part of the crystal structure of acid aluminium orthophosphates : $Al_2(H_{2-x}PO_4)_3(H_{3x}PO_4)\cdot 6H_2O$ (polyhedral representation) (from ref. 14).

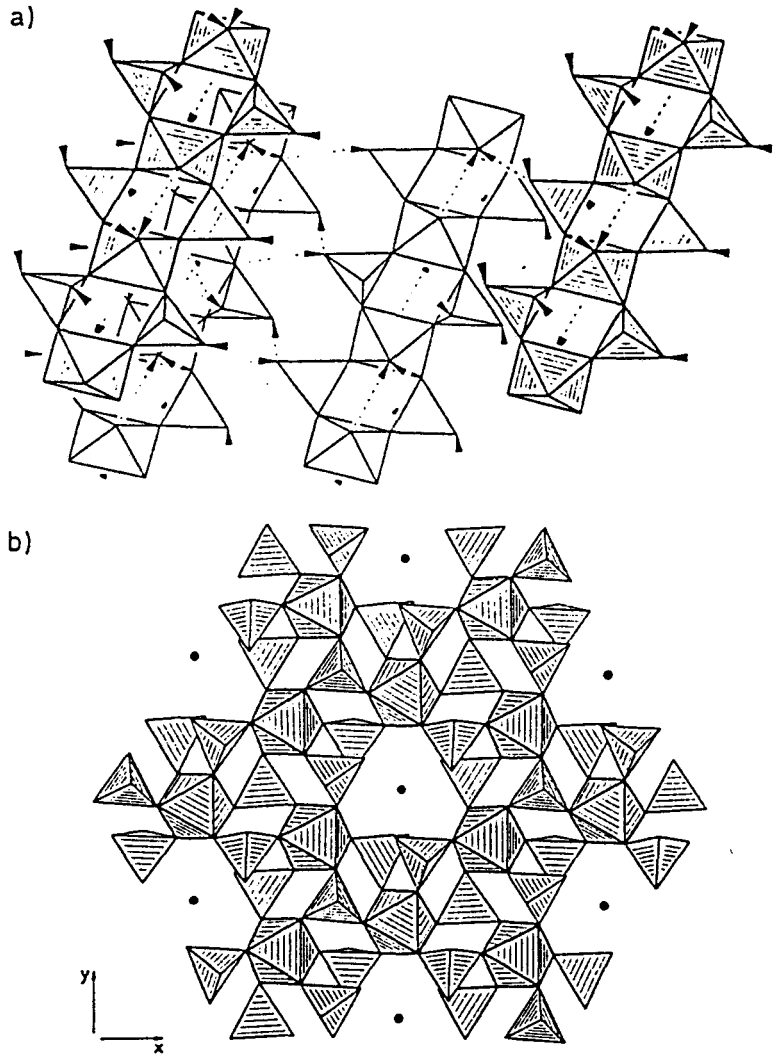

Figure 8. Part of the crystal structures of acid aluminium orthophosphates (polyhedral representation). (a) $Al(H_2PO_4)(HPO_4)\cdot H_2O$; polyhedron linkages directed upwards in this projection are indicated by shading. The hydrogen atom position are shown by wedges Inter- and intra-molecular hydrogen bonds are shown by broken lines. (b) $H_3O[Al_3(H_2PO_4)_6(HPO_4)_2]\cdot 4H_2O$; the filled circles in the middle of the holes represent the H_3O^+ sites (from ref. 14).

$Al_2(H_{2-x}PO_4)_3(H_{3x}PO_4)\cdot 6H_2O$ contains two different units stacked in the direction of "C" crystallographic axis. The first one is isolated PO_4 tetrahedra and the other one is two $Al(O_p)_3(O_{H2O})_3$ octahedra bound with three PO_4 tetrahedra as shown in Fig. 7.

$Al(H_2PO_4)(HPO_4)\cdot H_2O$ has a characteristic layered structure which consists of isolated $Al(O_p)_5(O_{H2O})$ octahedra linked by $PO_2(O_H)_2$ and $PO_3(O_H)$ tetrahedra (Fig. 8a). The $H_3O[Al_3(H_2PO_4)_6(HPO_4)_2]\cdot 4H_2O$ compound contains zeolite-like micropores with H_3O^+ sites in the middle of the micropore (Fig.8b).

Fig. 9 gives an estimation of the thermal stability of the crystalline aluminium orthophosphate described in Table 4. It depends predominantly on their water content and on the nature of the linkages between the polyhedra. Thermal treatments of hydrated aluminium orthophosphate converts them generally to lower hydrated phases. The highly hydrated phase like $Al_2(H_{2-x}PO_4)_3(H_{3x}PO_4)\cdot 6H_2O$ decomposes at 70 °C while the least hydrated form of Trolleite is stable up to 650 °C. Note also that the completely dehydrated $AlPO_4$ phase is stable up to 1800 °C. When present in catalyst formulation, it will not decompose under the conventional calcination procedures.

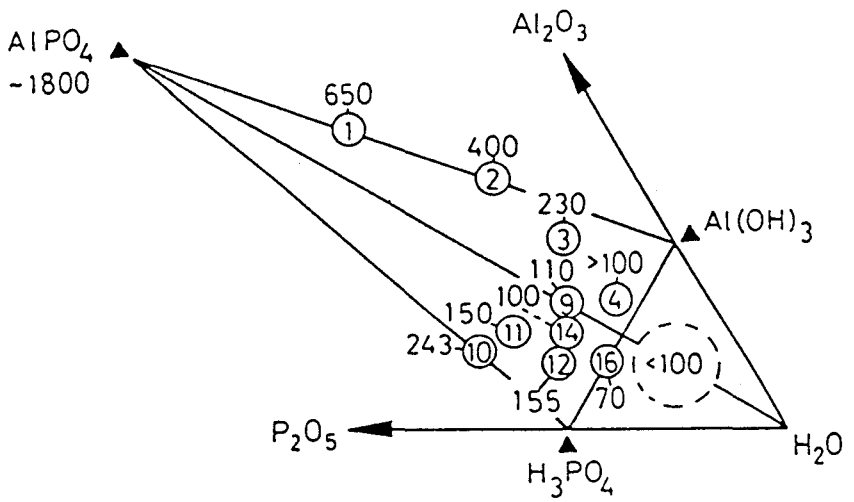

Figure 9. The thermal stability of some aluminium orthophosphates. The phases are numbered into the different circles according to table 4 and the temperatures are reported in °C (from ref. 14).

In addition, a lot of crystalline $AlPO_4$-N (N=5,8,11,14 etc.) which possess a zeolite-like structure are reported (15,16). VPI-5 has been also known as a crystalline aluminophosphate which has very large pores consisted of 18-menbered rings (16).

Let us note also that amorphous aluminium orthophosphate or some

specific surface structures of aluminium orthophosphate could be present and very important in hydrotreating catalysts. It has been revealed (18) that amorphous $AlPO_4$ contains four, five and six fold-coordinated aluminium ions at its surface.

1.2.2.9 "Mo-P" and "W-P" heteropoly compounds

Association of molybdates (tungstates) with phosphate-like structures conducts to a class of compounds which are chemically named heteropoly compounds or heteropoly acids of Mo or W (19, 20). The heteropoly anions which may contain Mo, W, P and also other elements are neutralised, both in the solid state and in solution, by a large variety of cations such as H^+ , NH_4^+, Na^+ etc.. In this review, we will present only some "Mo-P" heteropoly compounds which have certainly an important role in hydrotreating catalysts during the catalyst preparation (impregnation) or as supported oxidic phases. In general, "Mo-P" heteropoly compounds have the main following properties :

1) High solubility in water or polarized solvents such as alcohols, ethers and ketones. However, larger counter cations such as K^+, Rb^+, Cs^+ and NH_4^+ often decrease their solubility,
2) High stability in acid solutions,
3) Stronger acidity than molybdic acid,
4) Important and interesting oxidizing or reducing behaviors.

The phosphomolybdates ("Mo-P" heteropoly compounds) are basically composed of PO_4 tetrahedra and MoO_6 octahedra. Several structures can be obtained depending on the P/Mo ratio. Table 5 shows the list of such "Mo-P" heteropoly compounds.

Table 5. Chemical formulation of some "Mo-P" heteropoly anions (adapted from ref. 19)

Type	P/Mo ratio	Typical anions [a)]
"$Mo_{12}P$"	1 :12	$[PMo_{12}O_{40}]^{3-}$
"$Mo_{11}P$"	1 :11	$[PMo_{11}O_{39}]^{7-}$
"$Mo_{10}P$"	1 :10	$[PMo_{10}O_{35}]^{5-}$
"$Mo_{18}P_2$"	1 :9	$[P_2Mo_{18}O_{62}]^{6-}$
"Mo_9P"	1 :9	$[PMo_9O_{31}(HO)_3]^{6-}$
"Mo_6P"	1m :6m	$[P^{III}Mo_6O_{24}H_6]^{3-}$
"$Mo_{17}P_2$"	2 :17	$[P_2Mo_{17}O_{60}]^{8-}$
"Mo_5P_2"	2 :5	$[P_2Mo_5O_{23}]^{6-}$

a) Formal oxidation states of P and Mo are P^V and Mo^{VI}, respectively, unless otherwise stated.

The elements Co, Ni or Al can be also used as counter ions or incorporated in the heteropoly anions structure. For example, one can mention $Co_3[PMo_{12}O_{40}]_2 \cdot 34H_2O$ and $Ni_3[PMo_{12}O_{40}]_2 \cdot 34H_2O$. The corresponding phosphotungstates compounds have analogous structures and rather similar chemical properties with those of "Mo-P" heteropoly compounds. However, thermal stability or redox potential could be quite different.

The structure of some heteropoly compounds is shown in Fig. 10 (21). The "$Mo_{12}P$" heteropoly compound (Fig. 10a) is well known as a Keggin structure where twelve MoO_6 octahedra are surrounding a central PO_4 tetrahedra. Each four oxygen atoms of the central PO_4 are shared with three MoO_6 octahedra and four of six oxygen atoms in the MoO_6 octahedra are shared with the other MoO_6. Then only one oxygen in each MoO_6 is individually bound to the Mo atom. The structure of "$Mo_{10}P$" heteropoly anions is unknown yet but it is considered to be of dimeric structure. "$Mo_{11}P$" (Fig. 10b) heteropoly compound is more stable for reduction treatment than "$Mo_{12}P$" while the "Mo_9P" (Fig. 10e) heteropoly anion is less stable for reduction than "$Mo_{12}P$". "$Mo_{18}P_2$" (Fig. 10c) heteropoly anion has a dimeric structure with two central PO_4 tetrahedra surrounded by eighteen MoO_6 octahedra. Two different hydration forms are known in the "$Mo_{18}P_2$" compounds such as $H_6[P_2Mo_{18}O_{62}] \cdot 33H_2O$ (orange) and $H_6[P_2Mo_{18}O_{62}] \cdot 37H_2O$ (bride orange) while the later is unstable at ambient temperature. The precise structure of "Mo_6P" and "$Mo_{17}P_2$" are also unknown yet. The structure of "Mo_5P_2" is shown in Fig. 10d. It is interesting to note that the P atoms in the "Mo_5P_2" structure are exposed to the outer surface of the ion while those in the "$Mo_{12}P$" and "$Mo_{18}P_2$" are surrounded by the molybdenum octahedra.

Alkaline treatments transform these "Mo-P" heteropoly compounds into more stable heteropoly species with lower P/Mo ratio, and finally lead to simple "MoO_4" molybdate and phosphate. For example, the overall degradation of one "$Mo_{12}P$" heteropoly compound is completed by 20 to 28 moles of NaOH. On the contrary, the transformation can also proceed by the addition of large amount of phosphoric acid. In this case, it is attributed to the formation of new central PO_4 tetrahedra with addition of phosphate. The equilibria of "Mo-P" containing solutions as a function of hydrogen ion concentration are shown in Figure 11 (22).

Thermal treatment also lead to the degradation of heteropoly compounds. For example, by thermal treatment, the "$Mo_{12}P$" heteropoly compound decomposes into P_2O_5 and MoO_3 above 450 °C with gradual hydration water elimination. Griboval et al. (23) reported, however, that a partly reduced form of $[PMo_{12}O_{40}]^{7-}$ is highly thermally stable even above 400 °C.

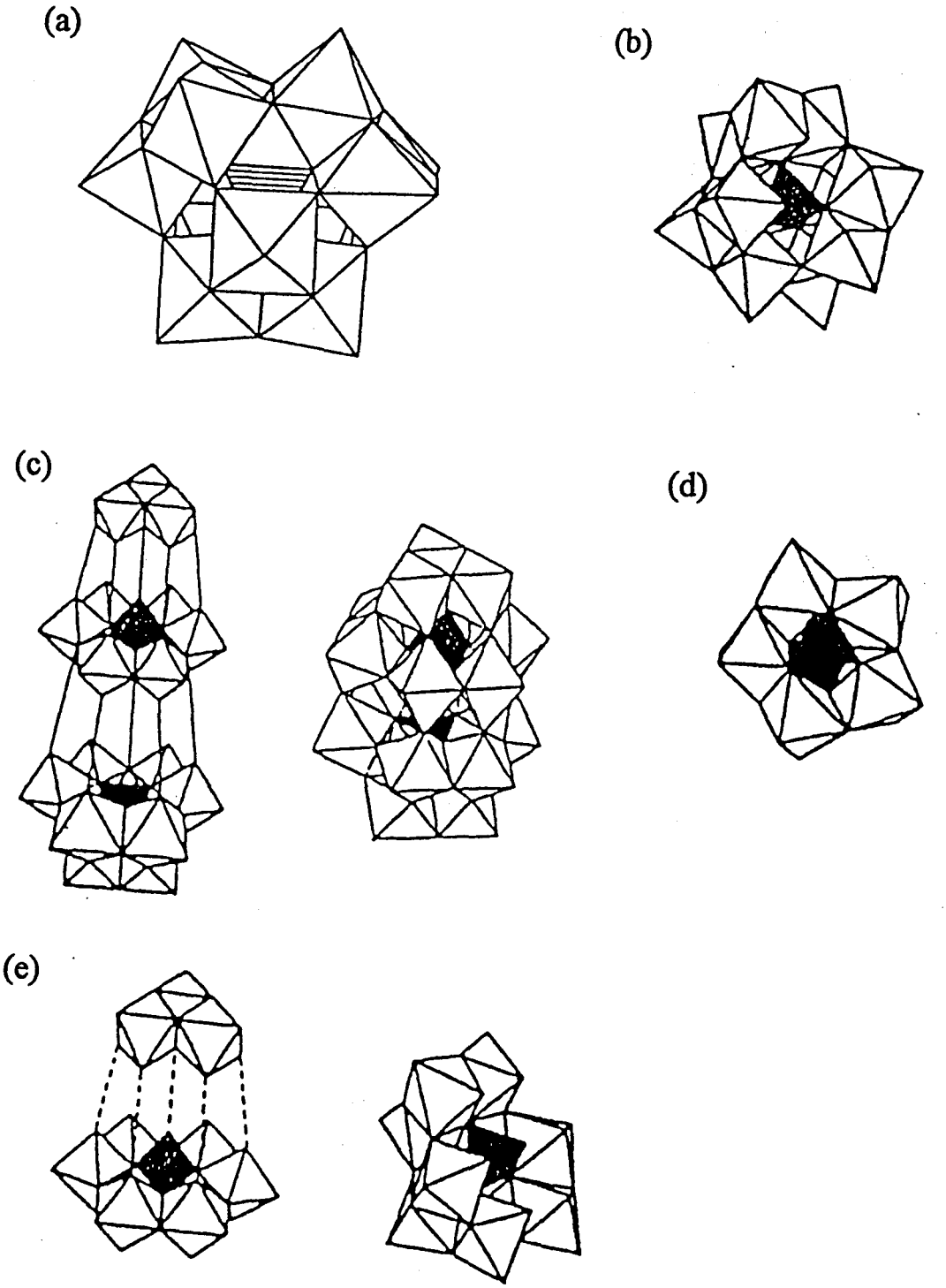

Figure 10. Structures of some "Mo-P" heteropoly anions. (a)"$Mo_{12}P$", (b)"$Mo_{11}P$", (c)"$Mo_{18}P_2$", (d) "Mo_5P_2" and (e) "Mo_9P". Shadowed and white polyhedra indicate PO_4 tetrahedra and MoO_6 octahedra, respectively. (adapted from ref. 19 and 21).

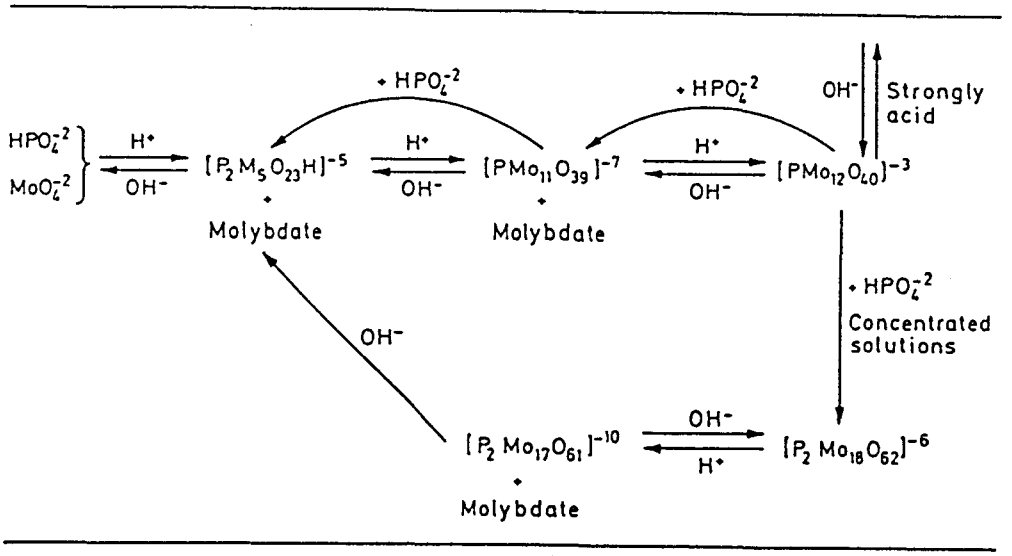

Figure 11. Equibria in molybdate-phosphate solutions as a function of hydrogen ion concentration (from ref. 22).

The order of stability also depends on the nature of the central atom (Si>Zr, Ti> Ge>P>As) and on the nature of the surrounding anion groups (W>Mo>V). In the light of hydrotreating catalysts, such a classification has some interest. If, for example, introduction of Si into alumina as a support (Silica-Alumina, zeolite etc.) leads to the formation of Si-Mo or Si-W heteropoly compounds, they will not be degraded during the calcination procedures.

1.2.2.10 Other phosphorus compounds

In addition to the P compounds described above, there are many other types of P-containing compounds like organophosphates, some of which might be present on specific fraction of the surface of hydrotreating catalysts in working conditions. Some of these compounds are represented below (24):

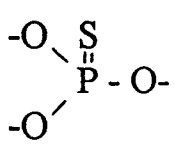

phosphorothioates
(phosphorothionates)

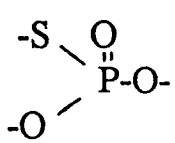

phosphorothiolates

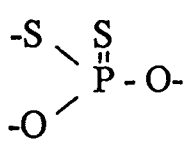

phosphorodithioates
(phosphorothionothiolates)

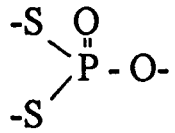

phosphorodithiolates

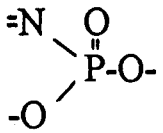

phosphoramides (phosphoramidates)

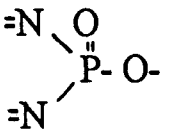

phosphorodiamidates

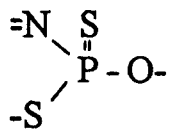

phosphoramidothionates

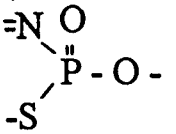

phosphoramidothiolates

It is quite possible that these compounds participate in the hydrotreating reactions as intermediates or as new active sites. For example, Thompson (25) reported that a sulphur radical is predominantly lost from a compound named methamidophos (Fig. 12). If a sulphur (or a nitrogen) containing compound further reacts with the methamidophos ion formed after sulphur abstraction, a catalytic desulphurization (or denitrogenation) cycle could be achieved. However, no evidence of such intermediates in the author's knowledge has been ever cited in literature yet.

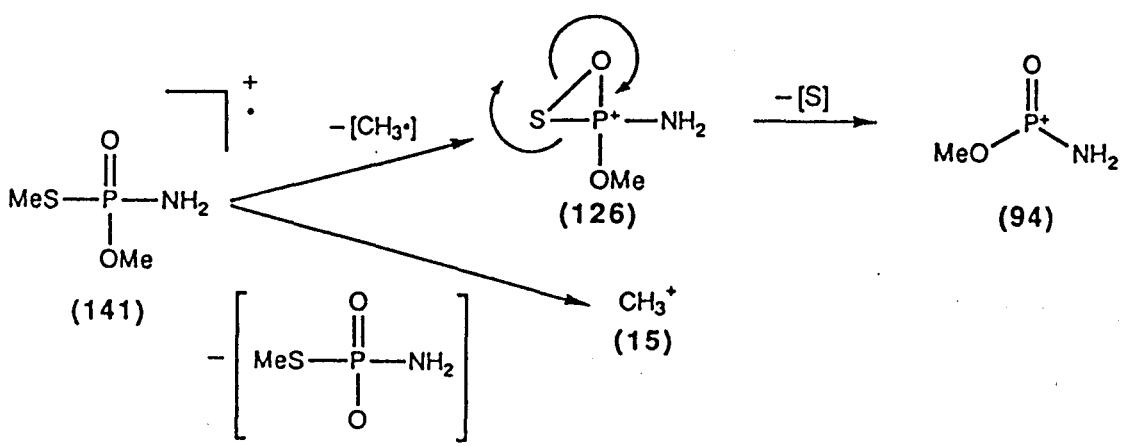

Figure 12. Schematic representation of CH_3^+ and S radical elimination from the compound "methamidophos" (from ref. 25).

1.2.2.11 Vibrational and NMR data of selected P-based reference compounds

To identify the above mentioned P compounds as well as Al, Mo, Co and Ni related species which might be contained in hydrotreating catalysts, it is convenient to use spectroscopic techniques such as NMR, IR, UV, Raman spectroscopies and XRD. Especially, XRD is the most useful tool to characterize well crystalline bulk compounds. Some typical IR and NMR data reported in literature are shown in Tables 6 and 7, respectively.

Table 6. List of IR vibration data of selected P-based reference compounds.

Compounds	Wave number (cm^{-1})	Ref.
$AlPO_4$	3795,3680,1130,735,715	26,27
"$PMo_{12}O_{40}$"	1070,965,875,790,590,485	28,29
"$PMo_{11}O_{39}$"	1110,1060,930,900,860,790,742	20
NiMoP heteropoly compound	815,730	30
Aluminium nickel phosphates	1119,930,490	31
"$AlMo_6$" heteropoly	945,920,890,665,445	30,31

Table 7. List of ^{31}P-NMR chemical shift data of selected P-based reference compounds.

Compounds	Chemical shift (ppm)	ref.
"$PMo_{12}O_{40}$"	- 3.9 to - 4.5	20
"PMo_9O_{34}"	- 4.1	20
"$P_2Mo_{18}O_{62}$"	- 3.1	20
"$P_2Mo_5O_{23}$"	2.2	26
$AlPO_4$	- 25 to - 30	32
crystalline $AlPO_4$	- 32	33
$AlPO_4$-T	- 29.5	34
$AlPO_4$-C	- 27.1	34
H_3PO_4	0	-

1.2.3. Preparation of alumina based hydrotreating catalysts containing P, Mo and Co or Ni

The objectives for optimizing the preparation of hydrotreating catalysts are to "put altogether" the selected ingredients (P, Mo, Co or Ni and the alumina) in order to obtain solids which satisfy specific requirements such as high metal dispersion, high metal loading, high specific surface area, low incorporation of some elements (P, Co, Ni) into the alumina framework, etc. The alumina support by itself can be used as a powder, as a preformed material like pellets or extrudates, or as its precursor forms. The goal of this part is not to extensively describe and discuss all the methods relative to preparation of supported catalysts but only to schematically present the most commonly used procedures. Fig. 13 gives the general preparation procedures used for obtaining alumina-based hydrotreating catalysts with P, Mo and Co (or Ni). The complexity of the system, but also its richness, makes possible that each element can be introduced alone or with other elements at a given step and that the order of element introduction can be permuted. Between each step, procedure of drying or calcination can be carried out or not. All these refinements will be completely examined in this paragraph.

1.2.3.1 Impregnation method (Fig. 13a and 13b)

The dry impregnation method (or incipient wetness impregnation method) is one of the most popular catalyst preparation technique (see also Table 11). It consists to impregnate the support with a solution containing the elements to be deposited which volume is exactly the same as the water pore volume of the support used. It is very easy to perform and is convenient to control the metal loading(s) and the physicochemical properties of catalysts to be obtained. However, the maximum metal loading(s) are limited by the solubility of metal salts. The impregnation method is further classified into co-impregnation and sequential impregnation. With this impregnation method, the sequences of P and metal introduction and the pH of impregnation solutions should be taken with great attention because they affect significantly on the resulting physicochemical properties and consequently on the catalyst performance (see paragraphs 1.2.5.4 and 1.2.6).

1.2.3.2 Equilibrium adsorption (Fig. 13a and 13b)

Equilibrium adsorption is also a popular method to prepare P-containing hydrotreating catalysts. The main preparation procedure is similar to the above impregnation methods. However, it consists to contact a very large volume of

solution containing the element to be deposited with the support, and then wait enough time in order to reach adsorption equilibrium between ions and the support surface. In this method, well dispersed metal species can be easily achieved although there is an effective disadvantage for a flexible control of all the metal loadings. Furthermore, this method is suitable for elucidating the limitations of monolayer dispersion and the strength of interaction between P, the other metals and the support. Once again, co-impregnation or sequential equilibrium adsorption can be performed as well as the impregnation method.

1.2.3.3 Precipitation method or hydrogel method **(Fig. 13c)**

In the precipitation method, the metal components and P are directly introduced in a precursor of the support like an alumina hydrogel. This method enables to get high metal loading and SSA but the metal dispersion is not always optimized. In addition, it is often difficult to control the P-Mo, Co-Mo or Ni-Mo interactions. Moreover, there might be also some difficulties to control the pore structure and the mechanical strength of the obtained catalysts.

1.2.3.4 Sol-gel method **(Fig. 13d)**

Recently, the present authors proposed a new catalyst preparation method, so called the «sol-gel» method (35). With this sol-gel method, P is introduced simultaneously with the other active metal components before hydrolysis of an aluminium alkoxide. This method is generally expected to obtain well dispersed high metal loadings (i.e. more than 30 wt% of Mo as the element) with extremely high SSA (from 300 to 600 m^2/g). Furthermore, this method is suitable for the study and identification of surface species because of its high SSA and high metal loadings. However, the sol-gel preparation method may cost too much compared with other preparation methods described above as aluminium alkoxide precursors are normally very expensive.

Moreover, the combination of different preparation methods described in Fig. 13 can give further variations in its preparation procedure and may provide interesting catalysts.

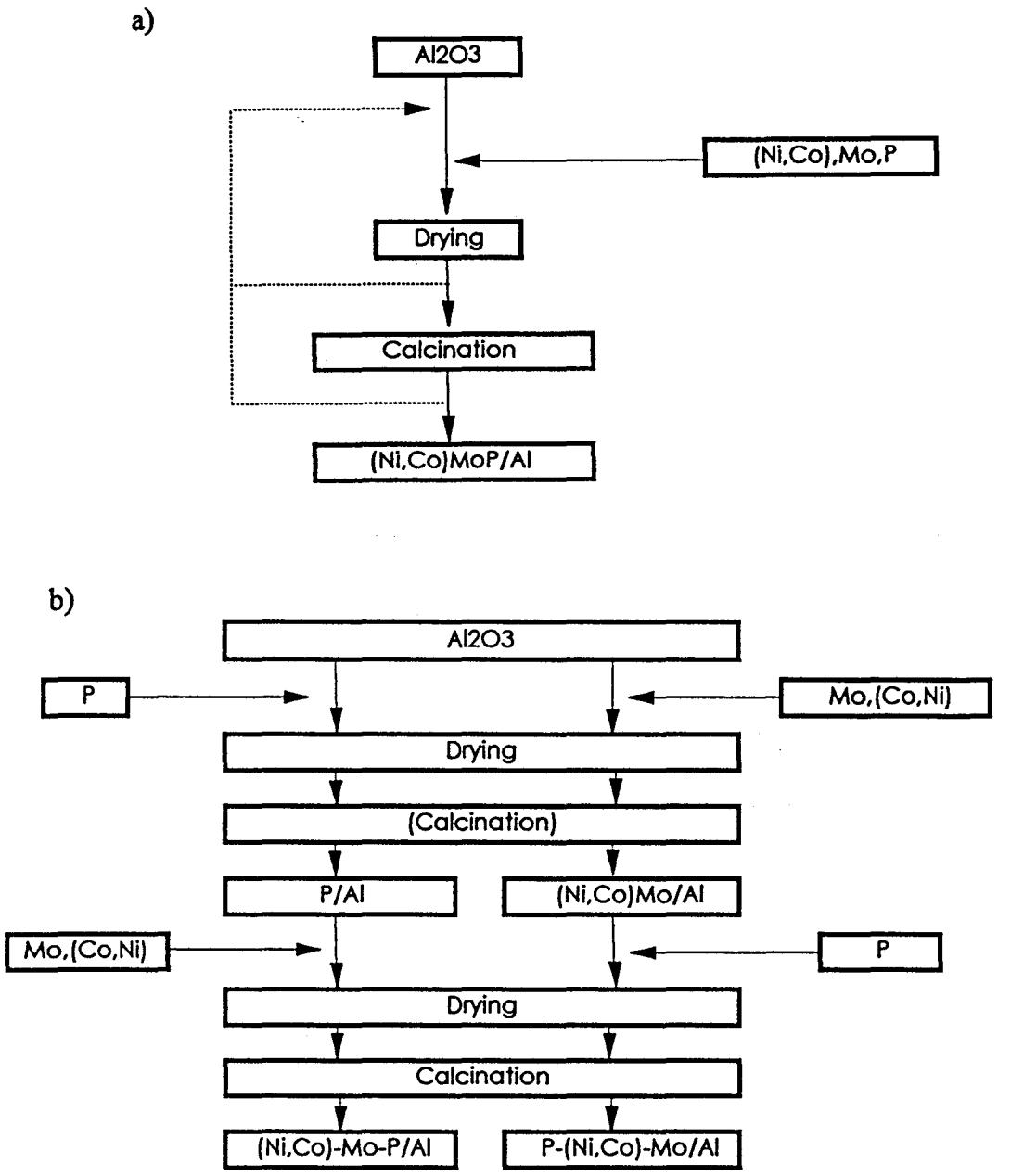

Figure 13. Procedures used for preparing alumina-based hydrotreating catalysts containing P, Mo and Co or Ni. (a) Impregnation or equilibrium adsorption method (co-impregnation), (b) Impregnation or equilibrium adsorption method (sequential impregnation)

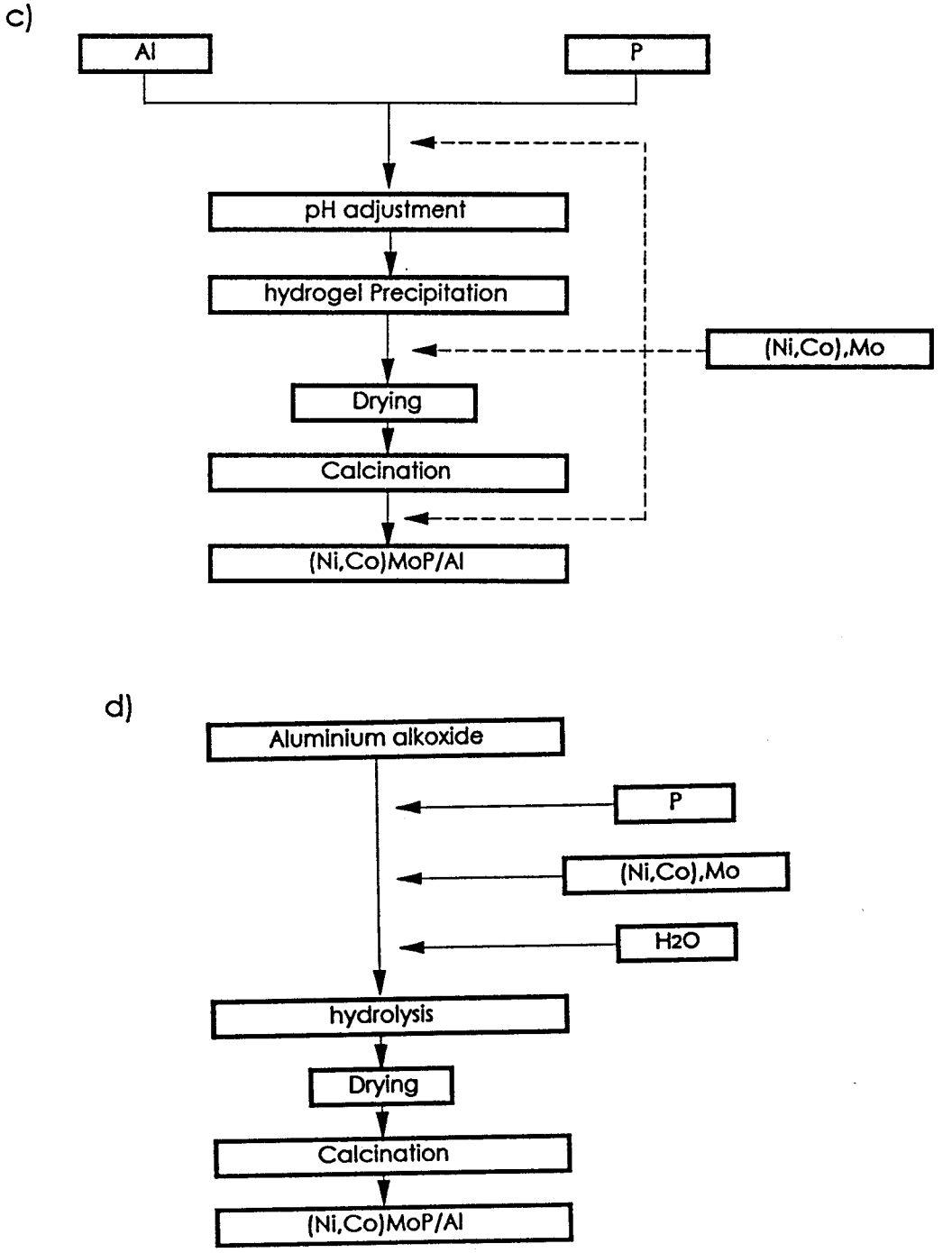

Figure 13. Procedures used for preparing alumina-based hydrotreating catalysts containing P, Mo and Co or Ni (continued). (c) Precipitation or hydrogel method and (d) Sol-gel method.

In the above preparations, ammonium heptamolybdate, cobalt nitrate or nickel nitrate are preferably used as Mo, Co and Ni precursors, respectively. As a P precursor, phosphorus pentoxide, phosphoric acid or their anion derivatives such as ammonium dihydrogen phosphate ($NH_4H_2PO_4$) are commonly used because they are highly water soluble and only phosphorus oxide remain after calcination. Especially, it is reported that the $NH_4H_2PO_4$ precursor gives weak interaction with the alumina support (36).

In addition, some research group recently start to use some heteropoly compounds as "Mo-P" precursors for preparation of hydrotreating catalysts (23,26,37). As described in paragraph 1.2.2, the heteropoly compound have unique structures and properties by themselves. In fact, they have high activity for several important reactions such as a mild oxidation (20). It is very attractive, therefore, to use them to obtain higher activity and unique selectivity.

1.2.4. Adsorption properties of P on hydrotreating catalysts

To understand the complex behavior of P interaction with alumina and the other metal species, it is very important to examine the chemistry involved in the preparation steps. In this part, adsorption properties of P are mainly presented and discussed.

1.2.4.1 Adsorption of P oxo-species on alumina

P oxo-species adsorbed on alumina are in a well dispersed state up to 2.9 $\times 10^{-6}$ P atom/pm^2 (or 2.9 P atom/nm^2) of alumina surface (38). IR spectroscopy permitted to identify several types of hydroxyl groups on the γ-alumina surface such as type Ia (tetrahedral Al-OH ; 3780 cm^{-1}), type Ib (octahedral Al-OH ; 3795 cm^{-1}), type IIa, IIb (bridged OH between two Al atoms ; 3736 cm^{-1}) and type III (bridged OH between three Al atoms ; 3697 cm^{-1}) as shown in Fig. 14 (39).

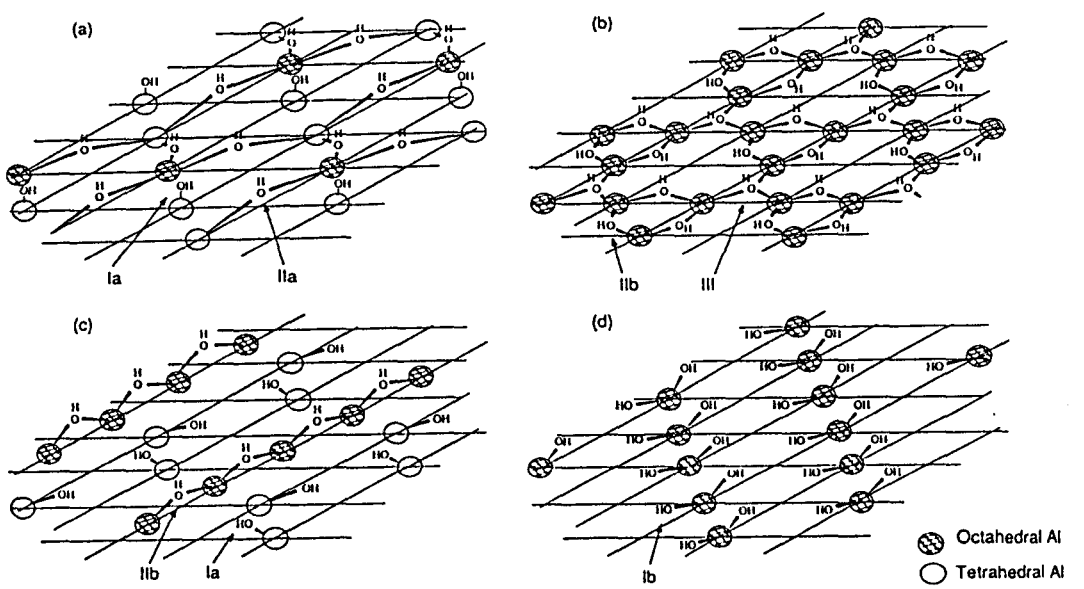

Figure 14. Idealized low Miller index surface planes of γ-alumina and nature of the different hydroxyl groups. (a) A layer, parallel to the (111) plane, (b) B layer, parallel to the (111) plane, (c) C layer, parallel to the (110) plane and (d) D layer, parallel to the (110) plane (from ref. 39).

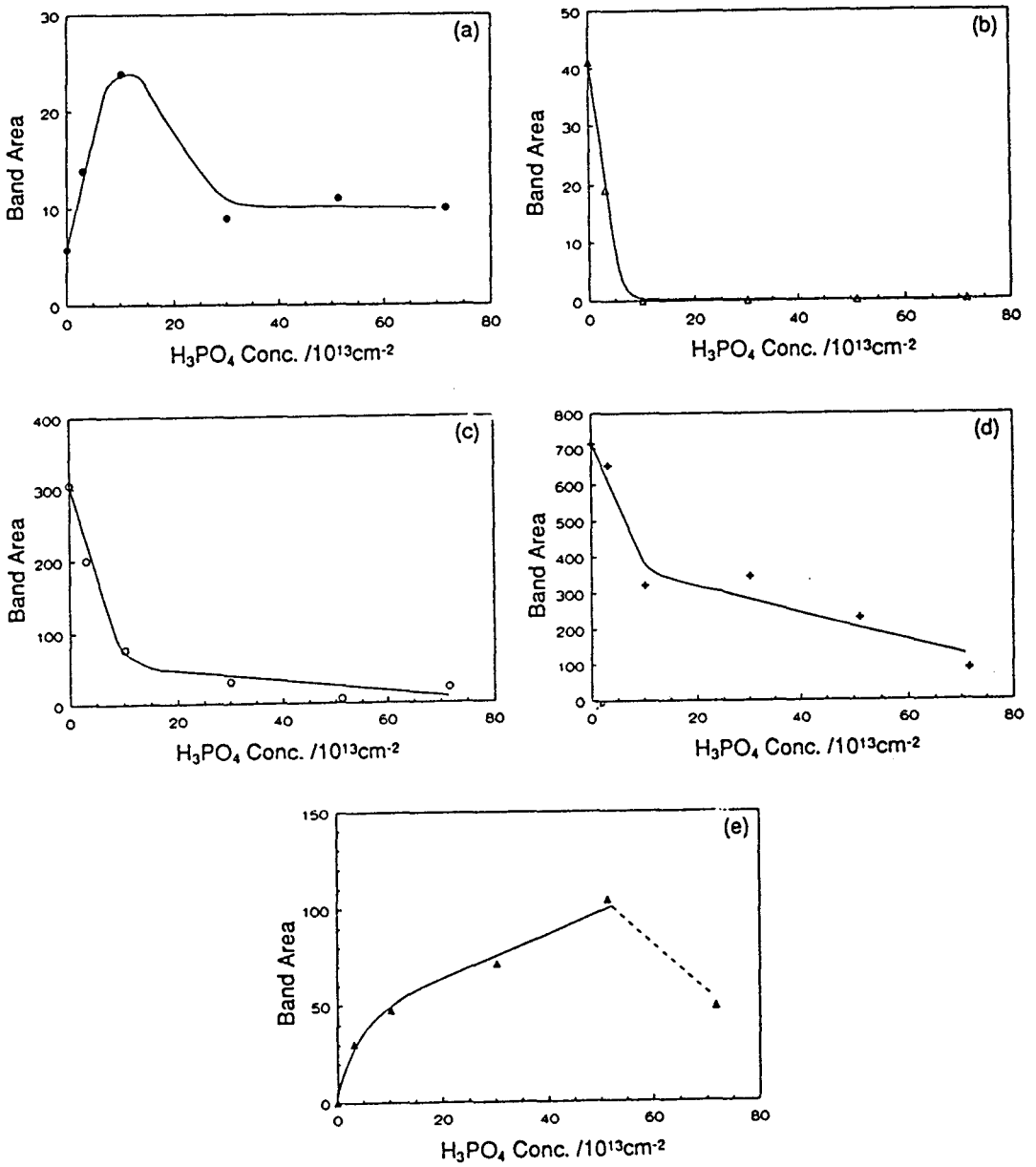

Figure 15. Effect of the surface concentration of phosphoric acid on the OH stretching region of P/Alumina samples : (a) 3795 cm^{-1} band (Ib sites), (b) 3780 cm^{-1} band (Ia sites), (c) 3736 cm^{-1} band (IIa and IIb sites), (d) 3697 cm^{-1} band (III sites) and (e) 3676 cm^{-1} band (P-OH sites) (from ref. 40).

At low P content, the P oxo-species interact with both basic and acid Al-OH while the Mo oxo-species interact predominantly with basic Al-OH. In general, the basic type Ib OH groups should be more reactive with P oxo-species than the acid ones.

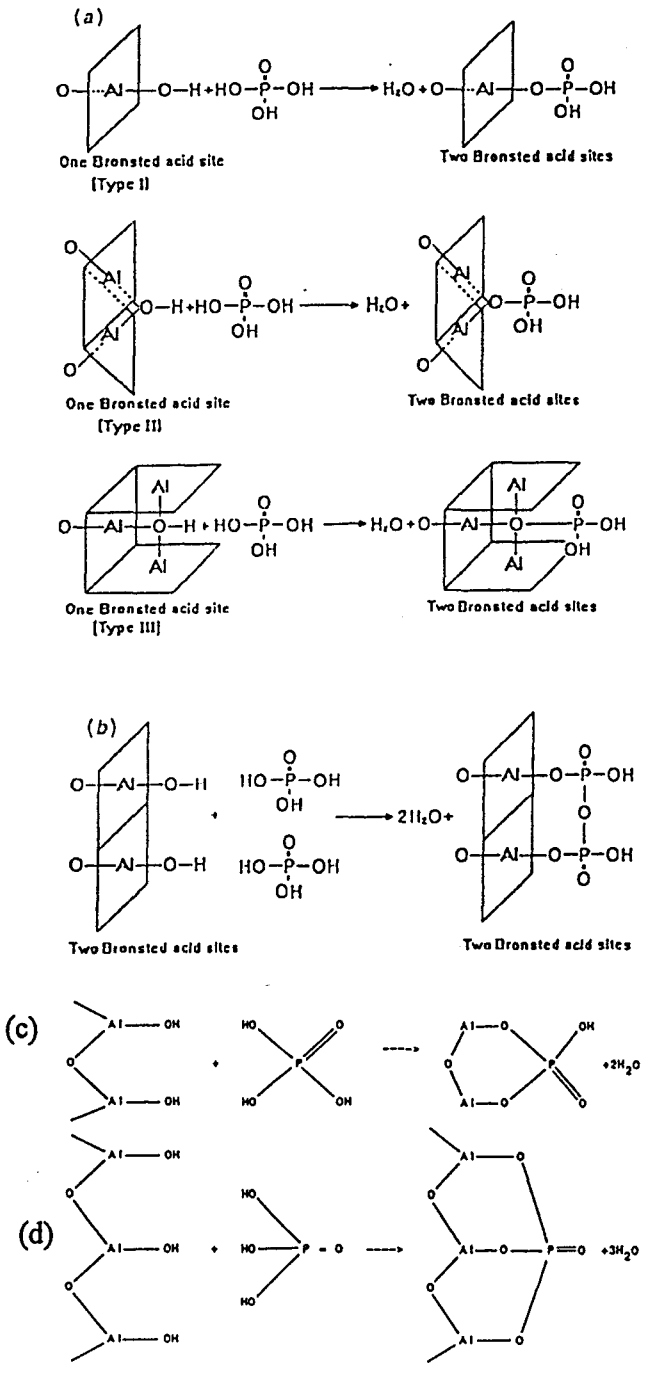

Figure 16. Schematic representation of interaction between H_3PO_4 and alumina surface OH ; (a) the formation of two Brönsted acid sites (B sites) from the adsorption of one H_3PO_4 on one OH site on the alumina, (b) the formation of two B sites from two H_3PO_4 and two OH sites (the interaction between neighboring P-OH bands), (c) the formation of one B sites from one H_3PO_4 and two OH sites, (d) the formation of site with no Brönsted acidity from one H_3PO_4 and three OH sites (adapted from ref.42 and 43).

However, Lewis and Kydd (40) found from an IR study that the amount of basic type Ib OH increases with addition of P up to a concentration of 10×10^{13} H_3PO_4 molecules/cm^2 (Fig. 15a). They suggested that OH groups of types II and III react with H_3PO_4 and leads to the formation of type Ib OH according to the following reaction :

$$\underset{\text{(Type II)}}{\text{Al-O(H)-Al}} + H_3PO_4 + H_2O \rightarrow \underset{\text{(Type I)}}{\text{Al-OH}} + \text{Al-O-P(=O)-(OH)}_2 + (H_3O^+) \qquad \text{Eq. (4.1)}$$

In addition, new P-OH groups (3676 cm^{-1}) are generated by the P loading up to 50×10^{13} H_3PO_4 molecules/cm^2 (Fig. 15e). At high P loading, the interaction between neighboring P-OH groups starts to form polymeric oxo-P compounds and intensity of the P-OH band tends to decrease (40,41).

Concerning the interaction of phosphoric acid with the alumina surface, several adsorption sites have been considered as schematically shown in Fig. 16 (42,43). If H_3PO_4 interacts with one surface Al-OH through a single bond, one surface Al-OH will be replaced by two P-OH (Fig.16a). However, if H_3PO_4 interacts with alumina through two or three OH groups, it could result in the partial or total loss of hydroxyls (Fig. 16c or 16d). From IR and NMR data, it was shown that H_3PO_4 interacts with multiple basic OH groups on alumina at low P content while single bonding is predominant at high P content (44,45).

Concerning the adsorption of H_3PO_4 on the alumina, different mechanisms are proposed in the literature as shown below :

(A) Aqueous solution of phosphoric acid will protonate Al-OH through hydrogen bond during the impregnation step and then leads to the formation of Al-O-P bonds by dehydration during the calcination step (26,46).

$$\text{Al-OH} + H_3PO_4\,(aq.) \leftrightarrow \text{Al-O(H}^+\text{)-H-OPO(OH)}_2\,(aq.)$$

$$\xrightarrow{\text{(calcination)}} \text{Al-O-PO(OH)}_2 + H_2O \qquad \text{Eq. (4.2)}$$

(B) P species adsorb electrostatically on the protonated surface Al-OH (47).

$$AlOH_2^+ + H_2PO_4^- \xrightarrow{K_1} AlOH_2^+\text{-}H_2PO_4^- \qquad \text{Eq. (4.3)}$$

$$AlOH_2^+ + HPO_4^{2-} \xrightarrow{K_2} AlOH_2^+\text{-}HPO_4^{2-} \qquad \text{Eq. (4.4)}$$

(C) P species adsorb covalently on the protonated surface Al-OH group (48,49).

$$AlOH_2^+ + H_2PO_4^- \rightarrow AlH_2PO_4 + H_2O \qquad \text{Eq. (4.5)}$$

$$AlOH_2^+ + HPO_4^{2-} \rightarrow AlHPO_4^- + H_2O \qquad \text{Eq. (4.6)}$$

(D) "H_2PO_4" is supported on alumina by a ligand exchange with Al-OH groups, especially at low P content (26,58,130).

$$Al\text{-}OH + H_2PO_4^- \rightarrow Al\text{-}H_2PO_4 + OH^- \qquad \text{Eq. (4.7)}$$

Mikami et al. (50) concluded from a detailed kinetic study that the P species adsorb electrostatically rather than covalently on the alumina at low P content. They calculated the intrinsic value of the adsorption and desorption rate constants at 25 °C for the monovalent phosphate : $K_1 = 4.1 \times 10^5$ mol^{-1} dm^3 s^{-1} and $K_{-1} = 2.3$ s^{-1}, and those for the divalent phosphate are $K_2 = 1.1 \times 10^7$ mol^{-1} dm^3 s^{-1} and $K_{-2} = 2.7$ s^{-1}, respectively. However, considering the experimental result that the pH of solution rises by the adsorption, mechanisms (B) and (D) may proceed simultaneously.

Variations of the Zeta potential of several supports versus the pH of the impregnating solution, and the isoelectronic point (IEP) as a function of P loading are reported in Fig. 17a and 17b (51). The IEP decreases from ~ 8.8 to 7.4 up to 2 wt% P_2O_5 and then shows a steady value above 2 wt% P_2O_5. The total amount of phosphate ions ($H_2PO_4^-$ and HPO_4^{2-}) adsorbed on the alumina decreases with increasing pH because the alumina surface tends to be negatively charged above its IEP but the relative amount of HPO_4^{2-} exhibits a maximum around pH=8 (Fig. 18) (50).

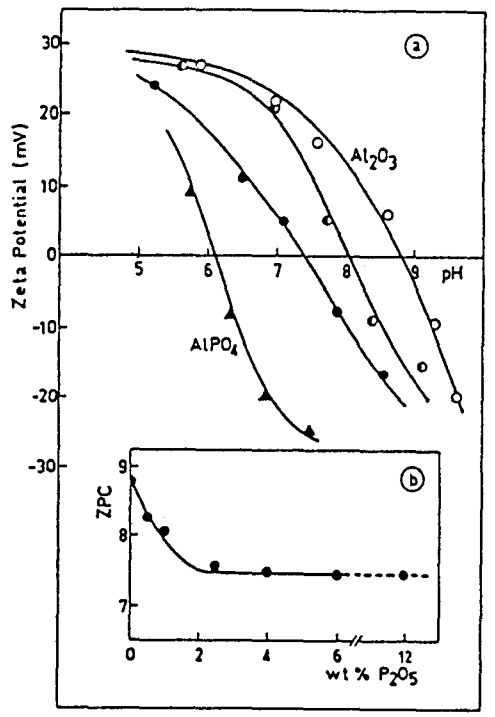

Figure 17. (a) Zeta potential at room temperature as a function of suspension pH of : alumina [open circle], $AlPO_4$ [triangle] , two different P/Al systems [closed or half closed circle]. (b) Variation of the isoelectoric point of P/Al samples as a function of phosphorus content (from ref. 51).

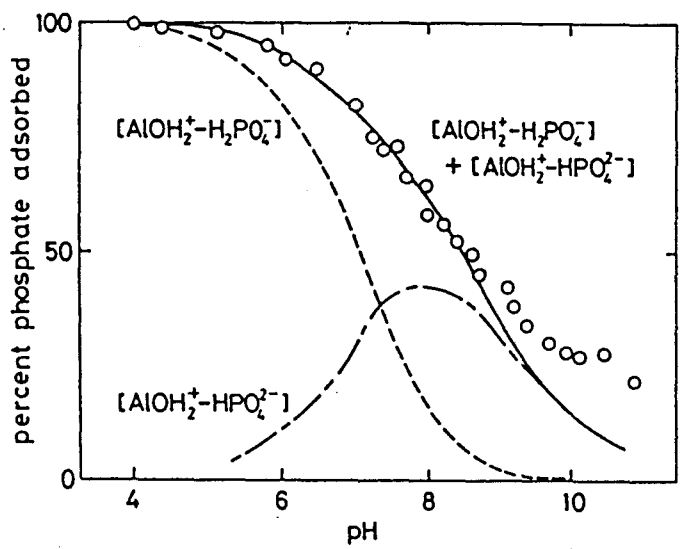

Figure 18. Variation of the amount of $H_2PO_4^-$ and HPO_4^{2-} adsorbed on alumina as a function of pH (from ref. 50).

Concerning the nature of adsorbed P species, Kraus (45) revealed, from detailed NMR investigations, that several states of P such as monophosphate, diphosphate, polyphosphate and $AlPO_4$ exist on the surface of γ-Alumina depending on the P content (Fig. 19). With increasing the P loading, the amount of polymeric phosphate tends to increase. It is remarkable to note that $AlPO_4$ is not detected at the low P loading, while it starts to be observed only above the P loading corresponding to theoretical P monolayer coverage. No crystalline $AlPO_4$ phase is observed with additional P loading. Considering the line broadening of ^{31}P-NMR , several types of $AlPO_4$ with a different degree of hydration and condensation might be also formed on the alumina (33).

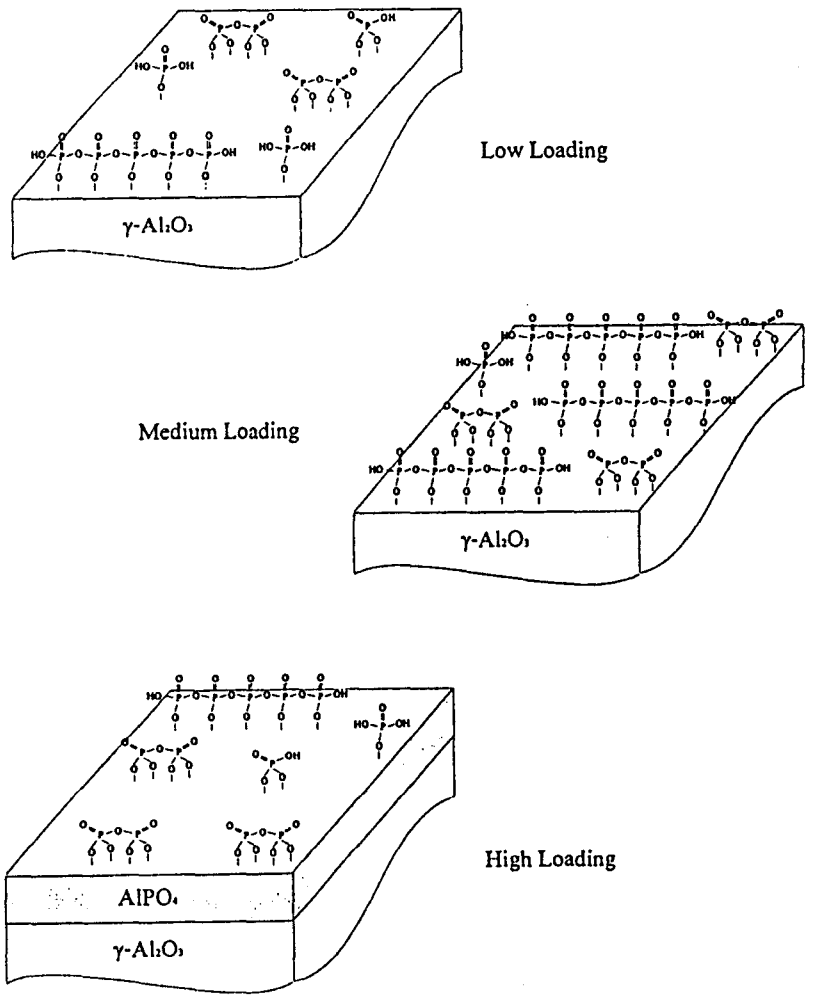

Figure 19. Possible phosphate structures on the surface of γ-Alumina (from ref. 45).

Petrakis et al. (43) also confirms that P oxo-species prefer to form surface amorphous aluminophosphate rather than the crystalline $AlPO_4$ phase at low P content due to thermodynamic limitation. For example, only 5 % of P can transform into the $AlPO_4$ phase even after calcination at 737 °C. On the other hand, Decanio et al. (33,52) detected crystalline $AlPO_4$ in dried P/Al and MoP/Al catalysts above 9 wt% and 4 wt% P loadings, respectively. This crystalline $AlPO_4$ transforms into amorphous $AlPO_4$ after calcination. Cruz Reyes et al. (53) also observed some hexagonal and orthorhombic crystalline $AlPO_4$ on W-P/Al catalyst by using HREM.

Kraus and Prins (36) also studied the difference between CoMoP/Al and NiMoP/Al catalysts on the formation of $AlPO_4$. They reported that $AlPO_4$ is preferably formed in the presence of Ni while Co-Mo-P compounds are mainly formed on CoMoP/Al catalysts.

1.2.4.2 Adsorption of molybdate and phosphate on alumina

The adsorption behavior of molybdate(s) in the presence of P oxo-species in solution or already deposited on alumina support (or vice-versa) has also been largely studied. For example, Fig. 20 shows the isothermal adsorption of solutions containing different concentrations of ammonium heptamolybdate (AHM).

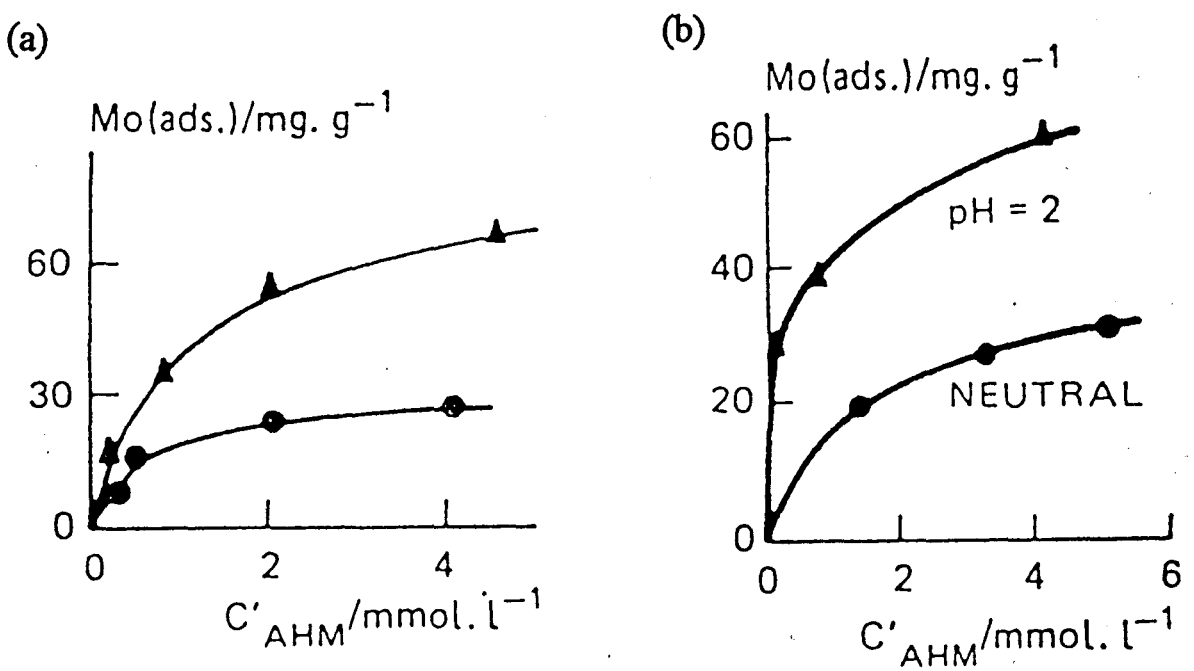

Figure 20. Adsorption isotherms of ammonium heptamolybdate (AHM) ;
(a) ▲ : on alumina and ● : on alumina after adsorption of $H_2PO_4^-$ (1.8 wt% of P)
(b) as a function of pH on alumina after adsorption of H_3PO_4 ; ▲ :pH=2 and ● : neutral condition (adapted from ref. 26).

In Fig. 20a, which corresponds to the sequential impregnation steps where P is adsorbed first before Mo, it is clear that less Mo is adsorbed on the P/Al support compared with impregnation of P-free alumina. However, the amount of Mo adsorption on the P/Al support also depends on the pH of the AHM solution (Fig. 20b). More Mo species tend to adsorb on the P/Al support under acid condition.

From an FTIR study (26), it appears that the heptamolybdate species interact not only with the OH groups of alumina but also with P-OH groups according to the surface reaction :

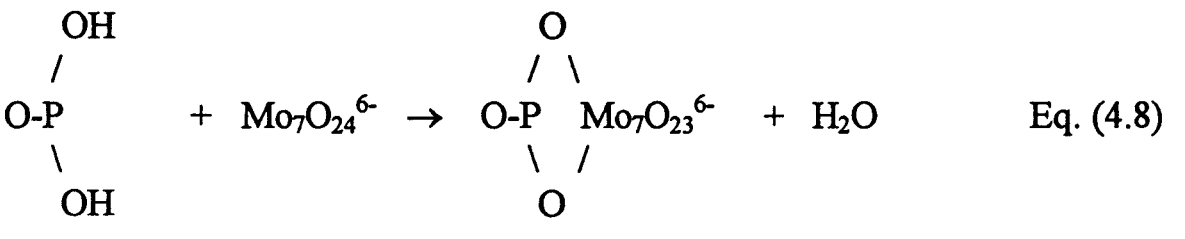

$$\text{O-P(OH)(OH)} + Mo_7O_{24}^{6-} \rightarrow \text{O-P(O)(O)}\,Mo_7O_{23}^{6-} + H_2O \qquad \text{Eq. (4.8)}$$

or

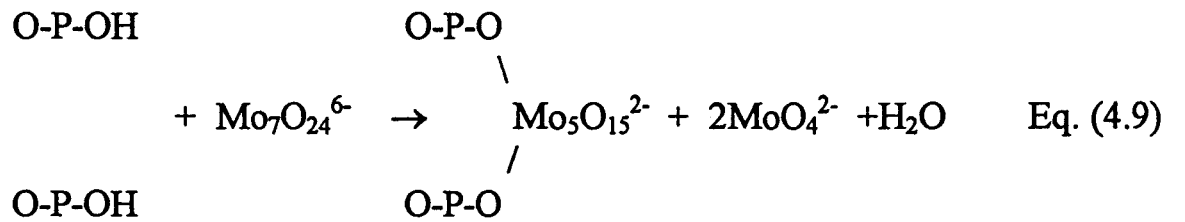

$$\text{O-P-OH} + Mo_7O_{24}^{6-} \rightarrow \text{O-P(O)-O-P(O)-O} + Mo_5O_{15}^{2-} + 2MoO_4^{2-} + H_2O \qquad \text{Eq. (4.9)}$$

The relative amount of Mo and P adsorbed onto γ-alumina from molybdate and/or phosphate solutions by sequences of pulses are shown in Fig. 21 (52). For the first pulses, the amounts of Mo and P retained are very high (~80 % and ~100 %, respectively) if the solutions contain only Mo and P. The amounts smoothly decrease by further pulses. On the other hand, the evolution during pulses with Mo + P solution which is equivalent to a co-impregnation is quite different. The Mo adsorption decreases significantly with addition of P due to the strong competition between P and Mo. In addition, the Mo adsorption decrease in the presence of P can be also explained by the formation of a phosphomolybdate (Equations 4.10 and 4.11) which has less affinity with alumina.

$$8H^+ + 5MoO_4^{2-} + 2HPO_4^{2-} \rightarrow P_2Mo_5O_{23}^{6-} + 5H_2O \qquad \text{Eq. (4.10)}$$

and

$$16H^+ + 5Mo_7O_{24}^{6-} + 14H_2PO_4^- \rightarrow 7H_2P_2Mo_5O_{23}^{2-} + 15H_2O \qquad \text{Eq. (4.11)}$$

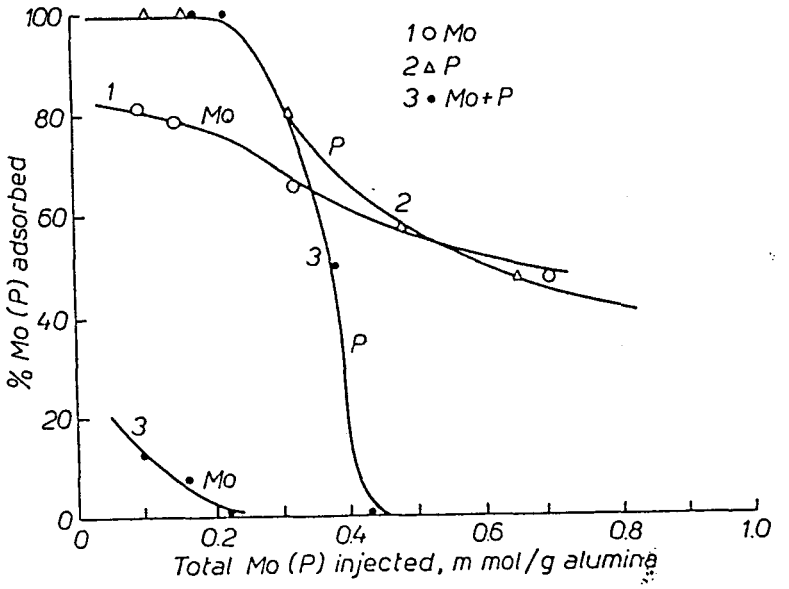

Fig. 21. Amount of Mo and P adsorption onto γ-alumina from the addition of each pulse of molybdate and phosphate solutions. (1) pulses of Mo solution, (2) pulses of P solution, (3) pulses of Mo+P solution (from ref. 52).

The addition of moderate amounts of P onto a Mo/Al catalyst increases the formation of octahedral molybdate (polymeric oxo-molybdate) rather than of tetrahedral MoO_4^{2-} while higher P loading leads to the formation of bulk MoO_3 and $Al_2(MoO_4)_3$ (33,122). $Al_2(MoO_4)_3$ might be formed by the following equation :

$$3\ MoO_3\ (bulk) + Al_2O_3\ (surface) \rightarrow Al_2(MoO_4)_3\ (surface) \quad \text{Eqs. (4.12)}$$

Han et al. (55) reported that the $Al_2(MoO_4)_3$ phase on alumina is easily hydrated with moisture in air and transforms to amorphous MoO_3 while $AlPO_4$ hardly reacts with water. Further addition of P in turn decreases the formation of $Al_2(MoO_4)_3$ since competitive adsorption between P and Mo oxo-species occurs on the alumina surface. Especially, P inhibits the formation of $Al_2(MoO_4)_3$ in the presence of nickel (56). The amount of deposited polymeric P-oxo compounds decreases in the presence of Mo probably through the formation of dispersed "Mo-P" heteropoly compounds (57).

1.2.4.3 Adsorption of "Mo-P" heteropoly compounds on alumina

As already mentioned in the chapter 1.2.3, phosphomolybdate heteropoly compounds have recently been used as new precursors for preparing hydrotreating catalysts. Indeed, the formation of some heteropoly compounds are effectively detected in the impregnation solution containing P and Mo oxo-species (46,58). Thus, the adsorption properties of "Mo-P" heteropoly compounds on alumina should be also very important. The chemistry of "Mo-P" heteropoly compounds in impregnation solution has been well investigated (21,59) and characteristic phase diagrams are reported in Fig. 22.

$P_2Mo_5O_{23}^{6-}$ reacts with basic OH groups on the alumina but it decomposes gradually into heptamolybdate ($Mo_7O_{24}^{6-}$) and/or poly oxo-molybdate (26,46,58). The increase of pH of the adsorption solution also helps the decomposition of heteropoly compounds since it pushes the equilibrium equations to the right side.

$$14PMo_{12}O_{40}^{3-} + 114OH^- \leftrightarrow 7P_2Mo_5O_{23}^{6-} + 19Mo_7O_{24}^{6-} + 57H_2O \quad \text{Eq. (4.13)}$$

$$7P_2Mo_5O_{23}^{6-} + 16OH^- \leftrightarrow 14HPO_4^{2-} + 5Mo_7O_{24}^{6-} + H_2O \quad \text{Eq. (4.14)}$$

More precisely, the degradation of "Mo-P" heteropoly compounds is reported to proceed successively as follows (26,129):

$$\text{"}Mo_{12}P\text{"} \rightarrow \text{"}Mo_{11}P\text{"} \rightarrow \text{"}Mo_5P_2\text{"} \rightarrow \text{"}Mo_7\text{"} \quad \text{Eq. (4.15)}$$

The stability of "Mo-P" heteropoly compounds also depends on the P/Mo ratio in the impregnation solution. At P/Mo ratio lower than 0.4, "Mo_5P_2" decomposes into "Mo_9P" and "$Mo_{11}P$" as follows (60) :

$$8H^+ + 15H_2O + 9H_2P_2Mo_5O_{23}^{4-} \rightarrow 5PMo_9O_{31}(H_2O)_3^{3-} + 13H_2PO_4^- \quad \text{Eq. (4.16)}$$

$$10H_2O + 11H_2P_2Mo_5O_{23}^{4-} \rightarrow 8H^+ + 5PMo_{11}O_{39}^{7-} + 17H_2PO_4^- \quad \text{Eq. (4.17)}$$

At the P/Mo ratio higher than 0.4, the phosphorus amount is high enough to push the equilibrium Eq. (4.16) or (4.17) to the left side and equilibrium Eq. (4.10) or (4.11) to the right hand. As a final result, all the Mo species in solution exist as stable "Mo_5P_2".

Furthermore, the stability of Mo-P compounds is attributed to their structural character. For example, $PMo_{12}O_{40}^{2-}$ and $P_2Mo_{18}O_{62}^{6-}$ are more stable than $P_2Mo_5O_{23}^{5-}$ on alumina (58).

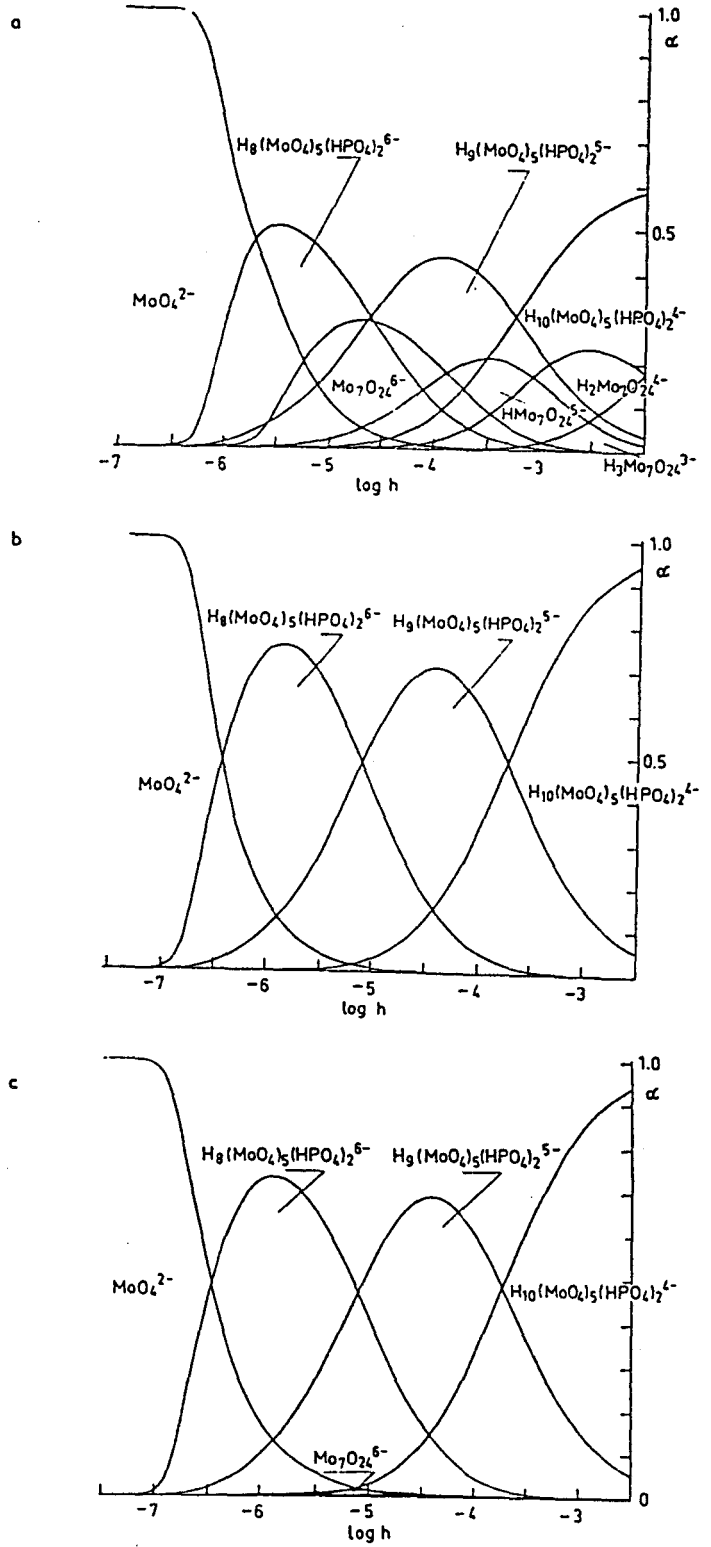

Fig. 22. Distribution diagrams $\alpha=f((\log h), B, C)$ of Mo-P oxo-species present in solution of impregnation. α is defined as the proportion of each Mo species in the total Mo. Log h, B and C represent - pH, initial concentration of Mo and P, respectively. Precipitates and species with $\alpha < 0.008$ have been omitted. (a) B=40 mM, C=10 mM, (b) B=50 mM, C=20 mM, (c) B=40 mM, C=20 mM (from ref. 59).

In the "Mo_5P_2", the two P atoms are localized at the exterior of ion where they are free to be in contact with the alumina surface while in "$Mo_{12}P$" and "$Mo_{18}P_2$", P is surrounded by MoO_6 octahedral shells and cannot interact easily with the alumina surface. Indeed, stability of "Mo-P" heteropoly compounds must strongly depend on both their nature and on impregnation conditions.

1.2.4.4 Adsorption of phosphate and promotor on alumina

On Ni-P/Al catalysts, presence of P prevents penetration of Ni into alumina and impedes the formation of $NiAl_2O_4$ after calcination (33,57,61). The released Ni species may form nickel phosphate or isolated Ni species. López Agudo et al. (62) reported that Ni and P species exist separately on NiP/Al catalysts considering XPS and EDX results. However, De Canio et al. (33) suggested that P oxo-species preferably forms nickel phosphate since the presence of P decreases drastically the amount of surface Ni^0 after reduction which might be derived from isolated Ni species. At this moment, it is difficult to conclude whether "Ni-P" or "Co-P" compounds are formed on alumina based catalysts or not. However, P may favor the formation of the $AlPO_4$ phase at 500 °C due to thermodynamic limitations (63) and also because of the strong interaction between P oxo-species and the alumina. On the contrary, the formation of Ni_2P is detected on carbon or on silica based catalysts at 370 °C as the Ni species and the support have weak interaction (64).

1.2.5. Characterization of P-containing hydrotreating catalysts

The presence of P in catalysts formulation significantly affects on some of their physicochemical properties such as pore structure, dispersion of active phases, acidity, thermal stability, reducibility, sulphidability and so on. In this part, the relation between P addition and physicochemical properties of hydrotreating catalysts are mainly presented and discussed for a better understanding on the P role.

1.2.5.1 Pore structure

The effect of phosphorus on the catalysts texture such as specific surface area (SSA), pore diameter (PD) and pore volume (PV) has been quite largely investigated (26,31,33,56,61,62,65,66,122). The SSA decreases with the P loading, irrespective of the preparation procedures. Especially, it is reported that the co-impregnation of "NiMoP" decreases the SSA more importantly than the sequential impregnation does (67).

The effect of P on PD depends on the catalysts preparation methods. The PD of catalysts prepared from impregnation method decreases with P loading while that from the hydrogel or sol-gel methods tends to increase in some cases. P compounds affect the hydrolysis and condensation step of alumina particles. Some patents also describe that P increases the PD of catalysts (68,69).

1.2.5.2 Thermal stability

Abbattista et al. (27) found that addition of P prevents crystallization of the γ-alumina phase and the transformation from γ to α-alumina in the system of Al_2O_3-$AlPO_4$. Stanislaus et al. (42) also reported that P improves significantly the thermal stability of the γ-alumina phase in P/Al catalysts. However, the same authors found that the positive effect of P is supposed to be cancelled in the presence of Mo due to the formation of aluminium molybdate. The thermal treatment of MoP/Al catalyst above 700 °C results in a considerable reduction of SSA and mechanical strength. P could not suppress the reaction between Mo and the alumina since the interaction between Mo and P might be rather minimal. The presence of Ni does not affect obviously the positive effect of P (42). On the other hand, Hopkins and Meyers (70) reported that the thermal stability of commercial CoMo/Al and NiMo/Al catalysts is improved by the addition of P.

It is therefore difficult to conclude at the moment whether the thermal stability of alumina is really improved by the addition of P in the presence of Ni, Co and Mo. However, its presence may not affect it significantly during the conventional hydrotreating conditions below 450 °C.

1.2.5.3 Acidity

1.2.5.3.1 P/Alumina catalyst and aluminophosphate

Petrakis et al. (43) reported from NH_3-TPD that strong acid sites are created in aluminophosphates. Abbattista et al. (27) also observed from IR measurements that Brönsted acid and strong Lewis acid sites are generated by P addition on the surface of Al_2O_3-$AlPO_4$. On the other hand, Morterra et al. (71) reported from an IR study that P decreases the amount of Lewis acid sites on P/Al_2O_3 but their strength increases. Poulet et al. (72) also supposed that the amount of Lewis acid sites decreases with P addition. Morales et al. (71,73) suggested that P increases only the number of weak acid sites on P/Al_2O_3 considering NH_3 and NaF adsorption. Stanislaus et al. (42,74) concluded that P eliminates strong acid sites and increases medium acid sites since activity of skeletal isomerization which needs strong acid sites decreases by P addition. Lewis and Kydd (40) also reported that the effect of P on surface acidity is minimal since cracking of cumene and of 1,3-diisopropylbenzene is very small. Jian et al. (75,76) also suggested that the addition of P does not induce enough acidity for C-N bond breaking of alkylamine.

1.2.5.3.2 Mo+P/Alumina catalysts

Sajkowski et al. (77) suggested from NH_3-TPD that P does not improve enough the acid strength of the Mo/Al system to affect its HDS or HDN activity. Iwamoto and Grimblot (57) found that a amount of interaction between P and the alumina affects significantly on the acidity of Mo/Al catalysts. For example, the catalysts prepared from P_2O_5 as a P precursor show lower acidity than those prepared from H_3PO_4 due to less interaction between P and alumina.

1.2.5.3.3 Mo +Promotor +P/Alumina catalysts

Walendziewski (66) observed that the acidity of CoMoP/Al measured by NH_3-TPD increases with P loading. Chadwick et al. (122) also reported that the surface acidity of NiMoP/Al measured by pyridine adsorption is slightly increased by P addition. Callant et al. (78) proposed that two acid sites associated respectively with the alumina support and the MoS_2 active phase exist on Ni-Mo-P/Al catalysts. Iwamoto and Grimblot (57) also concluded that P creates at least two acid sites both on alumina and on the Mo species. The later acid sites due to the OH groups associated with MoS_x are considered to be more stronger than those attributed to $AlPO_4$. The same authors revealed that the acidity measured by cyclopropane cracking increases in the order of NiP/Al < MoP/Al < NiMoP/Al (Fig. 23). The promotor Ni may enhance the acidity of Mo sites by modifying the electronic charge density of the MoS_2 active phase or by inducing more OH

groups into the MoS_2 slab.

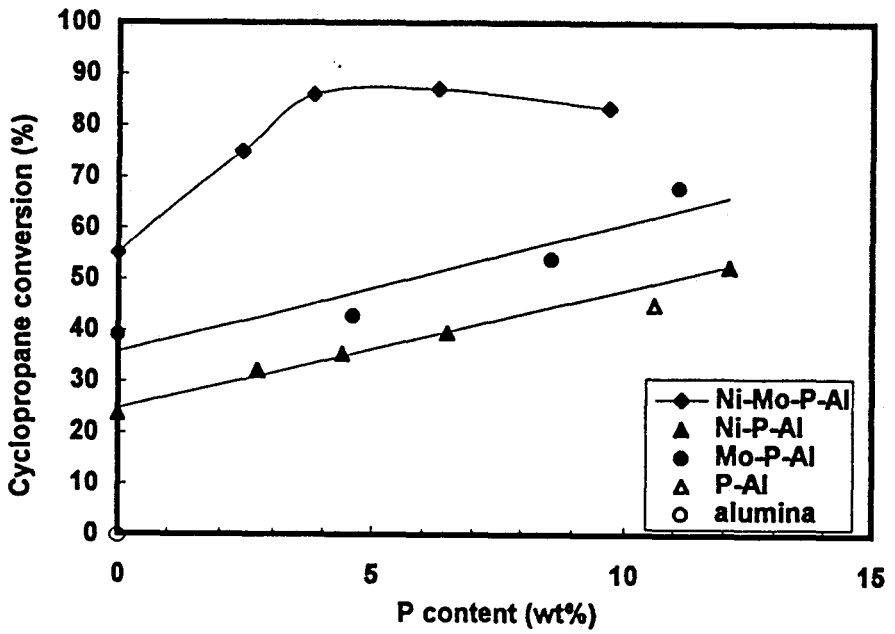

Fig. 23. Comparison of acidity of NiP/Al, MoP/Al and NiMoP/Al catalysts as measured by cyclopropane (CP) cracking as a function of P content (from ref. 57).

On the contrary, Chen et al. (81) found that the amount of acid sites in CoMoP/Al catalysts measured by NH_3-TPD decreases with the increasing amount of P. Stanislaus et al. (42,74) concluded from NH_3-TPD that P reduces the number of strong acid sites but increases considerably the number of acid sites with medium strength in NiMoP/Al.

The great differences as reported above might be attributed to both the nature of catalysts tested and to the method of acidity measurement (total acidity determination or selective titration of acid sites of a specific strength). In addition, the protocoles for measurements (temperature and duration of outgassing before acidity determination etc.) may also affect significantly the results.

1.2.5.4. Dispersion and distribution of catalyst components

1.2.5.4.1 Influence of pH

The pH of impregnation solutions for depositing the active elements on the alumina is one important factor for preparing catalysts. For example, Jian and Prins (60) reported that more bulk molybdenum oxide, as detected by XRD, is present in MoP/Al catalyst when the pH of impregnation solution decreased from 9 to 1 by the addition of P (Fig. 24).

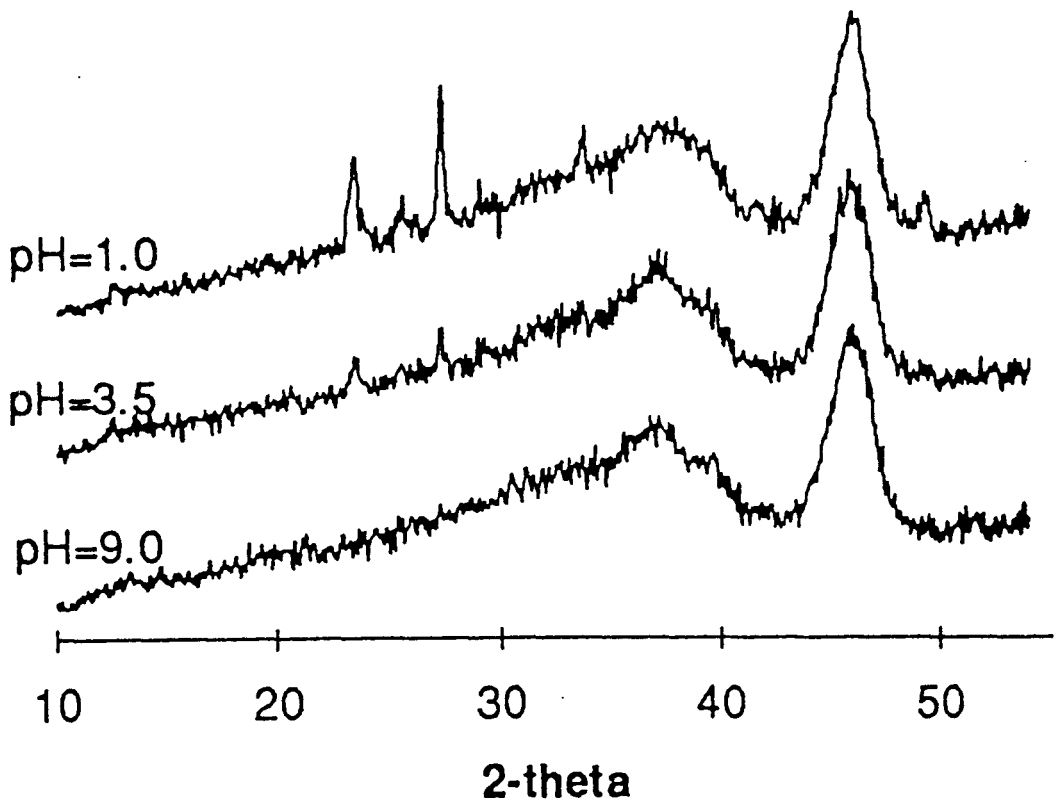

Fig. 24 Effect of the pH of co-impregnation solution on the dispersion of Mo species in MoP/Al catalysts (from ref. 60).

When pH of the impregnating solution is higher than the IEP of the support, the adsorption extent of PO_4^{3-} and MoO_4^{2-} anions decreases because the support surface is negatively charged in such conditions. If we consider that the driving force for adsorption is mainly imposed by electrostatic interaction, the anions can spread over the entire catalyst particle without formation of MoO_3 aggregates as the interaction of MoO_4^{2-} and the alumina surface is weak. On the

other hand, when pH of solution is lower than IEP where the support is positively charged, the molybdates present mainly as $Mo_7O_{24}^{6-}$ (according to $7MoO_4^{2-} + 8H^+ \leftrightarrow Mo_7O_{24}^{6-} + 4H_2O$) and phosphates strongly interact with support (see also paragraph 1.2.4.1). A good Mo dispersion can also been obtained in that case unless formation of bulky poly oxo-molybdate occurs. Indeed, in low pH condition, undesirable too much stronger adsorption of anions and precipitation of hydrated form of MoO_3 (molybdic acid) is often observed which consequently leads to give the characteristic lines of MoO_3 in XRD patterns after calcination of catalysts. Clearly, pH of impregnating solution has to be seriously controlled to optimize Mo dispersion.

1.2.5.4.2 Influence of the impregnation method

The impregnation method also affects the metal dispersion considerably. In sequential impregnation of P first followed by Mo on alumina, the SSA of support decreases and Al-OH groups are already occupied by phosphate. Therefore molybdate can not be stabilized on the support (see paragraph 1.2.4.2) and consequently, dispersion of MoO_3 tends to decrease. During this sequential impregnation, acid P-OH groups are also formed on the alumina which themselves can also enhance the adsorption of Mo species. In such case, the deposition of Mo species on the outer surface of catalysts particle is often observed (61). Stronger adsorption of PO_4^{3-} on alumina may also enforce the pore mouth plugging and prevents Mo penetration. Therefore, it is very difficult to achieve homogenous distribution by the sequential impregnation.

During co-impregnation of P and Mo, the formation of Mo-P heteropoly compounds has to be considered. It has been shown (45,58) that P and Mo forms "Mo_5P_2" heteropoly compound in stoichiometric proportion in the impregnating solution. Since the "Mo_5P_2" heteropoly compound has a relatively low affinity with alumina, Mo and P can spread over the entire support surface if the "Mo_5P_2" structure is unchanged until the impregnation completion. However, Cheng and Luthra (58) revealed by using ^{95}Mo-NMR that "Mo_5P_2" easily decomposes by contact with alumina after the impregnation. If the "Mo_5P_2" decomposes before reaching steady state, Mo and P adsorb on alumina so rapidly that the uniform profiles of Mo and P can not be achieved even in the co-impregnation conditions (61). Therefore, adjusting the proper pH and/or the atomic P/Mo ratio of the impregnating solution is needed to prevent the decomposition of "Mo_5P_2" and obtain well dispersed Mo species.

1.2.5.4.3 Influence of P content

The Mo dispersion also depends on the P content. Atanasova and co-

workers (61,79) reported that dispersion of Mo and Ni measured by XPS shows a steep increase at low P loading. The dispersion of molybdenum further increases with calcination while that of nickel decreases in NiMoP/Al catalysts. On the contrary, Sajkowski et al. (77) reported from an EXAFS investigation that P does not affect the size of polymolybdate species. Mangnus et al. (38) also presumed that the stacking of molybdates does not increase by the addition of P since the height of TPR peak at ~400 °C due to reduction of multi-layered Mo oxo-species is independent on the P content. Chadwick et al. (122) concluded that the dispersion of molybdenum decreases with P addition. Consequently, the MoS_2 slabs tend to grow by stacking of the MoS_2 layers.

Morales et al. (73) reported that the dispersion of Ni increases up to a loading of 6 wt% P_2O_5. Mangus et al. (38) also found that in CoP/Al catalysts, the dispersion of cobalt increases with P loading due to the formation of mixed Co-P species. However, López-Agudo et al. (62) reported that P prevents the homogeneous distribution of Ni and P over NiP/Al catalyst. With no doubt, a large amount of P in the catalyst formulation decreases the Mo dispersion and favors the formation of bulk MoO_3 and $Al_2(MoO_4)_3$ (80-83,122). McMillan et al. (120) reported however that the formation of $Al_2(MoO_4)_3$ is suppressed in the presence of Ni.

1.2.5.4.5 Effect of P on the MoS_2 and Ni sulphide dispersion

Eijsbouts et al. (84) reported that dispersion of Mo tends to increase by sulphidation but that of Ni decreases. Ramírez et al. (82) and Hubaut et al. (85) reported from HREM observations that P increases the stacking of the layered MoS_2 phase. These results were confirmed by Kemp et al. (86) who reported that P increases the stacking of MoS_2 for both CoMoP/Al and NiMoP/Al but decreases the length of the MoS_2 patches. It is considered that P prevents the growth of MoS_2 crystallites with an orientation parallel to the alumina surface by suppressing interactive Al-OH groups due to the $AlPO_4$ formation. However, Sajkowski et al. (77) reported conflicting data from EXAFS ; P does not affect the MoS_2 crystalline size. López-Agudo et al. (62) observed that the dispersion of Ni in NiP/Al decreases by sulphidation while it is not affected by P addition in oxide forms.

As a conclusion, the dispersion of metal components in oxide forms depends not only on the P content but also on the preparation procedures. Large amount of P favors the agglomeration of metal oxides. It should be considered that the non-uniform distribution of Mo over a catalyst particle at low P loading may considerably affect the XPS results. In activated form, as some discrepancies

exist, not only the preparation conditions but also activation conditions such as the nature of the presulphiding mixture and the sulphidation temperature may also affect the textural properties of the catalysts.

1.2.5.5 Effect of P on the activation of catalysts (reduction-sulphidation)

Since the hydrotreating catalysts are usually used under H_2 and H_2S, it is very interesting to understand the effect of P on reducibility and sulphidability of supported metals. It is also important to know if the phosphates by themselves are sensitive to such conditions. In this part, these properties will be discussed from XPS, TPR and TPS results. Note that the alumina support by itself is not chemically modified by the reduction - sulphidation treatments even if some hydrogen species and surface SH groups have already been identified (38,63).

1.2.5.5.1. Reduction

Bulk $AlPO_4$ or P/Al catalysts start to reduce above 730 °C. However, reduction is not completely finished even at 1000 °C (38). The quantitative data indicates that the phosphate mainly reduces into elemental phosphorus as the P_4 compound but the formation of phosphanes like PH_3 or P_2O_5 has been also detected as minor products. The reduced form P_4 goes out from the catalysts due to its extremely high vapour pressures. Therefore, it appears necessary to check the P loading of the catalysts after severe treatment conditions if some P has been removed as volatile compounds. Reduction of $AlPO_4$ is accelerated in the presence of reduced cobalt or molybdenum. At P / metal ratio ≤ 1, the $AlPO_4$ phase is completely reduced to metalphosphides such as CoP, Co_2P and MoPx ($x \leq 1$) and Al_2O_3 above 723 °C under H_2. Arunarkavalli (87) showed that the presence of P increases Ni reducibility, especially at low P content, by preventing the formation of nickel aluminate.

Sajkowski et al. (77) revealed, from XPS measurements, that the addition of P increases the amount of more easily reducible Mo species in Mo/Al catalyst. They presumed that P weakens the interaction between molybdates and the alumina surface due to the strong interaction between P and the alumina. Kinetic initial reduction rates (r_o) for several MoP/Al catalysts prepared by different preparation procedures were obtained by López-Cordero et al. (65). r_o of Mo-P/Al catalyst prepared from a sequential impregnation increases rapidly with increasing the P content up to 2.5 wt% P and then decreases slightly. On the other hand, r_o of co-impregnated MoP/Al catalysts varies only moderately. They interpreted their data by considering that P increases the amount of easily reducible octahedral molybdates such as poly oxo-molybdate multilayer and bulk

MoO_3 cluster and that this trend is more favored for the sequential impregnated Mo-P/Al catalysts.

On the other hand, Van Veen et al. (26) reported from TPR that Mo-P/Al catalyst is rarely reduced up to 700 °C due to formation of irreducible heteropoly species such as "Mo_5P_2", "Mo_6P" or "Mo_7P". Mangnus et al. (38) also reported TPR results indicating that the reducibility of a part of Mo species decreases with P loading due to the formation of mixed Mo-O-P species on MoP/Al catalysts. On CoMoP/Al catalysts, a new reduction peak appeared at 827 °C by the addition of P. This indicates that the strong polarization of the Co-O bond in a Co-Mo-O-P phase suppresses the complete reduction of the Co^{2+} ion at low temperature by comparison with the Co-Mo-O supported structure.

1.2.5.5.2 Sulphidation

It is interesting to know whether P is sulphided under conventional hydrotreating conditions or not. Mangnus et al. (63) investigated by TPS that P/Al and $AlPO_4$ are chemical unreactive with H_2S up to 723 °C. Chadwick et al. (122) also found no evidence of sulphided P formation from XPS measurements. These results indicate that P oxo-species do not transform to P sulphides or P oxy-sulphides during the classical conditions of the hydrotreating reactions.

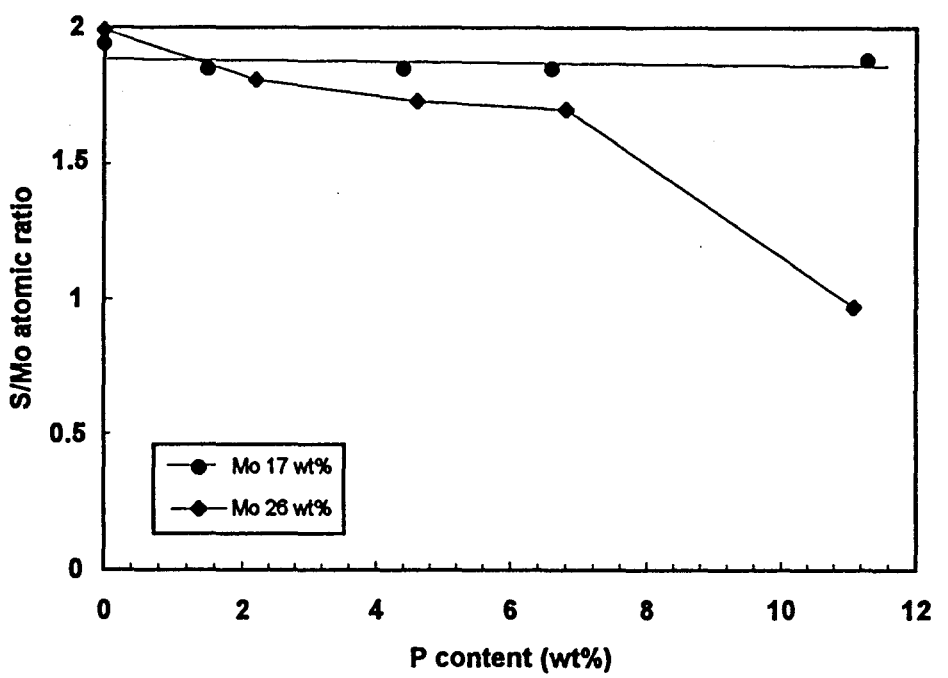

Fig. 25. Variation of the atomic S/Mo ratio measured after thiophene HDS as a function of P loading for MoP/Al catalysts. (from ref. 57).

Sajkowski et al. (77) reported that P does not affect the sulphiding behavior of Mo/Al catalysts. Mangnus et al. (63) also found that the S/Mo ratio in the MoP/Al catalysts after TPS measurements is independent of its P content and always shows a steady value of 2. Concerning solid state reactions, MoS_2 does not react with $AlPO_4$ to form MoP_x species (where x=1,2) below 1000 °C due to thermodynamic limitations (63). However, Poulet et al. (72) reported that P decreases the S/Mo ratio of a MoP/Al catalyst after sulphidation or after a subsequent hydrogen treatment. Jian and Prins (60) interpreted that the shift of NO adsorption bands toward higher frequency in the presence of P also indicates less sulphidation of Mo and Ni species in MoP/Al catalysts (60). Iwamoto and Grimblot (52) found that the sulphidability of molybdenum strongly depends on P and Mo content. P does not affect the sulphidability of Mo in the region of low P and Mo loading where they are present as individual species on the alumina. On the other hand, P decreases significantly the sulphidability of Mo at higher P and Mo content where they have some interactions (Fig. 25). This result may explain in part the above discrepancies of the different P effect on sulphidability.

In NiP/Al catalysts, López-Agudo et al. (62) reported that the sulphidability of Ni measured by XPS is not influenced by the P addition. On the other hand, Iwamoto and Grimblot (57) reported that P increases sulphidability of Ni in NiP/Al at 400 °C because P prevents the formation of stable nickel aluminate species. A similar explanation was also proposed for Ni reducibility (87).

At further higher sulphidation temperature, the effect of P on the sulphidability of Ni is completely different. Mangnus et al. (63) reported that the temperature of complete sulphidation of Co-P/Al increases with increasing the P content. The S/Co atomic ratio after sulphidation at 1000 °C decreases from 1.3 to 0.39 with P addition due to the formation of not sulphided compounds like cobalt phosphides, according to the following reactions :

$$CoS_{0.89} + AlPO_4 + 3.39\ H_2 \leftrightarrow 0.5\ Al_2O_3 + CoP + 2.5\ H_2O + 0.89\ H_2S \qquad \text{Eq. (5.1)}$$

and/or

$$2\ CoS_{0.89} + AlPO_4 + 4.28\ H_2 \leftrightarrow 0.5\ Al_2O_3 + Co_2P + 2.5\ H_2O + 1.78\ H_2S \qquad \text{Eq. (5.3)}$$

Fig. 26 represent the relative amount of Co in Co phosphides as a function of P content.

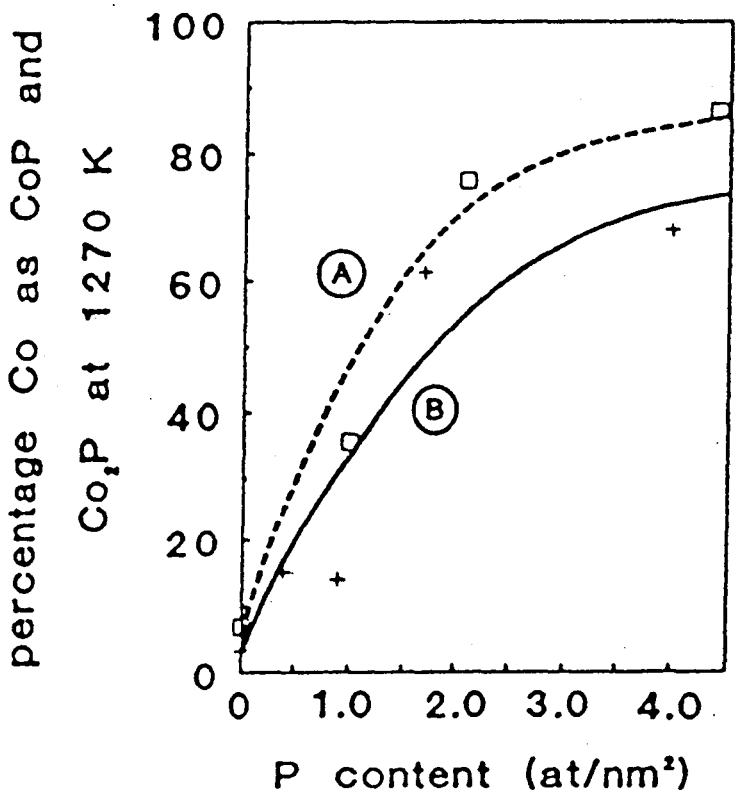

Fig. 26. The percentage of Co, which reacted with $AlPO_4$ and H_2 to CoP and Co_2P in the high temperature region (1000 °C) as a function of P content: (a) CoMoP/Al, (b) CoP/Al (from ref. 63).

The formation of Co_2P and Ni_2P needs severe condition as shown above (temperature between 723 and 1000 °C and high pressure). In the case of NiP/Al or NiMoP/Al catalysts, only $PH_3/H_2/H_2S$ treatment is effective to obtain the Ni_2P phase in conventional sulphidation conditions because P preferably interacts with the alumina support. However, carbon and silica supports which have less interaction with P can give the Ni_2P phase even in such conventional conditions (64). Andreev et al. (88) suggested the formation of the $NiPS_3$ compound after the sulphidation of NiMoP/Al. However, Robinson et al. (64) revealed that $NiPS_3$ decomposed to Ni_2P under the hydrotreating conditions, even in the presence of H_2S. Note however that $NiPS_3$ is an interesting phase to catalyze the oxidation of sulphide S^{2-} species (89). As a conclusion, the addition of P may increase the sulphidability of Ni or Co in Ni/Al or Co/Al up to about 700 °C due to the decreasing the amount of stable nickel aluminates but decreases it at higher temperature due to the formation of phosphides. However, the Ni_2P and Co_2P phases might be in a minor proportion on the alumina based catalysts at

conventional hydrotreating temperatures.

In CoMoS/Al or NiMoS/Al catalysts, Topsøe and co-workers (90) found from the IR spectra of NO adsorption that the P addition favors the less sulphided environment of the CoMoS or NiMoS phases. The present authors (57) also revealed that P decreases the sulphidability of Mo as in the case of Mo/Al. However, the addition of P has less positive effect on Ni sulphidability as the Ni species in NiMo/Al are predominantly associated with Mo species.

1.2.5.6 Vibrational and NMR data of P-based alumina catalysts

Following paragraph 1.2.2.11 of this review which reported some characteristic vibrational and NMR data of P-based reference compounds (Tables 6 and 7), it appears interesting to propose similar compilations concerning P-containing alumina catalysts in the dried and calcined forms. These vibrational and NMR data (Tables 8 - 10) are quite informative to characterize hydrotreating catalysts as their rather amorphous character make XRD analysis not informative enough.

Table 8. List of IR vibration data of selected P to based reference catalysts after drying and calcination.

Wave number	assignment	reference catalysts	ref.
3785 to 3800	Al(octa)-OH terminal Type Ib	Alumina	91
3760 to 3780	Al(tetra)-OH Type Ia	Alumina	91
3730 to 3745	Al-OH-Al double bridge Type IIa,b	Alumina	91
3697 to 3710	Al-OH-Al triple bridge Type III	Alumina	91
3677	P-OH	P/Alumina	71
3558	strongly hold water	P/Alumina	33
3250	interaction between neighboring P-OH or between P-OH and Al-OH	P/Alumina	40
1700 to 1300	physically adsorbed water	Alumina	92
1620	physically adsorbed water	Alumina	93
1220	phosphoryl group	P/Alumina	71
1180 to 1130	P-O (wavenumber decreases with decreasing bond order)	P/Alumina	71
1127 to 1152	formation of polyphosphate	NiMoP/Alumina	31
1120	P=O(t)	NiMoP/Alumina	30
1119	monolayer of phosphorus oxo-species	P/Alumina	30
1050	bridge band P-Ob-Mo	NiMoP/Alumina	30
1000 to 1100	P-O-Mo		31
945,920,730,815	P-Ni-Mo heteropoly compounds	NiMoP/Alumina	30
943,912,893 to 897	polymolybdate	dried NiMoP/Alumina	31
936	asymmetric ($PO_2(H_3)$)	dried NiMoP/Alumina	31
912 to 918	weakly bound bridge bands in MoO_4 tetrahedra	dried NiMoP/Alumina	30
900	asymmetric P-O-P stretching	P/Alumina	27
840	symmetric ($PO_2(H_2)$)	dried NiMoP/Alumina	31
815	asymmetric P-O-P stretching	P/Alumina	27
730 to 750	P-O-P in polyphosphate	NiMoP/Alumina	31
700 to 550	Al-O stretching	P/Alumina	27

Table 9. List of 27Al-NMR chemical shift data of selected P-based reference catalysts after drying and calcination.

Chemical shift (ppm)	Assignment	reference catalyst	measurement conditions					ref.
			Resonance frequency (MHz)	pulse length (micro s)	recycling time (s)	spinning frequency (kHz)	reference sample	
71	tetrahedral Al	NiMoP/Alumina	130.32	5	10	2.5 to 4	$AlCl_3$	55
75 to 73	tetrahedral Al	gamma-Alumina						94
72	tetrahedral Al	P/Alumina	78.3	0.2-0.5		2	$KAl(SO_4)_2$	33
67	tetrahedral Al	calcined sol-gel Alumina	104.26				$Al(H_2O)_6$	93
53	tetrahedral Al	calcined sol-gel Alumina	78.2	3	2	3.5	$Al(H_2O)_6$	95
41.5	$AlPO_4$	bulk $AlPO_4$	130.32	5	10	2.5 to 4	$AlCl_3$	55
40	crystalline $AlPO_4$	P/Alumina	78.3	0.2-0.5		2	$KAl(SO_4)_2$	33
38	amorphous $AlPO_4$	P/Alumina	78.3	0.2-0.5		2	$KAl(SO_4)_2$	33
30	Al(5) or Al(4) tricluster	Al-Si glass						96
29 to 27	$Al(OAl)_5$							97
22	octahedral Al	NiMoP/Alumina	130.32	5	10	2.5 to 4	$AlCl_3$	55
20 to 0	octahedral Al	sol-gel Alumina						95
13	$[Al(OH)_n(H_2O)_{6-n}]_n(MoO_4)(n=1,2)$	MoP/Alumina	78.42		1	6 to 7	$KAl(SO_4)_2$	98
10	unreacted Al alkoxide	sol-gel Alumina	78.21	4		3		99
10 to 8	octahedral Al	gamma-Alumina						94
8	octahedral Al	NiMoP/Alumina	130.32	5	10	2.5 to 4	$AlCl_3$	55
7	octahedral Al	calcined sol-gel Alumina	104.26				$Al(H_2O)_6$	93
5	octahedral Al	alpha-Alumina	70.4	1.6		2.6	$Al(H_2O)_6$	100
4	octahedral Al	sol-gel Alumina	78.2	3	2	3.5	$Al(H_2O)_6$	95
4	$(Al_2(OH)_5)$,$(Al_3(OH)_8)$ etc.	dried Alumina	104.26			3.2	$Al(H_2O)_6$	93
0	octahedral Al	P/Alumina	78.3	0.2 to 0.5		2	$KAl(SO_4)_2$	33
0	$(Al(H_2O)_6)$ monomer	dried Alumina	104.26			3.2	$Al(H_2O)_6$	93
0	$(Al(OH_2)_m(OHC_3H_8)_{6-m})$	sol-gel dried Alumina	104,26			3.2	$Al(H_2O)_6$	93
-1	amorphous $Al_2(MoO_4)_3$	NiMoP/Alumina	130.32	5	10	2.5 to 4	$AlCl_3$	55
-8 to -11	octahedral $Al(OP)_n(OAl)_{6-n}$	$AlPO_4$+Al_2O_3	104.26	2	2	5 to 5.5	$Al(H_2O)_6$	101
-8 to -13.7	$Al_2(MoO_4)_3$	MoP/Alumina	78.3	0.2 to 0.5		2	$KAl(SO_4)_2$	33
-12		bulk $Al_2(MoO_4)_3$	130.32	5	10	2.5 to 4	$AlCl_3$	55
-13 to -22	octahedral $Al(OP)_6$							97
-14	$Al_2(MoO_4)_3$	calcined sol-gel Alumina	78.2	3	2	3.5	$Al(H_2O)_6$	95
-17 to -4.6	octahedral $Al(OAl)_6$	sol-gel dried Alumina	78.21	4		3		99

Table 10. List of 31P-NMR chemical shift data of selected P-based reference catalysts after drying and calcination.

chemical shift (ppm)	Assignment	reference compound	measurement conditions					ref.
			Resonance frequency (MHz)	pulse length (micro s)	recycling time (s)	spinning frequency (kHz)	reference sample	
11 to -5	tetrahedral $P(O)_4$							97
2 to -5	tetrahedral $P(OP)(O)_3$							102
-8 to -10	monomeric phosphate or short chain polyphosphate	dried P/Alumina	121.7	2		6-7	H_3PO_4	33
-10	terminal polymeric phosphate							
-10 to -20	polymeric phosphate	dried P/Alumina	121.7	2		6-7	H_3PO_4	33
-15	tetrahedral $P(OAl)_2(OH)_2$							97
-15 to -25	tetrahedral $P(OP)_2(O)_2$							97
-17 to -20	internal polymeric phosphate	MoP/Alumina	121.7	2		6-7	H_3PO_4	33
-20	tetrahedral $P(OAl)_3(OH)$							97
-23 to -34	tetrahedral $P(OAl)_4$							97
-24	tetrahedral P-O-Al, $P(OAl)_4$	$AlPO_4+Al_2O_3$	161.98	3	3.6	5-5.5	Na_2HPO_4	101
-25 to -30	$AlPO_4$		200.47	6	2	2.5-4	H_3PO_4	55
-25 to -26	crystalline $AlPO_4$	MoP/Alumina.P/Alumina	121.7	2		6-7	H_3PO_4	33
-29	$AlPO_4$	P/Alumina						26
-30 to -51	tetrahedral $P(OP)_2(OAl)_2$							97
-32	crystalline $AlPO_4$	dried P/Alumina	121.7	2		6-7	H_3PO_4	33

1.2.6. Catalytic activities in the presence of P-based catalysts

There are many catalytic reactions involved in the hydrotreating processes. Especially, removal of hetero atoms from the oil fractions such as HDS, HDN and HDM are reactions of primary importance in petroleum refining. In addition, side reactions like hydrogenation (HYD) and isomerization (ISOM) may considerably improve the quality of the products obtained. Hydrocracking (HYC) has also a considerable importance for up-grading of heavy fractions. In general, the effect of P in the catalyst formulations strongly depends on its P content. For high P loadings, P usually gives negative effect on the hydrotreating reactions. It is attributed to the decreases of SSA and of active phase dispersion. Modification of pore structure may also be important. For low and medium P content, different results are often found in the literature. This may be attributed to the large variety of physicochemical properties in the presence of P as shown in the previous part. In this part, we will examine both the positive and negative effects of P on the classical hydrotreating catalysts. Table 11 gives the main tendencies of P presence in catalyst formulations for hydrotreating reactions with mainly probe molecules.

1.2.6.1. Effects of P on HDS

It is very interesting to know at first whether a very small few quantity of P leads to noticeably changes in the catalytic performance. Ledoux et al. (103) reported that 120 ppm of P hardly affects the thiophene HDS activity and the physicochemical properties of a CoMo/Al-P catalyst. It is considered, therefore, that P rarely affects the HDS activity in such an impurity level.

Bouwens et al. (104), Eijsbouts et al. (84) and Iwamoto and Grimblot (35) reported that P has no detectable promotion effect on thiophene HDS over Mo-P/Al and MoP/Al catalysts. On the other hand, Fierro et al. (105) indicated that thiophene HDS activity over co-impregnated MoP/Al catalysts gives a maximum at 4 wt% P_2O_5 while that over sequential impregnated Mo-P/Al catalysts is rather independent on the P content. Kim and Woo (80) also reported that thiophene HDS activity over Mo-P/Al catalysts containing less than 5 wt% P is slightly higher than a P-free catalyst. Lewis and Kydd (91) showed that the positive effect of P on thiophene HDS activity is more significant at higher Mo loading.

Recently, "Mo-P" heteropoly compounds have been studied and used new P and Mo precursors. Van Veen et al. (26) revealed that the order of thiophene HDS activity varies with the reducibility of the molybdenum phase according to the following sequence :

monomolybdate < heptamolybdate < octamolybdate < "Mo_9P" < "$Mo_{11}P$".

Table 11 List of hydrotreating tests over P containing hydrotreating catalysts

Reaction	Chemical composition (wt%)				SSA*	Method of preparation		Reaction conditions						memo	ref.
	Co	Ni	Mo	P	(m2/g)			Reactant	T (°C)	P (kg/cm2)	Pretreatment	Additive	Selectivity	P effect	
HDS			7	4,2	280	SI		Thiophene	400	AP	PS			→	6
			7	1,8	270	SI		Thiophene	400	AP	PS 400 °C			→	109
			5,3	0,4 to 2,6	188	SI		Thiophene	350 to 400	AP	PS		butane ↗	→	19
			8	0,75 to 3	270	SI	Fe(2,8 %)-Mo-P	Thiophene	400	AP	PS			→	127
			17	1 to 11	503	SG		Thiophene	300	AP	PS			→	302
			27	1 to 11	503	SG		Thiophene					butane ↘	↗	
			6,3	0,4 to 2,7	189	CO		Thiophene	351 to 400	AP	PS			↗↗	19
			10	0,3 to 3,3	220	SI		Thiophene	300	AP	PS			↗↗	41
			0,8 to 3	1	193	SI		Thiophene	400	AP	PS 500 °C			↗	12
		3,2		4,2	280	SI		Thiophene	400	AP	PS			→	6
		7 to 18		1 to 16	503	SG		Thiophene	400	AP	PS			↗	312
		1	7	0,6 to 4,3	280	SI	Ni-Mo-P/Al	Thiophene	400	AP	PS			↗↗	6
		3,5	7	0,7 to 6,2	280	SI		Thiophene						↗↗	6
		2,3	10	0,6 to 6	266	CO		Thiophene	350	AP	PS			↗↗	10
		3	10	0,25 to 2,5	259	CO		Thiophene	350	AP	PS 300 °C			↗↗	56
		2,3	10	0,3 to 7	198	CO		Thiophene	400	AP	PS 500 °C			↗↗	33,44
		2,3	10	0,3 to 8	198	SI	P-Ni-Mo, Ni-Mo-P							↗↗	P-Ni-Mo < Ni-Mo-P 33,44
	2		8	120 (ppm)	240	HG + CO	CoMo/Al-P	Thiophene	198	AP	PS 400 °C			→	23
	uk		10	0,3 to 4	276	SI	Co-MoP/Al, pH = 3	Thiophene	400	AP	nPS		butane ↘	↗↗	82
		6	20	1 to 11	503	SG		Thiophene	300	AP	PS 400 °C			↗↗	312
	3		8	0,5 to 5	209	SI	P-Co-Mo, Co-Mo-P	Thiophene	400	AP	PS			↗↗	P-Co-Mo < Co-Mo-P 114
	(2)	(2)	9,6	2,1	uk	CO		DBT	350 to 370	35	PS 320 °C			↗↗	150
	3		8	4,5 to 21	uk	HG + SI		Residual oil	390	78	PS 320 °C			↗↗	60
		2,3	10	0,3 to 7	198	SI	Ni-Mo-P	gas oil	410	69	PS 440 °C	quinoline		↗↗	33
		2,3		0,4 to 2,6	188	SI, CO	NiP < Ni-P	gas oil + pyridine	325 to 375	30 bar	PS 350 °C	N 0,08 %		↗	NiP < Ni-P 4
		3,5		0,8 to 3,7	uk	CO	pH=2	(VGO)	360	53	PS350 °C			↗	16
HDN		uk	uk	uk	uk	CO		indole	350	25 to 81	PS			↗	55
		3	8	3 to 4	228	SI	Ni-MoP/Al	OPA	320	30	PS 370 °C	DMDS		↗	2,42
		1 to 3,5	7	0,6 to 6,2	280	SI		quinoline	350 to 390	30	PS	DMDS		↗	6
		2		1,5 to 10	uk	CO		HVGO	360	54	PS 350 °C			↗	11
		2	10	3,7	uk	CO		HVGO	360	54	PS 350 °C			↗	11
			10	3,8	uk	CO		HVGO	360	54	PS 350 °C			↗	11
		2,3		0,4 to 2,6	188	SI		gas oil + pyridine	325 to 345	30 bar	PS 350 °C	gas oil (S 1,28 %)		↗	4
		3,3		0,4 to 2,7	188	CO		gas oil + pyridine	326 to 345	31 bar	PS 350 °C	gas oil (S 1,28 %)		↗↗	4
		2,3	10	0,3 to 7	198	SI	Ni-Mo-P/Al	gas oil	410	69	PS 440 °C			→	33,44
		2,3	10	0,3 to 8	198	SI	Ni-Mo-P/Al	quinoline	410	69	PS 440 °C			↗↗	
		2	9,6	2,1	uk	CO		quinoline	308	60	PS			↗	low quinoline 150
		2	9,6	2,1	uk	CO		quinoline	308	60	PS			↗	high quinoline 150
			9,3	2,8	252	CO		pyridine	350	60	PS350 + PR350			↗↗	37,47
		3	8	1 to 4	228	SI	Ni-MoP/Al	piperidine	320	30	PS 370 °C	DMDS		↗↗	Ni-MoP/Al 42
		3	8	2 to 4	228	SI	Ni-MoP/Al	DHQ	320	30	PS 370 °C	DMDS		↗↗	42

* : specific surface area of support before preparation

( ):estimated value, uk:unknown

CO:co-impregnation,SI:sequential impregnation, EA:equilibrium adsorption, HG: hydrogel method, SG:sol-gel method, NS: not supported

AP: Atmospheric Pressure, PS:Presulphiding, PR:Prereduction

DIPB:diisopropylbenzene, DHQ:decahydroquinoline, OPA:ortho-propylaniline, DMDS:dimethyldisulphide

Table 11 List of hydrotreating tests over P containing hydrotreating catalysts (continued)

Reaction	Chemical composition (wt%)				SSA*	Method of preparation		Reaction conditions							memo	Ref.
	Co	Ni	Mo	P	(m2/g)			Reactant	T (°C)	P (kg/cm2)	Pretreatment	Additive	Selectivity	P effect		
		3	8	3 to 4	228	SI	Ni-MoP/Al	cyclohexene	320	30	PS 370 °C	DMDS		↗		2
			27	1 to 11	503	SG		cyclohexene	350	AP	PS 400 °C			↗		312
HYD	3		8	0,5 to 5	209	SI	P-Co-Mo, Co-Mo-P	1-hexene	400	AP	PS	H2S		↗	P-Co-Mo < Co-Mo-P	114
			9,3	2,8	252	CO		isoprene	50	AP	PS350 + PR547			↗		37 47
	uk		10	0,3 to 4	276	SI	Co-MoP/Al, pH = 3	Benzene	320 to 360	30	PS	thiophene + CS2		↗		82
		2,3	10	0,3 to 7	198	SI	Ni-Mo-P/Al	gas oil	410	69	PS 440 °C	quinoline		↗		33,44
			9,3	2,8	252	CO		toluene	350	60	PS350 + PR350			↗		37 ,47
			5,3	0,4 to 2,6	188	SI		1-hexene	300	AP	PR 500 °C			↗		18
						CO								↗		
	3		8	2	228	SI		cyclohexene	220 to 370	30	PS370	pentylamine,DMDS		↗		181
		6 to 18	20 to 27	1 to 16	503	SG		cyclopropane	280	AP	PS 400 °C		propane ↗	↗		312
HYC		2,3	10	0,3 to 7	198	CO		DIPB	400	AP	PR 500 °C			↗	Ni-Mo-P<P-Ni-Mo<NiMoP	33
						SI	P-Ni-Mo				PR 500 °C			↗		
						SI	Ni-Mo-P				PR 500 °C			↗		
						CO					PS 500 °C			↗	NiMoP<P-Ni-Mo<Ni-Mo-P	
						SI	P-NI-Mo				PS 500 °C			↗		
						SI	Ni-Mo-P				PS 500 °C			↗		
	3		8	0,5 to 5	209	SI	P-Co-Mo, Co-Mo-P	isooctene	400	AP	PS 500 °C			↗	P-Co-Mo < Co-Mo-P	114
		6 to 18	20 to 27	1 to 16	503	SG		cyclopropane	280	AP	PS 400 °C		propane ↗	↗	P<NiP<MoP<NiMoP	312
ISOM		27	1 to 11		503	SG		cyclohexene	350	AP	PS 400 °C			↗		312
			9,3	2,8		CO		pentadiene	50	AP	PS350 + PR547			↗		37
			2 to 4,6	0,4 to 2,5	208	EA		cyclohexene	400	AP	PR 400 °C			↗		49
HDM	12,2		6,5	4 to 2,5	-	NS		Residual oil	470	100	PS			↗		29

* : specific surface area of support before preparation

( ):estimated value, uk:unknown

CO:co-impregnation,SI:sequential impregnation, EA:equilibrium adsorption, HG: hydrogel method, SG:sol-gel method, NS: not supported

AP: Atmospheric Pressure, PS:Presulphiding, PR:Prereduction

DIPB:diisopropylbenzene, DHQ:decahydroquinoline, OPA:ortho-propylaniline, DMDS:dimethyldisulphide

Griboval et al. (23) also reported that partly reduced "$Mo_{12}P$" gives high thiophene HDS activity because it has stability high enough to maintain the Keggin structure even after calcination at 400 °C.

López-Agudo et al. (62) found that gas oil HDS activity over NiP/Al catalysts prepared by both co-impregnation and sequential impregnation increases with increasing the amount of P up to 6 wt% P_2O_5. Morales et al. (16) also reported that HDS activities of thiophene, VGO and deasphalted crude oil over NiP/Al catalysts give a maximum at 7wt% of P_2O_5. The correlation between HDS and the amount of octahedral Ni^{2+} in the oxide form of the catalysts suggests that octahedrally coordinated nickel cations are possible precursor of the active phase. Andreev et al. (88) reported that a catalyst made with $NiPS_3$ mixed with Al_2O_3 shows high activity for thiophene HDS while selectivity for hydrogenated products is lower than that obtained over NiMo/Al and CoMo/Al catalysts. They assumed from this result that the promotion effect of P over NiMoP/Al catalyst is attributed to the formation of the $NiPS_3$ phase during the presulphidation step. However, Robinson et al. (64) reported that $NiPS_3$ decomposes into Ni_2P under the typical hydrotreating conditions even in the presence of H_2S. Therefore, Ni_2P could be the actual active species rather than $NiPS_3$ for HDS if it exists on NiP/Al and NiMoP/Al catalysts. Iwamoto and Grimblot (57) also indicated that P addition increases thiophene HDS activity over NiP/Al sol-gel catalysts due to the increasing sulphidability of Ni.

Muralidhar et al. (106) reported that thiophene HDS activity over both Co-Mo-P/Al and P-Co-Mo/Al catalysts do not change at 0.5 wt% P loading while the activity decreases at 5wt% P loading. Ramselaar et al. (107) also showed that P has no positive effect on thiophene HDS over Fe-Mo-P/Al catalyst. Eijsbouts et al. (32,84) concluded that thiophene HDS over Ni-Mo/Al catalysts is not promoted considerably by P addition while the selectivity for unsaturated hydrocarbons increases slightly. On the other hand, Atanasova et al. (79) found that P gives a maximum activity for thiophene HDS at ~2 wt% P_2O_5 over NiMoP/Al catalysts. Walendzieski (66) observed a small maximum for thiophene HDS over Co-MoP/Al catalyst containing 1.5 wt% P while selectivity for hydrogenated product was lower than in the P-free catalyst. Chadwick et al. (122) also revealed that thiophene HDS over NiMoP/Al catalysts shows a broad maximum at ~1 wt% P. Lewis et al. (67,110) observed a high positive effect on thiophene and quinoline spiked gas oil HDS at ~1 wt% P, especially over Ni-Mo-P/Al catalysts where P is impregnated prior to the metal species. Kamp and Adams (114) reported that NiMoP/Al-P and CoMoP/Al-P catalysts prepared by the hydrogel method show higher HDS activity for cracked heavy gas oil (CCHGO) than conventional commercial catalyst. Chen et al. (60) reported that

HDS for atmospheric residue over CoMo/Al-P catalyst shows maximum activity at ~5 wt% P. They also correlated reducibility of molybdenum and the HDS activity as in the case of MoP/Al catalyst prepared from "Mo-P" heteropoly compounds as a P precursor.

Kushiyama et al. (113) reported that P also promotes HDS activity for crude oil over highly divided unsupported Mo and Co-Mo sulphide catalysts with a maximum for the P/(Co+Mo) molar ratio of 2. This is interesting as P may directly modify the metal components without the alumina support.

It can be concluded that P shows no effect or very small positive effect on thiophene HDS but decreases selectivity for hydrogenated products over Mo/Al catalysts. However, the presence of P seems to be effective in promoted Mo-based catalysts, especially in NiMoP/Al catalyst.

1.2.6.2 Effects of P on HDN

The positive effect of P has been mostly reported on HDN reactions for both model compounds and industrial processes. Topsøe et al. (90) indicated that indole HDN is enhanced by P addition. Eijsbouts et al. (32,84) reported that quinoline HDN activity increases with the addition of P, especially over Ni-Mo-P/Al catalysts. P addition increases the selectivity for unsaturated N-free hydrocarbons production (propylbenzene). On the other hand, Poulet and co-workers (72,85) and Jian et al. (75,109) reported that P has negative effect for pyridine HDN over MoP/Al catalyst. These results make the effect of P on HDN really unclear. Interestingly, Jian and Prins (75) found that the effect of P essentially depends on the nature of the reactants and intermediates. For example, P indicates a positive effect on the quinoline, ortho-propylaniline (OPA) and indole HDN reactions and a negative effect on pyridine, piperidine and decahydroquinoline (DHQ) HDN over NiMoP/Al catalysts.

Eijsbouts et al. (32,84) proposed that P does not modify the active Ni-Mo-S phase itself but rather allows creation of new active sites associated either with acid $AlPO_4$, with other metal phosphates (ex. Ni-phosphate) or with modification of Ni and Mo sulphide since the effect of P on the HDN activity does not correspond to changes in the dispersion of Ni or Mo species. Especially, they suggested that the improvement of HDN activity is strongly attributed to the $AlPO_4$ formation since the quinoline HDN performance over a dual catalytic bed made of NiMo/Al and P/Al remarkably increases by comparison with the performance obtained in a single NiMo/Al catalyst. Lewis et al. (67,110) also reported that the addition of 1 to 3 wt% P into NiMoP/Al catalysts gives the maximum HDN activity for gas oil and quinoline due to optimised surface acidity.

López Agudo et al. (62) also proposed that pyridine HDN over Ni-P/Al and NiP/Al catalysts is promoted by acid groups of the $AlPO_4$ phase which are effective for C-N bond hydrogenolysis. Ramírez de Agudelo and Morales (56) indicated that HDN of VGO over NiP/Al catalyst is enhanced by improving the hydrogenolysis step. However, other predicted that the P/Al catalyst itself has very low activity for C-N or C-C bond breaking of hydrocarbon (75,67).

A detailed kinetic study by Jian and Prins (75) revealed that P addition decreases the C-N bond cleavage (rate constants k_1' and k_2') and subsequent alkenes hydrogenation (rate constant k_3') steps in piperidine and DHQ HDN (Fig. 27a, 27b and Table 12a). On the other hand, the presence of P increases aromatic ring HYD for ortho-propylaniline (OPA) (rate constant k_1' in Fig. 27c and Table 12b). This result indicates that P presence increases only hydrogenation of aromatic ring but shows no positive effect on the C-N bond cleavage. If the former reaction is a rate determining step, the overall HDN reaction is promoted. For example, P only promotes the HDN reaction when intermediate species have an aniline-like structure for which the rate control step is hydrogenation of the aromatic rings. This is the case for aniline HDN through the formation of cyclohexylamine, for indole through the formation of o-ethylaniline, or for quinoline through the formation of ortho-propylaniline.

Jian et al. (2) also investigated the complex influence of H_2S on pyridine and piperidine HDN over MoP/Al and Ni-MoP/Al catalysts (Table 13). The presence of H_2S itself decreases the HYD of pyridine into piperidine but increases piperidine HDN, especially over Ni-MoP/Al catalysts. As a consequence, HDN activity of pyridine increases even if the total conversion is suppressed. Callant et al. (78) also revealed that adsorption of H_2S on NiMoP/Al catalyst has a positive effect on the C-N bond cleavage but has a detrimental effect on the HYD of indole. The increase in the H_2S partial pressure preferably transforms indoline into o-ethylaniline by a ring opening mechanism while the decrease in H_2S partial pressure leads to the formation of octahydro-1H-indole which is the totally hydrogenated N-containing compound (Fig. 27d).

The concentration of N-containing compounds on the catalyst surface also affects the HDN activity. Van Veen et al. (108) reported that quinoline HDN over P-containing NiMoP/Al is more influenced by the concentration of N-containing compounds in feed than over P-free NiMo/Al catalysts. They proposed that high concentration of quinoline strongly adsorbed on the catalyst active sites hampers the reaction. For lower concentration of N-containing compound, the quinoline HDN activity over NiMoP/Al catalysts is higher than over NiMo/Al catalysts and correlates to their acidity.

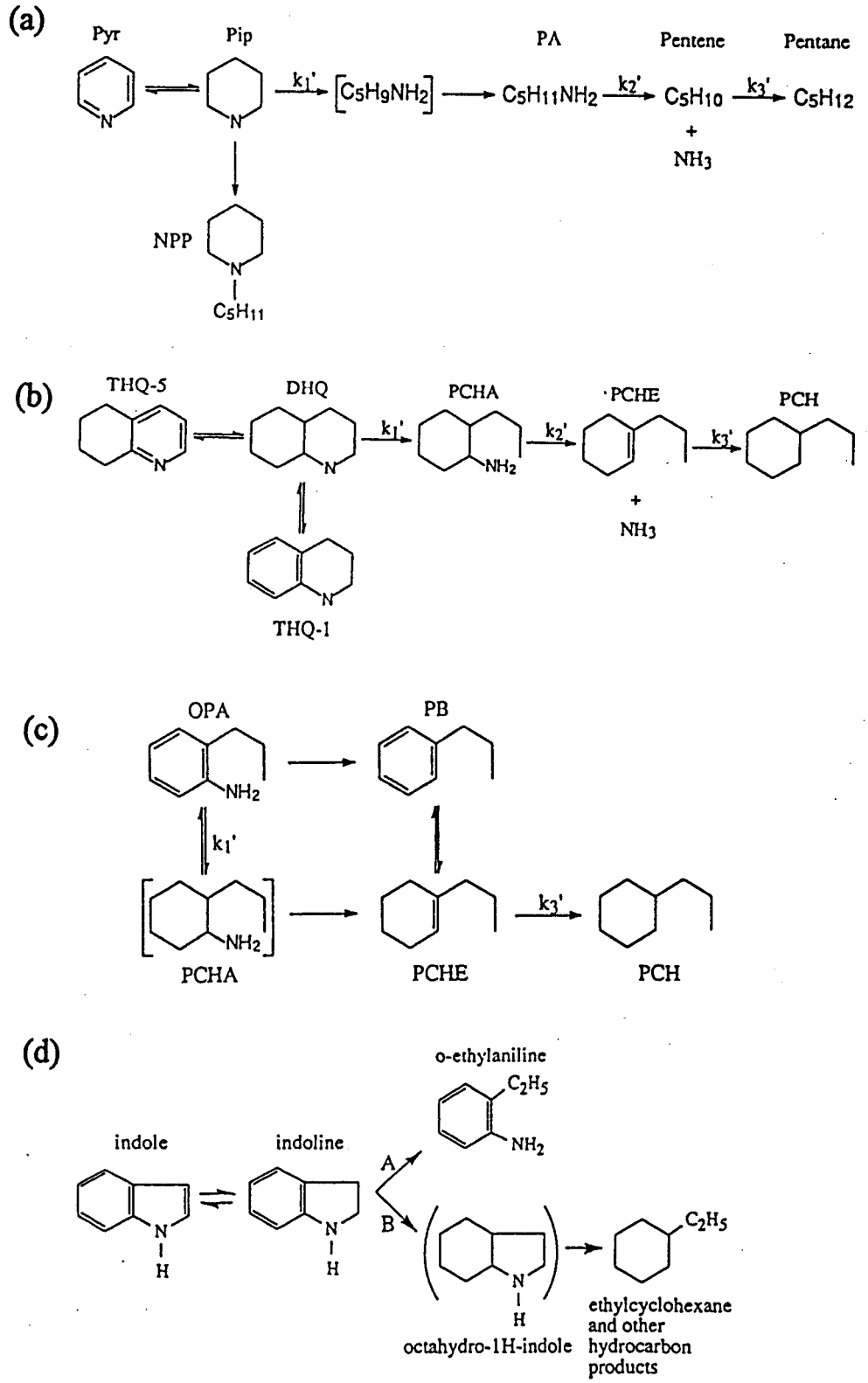

Fig. 27. HDN reaction networks of (a) Piperidine, (b) Decahydroquinoline, (c) Ortho-propylaniline and (d) indole (adapted from ref. 75 and 78).

Table 12. [a]Effective rate constants for the HDN reactions of piperidine and decahydroquinoline (10^2 mol reactant/h g-catalyst). (see reaction network in Fig. 27(a) and (b)), [b]Effect of P on the HDN reaction of ortho-propylaniline (see reaction network in Fig. 27(c)) (from ref. 75)

(a)

Catalyst	Piperidine			Decahydroquinoline		
	k'_1	k'_2	k'_3	k'_1	k'_2	k'_3
$NiMo/Al_2O_3$	0.82	7.4	4.8	0.87	18.7	8.6
$NiMoP(1)/Al_2O_3$	0.65	7.5	3.6	0.77	18.0	7.7
$NiMoP(2)/Al_2O_3$	0.60	7.3	3.2	0.71	16.8	6.5
$NiMoP(4)/Al_2O_3$	0.44	5.4	2.4	0.55	14.4	5.3

(b)

Catalyst	HDN (%)	Product composition (%)			Rate constant	
		PCH	PCHE	PB	k'_1	k'_3
$P(2)/Al_2O_3$	0	0	0	0	0	0
$NiMo/Al_2O_3$	23.5	17.8	4.8	0.9	0.84	14.1
$NiMoP(1)/Al_2O_3$	30.2	21.3	7.4	1.5	1.13	11.4
$NiMoP(2)/Al_2O_3$	34.6	23.7	9.1	1.8	1.34	10.4
$NiMoP(4)/Al_2O_3$	29.9	16.7	11.4	1.8	1.12	6.9

Table 13. Influence of H_2S and P presence in the HDN of pyridine. (from ref. 109) (a) Conversion of pyridine (%), (b) Piperidine production (%), (c) C_5 production (HDN reaction) (%), (d) Ratio of saturated hydrocarbon in C_5 products (from ref. 109)

catalyst	$H_2S/H_2 = 0$				$H_2S/H_2 = 3.0 \times 10^{-3}$			
	conv(a)	pip(b)	C_5(c)	$C_5°/C_5^=$(d)	conv	pip	C_5	$C_5°/C_5^=$
Mo/Al_2O_3	40	34	3.9	1.7	26	16	7	4.0
$MoP(2)/Al_2O_3$	40	34	3.3	1.2	29	19	7	3.9
$NiMo/Al_2O_3$	57	49	4.3	4.0	48	18	24	3.8
$NiMoP(2)/Al_2O_3$	57	49	4.5	2.9	45	20	20	2.0

All these results suggest that the HDN activity is related at least to two different active sites as CUS associating HYD sites and acid sites which are responsible C-N bond cleavage. The NiMoP/Al catalyst has less surface anionic vacancies than the P-free NiMo/Al catalysts due to a worse Mo dispersion or sulphidability. Adsorption of H_2S transforms the CUS according to the following scheme.

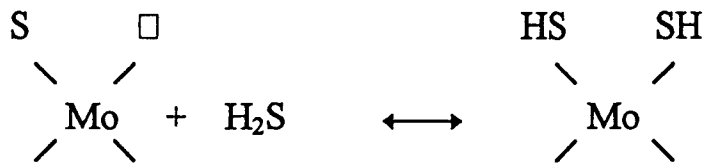

Since both HYD and C-N bond cleavage are necessary for HDN reactions, the optimization of P and H_2S concentration is needed to obtain a maximum HDN activity.

Jian and Prins (112) also reported that the nature of active sites are not chemically modified but the total number or geometric feature of active sites are changed by P addition, since the presence of P rarely change the activation energies and heat of adsorption but increases the adsorption constant of N-containing compounds or NH_3 (Fig. 28).

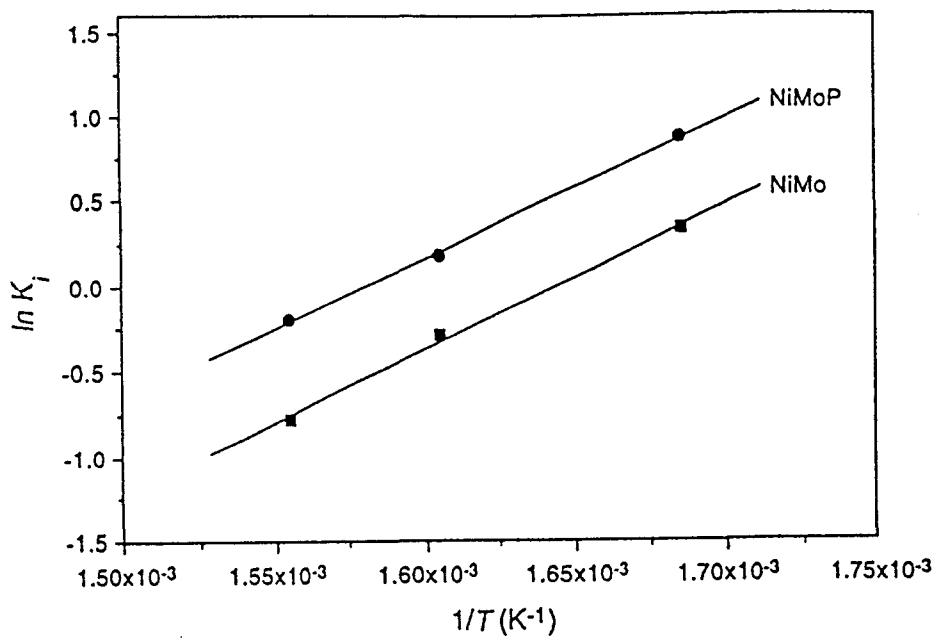

Fig. 28. The adsorption constant of ortho-propylaniline as a function of temperature over NiMo(P)/Al catalysts (from ref. 112).

On the contrary, Topsøe and co-workers (90) proposed that HDS, HDN and HYD reactions take place on the same catalytic sites and the effect of P is rather to decrease the amount of poisoning N adsorbed species than that of H species on the active sites (Table 14). Consequently, total HDN reaction is activated by P addition.

In short, the effect of P on HDN reactions is quite complicated and, therefore, is still in the matter of debate.

Table 14. Comparison of the equilibrium constants of different reactions at 350 °C for different alumina based catalysts. (from ref. 90)

Reaction	Catalyst			
	Mo	Co-Mo	Ni-Mo	Ni-Mo-P
$\frac{1}{2}H_2 + * \rightleftharpoons H-*$	$1.4 \cdot 10^0$	$1.5 \cdot 10^0$	$1.5 \cdot 10^0$	$1.5 \cdot 10^0$
$H_2S + * \rightleftharpoons S-* + H_2$	$80.4 \cdot 10^2$	$6.0 \cdot 10^2$	$4.6 \cdot 10^2$	$5.4 \cdot 10^2$
$NH_3 + * \rightleftharpoons N-* + 3/2H_2$	$118.8 \cdot 10^5$	$24.8 \cdot 10^5$	$19.4 \cdot 10^5$	$9.4 \cdot 10^5$

1.2.6.3 Effects of P on HYD

Effect of P on HYD during HDN processes have been previously considered. In this part, we examine other results concerning HYD. Fierro et al. (105) reported that selectivity of butane in thiophene HDS gives a maximum at 4 wt% of P_2O_5 for MoP/Al catalysts. López Cordero et al. (65) found that 1-hexene HYD on reduced MoP/Al and Mo-P/Al catalysts increased with increasing the amount of P, especially for sequentially impregnated Mo-P/Al catalysts. The addition of 1 to 3 wt% P into Ni-Mo/Al gives the maximum aromatic reduction for gas oil due to the optimum surface acidity (67,110).

On the other hand, Muralidhar et al. (107) found that the presence of P increases HYD of aromatic ring but decreases the successive HYD steps of alkene formed from ring opening reaction. The same authors also reported that 1-hexene HYD activity over Co-Mo-P/Al catalyst decreases with P loading. Hubaut

and co-workers (72,85) also reported that toluene HYD activity increases by P addition while isoprene HYD does not change by P addition over the MoP/Al. Jian et al. (109,112) also reported that HYD of cyclohexene decreases with the addition of P over Ni-MoP/Al catalysts. Iwamoto and Grimblot (111) confirmed that HYD of cyclohexene decreases with the addition of P over sulphided MoP/Al sol-gel catalysts while the selectivity of propane in C_3 products from cyclopropane cracking increases with the P content. Walendziewski (66) showed that benzene HYD decreases by the addition of 3 wt% P_2O_5. Jian et al. (112) also found that the presence of N-containing compounds inhibited the HDN reactions over NiMoP/Al at a relatively higher rate than over NiMo/Al catalyst due to the stronger adsorption rate.

These results suggest that the effect of P on the HYD reaction should strongly depend on reactants, nature of active sites and reaction conditions as well as during the HDN reaction. However, P may increase predominantly aromatic HYD as in the HDN reactions. The effect of hydrogen pressure is relatively important for the HYD reactions since a rather negative effect of P tends to be observed in the reactions performed under the atmospheric pressure.

1.2.6.4 Effects of P on HYC and ISOM

Lewis et al. (67) showed that diisopropylbenzene HYC over P/Al catalysts shows low activity while that over NiMoP/Al catalysts increases between 1 and 3 wt% P. On the other hand, Muralidhar et al. (107) reported that HYC activity of isooctene over Co-Mo-P/Al catalysts decreases with increasing the amount of P. Iwamoto and Grimblot (57) reported that HYC of cyclopropane increases with P loading, especially over NiMoP/Al catalysts.

Poulet et al. (72) reported that isomerization activity from trans → cis pentadiene over MoP/Al catalyst decreases with P addition. Gishti et al. (52) also reported that activity for skeletal isomerization of cyclohexene to methyl cyclopentenes over reduced MoP/Al was reduced by P addition. Iwamoto and Grimblot (111) reported, however, that isomerization of cyclohexene over sulphided MoP/Al sol-gel catalyst increases with the P addition.

1.2.6.5 Effects of P on HDM

The result of HDM over P containing catalysts are very scarce because simple model reactions like thiophene HDS and pyridine HDN are generally preferred from the reason of facility of experiments and interpretation in principle. Moreover, the control of catalyst pore distribution, which may also considerably affects the HDM results, makes this kind of studies more difficult. Kushiyama et al. (113) reported that the addition of P improves HDM activity of crude oil over

unsupported Mo and Co-Mo soluble catalysts. They proposed that P interact strongly with the V-containing compounds in the feedstock. The positive effect of P on HDM can be also found frequently in patents (see for example ref. 115).

1.2.6.6 Effect of P on coke formation and catalytic life

Fitz Jr. and Rose (44) reported that the presence of P decreases the amount of coke and increases its H/C ratio during thiophene-cyclohexene hydrotreating reactions. Spojakina et al. (31) also showed that P decreases coke formation in thiophene HDS reaction. Lewis et al. (67) reported that at the optimum P loading, the catalyst life for light gas oil (LGO) HDS reaction is improved by maintaining its SSA. However, no clear correlation was reported between SSA and the amount of coke deposition.

1.2.7. Structural models of P containing hydrotreating catalysts

Based on their characterizations and reaction tests, structural models of P-containing hydrotreating catalysts have been proposed in literature.

Poulet et al. (72) reported a structural model of MoP/Al catalysts (Fig. 29) in which P exists in three different states :

1) Isolated P oxo-species in interaction with alumina
2) P directly incorporated into the MoS_2 slab
3) P oxo-species bound to both MoS_2 and the alumina support

Mangnus et al. (63) also proposed a structural model for Co-Mo-P/Al catalysts (Fig. 30) where P mainly exists as $AlPO_4$ on the aluminium surface. In this model, a part of Mo sites at the edges of the MoS_2 slab interacts with $AlPO_4$ through Co-Mo-O-P linkages.

It is also reported that no obvious difference exist between P-containing catalysts and P-free ones (76,77,122). The P effect would be to affect only the morphology of the MoS_2 slabs and consequently to change the number of active sites and their steric hindrance.

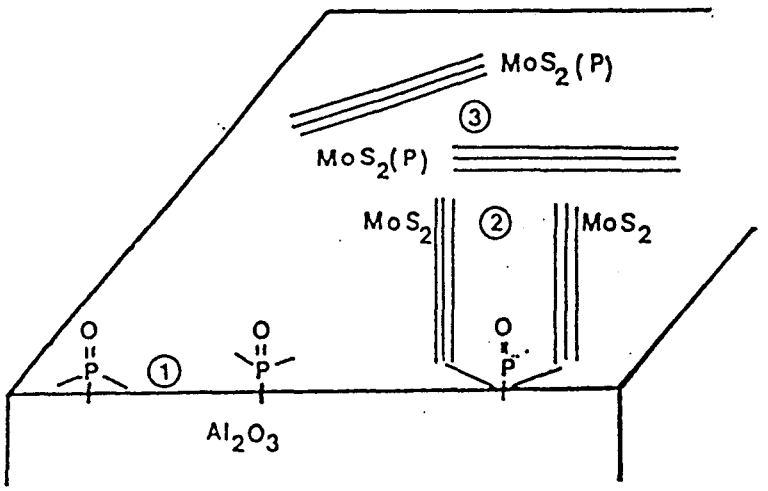

Fig. 29. Schematic representation of P location in the MoP/Al catalyst (from ref. 72). (1) P oxo-species adsorbed on alumina, (2) P oxo-species bound to both MoS_2 slabs and the alumina support, (3) P directly incorporated into the MoS_2 slab.

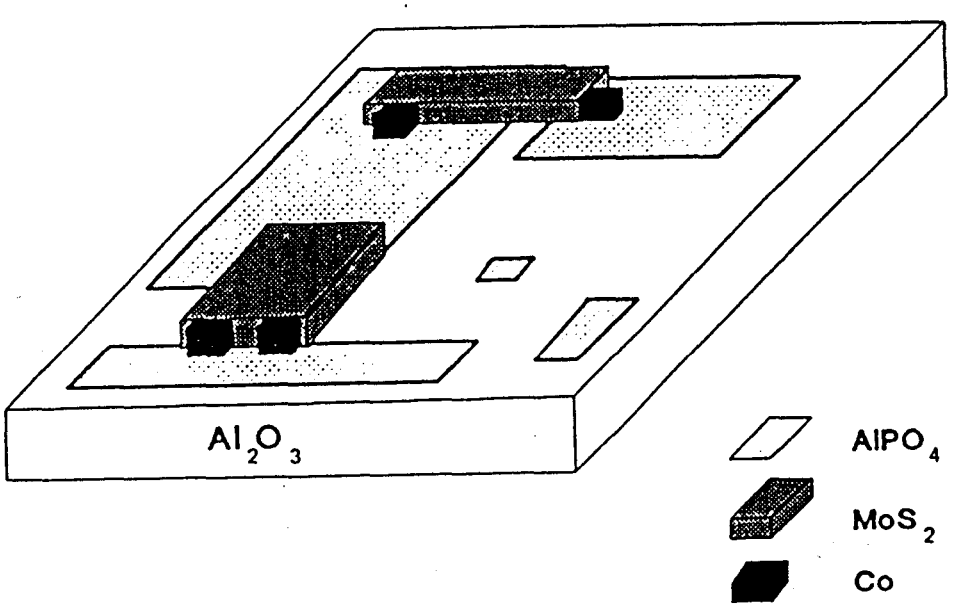

Fig. 30. Schematic model for sulphided CoMoP/Al catalyst (from ref. 63).

1.2.8. Effect of P on other hydrotreating catalysts

1.2.8.1 W-based catalysts

Much less studies on the W-based hydrotreating catalysts are found in the literature compared with those of Mo-based catalysts. It is expected, however, that P might give almost same effects on the preparation, textural, structural properties and reactions as those in the case of Mo-based catalysts since tungsten has a lot of chemical characteristics of Mo. Atanasova et al. (116) reported that P increases thiophene HDS activity especially over a sequentially impregnated NiW-P/Al catalyst. Halachev et al. (117) found that P gives maximum HYD activity of naphthalene at 0.6 wt% P_2O_5. Cruz Reyes et al. (53) reported that P notably enhances gas oil HDS and pyridine HDN over W/Al catalyst.

1.2.8.2 Carbon supported catalysts

P decreases thiophene HDS significantly over CoMo/C catalysts (104,118,119). The weak interaction between P oxo-species and the carbon support favors the formation of cobalt phosphate and/or phosphine in the presence of H_2 and leads to the poisoning of the active phases. This is not the case with the alumina support because the strong interaction between P and Al forms preferably $AlPO_4$ which is not converted into phosphine.

On the other hand, Robinson et al. (64) found that Ni-P/C catalysts show high activity for quinoline HDN due to the formation of Ni_2P

1.2.9. Impact of P introduction into industrial catalyst formulations

Since the addition of P on commercial hydrotreating catalysts may be sometimes the subject to confidential aspects, it is less opened in general literature. However, according to a report in Oil and Gas Journal (119), it appears that several commercial catalysts suppliers provide P-containing catalysts (for example, catalysts TK-551 and TK771 from Haldor Topsøe A/S, or IMP-DSD-3 and IMP-DSD-5 from Instituto Mexicano Del Petroleo) while the effect of P is not clarified.

In addition, the advantage of P addition in catalyst formulations are often found in patents where the positive effects of P are roughly categorised into the following aspects :

(1) the optimization of either the pore structure or dispersion and states of Co(Ni) + Mo by P addition,
(2) the optimization of synergy effects between P and the other additives,
(3) the optimization of catalyst preparation using specific types of phosphorus

precursors,

(4) the use of P containing catalysts under specific reaction conditions as well as their combination with other hydrotreating catalysts or processes.

1.2.10. General discussion and conclusion

The P content, the nature of the P precursor, the way of P introduction significantly affect the textural and structural properties of catalysts. Therefore, it is very important to determine the optimum preparation and activation conditions of hydrotreating catalysts to obtain the desirable catalytic performances. Especially, pH of solution and the P/Mo atomic ratio are important factors to obtain active hydrotreating catalysts. But more generally, many other factors influence the results presented above. In this part, a review of the main effects in relation with P introduction in the catalysts will be discussed and summarised.

1.2.10.1 Effect of P on preparation

P has two main positive effects on the catalysts preparation.

1) The solutions containing Mo and Co+Mo or Ni+Mo precursors tend to be unstable without proper additives. Indeed, light orange or green precipitation within few minutes after dissolving each metallic salts is often observed in the preparation of Co+Mo or Ni+Mo solution, respectively. The P addition stabilises such impregnation solution via formation of "Mo-P" or "Ni-P" oxo-compounds. Therefore, the presence of P allows to increases the dispersion of the metal species supported on the resulting catalysts.

2) As the above Mo-P oxo-compounds have less interaction with the alumina support, they can spread over the entire surface of the support particles. Especially, the co-impregnation method with high P/Mo atomic ratio is suitable to obtain the highly dispersed state of supported metals. On the other hand, in sequential impregnation in which P is introduced first, Mo tends to deposit on the outer surface of the catalyst particles probably due to the rather strong interaction between Mo and phosphated alumina. Large amounts of P decrease the dispersion of metal components since the stronger affinity between P and alumina prevents the interaction between metals and the support. Fig. 31 reports a diagram which schematically represents all the possible interactions relative to the presence of P oxo-species in the catalyst preparations.

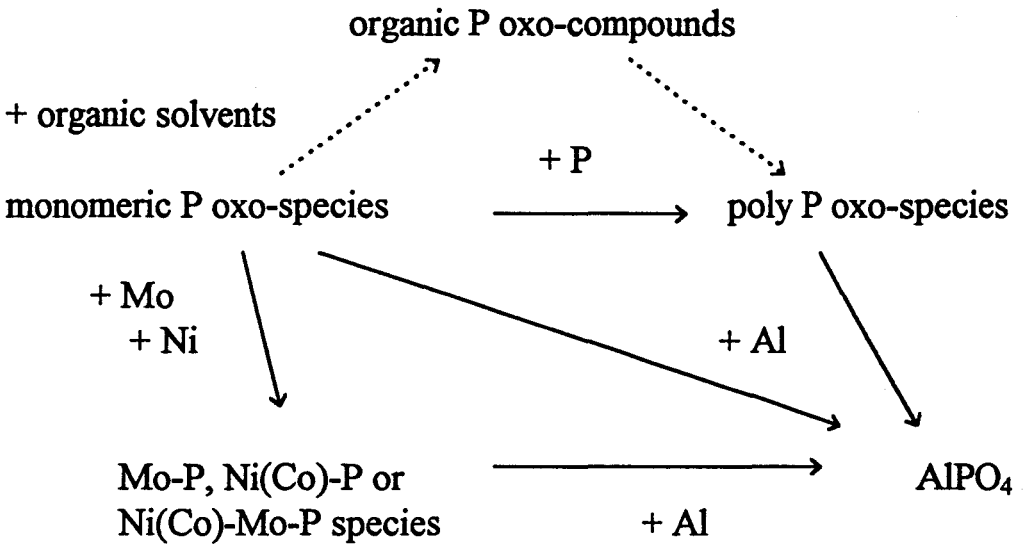

Fig. 31 Schematic diagram of representing the different P oxo-species obtained during catalyst preparation

1.2.10.2 Effect of P on textural and structural modifications of catalysts

This is one of the most unclear point of whether P can interact with Mo species or not in the final catalyst. In the impregnation steps, P and Mo oxo-species react to form some heteropoly compounds. However, they can decompose by impregnation itself or by calcination since they are usually quite unstable. One exception is reported for reduced heteropoly "$Mo_{12}P$" anion which is stable even after calcination at 400 °C (23). The interaction between the P and Mo species after calcination or sulphidation may depend on the P content. P may not modify the Mo species at low P content where the Al-OH groups reacting with the Mo and P species are still remaining. In this case, P and Mo species might be supported on alumina independently. With increasing the P loading, it starts to interact with the Mo oxo-species by sharing their oxygen atom. This interaction may be maintained even after sulphidation (at least in part) because P decreases sulphidability of the Mo oxo-species. This oxygen remaining in MoS_2 slabs (Mo oxy-sulphide) contributes to the generation of strong acid sites as well as in $AlPO_4$. Too much P then favors the segregation of bulk Mo oxide such as MoO_3 and $Al_2(MoO_4)_3$.

It is remarkable to note that $AlPO_4$ is not detected at the low P loading, while it starts to be observed only above the P loading corresponding to theoretical P monolayer coverage (131).

Co_2P in certain conditions. However, they would be present as minor species on the alumina based catalysts because P has stronger affinity with alumina rather than with Ni or Co species in conventional hydrotreating conditions.

The formation of mixed Mo-P-S compounds is thermodynamically restricted below 1000 °C (63). This indicates that the S atoms in MoS_2 are not replaced by P atoms directly. In the same way, P does not regularly occupy the edges of the MoS_2 platelets through S atoms as in the case of Co-Mo-S or Ni-Mo-S phases. The formation of P(white), P(red) and P(black) on catalysts can be also excluded because they have extremely high vapour pressure under the hydrotreating conditions.

P also modifies the textural properties of the MoS_2 slabs (depending on the P content). It tends to increase the number of MoS_2 stacked layers. These modifications might give the following positive effects on the catalyst :

-Optimise the steric CUS configuration,

-Increase the proportion of the NiMoS(II) phase which has a higher hydrogenation activity and less steric hindrance

-Optimize the ratio of rim and edge sites in the MoS_2 slabs (see the model described by Daage and Chianelli (124)),

Considering all the investigations above, the present authors proposed a structure of the active phase of MoP/Al and NiMoP/Al catalysts in Fig. 32. P creates at least two species on the catalysts. The one is isolated P oxo-species on alumina (monomeric or polymeric P oxo-species and $AlPO_4$ are not shown in the figure). The other is P interacting with both alumina and MoS_2. It prevents the complete sulphidation of molybdenum oxo-species and creates acid OH groups in MoS_2 slabs. If Co or Ni is present, it can occupy the edges of MoS_2 as in the classical CoMoS and NiMoS phases.

1.2.10.3 Effect of P on hydrotreating reactions

P has positive effects on isomerization and hydrogenolysis reactions which require acid properties. P also improves the HYD reaction of aromatic rings, especially over NiMoP/Al catalysts. P shows minor effect on thiophene HDS while it may improve the HDS activity of heavier sulphur containing molecules such as VGO in which the HYD of aromatic rings before C-S bond scission is effective. P also promotes HDN reactions in which HYD of aromatics rings is the rate determining step. In any cases, large amounts of P is detrimental on all the hydrotreating reactions.

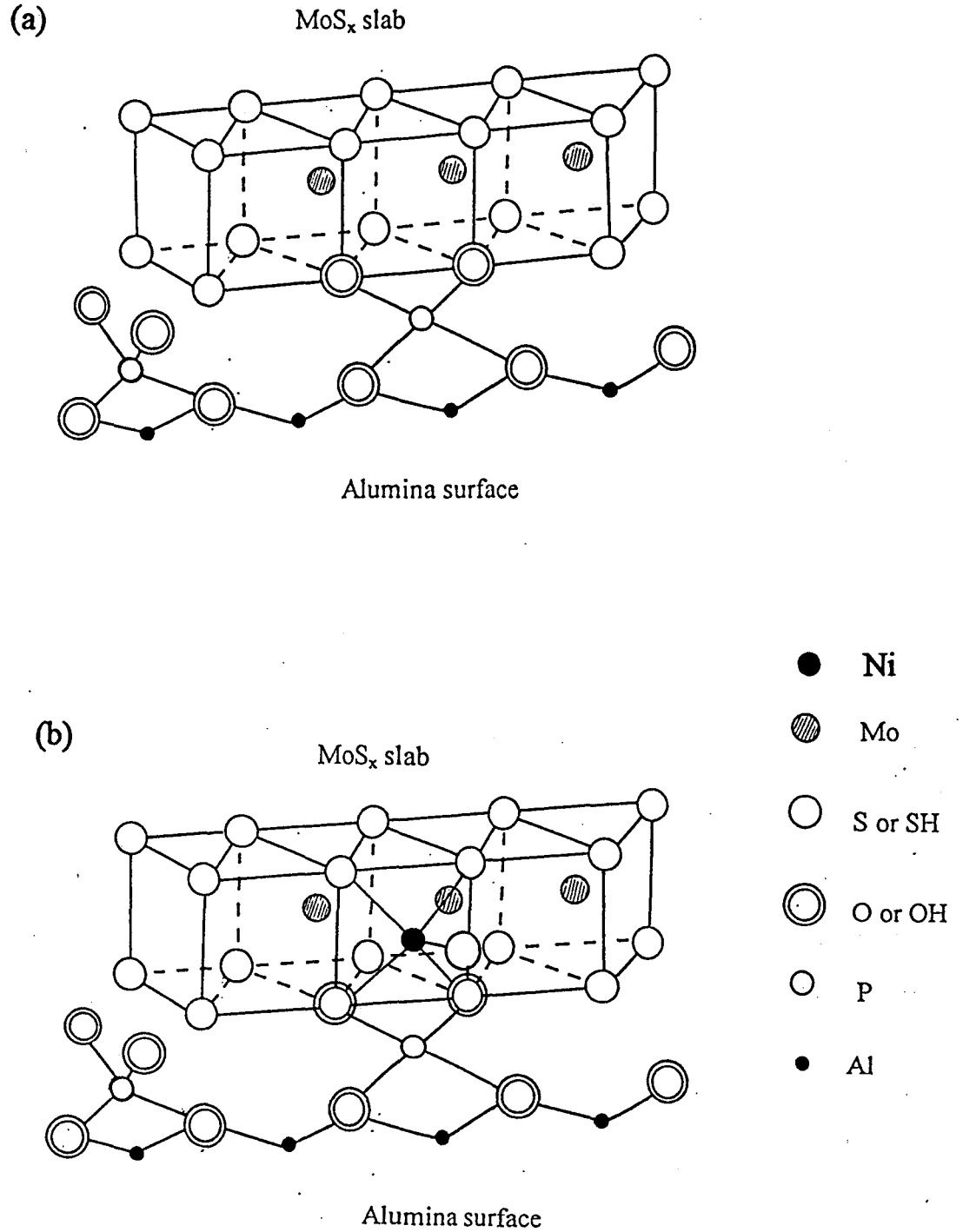

Fig. 32. A model representing interaction between MoS_2 and the alumina through P oxo-species. (a) unpromoted MoP/Al, (b) Ni-promoted MoP/Al.

Here, let us discuss why P can predominantly improve HYD of aromatic rings. Recently, Daage and Chianelli (124) proposed that HDS/HYD selectivity during conversion of DBT strongly depends on the MoS_2 slab morphology (number of MoS_2 stacked layers) in unsupported catalysts. The HYD reaction mainly proceeds on rim sites while both rim and edge sites are responsible for HDS reaction. This means that stacking of the MoS_2 layers enhances HDS rather than HYD. However, this is not in agreement with experimental P effect because the addition of P preferably increase MoS_2 stacking but promotes HYD of aromatic rings. Spojakina et al. (31) proposed that the presence of P increases both dispersion of molybdenum and prevents the penetration of Ni into the alumina support. In such a case, P contributes to the optimization of Ni/Mo ratio on the active phase and increase the amount of nickel available to form the Ni-Mo-S active phase which could be also profitable for HYD.

Another possibility could be considered on the basis of modelled active sites proposed by Hubaut et al. (125) on the basis of a previous investigation by the same group (126) (Fig.34). In this model, the reactions involved in the hydrotreating schemes over Mo/Al catalysts are associated with its CUS configuration. HYD of aromatic compounds (toluene and pyridine etc.) and ISOM of diene need a ^{2}M-^{2}M or ^{2}M-^{3}M sites while ^{3}M-^{3}M sites are responsible for complete diene HYD and pyridine HDN (where ^{x}M means number of CUS around one edge Mo atm). As P decreases the amount of exchangeable oxygen atoms around Mo atom (low sulphidability of the Mo/Al), the proportion of ^{2}M sites may relatively increase. Thus, HYD of aromatic rings and some HDN reactions could be promoted.

Furthermore, Moreau et al. (127) proposed that the aromatic HYD reaction is favored on stronger electron withdrawing sites (higher oxidation state) and hydrogenolysis is on slightly electron donating sites (lower oxidation state). This is also in well agreement with the P effect which decreases sulphidability of Mo with remaining oxygen atoms in MoS_2 slab.

In addition, there is one important question whether the effect of P is mainly related with increasing the acidity or with the generation of new hydrogenation sites. One possible explanation is to consider that Brönsted acid sites work also as hydrogenation sites. In terms of reaction involving hydrogen species, acid sites and HYD sites could be considered as the same but the difference between them is whether hydrogen stays essentially at the catalyst surface or is incorporated in the reactant at the end of reaction. If the hydrogen species on the Brönsted acid sites can be consumed by the reactants and immediately compensated by spillover hydrogen under the hydrotreating conditions, acid sites can act as hydrogenation sites.

Indeed, Kanai et al. (128) proposed that the Brönsted acid site gives hydrogenation activity in specific conditions.

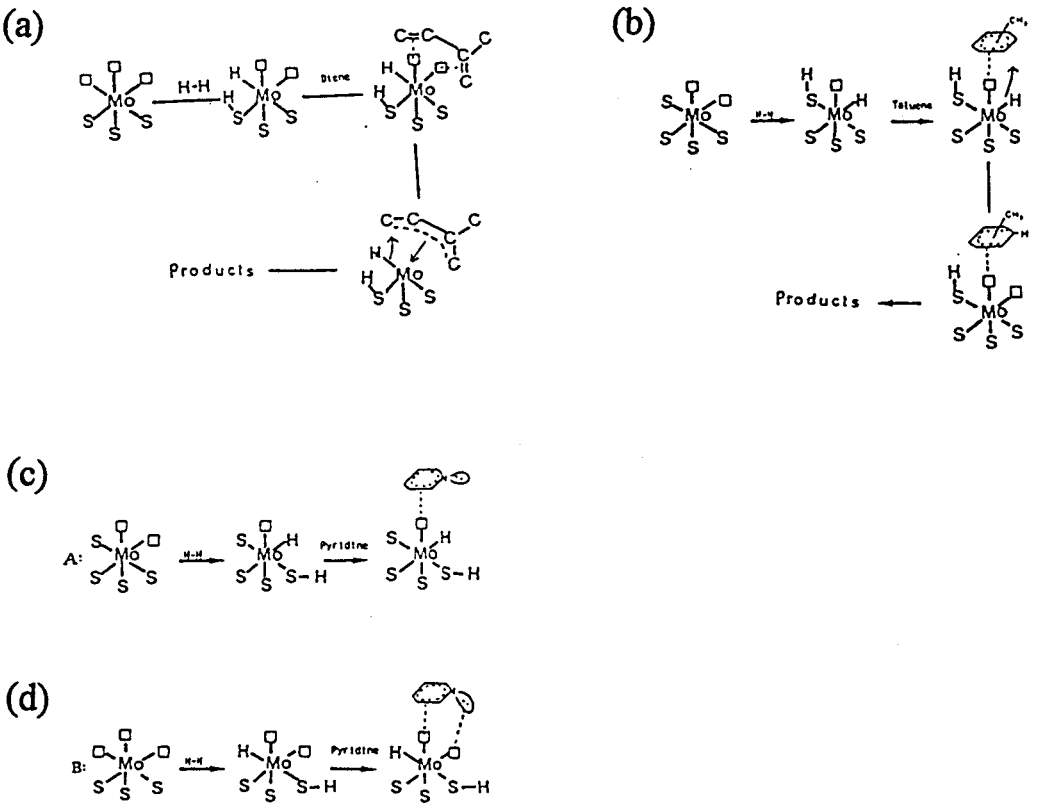

Fig. 33. Probe molecule transformations on coordinative unsaturated sites (CUS) of MoS_2 (adapted from ref. 125): (a)ISOM and HYD of diene, (b) HYD of toluene, (c) HYD of pyridine, (d) HDN of pyridine.

1.2.10.4 Other possible effects of phosphorus

In addition to the above investigation, effects of P have been proposed from different point of views :

1) P decreases the polarization of Mo-S bonds and increase its covalent character. Since Mo-based catalyst with a high covalency of Mo-S bonds is supposed to have a high HDS activity, P can improve HDS activity (80).

2) P increases the formation of octahedral Mo, Co and Ni which would be the precursors of active phases (33,73).
3) P promotes strongly hydrogen activation properties of MoP/Al catalysts (52).

As a final conclusion, a lot of efforts, whose the main results are reported in this review, has already revealed that addition of P in alumina based hydrotreating catalysts produces notable changes on either their textural, structural properties or reactivity. Some of these changes induce better performances in the hydrotreating reactions if key parameters during preparation are correctly controlled. However, there are still many questions to be answered about the exact locations of P in the catalysts and its role. Some interesting perspectives and explanations can be found in the literature but without any doubt, the challenge to continuously improve hydrotreating catalysts, namely by the P addition, is still open.

List of Reference

No.			Authors					article	vol	no.	page	year
1	O.Weisser	S.Landa	(Pergamon press)					Sulphide Catalysts, their				1973
								properties and applications				
2	R.Prins	V.H.J. de beer	G.A.Somorjai					Catal. Rev.	31		1	1989
3	H.Topsoe	B.S.Clausen	F.E.Massoth	(Springer-Verlag)				Catalysis	11			1996
4								USP327280				1966
5								US3446730				1969
6	P.C.Weast	M.Astle	(CRC press. Inc.)					Handbook of Chem. and Phys.			B-29	1981
7	A.F.Wells	(Oxford)						Structural Inorg. Chem.			638	1962
8	K.B.King(ed.)	(John wiley & sons Inc.)						Encyclopedia of Inorg. Chem.	6			
9	R.Steudel	(Walter de Gruyter Berlin)						Chem. of non-Metals			307	1977
10	W.Weng	J.L.Baptista						J.Sol-Gel. Sci.Tech.	8		645	1997
11	J.Livage	P.Barboux	M.T.Vandenborre	C.Schmutz	F.Taulelle			J.Non-Cryst.Solids	147&148		18	1992
12	D.E.Rogers	G.Nickless	(Ed.) Gnickvess	(Elsevier)				Inorganic Sulfur Chem.	281			1968
13	G.A.Olah	(Wiley Interscience)						Friedel-Crafts Chem.			368	1973
14	R.Kniep							Angew.Chem.Int.Ed.Engl.	25		525	1986
15	C.Fernandez	J.P.Amoureux	J.M.Chezeau	L.Delmotte	H.Kessler			Microporous Mater.	6		331	1996
16	I.Balakrishnan	S.Prasad						Appl.Catal.	62		L7	1990
18	B.Rebenstorf	T.Lindblad	S.L.T.Andersson					J.Catal.	128		293	1991
19	G.A.Tsigdinos							Topics in Current Chem.	76		1	1978
21	L.Pettersson	I.Andersson	L.Öhman					Inorg.Chem.	25		4726	1986
22	P.Souchay	(Gauthier Villars)						Polyanions et polycations				1963
23	A.Griboval	P.Blanchard	E.Payen	M.Fournier	J.L.Dubois			Stud.Surf.Sci.Catal.	106		181	1997
24	H.W.Chamber	C.M.Thompson	(ed.J.E.Chambers	P.E.Levi)	(Academic press)			Organophoshpates				1992
25	C.M.Tompson	T.Nishioka	T.R.Fukuta					J.Agric.Food.Chem.	31		696	1983
26	J.A.R.van.Veen	P.A.J.M.Hendriks	R.R.Andréa	E.J.G.M.Romers	A.E.Wilson			J.Phys.Chem.	94		5282	1990
27	F.Abbattista	A.Delmastro	G.Gozzelino	D.Mazza	M.Vallino	G.Busca	V.Lorenzelli	J.Chem.Soc.Faraday.Trans.	86	21	3653	1990
28	A.Spojakina	S.Damyanova						React.Kinet.Catal.Lett.	53	2	405	1994
29	T.K.Shokhireva	T.M.Yurieva	A.A.Altynnikov	V.F.Anufrienko	L.M.Plyasova			React.Kinet.Catal.Lett.	47	2	177	1992
	G.S.Litvak	A.A.Spojakina	N.Kostova									
30	P.Atanasova	T.Halachev						Appl.Catal.	48		295	1989
31	A.Spojakina	S.Damyanova	L.Petrov					Appl.Catal.	56		163	1989
32	S.Eijsbouts	L.V.Gruijthuijsen	J.Volmer	V.H.J.de Beer	R.Prins			Stud.Surf.Sci.Catal.	50		79	1989
33	E.C.DeCanio	J.C.Edwards	T.R.Scalzo	D.A.Storm	J.W.Bruno			J.Catal	132		498	1991
34	C.Fredericci	S.F.Dominguez						Materials Res; Bull.	31	2	235	1996
35	R.Iwamoto	J.Grimblot						Stud.Surf.Sci.Catal.	106		195	1997
36	H,Kraus	R.Prins						J.Catal.	170		20	1997
37	Y.Okamoto	T.Gomi	Y.Mori	T.Imanaka	S.Teranishi			React.Kinet.Catal.Lett.	22	3-4	417	1983
38	P.J.Mangnus	J.A.R.van,Veen	S.Eijsbouts	V.H.J.de Beer	J.A.Moulijn			Appl.Catal.	61		99	1990
39	H.Knözinger	P.Ratnasamy						Catal. Rev.Sci.Eng.	17	1	31	1978
40	J.M.Lewis	R.A.Kydd						J.Catal	132		465	1991
41	A.Morales	M.M.Ramírez de Agudelo		F.Hernandez				Appl.Catal.	41		261	1988
42	A.Stanislaus	M.Absi-Halabi	K.Al-Dolama					Appl.Catal.	39		239	1988
43	D.E.Petrakis	M.J.Hudson	P.J.Pomonis	A.T.Sdoukos	T.V.Bakas			J.Mater.Chem.	5	11	1975	1995

44	C.W.Fitz.Jr	H.F.Rase						Ind.Eng.Chem.Res.Dev.	22		40	1983
45	H.Kraus							Thesis, ETH Nr.11620				
46	H.Kraus	R.Prins						J.Catal.	164		251	1996
47	J.A.Davis	J.O.Leckie						J.Coloid Int.Sci.	74		32	1980
48	A.Breeuwsma	J.Lyklema						J.Coloid Int.Sci.	43		437	1973
49	C.P.Huang							J.Coloid Int.Sci.	53		178	1975
50	N.Mikami	M.Sasaki	K.Hachiya	R.D.Astumian	T.Ikeda	T.Yasunaga		J.Phys.Chem.	87		1454	1983
51	R.Lopez Cordero	F.J.G.Llambias	J.M.Palacios	J.L.G.Fierro	A.Lopez Agudo			Appl.Catal.	56		197	1989
52	K.Gishti	A.Iannibello	S.Marengo	G.Morelli	P.Tittarelli			Appl.Catal.	12		381	1984
53	J.C.Reyes	M.A.Borja	R. Lopez Cordero	A.Lopez Agudo				Appl.Catal.	120	A	147	1994
54	R.Hubaut	O.Poulet	S.Kasztelan	J.Grimblot				J.Mol.Catal.	81		301	1993
55	O.H.Han	C.Y.Lin	G.L.Haller					Catal.Lett.	14		1	1992
56	M.M.Ramírez de Agudelo		A.Morales					Proc.9th Int.Cong.Catal.	1		42	1988
57	R.Iwamoto	J.Grimblot						to be published				
58	W.C.Cheng	N.P.Luthra						J.Catal.	109		163	1988
59	L.Pettersson							ACTA Chem.Scandinavian	25		1956	1971
60	M.Jian	R.Prins						Bull.Soc.Chim.Belg.	104	4-5	231	1995
61	P.Atanasova	J.Uchytil	M.Kraus	T.Halachev				Appl.Catal.	65	1	53	1990
62	A.Lopez Agudo	R.Lopez Cordero	J.M.Palacios	J.L.Fierro				Bull.Soc.Chim.Belg.	104	4-5	237	1995
63	R.J.Mangnus	A.D.van.langeveld	V.H.J.de.Beer	J.A.Moulijn				Appl.Catal.	68		161	1991
64	W.R.A.M.Robinson	J.N.M. van Gestel	T.I.Koranyi	S.Eijsbouts				J.Catal.	161		539	1996
	A.M.van der Kraan	J.A.R.van,Veen	V.H.J.de Beer									
65	A.Lopez Cordero	N.Esquivel	J.Lazaro	J.L.G.Fierro	A.Lopez Agudo			Appl.Catal.	48		341	1989
66	J.Walendziewski							React.Kinet.Catal.Lett.	43	1	107	1991
67	J.M.Lewis	R.A.Kydd	P.M.Boorman	P.H.Van.Rhyn				Appl.Catal.	84		103	1992
68								USP4066572				1978
69								USP4202798				
70	P.D.Hopkins	B.L.Meyers						Ind.Eng.Chem.Res.Dev.	22		421	1983
71	C.Morterra	G.Magnacca	P.P.de.Maestri					J.Catal	152		384	1995
72	O.Poulet	R.Hubaut	S.Kasztelan	J.Grimblot				Bull.Soc.Chim.Belg.	100	n11-12	857	1991
73	A.Morales	M.M.Ramírez de Agudelo						Appl.Catal.	23		23	1986
74	A.Stanislaus	M.Absi-Halabi	K.Al-Dolama					Appl. Catal.	50	3	237	1989
75	M.Jian	R.Prins						Catal.Lett.	35		193	1995
76	M.Jian	F.Kapteijn	R.Prins					J.Catal.	168		491	1997
77	D.J.Sajkowski	J.T.Miller	G.W.Zajac					Appl.Catal.	62		205	1990
78	M.Callant	K.A.Holder	P.Grange	B.Delmon				Bull.Soc.Chim.Belg.	104	4-5	245	1995
79	P.Atanasova	T.Halachev	J.Uchytil	M.Kraus				Appl. Catal	38		235	1988
80	S.I.Kim	S.I.Woo						J.Catal.	133		124	1992
81	Y.W.Chen	W.C.Hsu	C.S.Lin	B.C.Kang	S.T.Wu	L.J.Leu	J.C.Wu	Ind.Eng.Chem.Res.	29		1830	1990
82	J.Ramirez	V.M.Castano	C.Leclercq	A.Lopez Agudo				Appl.Catal.	83	General	251	1992
83	R.Lopez Cordero	S.López Guerra	J.L.G.Fierro	A.Lopez Agudo				J.Catal.	126		8	1990
84	S.Eijsbouts	J.N.M.van,Gestel	J.A.R.van,Veen	V.H.J.de Beer	R.Prins			J.Catal	131		412	1991
85	R.Hubaut	O.Poulet	S.Kasztelan	E.Payen	J.Grimblot			Proc.Symp.Adv.Hydrotreat.Catal.			548	1994
86	R.A.Kemp	R.C.Ryan	J.A.Smegal					Proc.9th Int.Cong.Catal.	1		128	1988
87	T.Arunarkavalli							Proc.Indian Acad. Sci.	108	1	27	1996

88	A.Andreev	Ch.Vladov	L.Prahov	P.Atanasova				Appl.Catal.	108	A	L97	1994
89	E.Manova	C.Severac	A.Andreev	R.Clément				J.Catal.	169		503	1997
90	H.Topsoe	B.S.Clausen	N.Topsoe	P.Zeuthen				Stud. Surf. Sci. Catal.	63		77	1989
91	J.M.Lewis	R.A.Kydd						J.Catal	136		478	1992
92	P.M.Boorman	R.A.Kydd	T.S.Sorensen	K.Chong	J.M.Lewis	W.S.Bell		Fuel	71	January	87	1992
93	Y.Kurokawa	Y.Kobayashi	S.Nakata					Heterogeneous Chem.Rev.	1		309	1994
94	T.Tsuchida	S.Ohta	K.Horigome					J.Mater.Chem.	4	(9)	1503	1994
95	I.H.Cho	S.B.Park	J.H.Kwak					J.Mol.Catal.	104	A	285	1996
96	S.H.Risbud	R.J.Kirkpatrick	A.P.Taglialavore	B.Montez				J.Am.Ceram.Soc.	70	1	C10	1987
97	R.K.Brow	R.J.Kirkpatrick	G.L.Turner					J.Am.Ceram.Soc.	73	(8)	2293	1990
98	J.C.Edwards	E.C.Decanio						Catal.Lett.	19		121	1993
99	S.Rezgui	B.C.Gates						Chem.Mater.	6		2386	1994
100	D.Muller	W.Gessner	H.J.Behrens	G.Scheler				Chem.Phys.lett.	79	1	59	1981
101	F.M.Bautista	J.M.Campelo	A.Garcia	D.Luna	J.M.Marinas	A.A.Romero		Appl.Catal.	96		175	1993
102	N.R.Gazimzyanov	V.I.Mikhailov	V.V.Volod'ko					Kinet.Catal.	36	5	694	1995
103	M.J.Ledoux	A.Peter	E.A.Blekkan	F.Luck				Appl.Catal.	133	A	321	1995
104	S.M.A.M.Bouwens	J.P.R.Vissers	V.H.J.de Beer	R.Prins				J.Catal.	112		401	1988
105	J.L.G.Fierro	A.Lopez Agudo	N.Esquivel	R.Lopez Cordero				Appl.Catal.	48		353	1989
106	G.Muralidhar	F.E.Massoth	J.Shabtai					J.Catal.	85		44	1984
107	W.L.T.M.Ramselaar	S.M.A.M.Bouwens	V.H.J.de Beer	A.M. van der Kraan				Hyperfine Interactions	46		599	1989
108	J.A.R.van.Veen	H.A.Colijn	P.A.J.M.Hendriks	A.J.van Welsenes				Fuel Processing Technol.	35		137	1993
109	M.Jian	J.L.Rico,Cerdo	R.Prins					Bull.Soc.Chim.Belg.	104	4-5	225	1995
110	J.M.Jones	R.A.Kydd	P.M.Boorman	P.H.Van.Rhyn				Fuel	74	12	1875	1995
111	R.Iwamoto	J.Grimblot						J.Catal.	in press			
112	M.Jian	F.Kapteijn	R.Prins					J.Catal.	168		491	1997
113	S.Kushiyama	R.Aizawa	S.Kobayashi	Y.Koinuma	I.Uemasu	H.Ohuchi		Appl.Catal.	63		279	1990
114	R.A.Kemp	C.T.Adams						Appl.Catal.	134		299	1996
115								USP4520128				1985
116	P.Atanasova	Ch.Vladov	T.Halachev					Bull.Soc.Chim.Belg.	104	4-5	104	1995
117	T.Halachev	P.Atanasova	A.Lopez Agudo	M.G.Arias	J.Ramirez			Appl.Catal.	136	A	161	1996
118	S.M.A.M.Bouwens	A.M.van.der.Kraan	V.H.J.de.Beer	R.Prins				J.Catal	128		559	1991
119	A.K.Rhodes							Oil & Gas Jounal	Oct.	2	35	1995
120	M.McMillan	J.S.Brinen	G.L.Haller					J.Catal	97		243	1986
121	J.L.R.Cerda	R.Prins						Bull.Soc.Chim.Belg.	100	n11-12	815	1991
122	D.Chadwick	D.W.Aitchison	R.Ohlbaum	L.Josefsson				Stud. Surf. Sci. Catal.	16		323	1983
123	A.Stanislaus	B.H.Cooper						Catal.Rev.	36	1	75	1994
124	M.Daage	R.R.Chianelli						J.Catal.	149		414	1994
125	R.Hubaut	J.P.Bonnelle	J.Grimblot					Trends in Phys.Chem.	2		277	1991
126	S.Kasztelan	A.Wambeke	L.Jalowiecki	J.Grimblot	J.P.Bonnelle			J.Catal.	124		12	1990
127	C.Moreau	C.Aubert	R.Durand	N.Zmimita	P.Geneste			Catal. Today	4		117	1988
128	J.Kanai	J.A.Martens	P.A.Jacobs					J.Catal.	133		527	1992
129	M.A.Castillo	P.G.Vazquez	M.N.Blanco	C.V.Caceres				J.Chem.Soc.Franday Trans.	92	17	3239	1996
130	J.A.R.van.Veen	P.A.J.M.Hendriks	E.J.G.M.Romers	R.R.Andréa				J.Phys.Chem.	94		5275	1990
131	E.R.H.van.Eck	A.P.M.Kentgens	H.Kraus	R.Prins				J.Phys.Chem.	99		####	1995

DEUXIEME PARTIE : Préparation, caractérisation et performances catalytiques de solides à base de P, Mo, Ni et alumine élaborés par voie Sol-Gel

2.1 Introduction

To prepare Ni-Mo-P-Alumina hydrotreating catalysts, several routes such as conventional impregnation, equilibrium adsorption, precipitation and sol-gel methods can be generally selected depending on the objectives (see chapter 1.2). In the choice of catalysts preparation, the sol-gel method is extremely interesting from the following points of view :

1. Easy preparation procedure as catalyst formulations can be obtained directly in two steps (drying and calcination steps).
2. High surface area (i.e. more than 400 m^2/g) can be easily achieved.
3. High metal loading (i.e. more than 30 wt% of Mo) can be easily obtained.
4. High metal dispersions can be achieved at the above high metal loading.
5. Catalytic activity higher than the ones obtained on conventional catalysts can be obtained.
6. Suitable for surface science characterizations because of their high metal loadings and high surface area. It is possible to detect species whose role is very important in relatively minor quantity.

In this part, the effects of P on the textural, structural and catalytic properties of Ni-Mo-P-Alumina based hydrotreating catalysts prepared by an advanced sol-gel method are investigated to show their improvements.

Background on sol-gel preparation of solids

In general, reactions involved in sol-gel chemistry are classified as follows.

Exchanging of alcoholate groups

A part of alcoholate groups (OR) of metal (M) alkoxides are exchanged by molecules of the alcoholic solvent.

$$M(OR)_n + m\,R'OH \rightarrow M(OR)_{n-m}(OR')_m + m\,ROH \quad (n \geq m)$$

The exchanging rate increases when the steric factor of the alcoholate decreases.

Ex. $O_{Me} > O_{Et} > O_{Pr} > O_{Bu}^{sec} > O_{Bu}^{t}$

The hydrolysis step

The OR groups are released from the metal alkoxide by a nucleophilic attack of H_2O.

$M(OR)_n + x\,H_2O \rightarrow M(OR)_{n-x}(OH)_x + x\,ROH$ [if n>x]

or

$M(OR)_n + n\,H_2O \rightarrow M(OH)_n + n\,ROH$

<u>The condensation step</u>

Furthermore, the condensation reactions take place with competition between three reactions.

i) alcooxolation

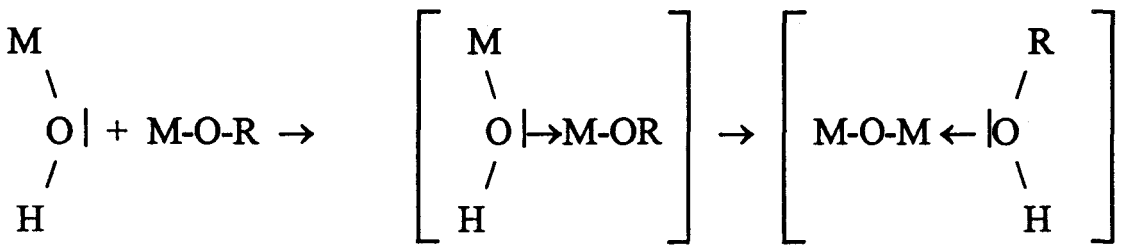

$\rightarrow$ M-O-M + ROH

ii) Oxolation

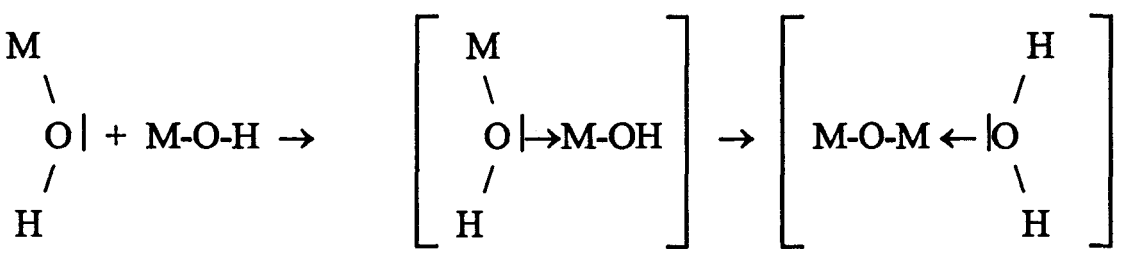

$\rightarrow$ M-O-M + H_2O

iii) Olation

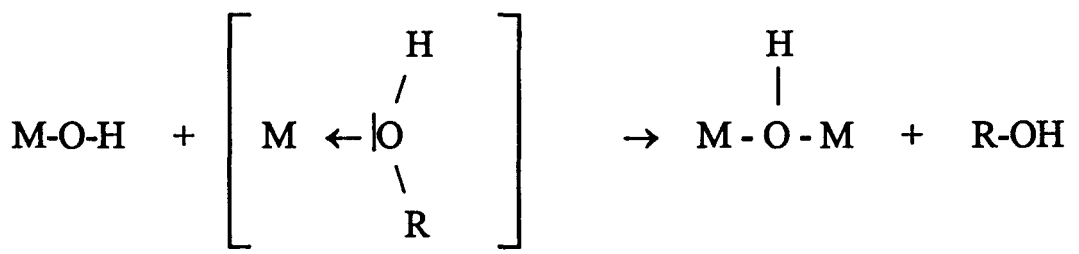

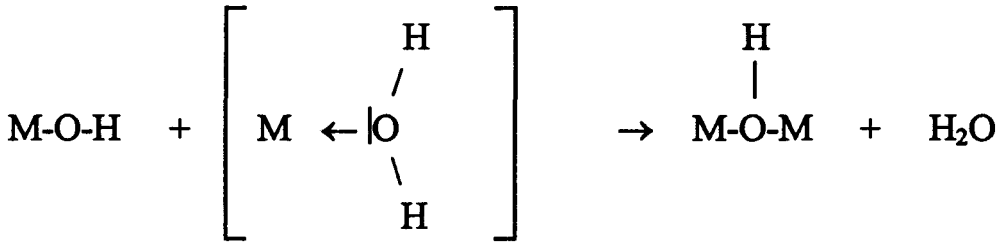

The physico-chemical properties of resulting solids depend on all the reactions written above and consequently on the nature of metal center M, nature of alkoxide groups, ratio between the solvent to alkoxide, reaction conditions and so on.

2.2 Le système Mo-P-Alumine

2.2.1

Genèse, structure et propriétés catalytiques du système Mo-P-Alumine préparé par voie sol-gel

(Cette partie a été publiée dans ***Studies in Surface Science and Catalysis, 106, 195 (1997).***)

Genesis, Characterizations and HDS Activity of Mo-P-Alumina Based Hydrotreating Catalysts Prepared by a Sol-Gel Method

R. Iwamoto [a,b] and J. Grimblot [a]

[a] Laboratoire de Catalyse Hétérogène et Homogène, URA CNRS D402, Université des Sciences et Technologies de Lille, 59655 Villeneuve D'Ascq Cédex, France

[b] Central Research Laboratories, Idemitsu Kosan Co., Ltd., 1280 Kami-izumi Sodegaura, Chiba, Japan

ABSTRACT

Mo oxide - P oxide - Aluminum catalysts with a wide range of P loading (0-14 wt%) were prepared by a sol-gel method to elucidate the role of phosphorous on the textural, structural and catalytic properties of Mo based catalysts. Two different Mo loadings (expected ~20 and ~30wt%Mo) and two kinds of P precursors (phosphoric acid, phosphorus pentoxide) were examined. The structural properties of dried and calcined forms were studied by means of various characterization techniques. Specific surface area (S.S.A.) of catalysts were decreased proportional to the P loading in every series. Especially, the S.S.A. in the series of P_2O_5 precursor decreased drastically above 7.7wt%P loading. XRD measurements revealed that excess loading of Mo and P within the alumina framework provokes aggregation of bulk MoO_3 (above 6.8wt%P in the series of 30wt%Mo for H_3PO_4 precursor and above 5.5wt%P in the series of P_2O_5 precursor). From IR measurements, it was found that P and Mo atoms interact with equivalent sites of alumina. From NMR measurements, predominant formation of Mo-P heteropoly complex were observed in the drying step. P interacted strongly not only with alumina framework but also with P itself. P_2O_5 prefers to polymerize by calcination. It was also found that Mo enhanced the interaction of P with alumina through the formation of P-Mo heteropoly complex. Water extraction tests revealed that Mo and P interacts strongly with the alumina framework. The HDS activity was not promoted by P while excess P decreased HDS activity with the formation of bulk MoO_3.

1. INTRODUCTION

The active phase of hydrotreating catalysts generally consists of Mo sulfide deposited on γ-alumina which was produced by calcination of alumina hydroxides precursors. The Mo precursor is usually introduced to alumina by conventional dry or wet impregnation methods. However, only up to 10-12 wt% Mo can be dispersed by these methods. In previous works, new preparation methods of well-dispersed Mo precursor based on a sol-gel method were proposed [1][2]. In this sol-

gel method, alumina is obtained by hydrolysis of aluminium tert-butylate or aluminium sec-butylate. Mo is incorporated homogeneously with the alumina precursor during the support preparation. This advanced method can give at least 30 wt% of well dispersed Mo and higher HDS activity than conventional catalysts. Indeed, the physico-chemical properties of resulting solids depend on the reactions involved in the sol-gel process (hydrolysis, condensation through alcooxolation, oxolation or olation steps), on the nature of the metal or the associated alkoxide and finally on the reaction condition (temperature, the ratio between the solvent and alkoxide). Furthermore, the sol-gel preparation method is very convenient not only for obtaining active catalysts but also for investigating what happens on the surface of catalysts because of their unique high S.S.A..

To achieve higher activity with the sol-gel catalyst, it is useful to investigate the effect of promoter and additives such as Co, Ni and P on the Mo-based sol-gel catalysts. The role of P on the HDS activity for Mo based hydrotreating catalysts has been studied by many researchers, while the precise effect has not been well understood yet [3-5]. Eijsbouts et al. reported that P had no effect on the HDS activity for MoO_3/Al_2O_3 [3]. On the other hand, Lewis et al. and Kim et al. reported a positive effect for HDS reaction in the region of low P loading [4][5].

In this work, we wished to elucidate the role of P on the Mo-P-alumina sol-gel catalysts which contain high loading of Mo and a wide range of P amounts. Their main structural and textural properties will be compared as well as their performance in thiophene HDS.

2. EXPERIMENTAL

2.1 Catalyst preparation

Mo-P-Alumina catalysts were prepared on the basis of a sol-gel method according to the procedures in Figure 1. Alumina was prepared by the hydrolysis of aluminium sec-butylate (ASB) dissolved in 2-butanol (2BN) and 1,3-butanediol (13BD). Mo and P were incorporated with the alumina precursor during the gel preparation. Mo was added to the aluminium alkoxide before hydrolysis as a dispersion of ammonium heptamolybdate (AHM) in 13BD. P was introduced by different ways depending on the nature of precursor. P_2O_5 precursor was introduced in ASB solution after dissolving in 2BN (Route A). On the other hand, 99% of ortho-phosphoric acid (H_3PO_4 precursor) was dissolved in 13BD simultaneously with AHM (Route B). The catalysts obtained at each stage are noted to MPD(X-Y)H, MPC(X-Y)P where the MPD, MPC means dried and calcined sample, X,Y means expected loadings in wt% of Mo and P respectively. H, P refer to the nature of P precursor such as H_3PO_4 or P_2O_5 respectively. The ratio of H_2O/ASB was usually kept at 10. It was noted however as * if H_2O/ASB was increased to 100.

2.2 Catalysts characterization

The chemical compositions were provided by "Service Central d'analyse du CNRS" (Vernaison, France). The obtained powders were characterized by BET

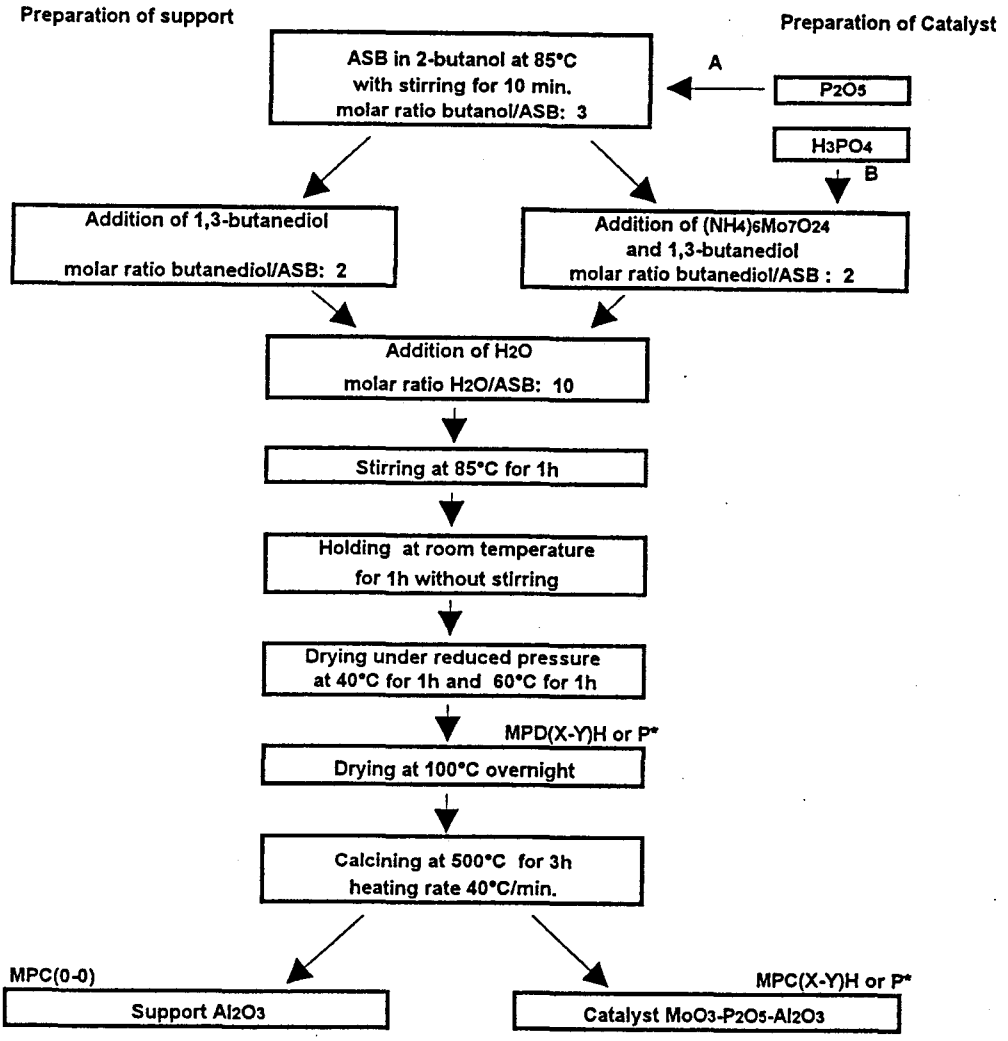

Figure 1. Procedure for preparation of Mo-P-Al sol-gel catalysts

specific surface area (QUANTASORB Jr., Quantachrome; pretreated at 200°C for 30 min.), X-ray powder diffraction(XRD) (Siemens D5000 Diffractometer equipped with a goniometer, a monochromator and a Cu X-ray tube), Infrared Spectroscopy (FTIR, Nicollet510 Spectrometer, sample was pelleted with KBr), ^{27}Al-NMR (BRUKER ASX400; resonance frequency 104.26MHz, recycling time 3 sec., pulse length 1 μsec., spinning frequency 15kHz and reference $Al(H_2O)_6^{3+}$) and ^{31}P-NMR (BRUKER ASX100; resonance frequency 40.53MHz, recycling time 40 sec., pulse length 2 μsec., spinning frequency 7kHz and reference H_3PO_4).

2.3 Catalytic activity (HDS)

Hydrodesulfurization of thiophene was carried out at atmospheric pressure in a flow type reactor packed with 0.2g of catalyst. The catalyst was sulfided at 400°C for 2h with a H_2/H_2S (90/10) mixture gas at flow rate of 50 ml/min. After cooling down to 300°C, thiophene purified by vacuum distillation was introduced in the reactor at constant pressure (50 torr) with a flow of dried hydrogen (10ml/min.). The reaction products were analyzed by gas chromatography.

3. RESULTS AND DISCUSSION

3.1 Specific surface area and chemical composition

Table 1 shows chemical composition and specific surface area per gram of calcined catalyst (S.S.A.) of all prepared samples. Amounts of Mo and P were almost those expected except for MPC(30-14)P*. It is suggested that excess water enhanced dissolution of AHM and prevents incorporation with alumina. As already reported in a previous report [1][2], the bare alumina MPC(0-0) and Mo oxide alumina such as MPC(20-0), MPC(30-0) have higher S.S.A. compared with conventional ones [6]. With introducing P, the S.S.A. decreased proportional to the amount of P loading in every series. Especially, the S.S.A. decreased drastically above 7.7wt%P loading in the series of P_2O_5 precursor. It is presumed that P and cracked alcohol residues may block the porosity of sample because large amount of carbon (5.9wt%) was found on the MPC(30-13)P. However the corresponding MPC(30-14)P* which was prepared with increasing H_2O/ABS ratio showed less carbon residue but still low S.S.A. ($13 m^2/g$).

Table 1.
Chemical composition and S.S.A. of prepared catalysts

Catalysts	Mo (wt%)	P (wt%)	Carbon(wt%)	S.S.A.(m^2/g)
MPC(0-0)	0	0	0.5	503
MPC(20-0)H	17.5	0	0.2	586
MPC(20-1)H	17.9	1.6	0.3	570
MPC(20-2)H	17.3	2.2	0.2	560
MPC(20-3)H	17.2	3.1	0.2	559
MPC(20-4)H	17.9	4.4	0.2	525
MPC(20-7)H	16.8	6.6	0.3	505
MPC(20-11)H	16.4	11.3	0.3	428
MPC(30-0)H	26.0	0	-	523
MPC(30-1)H	25.9	1.1	0.1	505
MPC(30-2)H	26.5	2.2	0.1	443
MPC(30-5)H	25.3	4.6	0.1	411
MPC(30-7)H	25.8	6.8		405
MPC(30-11)H	25.3	11.1	0.1	263
MPC(30-1)P	28.3	1.7	0.3	508
MPC(30-3)P	27.7	2.7	0.6	490
MPC(30-6)P	25.5	5.5	0.2	439
MPC(30-8)P	26.7	7.7	0.2	238
MPC(30-13)P	25.3	12.7	5.9	4
MPC(30-14)P*	16.5	13.7	0.3	13
MPC(0-11)H	0	10.6	0.3	474
MPC(0-10)P	0	12.1	-	486

3.2 X-ray powder diffraction (XRD)

(a)H_3PO_4 precursor

Figure 2 shows the XRD patterns of sol-gel catalysts obtained from the H_3PO_4 precursor. The bare alumina MPC(0-0) can be identified as poorly

crystalline γ-Al_2O_3. For P oxide-alumina MPC(0-11)H and Mo oxide-alumina MPC(30-0), no peak corresponding to P or Mo oxo-compounds can be detected. It is suggested therefore that Mo and P exist as a well dispersed species. It was also observed that incorporation of Mo and/or P with alumina prevents the formation of structured γ-Al_2O_3. They seem to be present in an amorphous matrix. For Mo-P-Al, the well dispersed state of Mo oxide is kept up to MPC(20-11)H in the series of 20wt%Mo (not shown here) and up to at least MPC(30-5)H in the series of 30wt%Mo. However, bulk MoO_3 can be identified above MPC(30-7)H. This result means that high loading of Mo and P within the alumina framework provokes aggregation of bulk Mo oxide.

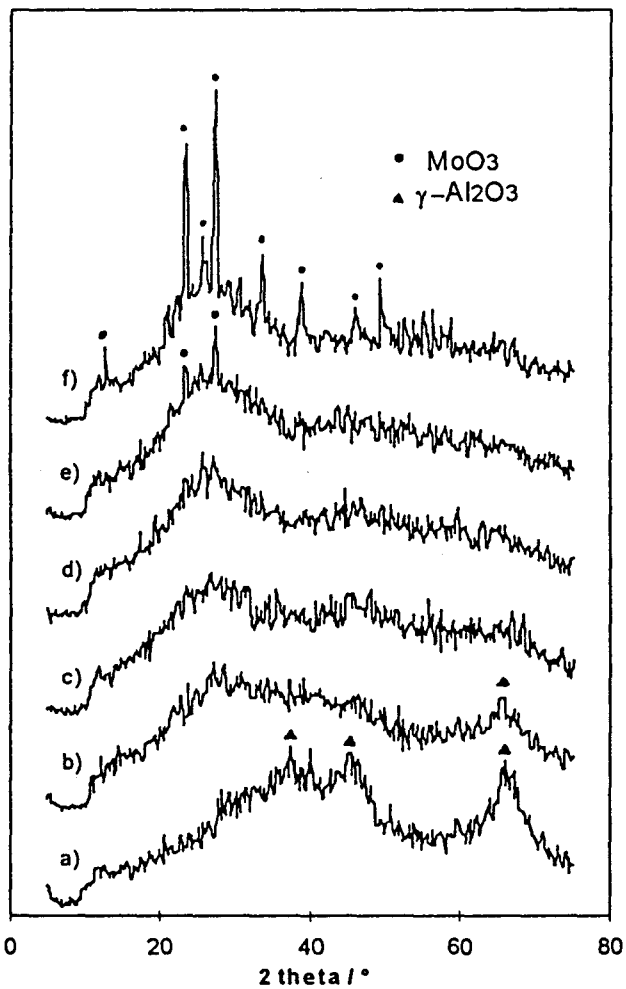

Figure 2. XRD patterns of Mo-P-Al sol-gel catalysts prepared from the H_3PO_4 precursor. (a)MPC(0-0), (b)MPC(0-11)H, (c)MPC(30-0), (d)MPC(30-5)H, (e)MPC(30-7)H, (f)MPC(30-11)H

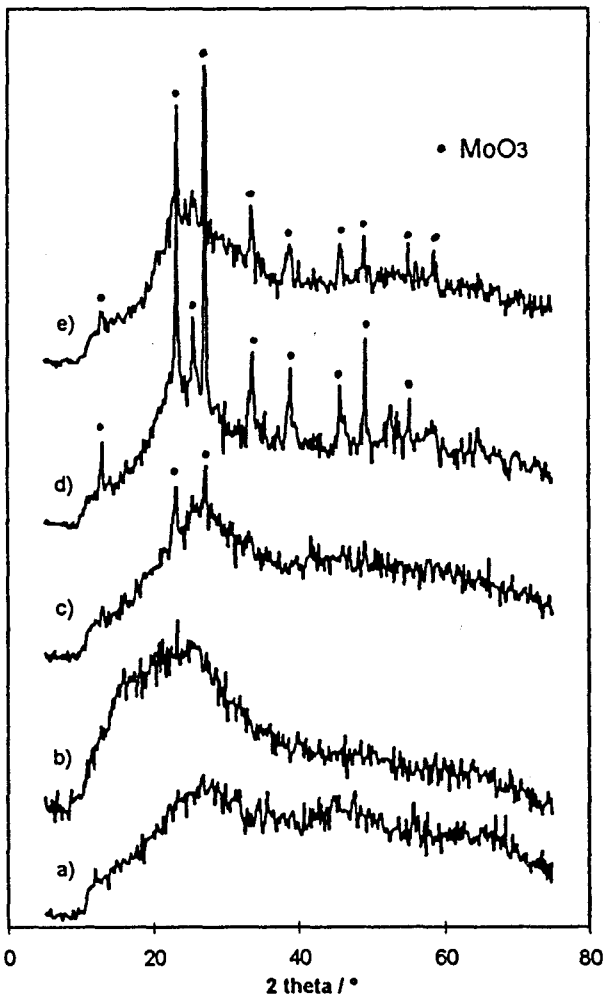

Figure 3. XRD patterns of Mo-P-Al sol-gel catalysts prepared from the P_2O_5 precursor (a)MPC(30-0), (b)MPC(30-3)P, (c)MPC(30-6)P, (d)MPC(30-13)P, (e)MPC(30-14)P*

(b)P_2O_5 precursor

Figure 3 shows the X-ray powder diffraction patterns of sol-gel catalysts obtained from the P_2O_5 precursor. The addition of P_2O_5 precursor showed similar effect as the H_3PO_4 precursor. However, the intensity of bulk MoO_3 in MPC(30-6)P which contains 5.5wt%P was almost the same as that observed in MPC(30-7)H which contains 6.8wt%P. It was concluded therefore that the P_2O_5 precursor enhanced the formation of bulk MoO_3 compared with H_3PO_4 precursor at the same loading of Mo.

3.3 Infrared spectroscopy

(a)H_3PO_4 precursor

The assignment of IR bands in Mo-P-Alumina based catalysts have been already reported by many researchers [7-13]. Figure 4 shows IR spectra of dried and calcined catalysts obtained from the H_3PO_4 precursor.

For all dried catalysts, a broad band at ~750 cm^{-1} which is assigned to Al-O stretching was observed. Furthermore, many small bands and shoulders were observed (i.e. at 1458, 1370, 1135 and 1055 cm^{-1} etc.), though it is sometimes difficult to identify. These bands could be assigned to residual alcoholate incorporated in the alumina framework or supported metal complexes, because they are well corresponding to IR spectra of the solvents (2BN,13BD). This fact indicates that the hydrolysis reaction of ASB does not proceed completely in this preparation condition. Bands at 1070 cm^{-1} for MPD(0-0) and MPD(0-11)H is considered as sol-gel boehmite [7]. P containing catalysts such as MPD(30-11)H, MPD(0-11)H have a broad band at ~1100 cm^{-1}. This band can be decomposed into three bands at 1115, 1080 and 1055 cm^{-1} which is assigned to stretching vibration of $P=O_t$, P-O and P-O-Mo of heteropoly acid [8][9]. This result assumes that P-Mo heteropoly compound was formed during the gel precipitation. Specific bands at ~1404, 900 and 845 cm^{-1} which can be assigned to AHM were observed in MPD(30-11)H. It is considered that P prevents the incorporation of Mo within the alumina framework even at the drying step since the intensity of these bands are well correlated to the P content.

For the calcined samples, all the spectra are rather broad. With increasing loading of P, a large broad band appeared again at about 1100 cm^{-1} which can be decomposed into two bands at 1125 and 1090 cm^{-1}. They are assigned to the $P=O_t$ and P-O respectively [9][10]. In MPC(30-11)H, bands at 1000, 880 and 823 cm^{-1} which are assigned to bulk MoO_3 were also detected. This result is in well agreement with the results of XRD. It is suggested that the main part of MoO_3 derived from decomposition of bulk AHM with calcination.

In MPC(0-0), characteristic three bands at 1640, 1503 and 1425 cm^{-1} which might be assigned to physically or coordinately adsorbed H_2O were observed. However, the two of three bands were disappeared with the introduction of Mo and/or P [11]. This result indicates that Mo and P are interacting with equivalent sites of Al_2O_3. This is a reason why a part of Mo cannot interact with Al_2O_3 when P content increases.

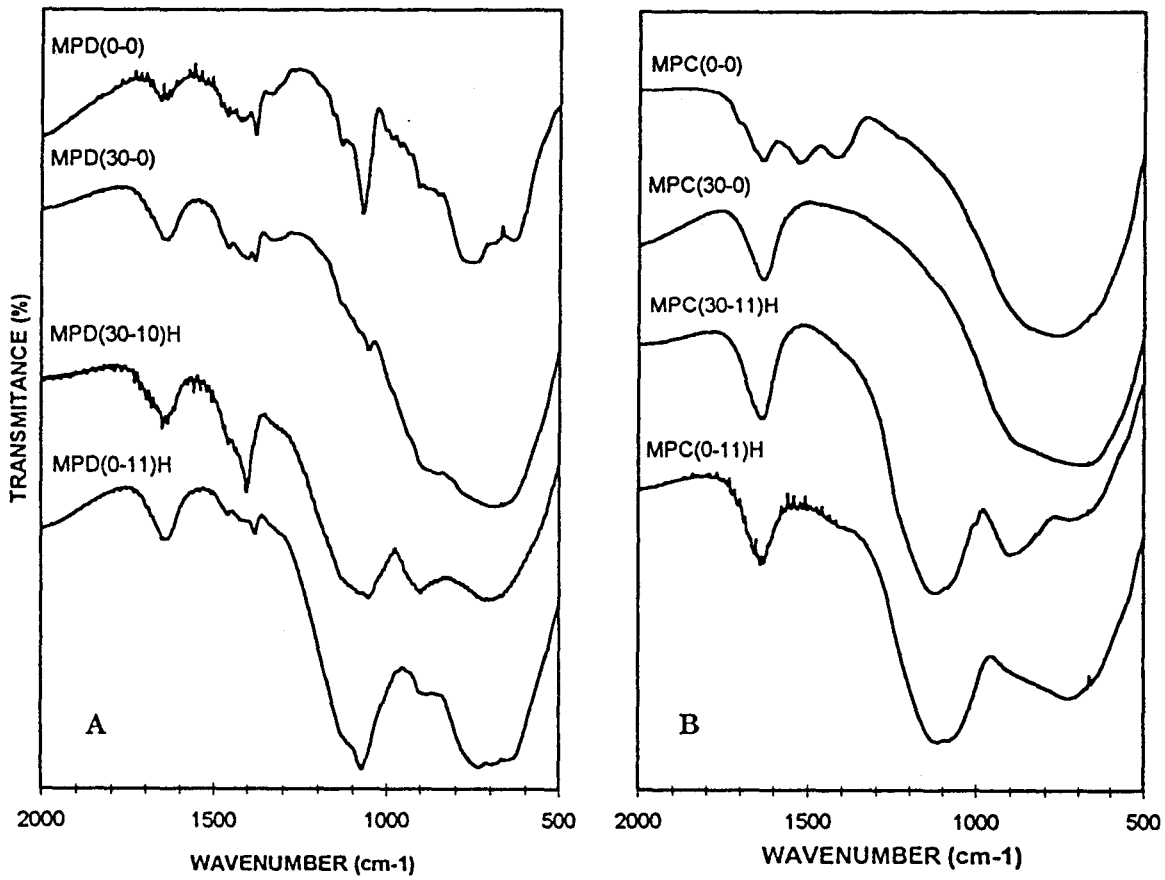

Figure 4. IR spectra of Mo-P-Al sol-gel catalysts prepared from the H_3PO_4 precursor. (A: after drying 100°C , B: after calcination at 500°C).

(b) P_2O_5 precursor

Figure 5 shows IR spectra of dried and calcined catalysts obtained from the P_2O_5 precursor. In MPD(0-10)P, a characteristic band which might be assigned to monomeric P species observed at 1000 cm^{-1}. In MPC(30-13)P, intensity of bands for the residual alcoholate was much more higher than those in MPD(30-11)H. It is suggested that P_2O_5 prevents the hydrolysis of ASB and eventually, it remains more alcoholate in the final compound. It is also assumed that part of these bands are attributed to organic P complex formed with the alcohol solvent, since the same IR spectra was obtained from dried P_2O_5 after dissolving it in 2BN. From the literature, the formula of these complexes are $PO(OH)_2(Obut)$, $PO(OH)(Obut)_2$ or $PO(Obut)_3$ [12]. These complexes are considered to be formed by the following reactions.

$$P_2O_5 + 2but\text{-}OH + H_2O \rightarrow 2PO(OH)_2(Obut) \quad (1)$$

$$P_2O_5 + 4but\text{-}OH \rightarrow 2PO(OH)(Obut)_2 + H_2O \quad (2)$$

$$P_2O_5 + 6but\text{-}OH \rightarrow 2PO(Obut)_3 + 3H_2O \quad (3)$$

For calcined samples, MPC(0-10)P showed broad bands between 1000 and 1330 cm^{-1} which are assigned to highly polymerized P oxo-compounds [13][14]. For MPC(30-13)P, the intensity of bands at 1090 and 1125 cm^{-1} which are assigned to P-O and P=O_t vibration decreased comparing with those in MPC(30-11)H. On the contrary, the intensity of band at 1200 cm^{-1} which is assigned to polymeric P oxo-compounds increased. It is suggested that MPC(30-13)P contains also more polymerized P oxo-species than MPC(30-11)H. If the ratio of H_2O/ASB increases from 10 to 100, the bands at 1330 cm^{-1} increased significantly. This means that the excess of water during the gel preparation provokes the aggregation of P. It is assumed that P has less interaction with alumina in the drying stage because a large part of P is involved in complexes with the alcohol solvent. In such a case, P prefers to polymerize than to interact with the alumina framework. The bands for bulk MoO_3 were also observed at 1000, 880, and 823 cm^{-1} in MPC(30-13)P and MPC(30-14)P*.

From the IR measurements, it was found that the P precursor affects significantly on the physicochemical properties of resulting catalysts.

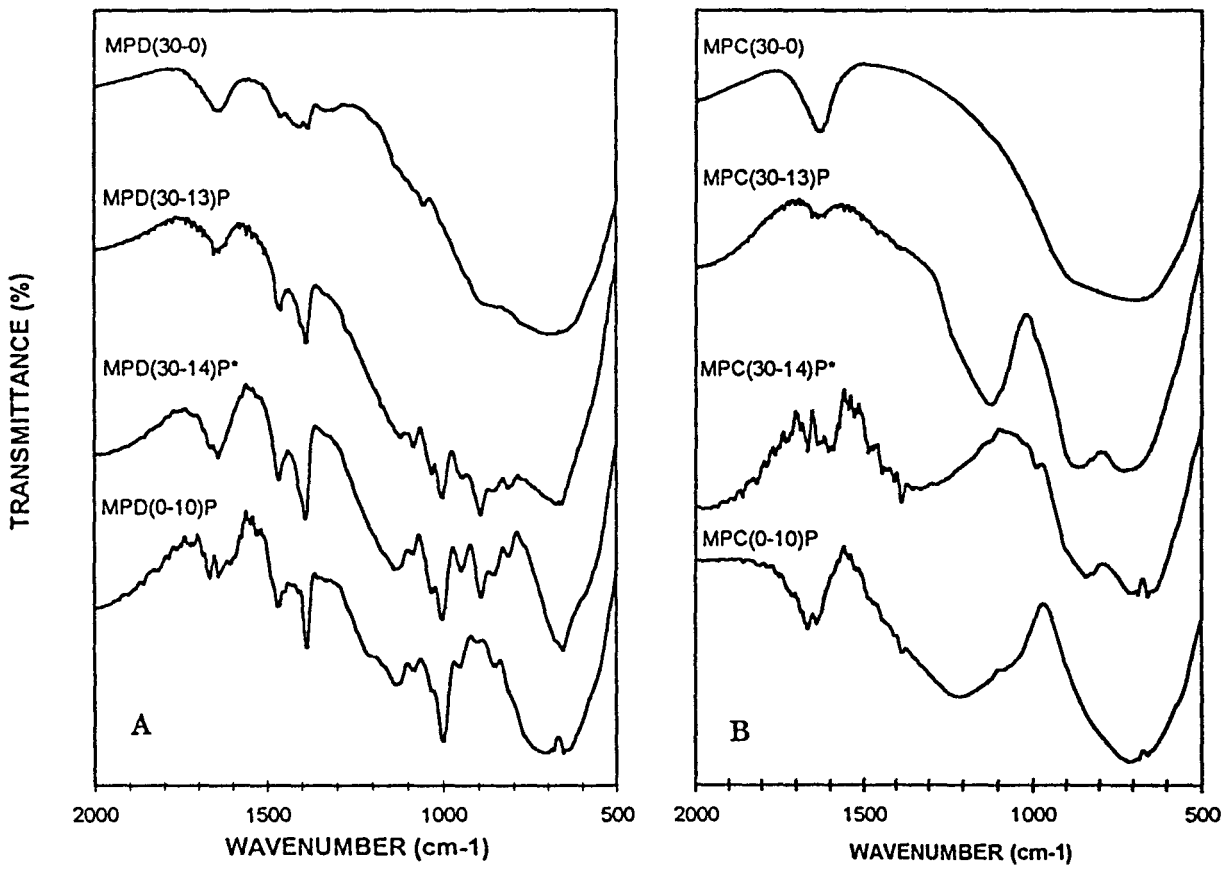

Figure 5. IR spectra of Mo-P-Al sol-gel catalysts prepared from the P_2O_5 precursor. (a) after drying 100°C , (b) after calcination at 500°C.

3.4 ^{27}Al-NMR

(a)H_3PO_4 precursor

Top peak value of ^{27}Al-NMR spectra are listed in Table 2. The assignment of ^{27}Al-NMR spectra in this region have already been reported by many researchers [15-22]. MPD(0-0) has a single broad signal at 7.2 ppm. This signal is assigned to octahedral alumina [15]. For all the Mo and P containing catalysts, tailing of spectra between 0 and -30 ppm or even presence of a shoulder at -5 ppm were observed depending on the content of Mo or P. This tailing should correspond to octahedral surface aluminium sites shell in which P or Mo are located in a second coordination [16]. These signals seem to be characteristic for sol-gel catalysts since surface informations are emphasized by the extremely large S.S.A.. In addition, P containing catalysts showed another weak signal at ~41 ppm which is assigned to $AlPO_4$. This result indicates that P interacts strongly with alumina framework even in the drying step. It was also revealed that the amount of interaction between P and alumina increased in the presence of Mo because the intensity of $AlPO_4$ in MPD(30-11)H was more stronger than that in MPD(0-11)H.

Table 2.
Results of ^{27}Al -NMR obtained from the Mo-P-Al sol-gel catalysts

Catalysts	Before calcination (ppm)				After calcination (ppm)			
MPD(0-0)		7.2			65.5	33.0	6.9	
MPD(0-11)H	40.2	7.1			65.5	39.0	6.6	-12.0
MPD(20-0)		6.5			62.2	30.0	5.2	
MPD(30-0)		6.2	-5.0		54.7	27.3	5.3	-13.6
MPD(20-11)H	41.2	6.0	-5.0		55.0	37.8	4.8	-13.6
MPD(30-11)H	41.2	5.9	-5.0			36.7	6.6	-13.6
MPD(30-13)P		13.7	-1.1			36.7	27.0	13 -2.9 -14.1
MPD(30-14)P*		13.6	-0.4			37.9	26.8	-2.9 -12.4
MPD(0-10)P	61.0	33.0	5.2		55.0		26.8	6.3

On the calcined bare alumina MPC(0-0), another new signal of tetrahedral aluminium site was observed at ~65 ppm [15]. Furthermore, a broad shoulder appeared at 33 ppm which might be attributed to 5-fold coordinated aluminium sites [17]. This signal is characteristic for the sol-gel alumina since it possesses a highly disordered and poorly crystalline structure as shown by XRD. The signal at ~30 ppm is also observed in the Mo loaded catalysts such as MPC(20-0) or MPC(30-0). The intensity of this signal increased with the increasing amount of Mo. This could be assigned to 5-fold coordinated aluminium sites since introduction of Mo prevents the crystallization of alumina and leads to much more distortion as already shown by XRD. However, another explanation as being due to the presence of a surface tetrahedral $Al(OMo)_4$ cannot be neglected.

Furthermore, MPC(30-0) gave a weak shoulder spectra at -13.6 ppm which is assigned to $Al_2(MoO_4)_3$ [18]. This compound is supposed to be derived from a following equation.

$$3\ MoO_3(bulk) + Al_2O_3(surface) \rightarrow Al_2(MoO_4)_3 \quad (4)$$

The formation of $Al_2(MoO_4)_3$ is more apparent in MPC(30-11)H, because the high P loading favors the formation of bulk MoO_3. However, MPC(0-11)H which contains only P also showed the shoulder signal at ~-13 ppm. This signal can be assigned to $Al(OP)_6$ in this case [19]. Hence, the signal of ~-13, 14 ppm might be considered as multiple states of octahedral surface alumina in which terminal OH are exchanged by Mo or P.

The spectra for $AlPO_4$ was observed at 37 to 39 ppm for all the P containing catalysts. Though the $AlPO_4$ already existed in the drying step, the main part of $AlPO_4$ forms during calcination. The intensity of $AlPO_4$ for MPC(20-11)H and MPC(30-11)H were much more stronger than that for MPC(0-11)H catalyst. This result indicates again that Mo provokes the formation of $AlPO_4$. Concerning the chemical shift, the top peak values of 6, 5 and 4-fold aluminium sites tend to decrease with the increasing amount of Mo. This might be caused by the increase in distortion of the alumina framework or by the decreases of the aluminium density in the shell of each aluminium sites when the Mo loading increases [20].

(b) P_2O_5 precursor

MPD(0-10)P had three signals at 61 ppm(weak), 33 ppm(weak) and 5.2 ppm(strong) which correspond to tetrahedral, 5-fold and octahedral aluminium sites respectively. MPD(30-13)P showed a large broad signal at -1.1 ppm and a small sharp signal at 13.7 ppm. The former signal could be assigned to less condensed octahedral aluminium sites [15]. The later signal might be assigned to $(Al(OH)_n(H_2O)_{6-n})(MoO_4)$ or $Al(OP)_5$ [19][21]. This result suggests that the P_2O_5 precursor prevents drastically the hydrolysis and condensation of the Al-alkoxide. Zaharescu et al. also reported that the rate of hydrolysis and condensation of Si-alkoxide is strongly influenced by PO(OR)x complexes in the P-TEOS system [22]. P complexes might affect on the accessibility of the metal alkoxide to water molecules or to other alkoxides for condensation.

In calcined catalysts, MPC(0-10)P showed also three signals at 55 ppm, 26.8 ppm(strong) and 6.3 ppm(strong) which correspond to tetrahedral, 5-fold and octahedral aluminium sites respectively similar to MPD(0-10)P. However, their respective populations were strongly modified. It is remarkable that no signal for the $AlPO_4$ was observed in MPC(0-10)P even after calcination. MPC(30-13)P gave a large broad signal at 36.7 ppm and a small sharp signal at -14.1 ppm which are assigned to $AlPO_4$ and $Al_2(MoO_4)_3$ or $Al(OP)_6$ respectively.

3.5 ^{31}P-NMR

(a)H_3PO_4 precursor

Table 3 shows the top peak value of ^{31}P-NMR spectra. The assignment of ^{27}P-NMR spectra in this region has been also reported by several researchers [23-27]. For the dried MPD(0-11)H, a broad signal which could be decomposed into 2 signals at -11 and -21 ppm was obtained. They are assigned to monomeric and polymeric P oxo-species respectively [23]. On the other hand, the Mo and P containing catalysts such as MPD(20-11)H, MPD(30-5)H and MPD(30-11)H showed another signal at about -15 ppm. This signal could be assigned to a P-Mo heteropoly compound in agreement with the IR observation. All the calcined catalysts showed broad overlapping signals at about -18 and ~-24 ppm which corresponds to polymeric P oxo-species and $AlPO_4$ respectively. Mo containing catalysts such as MPC(20-11)H and MPC(30-11)H gave less polymeric P than MPC(0-11)H. It is suggested that Mo is effective for dispersing P on the alumina through the formation of a P-Mo heteropoly complex. It was found that the top peak value of $AlPO_4$ signal for MPC(30-5)H and MPC(30-11)H shifts 2 ppm to the lower value.

Table 3.
Results of ^{31}P-NMR obtained from the Mo-P-Al sol-gel catalysts.

Catalysts	Befor calcination (ppm)			After calcination (ppm)	
MPD(0-11)H	-11		-21	-18	-24
MPD(20-11)H	-11	-15.9	-21	-18	-24
MPD(30-5)H	-11	-14.3		-18	-26
MPD(30-11)H	-11	-15.9	-21	-18	-26
MPD(30-13)P	-4 to -11	-14.6	-21	-19	-25
MPD(30-14)P*	-4 to -11	-14.6	-21	-18	-23
MPD(0-10)P	-4 to -11		-21	-19	

b)P_2O_5 precursor

MPD(0-10)P showed several overlapping signals between -4 and -11 ppm which might be assigned to multiple states of monomeric P such as $PO(OH)(OBut)_2$ and $PO(OBut)(OH)_2$ including their isomer structures. Zaharescu et al. reported that these complexes are not hydrolyzed by water [22]. MPD(30-13)P showed another signal at -14.6 ppm which is assigned to a Mo-P heteropoly compounds. This result means that a part of the organic P can form complexes with Mo as well as the H_3PO_4 precursor. Considering from the equilibrium studies by Jian et al. and Cheng et al. [24][25], it is supposed, that the P-Mo heteropoly compound was formed, for example, by the following reactions.

$$2H^+ + 14PO(OH)_2(OBut) + 5Mo_7O_{24}^{6-} \rightarrow 7H_2P_2Mo_5O_{23}^{4-} + 14But\text{-}OH + H_2O \quad (5)$$

or

$$Mo_7O_{24}^{6-} + 4H_2O \rightarrow 7MoO_4^{2-} + 8H^+ \quad (6)$$

and

$$6H^+ + 2PO(OH)_2(OBut) + 5MoO_4^{2-} \rightarrow H_2P_2Mo_5O_{23}^{4-} + 2But\text{-}OH + 3H_2O \quad (7)$$

After calcination, it was found that MPC(0-10)P showed only polymeric P at ~-19 ppm. No signal for the $AlPO_4$ was obtained at -24 ppm in agreement with ^{27}Al-NMR. It is considered that the P_2O_5 precursor tends to polymerize rather than to interact with the alumina framework because the alcoholate P complexes prevent the interaction with alumina. On the other hand, MPC(30-13)P showed two overlapping signals at -19 and -25 ppm which are attributed to the polymeric P oxo-species and the $AlPO_4$ respectively. These data indicate that the P-Mo heteropoly compounds induce the formation of $AlPO_4$. In the "$P_2Mo_5O_{23}$"structure, the two P atoms are located at top and bottom of the cluster respectively [25]. Therefore, it is thought to be easier for P to be in contact with the alumina framework.

From the above investigation, it was found that the hydrolysis and condensation reaction of the Al-alkoxide are extremely prevented by the P_2O_5 precursor. Therefore, another MPC(30-14)P* was prepared with increasing the ratio of H_2O/ASB=100 to accelerate the hydrolysis and condensation reactions. Figure 5 showed, however, that MPC(30-14)P* gave much more polymeric P oxo-species than MPC(30-13)P. It is considered that excess water shifted the equilibrium equation (5) and (7) to the left hand and consequently prevented the hydrolysis of alcoholate P precursor. Since increasing the H_2O/ASB ratio did not improve the hydrolysis reaction, P_2O_5 might prevent the access of alkoxide molecules to each other.

The amounts of Mo and P remaining after water extraction were also investigated in Table 4. In general, MoO_3, H_3PO_4 and heteropoly compounds are easily extracted by water while monolayer molybdate and $AlPO_4$ are hardly extracted [26][27]. The extent of extraction depends strongly on the strength of

Table 4.
Effect of water extraction on the atomic ratio Mo/Al and P/Al

Catalysts	Before water extraction		After water extraction	
	Mo/Al	P/Al	Mo/Al	P/Al
MPC(20-0)	0.13	-	0.14	-
MPC(20-11)H	0.18	0.37	0.14	0.40
MPC(30-0)	0.23	-	0.25	-
MPC(30-11)H	0.36	0.50	0.21	0.55

interaction between those compounds and support. It was found that the amount of Mo and P for MPC(20-0), MPC(20-11)H, MPC(30-0) catalysts after the water extraction gave almost same value as that of the initial catalysts. Therefore, all the Mo and P oxo-species in these catalysts have strong interaction with the alumina surface. On the other hand, the amount of Mo for MPC(30-11)H apparently decreases with the water extraction. Therefore, it is considered that a part of Mo cannot interact with alumina and leads to the formation of bulk MoO_3.

As the main conclusions from the characterizations, it appears that reactivity of P with Mo and alumina depends strongly on the nature of the P precursor and on the preparation conditions.

The scheme of interaction between P and other component is shown in Figure 6.

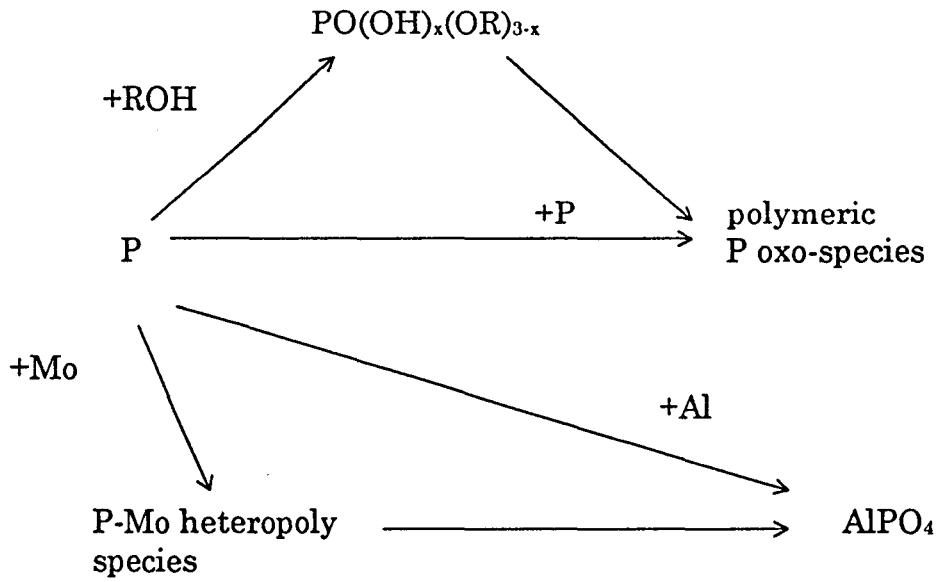

Figure 6. Schematic diagram for P transformation

3.6. Thiophene HDS activity

(a)H_3PO_4 precursor

Figure 7 shows the thiophene HDS activity and selectivity for the sol-gel Mo-P-Al catalysts prepared from the H_3PO_4 precursor as a function of P content. It was found that no effect was detected in the series of 20wt%Mo. On the other hand, a negative effect was obtained above 4wt%P in the series of 30wt%Mo. The decrease in the HDS activity should be attributed to the formation of bulk MoO_3 since bulk MoO_3 possesses less activity than dispersed Mo. Selectivity of C_4 products did not changed significantly while the selectivity of hydrogenated compound (butane) decreased slightly with the formation of bulk MoO_3

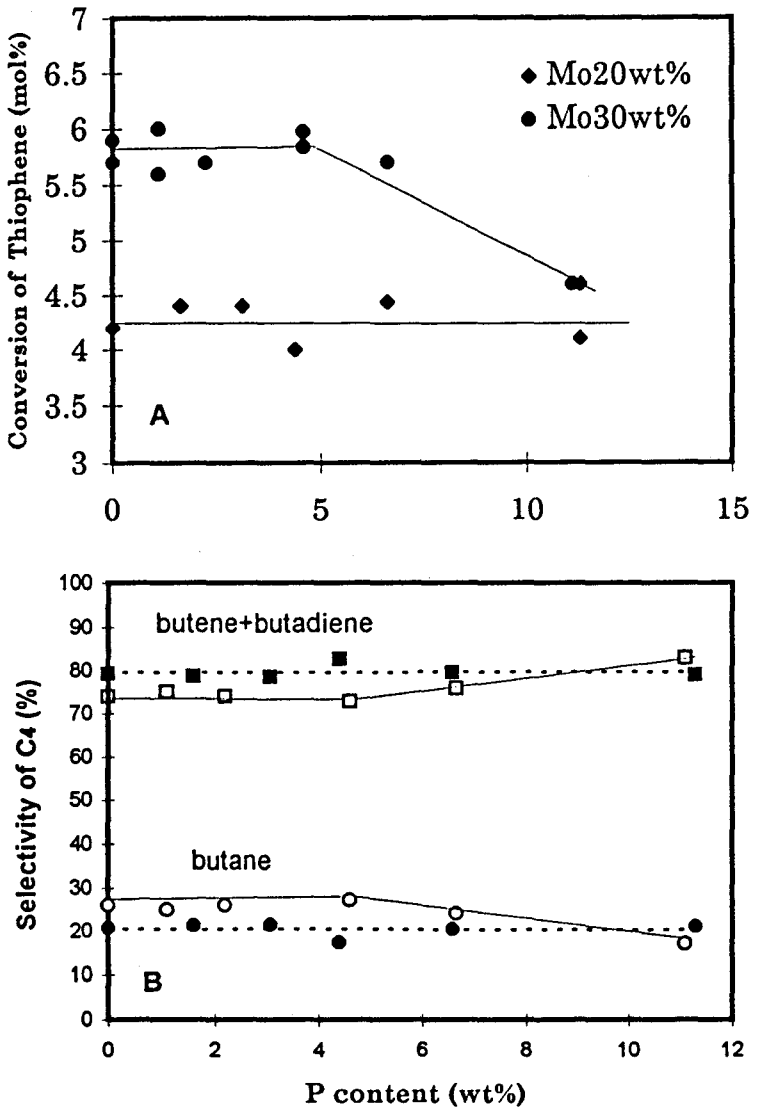

Figure 7. Thiophene HDS activity and selectivity products on Mo-P-Al sol-gel catalysts prepared from H_3PO_4 precursor. In B, ■,● mean the series of 20wt%Mo and □,○ mean the series of 30wt%Mo.

b)P_2O_5 precursor

Figure 8 shows the thiophene HDS activity and selectivity for the Mo-P-Al sol-gel catalysts prepared from the P_2O_5 precursor. The almost same trend was obtained as the H_3PO_4 precursor, though the activity started to decrease above ~4wt%P. This limit is lower than that found in H_3PO_4 series because the P_2O_5 precursor favors the formation of bulk MoO_3 and carbon in the preparation procedure (see Table 1). It is considered that only dispersion of Mo affects on the thiophene HDS activity in Mo-P-Alumina sol-gel catalysts.

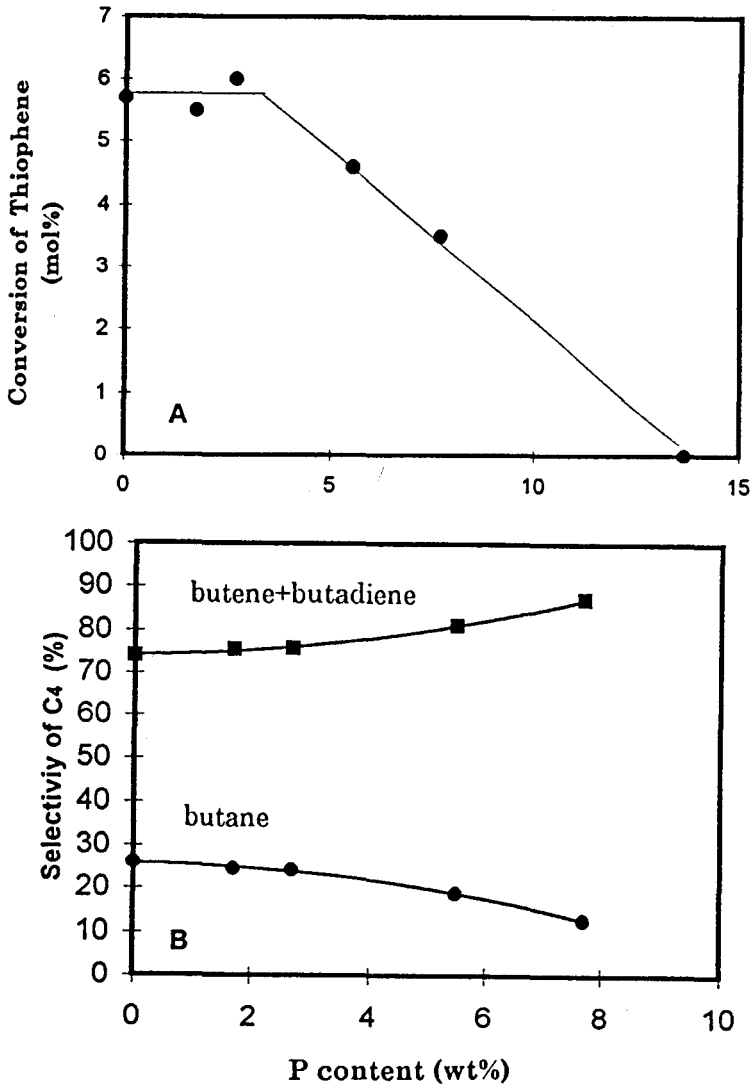

Figure 8. Thiophene HDS activity and selectivity of C_4 products on Mo-P-Al sol-gel catalysts prepared from P_2O_5 precursor.

4. CONCLUSION

Mo-P-Al sol-gel catalysts with a wide range of P loading were prepared to elucidate the role of phosphorous on the textural, structural and catalytic properties of Mo based catalysts. It was found that the amount of P, the nature of P precursors and the preparation conditions affect significantly on the physicochemical properties and HDS activity. In drying step, predominant formation of a P-Mo heteropoly complex was observed. With calcination, P interacts strongly not only with the alumina framework but also with P itself. The interaction between P and alumina was enhanced in the presence of Mo via the formation of a P-Mo heteropoly complex. The P_2O_5 precursor prevents strongly the hydrolysis and condensation of the Al-alkoxide. The P_2O_5 has less interaction with alumina in the drying step and tend to polymerize by calcination. The HDS activity was not promoted by P and decrease with the formation of bulk MoO_3.

REFERENCE

[1] E. Etienne, E. Ponthieu, E. Payen, and J. Grimblot, J. Non-Cryst. Solids 147 &148, 764 (1992)

[2] L. Lebihan, C. Mauchaussé, L.Duhamel, J.Grimbot and E.Payen J.sol-gel Scien. Tech., 2,837 (1994)

[3] J. M. Lewis and R. A.Kydd, J. Catal., 136, 478 (1992)

[4] S. Eijsbouts, J. van Gestel, J. A. R. van Vean, V. H. J. de Beer and R.Prins, J.Catal., 131, 412 (1991)

[5] S. I. Kim and S. I. Woo, J.Catal., 133, 124 (1992)

[6] S. M. A. M. Bouwens, J. P. R. Vissers, V. H. J. de beer and R. Prins, J. Catal., 112 (1988)

[7] E. Ponthieu, E. Payen, G. M. Pajonk and J. Grimblot, J. Sol-Gel, Sci.Tech., 8, 201, (1997)

[8] A. Spojakima and S. Damyanova, React. Kinet. Catal., 53, 2, 405 (1994)

[9] P. Atanasova and T. Halachev, Appl. Catal., 48, 295 (1989)

[10] J. M. Lewis and R. A. Kydd, J. Catal., 132, 465 (1991)

[11] P. M. Boorman, R. A. Kydd, T. S. Sorensen, K. Chong, J.M.Lewis and W. S. Bell, Fuel, 71, january, 87, (1992)

[12] W. Weng and J.L.Baptista, J.Sol-Gel.Sci.Tech., 8, 645, (1997)

[13] A. Spojakima and S. Damyanova and L. Petrov, Appl. Catal., 56, 163, (1989)

[14] C. Morterra, G. Magnacca and P. P. de Maestri, J. Catal., 152,384 (1995)

[15] Y. Kurokawa,Y. Kobayashi and S. Nakata, Hetero. Chem. Rev., 1, 309 (1994)

[16] F. M. Bautista, J. M. Campelo, A. Garcia, D. Luna, J. M. Marina and A. A. Romero, Appl. Catal., 96, 175 (1993)

[17] S. H. Risbud, R. J. Kirkpatrick, A. P. Taglialavore and B. Montez, J. Am. Ceram. Soc., 70, 1, C10 (1987)

[18] I. H. Cho, S. B. Park and J. H. Kwak, J. Mol. Catal., 104, A, 285, (1996)

[19] R. K. Brow, R. J. Kirkpatrick and G. L. Turner, J. Am. Ceram. Soc.,73 (8), 2293 (1990)

[20] S. Rezgui, B. C. Gate, Chem. Mater., 6, 2386 (1994)

[21] J. C. Edwards and E.C.Decanio, Catal. Lett., 19, 121, (1993)

[22] M. Zaharescu, A. Vasilescu, V. Badescu and M. Radu, J. Sol-Gel, Sci.Tech., 8, 59, (1997)

[23] E.C.Decanio, J. C. Edward, T. R. Scalzo, D. A. Storm and J. W. Bruno, J. Catal., 132, 498, (1991)

[24] M. Jian and R. Prins, Bull. Soc. Chim. Belg., 104, n4-5, 104 (1995)

[25] C. Cheng and N. P. Luthra, J. Catal., 109, 163, (1988)

[26] N. R. Gazimzyanov, V. I. Mikhailov and V. V. Volod'ko, Kinet. Catal., 36,5,694, (1995)

[27] P. Atanasova, J. Uchytil, M. Kraus and T. Halachev, Appl. Catal., 65, 53 (1990)

2.2.2

Propriétés acides et hydrogénantes des catalyseurs Mo-P-Alumine préparés par voie sol-gel

(Cette partie est sous presse à ***Journal of Catalysis.***)

JOURNAL OF CATALYSIS 172, 000–000 (1997)
ARTICLE NO. CA971855

RESEARCH NOTE

Acidity and Hydrogenation Properties of Mo-P-Alumina Catalysts Prepared by a Sol–Gel Method

Ryuichiro Iwamoto*,† and Jean Grimblot*,[1]

*Laboratoire de catalyse hétérogène et homogène, URA CNRS 402, Université des Sciences et Technologies de Lille, 59655 Villenueve d'Ascq Cedex, France; and †Central Research Laboratories, Idemitsu Kosan Co. Ltd., 1280 Kami-izumi, Sodegura, Chiba, 299-02, Japan

Received February 27, 1997; revised July 14, 1997; accepted July 14, 1997

The decrease of the S, N, and metal compounds (Ni, V) in petroleum fractions is an important task to solve recent environmental problems. For this purpose, improvements of Mo-alumina based catalysts by addition of promotors (Co, Ni) (1–3) and also by incorporation of P (4–8) have deserved a considerable interest. However, the role of P in the catalysts formulations is still a matter of controversy (4–23). Several studies (9–18) using IR spectroscopy, temperature-programmed desorption of basic molecules, and surface reactions have tried to show the influence of P on the acid–basic properties of the catalysts. P has an effective influence, but the debate still exists as different techniques are used to probe the catalysts and also because they are prepared according to different methods with various amounts of P. Relevant studies (12, 19–23) also pointed out the influence of P in catalytic reactions, namely in hydrogenation reactions, in terms of changes of the activity and selectivity as well. Once again, the P loading, the way to introduce it in the catalyst, and the nature of the reactant lead to different conclusions.

In a previous paper (24), we have shown that catalysts prepared by a sol–gel method exhibit higher hydrodesulphurization (HDS) activity than conventional catalysts as it was possible to obtain high Mo loadings up to 30 wt% (in Mo) as well dispersed Mo oxo-species. Recently (25), we extended this preparation procedure to investigate Mo-P-alumina catalysts. Textural and structural characteristics were extensively discussed with data on HDS of thiophene. In the present note, we wished to elucidate the role of P on the acidity and hydrogenation property of those Mo-P-alumina catalysts containing ~26 wt% of Mo and up to 11 wt% of P. Cyclohexene (CHE) hydrogenation and cyclopropane (CP) were the selected reactions to test the hydrogenation and acidity changes induced by P.

The procedures for the catalysts preparation and their textural and structural characteristics are extensively described in Ref. (25). The alumina precursor is the aluminium secbutylate. Mo as ammonium heptamolybdate and P as P_2O_5 or H_3PO_4 are incorporated during the gel formation. Among the two series prepared with ~17 wt% Mo and ~26 wt% Mo, only the second one has been considered in this work as it shows higher HDS activity, despite a decrease of the specific surface area for the highest P loading. Nomenclature of the catalysts is the same as previously (25).

Hydrogenation of cyclohexene (CHE) was carried out at atmospheric pressure in a flow-type reactor with 0.2 g of catalyst presulphided at 400°C for 2 h with a H_2/H_2S (90/10) gas mixture (50 ml · min^{-1}). Then, CHE was introduced in the reactor at 350°C at constant partial pressure (100 Torr) with dry H_2 at a total gas flow rate of 10 ml · min^{-1}. The reaction products were analyzed by gas chromatography, at the steady state, 2 h after introduction of CHE. Cracking of cyclopropane (CP) was carried out at atmospheric pressure in a flow-type reactor with 0.2 g of catalyst. Two reaction conditions were used. In the first case, activity was measured at 350°C in the absence of H_2 on the oxidic catalysts with a CP/He (5/95) gas mixture at a flow rate of 5 ml · min^{-1}. For the second condition, activity was measured at 350°C in the presence of H_2 on the presulphided catalysts (same conditions as above). A CP/He/H_2 (2.5/47.5/50) gas mixture at a total flow rate of 10 ml · min^{-1} was used. Conversion of CP was determined by gas chromatography, at the steady state, 1 h after introduction of CP.

The results on CHE hydrogenation obtained with the Mo-P-alumina catalysts prepared with H_3PO_4 as the P precursor are reported on Table 1. Whatever the P content, the CHE conversion remains constant at about 26%. The main products are isomerized molecules like methylcyclopentane (MCPA) and methylcyclopentenes (MCPE), a totally hydrogenated molecule as cyclohexane (CHA) and the corresponding dehydrogenated benzene (BZ). Less than 1% of converted CHE is distributed in lighter fragments. The product distribution shows (Table 1) that the amount of BZ is quite independent on the P content while the amount of

[1] Corresponding author. E-mail: jean.grimblot@univ.lille1.fr.

0021-9517/97 $25.00

TABLE 1

Results of Cyclohexene (CHE) Hydrogenation at 350°C over Sulphided Mo-P-Alumina Sol–Gel Catalysts

Catalysts[a]	Mo (wt%)	P (wt%)	S.S.A. (m^2/g)	CHE conv. (%)	Product distribution (%)[b]			
					MCPA	MCPE	CHA	BZ
MPC(30-0)	26.0	0	523	27.2	3	10	63	24
MPC(30-2)H	26.5	2.2	443	24.7	4	14	66	16
MPC(30-5)H	25.3	4.6	411	27.4	5	20	55	20
MPC(30-7)H	25.8	6.8	405	26.3	6	27	48	19
MPC(30-11)H	25.3	11.1	263	26.2	7	39	38	16

[a] Nomenclature of catalysts is defined in Ref. (25). H means a preparation with H_3PO_4 as a P precursor.
[b] MCPA = methylcyclopentane , MCPE = methylcyclopentenes, CHA = cyclohexane, BZ = benzene.

isomerized molecules (MCPA + MCPE) increases with the P loading. Conversely, the proportion of CHA decreases with the P loading. Thermodynamic data indicate that the dehydrogenation reaction is favored at the working condition used. This can explain the presence of BZ in similar amount on all the sudied catalysts. Clearly, in the sulphided state, introduction of P in the catalyst formulation enhances acidity as CHE isomerization is promoted, whereas the hydrogenation potentiality decreases. This last result is similar to some observations reported by Walendziewski (12), Muralidhar *et al.* (22), and Poulet *et al.* (23) who found that hydrogenation of benzene, hexene, or isoprene respectively decreases with the addition of P in sulphided Co–Mo or Mo-alumina catalysts. However, inverse effects can also be found; for example, toluene hydrogenation increases in the presence of P in a Mo-alumina catalyst (23). The nature of the molecule to hydrogenate, the preparation method of the catalyst, and the amount of P have a strong influence on the hydrogenation ability of the catalysts. The isomerization results shown in Table 1 seem to indicate that P is directly participating in the structure of the active phase and/or influences the strength of the acid sites as C–C bond hydrogenolysis is noticeably enhanced. In the oxidic Mo-P-alumina catalysts, we have already shown, mainly by IR and NMR spectroscopies, that P may interact with Mo to form P–Mo heteropoly species and also with the alumina framework. After sulphidation, the catalysts may have a memory effect of these interactions.

Cracking of CP will be considered first on the oxidic catalysts in the absence of H_2 in the reacting mixture. In the experimental conditions used, pure alumina does not show any evidence of cracking activity, whereas the catalysts containing Mo and/or P are active. The products obtained by CP cracking are mainly propane and propene. In some cases, small amounts of CH_4, C_2H_4, C_4H_6, and C_4H_8 are also obtained. Figure 1 shows the influence of the P content and of the nature of the P precursor (P_2O_5 or H_3PO_4) used to prepare the Mo-P-alumina catalysts on the CP conversion. The catalyst without P (catalyst MPC(30-0)) has already a high acidic potentiality as conversion of CP is 90.8% with a yield in ethylene of only 0.1%. This result has to be compared with the conversion obtained on a catalyst containing only P. For example, the MPC(0-11)H catalyst (10.6 wt% P, 474 $m^2 \cdot g^{-1}$) shows a CP conversion of 88% with no production of ethylene. It seems therefore that introduction of P or Mo in the alumina catalyst develops similar acidity with respect to CP conversion. The combination P–Mo is more efficient for CP cracking when H_3PO_4 is used as the P precursor. The activity increases quite linearly with the P content to reach 98.1% with a C_2H_4 yield of 1.4% for the MPC(30-11)H catalyst. Since the presence of both Mo and P increases the CP conversion and also increases the relative yield of ethylene, it is suggested therefore that the acid sites are probably stronger on the mixed Mo–P oxidic catalysts than on the oxomolybdate species or on the aluminium phosphate. On the other hand, CP conversion for the series prepared from P_2O_5 as a P precursor decreases with P loading, the effect being already noticeable at low

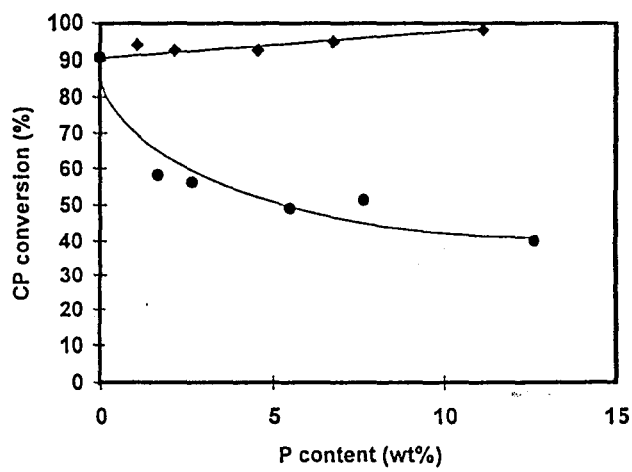

FIG. 1. The effect of the phosphorus precursor on the cyclopropane conversion. The catalysts were not sulphided prior to the tests and the reaction was carried out at 350°C in the absence of H_2: ◆, H_3PO_4 as a P precursor; ●, P_2O_5 as a P precursor.

P loading, where the decrease of the specific surface area is not yet dramatic (25). Clearly, the way of introducing P in the catalyst formulation has a strong influence on their acidic behavior; this can in part explain the discrepancies noted in the literature about the role of P. The decrease of the CP conversion in the series prepared with P_2O_5 might be mainly attributed to fewer interactions between the P oxo-species and the alumina support.

Let us now consider the CP conversion over sulphided catalysts (only catalysts prepared with H_3PO_4 are considered). Figure 2 shows that the CP conversion, in the presence of H_2 in the feed, increases with the amount of P introduced in the catalysts. In parallel, the relative amount of C_2H_4 increases as well. Clearly, the sulphidation step of the catalysts has not inhibited the synergy between P and Mo for developing acid sites strong enough to crack CP and produce a minor amount of ethylene. However, we have no direct evidence of whether the strong acid sites due to the interaction between Mo and P in the sulphided catalysts are the same as the ones present in the oxidic precursors. But it is possible, as already mentioned in the part concerning the CHE conversion results, that the sulphided state of the catalysts have a memory effect of the P–Mo interaction. To show the effect of H_2 in the reactive mixture, the CP conversion has been measured in the same run with and without the presence of hydrogen over the sulphided MPC(30-7)H catalyst (Fig. 3). The CP conversion decreases drastically from ~95% in presence of H_2 to ~75% in the absence of H_2 while the activity recovers almost the same level when the hydrogen is reintroduced in the reactive feed. Such a positive effect of hydrogen in the reactive feed is a clear indication that CP cracking on Mo-P-alumina catalysts proceeds differently, at least in part, on the sulphided state and on the oxidic form, even if the conversion values are at the same level. On the sulphided catalysts, the effect of H_2 might be

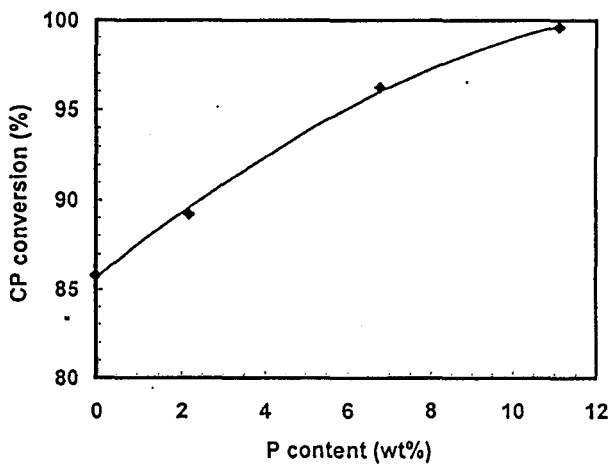

FIG. 2. The cyclopropane conversion over presulphided catalysts prepared from H_3PO_4 as a precursor. The reaction was carried out at 350°C in the presence of H_2.

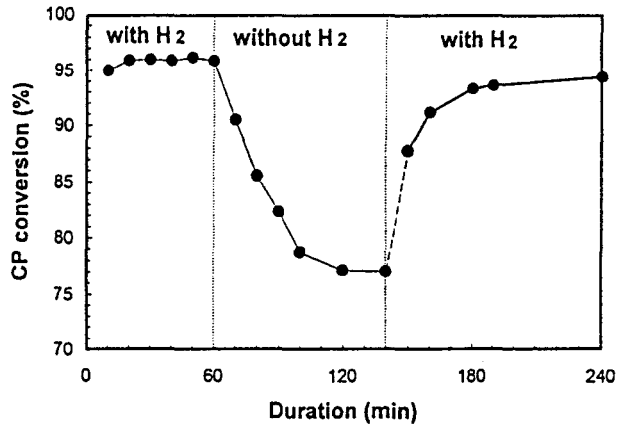

FIG. 3. The effect of hydrogen in the reactive feed on the cyclopropane conversion on the presulphided MPC(30-7)H catalyst.

to increase the quantity of acid SH groups (Brönsted sites) and/or to create coordinated unsaturated sites (CUS) which then act as Lewis acid sites. Since P has a negative effect on the Mo sulphidation extent (26), the presence of H_2 in the feed may also create acid OH groups associated with the Mo remaining oxo-species. The last possible effect of H_2 could be the modification of the P oxo-species, probably associated with the alumina framework, where the $P{=}O_t$ groups (identified by IR; see Ref. (25)) are giving P–OH surface species. At the present time, it is not possible to exclude one of these possibilities for explaining the positive effect of H_2. Note only that chemical analyses of the sulphided catalysts after tests in CP cracking with H_2 in the feed revealed a S/Mo atomic ratio decreasing from ~2.0 to ~1.7 with the increase of the P content. This result could be associated with a worse sulphidability of the Mo oxo-species in the presence of P or also with the formation of smaller MoS_2 crystallites. In such a case, the relative amount of Mo at the edges of the MoS_2 patches is optimal (see the geometrical model of Kasztelan *et al.* (27, 28)) with, consequently, the presence of an optimal number of CUS created by the effect of H_2 (29). Nevertheless, the other possible effects of H_2, as mentioned before, cannot be ruled out. Anyway, it is considered that the P addition in Mo-alumina-based catalysts does not increase the strength of acid sites enough to enhance hydrogenolysis of C–S as the HDS activity of thiophene at atmospheric pressure is not deeply modified (25).

REFERENCES

1. Prins, R., De Beer, V. H. J., and Somorjai, G. A., *Catal. Rev.* **31**(1 & 2), 1 (1989).
2. Delmon, B., *Stud. Surf. Sci. Catal.* **53**, 1 (1989).
3. Topsøe, H., Clausen, B. S., and Massoth, F. E., *in* "Catalysis" (J. R. Anderson and M. Boudart, Eds.), Vol. 11. Springer-Verlag, Berlin, 1996.
4. Kim, S. I., and Woo, S. I., *J. Catal.* **133**, 124 (1992).
5. Bouwens, S. M. A. M., Vissers, J. P. R., De Beer, V. H. J., and Prins, R., *J. Catal.* **112**, 401 (1988).

6. Eijsbouts, S., Van Gestel, J., van Veen, J. A. R., De Beer, V. H. J., and Prins, R., *J. Catal.* **131**, 412 (1991).
7. Chadwick, D., Aitchison, D. W., Ohlbaum, R., and Josefsson, L., *Stud. Surf. Sci. Catal.* **16**, 323 (1982).
8. Hendriks, J. A. J. M., Andéa, R. R., Romers, E. J. G., and Wilson, A. E., *J. Phys. Chem.* **94**, 5282 (1990).
9. Morterra, C., Magnacca, G., and De Maestri, P. P., *J. Catal.* **152**, 384 (1995).
10. Abbattista, F., Delmastro, A., Gozzelino, G., Mazza, D., and Vallino, M., *J. Chem. Soc. Faraday Trans.* **86**(21), 3653 (1990).
11. Petrakis, D. E., Hudson, M. J., Pomonis, P. J., Sdoukos, A. T., and Bakas, T. V., *J. Mater. Chem.* **5**(11), 1975 (1995).
12. Walendziewski, J., *React. Kinet. Catal. Lett.* **43**(1), 107 (1991).
13. Morales, A., Agudelo, M. M. R., and Hernandez, F., *Appl. Catal.* **41**, 261 (1988).
14. Stanislaus, A., Absi-Halabi, M., and Al-Dolama, K., *Appl. Catal.* **39**, 239 (1988).
15. Chen, Y. W., Hsu, W. C., Lin, C. S., Kang, B. C., Wu, S. T., Leu, L. J., and Wu, J. C., *Ind. Eng. Chem. Res.* **29**, 1830 (1990).
16. Sajkowski, D. J., Miller, J. T., and Zajac, G. W., *Appl. Catal.* **62**, 205 (1990).
17. Lewis, J. M., Kydd, R. A., Boorman, P. M., and Van Rhyn, P. H., *Appl. Catal.* **84**, 103 (1992).
18. Callant, M., Holder, K. A., Grange, P., and Delmon, B., *Bull. Soc. Chim. Belg.* **104**, 245 (1995).
19. Fierro, J. L. G., Lopez Agudo, A., Esquivel, N., and Cordero, V., *Appl. Catal.* **48**, 353 (1989).
20. Cordero, R. L., Esquivel, N., Lazaro, J., Fierro, J. L. G., and Lopez Agudo, A., *Appl. Catal.* **48**, 341 (1989).
21. Gishti, K., Iannibello, A., Marengo, S., Morelli, G., and Tittarelli, P., *Appl. Catal.* **12**, 381 (1984).
22. Muralidhar, G., Massoth, F. E., and Shabtai, J., *J. Catal.* **85**, 44 (1984).
23. Poulet, O., Hubaut, R., Kasztelan, S., and Grimblot, J., *Bull. Soc. Chim. Belg.* **100**, 857 (1991).
24. Lebihan, L., Mauchaussé, C., Duhamel, L., Grimblot, J., and Payen, E., *J. Sol-Gel Sci. Tech.* **2**, 837 (1994).
25. Iwamoto, R., and Grimblot, J., *Stud. Surf. Sci. Catal.* **106**, 195 (1997).
26. Iwamoto, R., and Grimblot, J., unpublished results.
27. Kasztelan, S., Toulhoat, H., Grimblot, J., and Bonnelle, J. P., *C.R. Acad. Sci. Paris* **299**(II), 289 (1984).
28. Kasztelan, S., Toulhoat, H., Grimblot, J., and Bonnelle, J. P., *Appl. Catal.* **13**, 127 (1984).
29. Wambeke, A., Jalowiecki, L., Kasztelan, S., Grimblot, J., and Bonnelle, J. P., *J. Catal.* **109**, 320 (1988).

2.2.3 Caractérisations des catalyseurs Mo-P-Alumine par ^{31}P, ^{27}Al MAS-RMN et 2-D ^{27}Al MQMAS-RMN

(Characterization of Mo-P-Alumina Sol-Gel Catalysts by Solid State ^{31}P, ^{27}Al MAS-NMR and 2-Dimensional ^{27}Al MQMAS-NMR)

Abstract

Conventional solid state ^{27}Al and ^{31}P Magic Angle Spinning Nuclear Magnetic Resonance (MAS-NMR) and an advanced two-dimensional ^{27}Al Multiple-Quantum MAS-NMR (2D-^{27}Al MQMAS-NMR) have been applied to characterize Molybdenum oxide-Phosphorus oxide-Alumina based hydrotreating catalysts (Mo-P-Alumina). These catalysts were prepared by a sol-gel method with high Mo loading (with Mo expected amounts of ~20 and ~30 wt%) and a wide range of P content (from 0 to 13 wt% of P). The chemical environments of Al and P strongly depend on the nature of the P precursor used in the sample preparation (H_3PO_4 or P_2O_5) and on the amount of P and Mo. From the ^{27}Al MAS-NMR measurements on dried P containing samples, formation of octahedral aluminium and of $AlPO_4$ (Al_{tetra}-O-P surface species) in small amount were observed. After calcination at 500 °C, the formation of tetrahedral and penta-coordinated aluminium was also observed, mainly in samples containing Mo. In fact, presence of molybdenum favors the interaction of phosphorus with the alumina framework, leading to important amount of Al_{tetra}-O-P. At higher P and Mo loadings, $Al_2(MoO_4)_3$ was also detected in the calcined sample. ^{31}P MAS-NMR measurements revealed the formation of monomeric or polymeric P oxo-compounds after drying and polymeric P oxo-compounds or $AlPO_4$ after calcination, respectively. Especially, the use of P_2O_5 as a P precursor conducts to the formation of polymerized P oxo-compounds rather than of $AlPO_4$ after calcination in the absence of Mo.

2D-^{27}Al MQMAS-NMR gave an extraordinary improved resolution compared with conventional ^{27}Al MAS-NMR. In dried samples, pure alumina and Mo-Alumina catalysts showed a single distorted octahedral aluminium site while P containing catalysts showed additional octahedral and tetrahedral aluminium sites interacting with phosphorus. After calcination, mainly octahedral and tetrahedral aluminium sites were observed in every catalysts. Al_{tetra}-O-P sites were also detected in P-containing Alumina catalysts but the octahedral Al-O-P sites were disappeared. In addition, a small amount of penta coordinated aluminium site was obtained in pure alumina. The presence of Mo introduces a large distortion into the alumina framework as the amount of penta coordinated aluminium sites is significantly increased in the presence of Mo.

2.2.3.1. Introduction

The active phase of hydrotreating catalysts generally consists of molybdenum sulfide MoS_2 deposited on γ-alumina. The molybdenum precursor is usually introduced on the Al_2O_3 support by a conventional wet impregnation method. However, only 10-12 wt% Mo can be dispersed by this procedure. In previous works, the present authors proposed a new catalyst preparation method based on a sol-gel synthesis to obtain well-dispersed Mo oxo-species on a high surface area alumina support which is obtained by hydrolysis of an aluminum alkoxide in the presence of Mo precursor (1, 2). This advanced method can produce powders containing up to ~30 wt% of well dispersed Mo and specific surface area higher than 400 $m^2.g^{-1}$. To improve the sol-gel hydrotreating catalysts, it appeared interesting to investigate the effects of phosphorus addition during the gel synthesis since P has already been reported as an excellent promotor for several hydrotreating reactions such as HDS (hydrodesulfurization), HDN (hydrodenitrogenation) and HYD (hydrogenation), as well as the classical promotors like Co and Ni (3-6). With phosphorus addition, it was found that the specific surface area of sol-gel catalysts decreases with increasing P loading but may remain relatively high in some cases (2). XRD (X-ray diffraction) measurements also revealed that large amounts of molybdenum and phosphorus in the catalyst formulation provoke aggregation of bulk MoO_3 (2).

Solid state NMR is widely known as one of the most useful techniques for characterizing catalysts which may be rather amorphous and with a large number of structural defects. In particular, a considerable number of studies has been carried out to investigate the chemical states and environments of P and Al in Mo-P-Alumina based hydrotreating catalysts (7-14). The state of P on the alumina strongly depends on its amount. At low P content, P is supported as well dispersed mono or diphosphates. With increasing the P loading, polymeric P oxo-compounds and $AlPO_4$ with different degrees of hydration are also formed. In the presence of both Mo and P, the formation of a Mo-P heteropoly anion like $P_2Mo_5O_{23}^{6-}$ is observed while it gradually decomposes to PO_4^{3-} and MoO_4^{2-} after impregnation on the alumina support (9,12). At higher P loading, the $Al_2(MoO_4)_3$ phase or $[Al(OH)_n(H_2O)_{6-n}]_n(MoO_4)$ (with n=1 or 2) species are also detected by ^{27}Al MAS-NMR after calcination. Aluminium cations are mainly located in octahedral or tetrahedral coordination sites while penta coordinated Al sites are also found in some cases (15,16).

Recently, Kraus and co-workers (17,18) applied new advanced NMR techniques such as ^{27}Al-^{31}P Rotational-Echo Double Resonance (REDOR), Transfer of Populations in Double Resonance (TRAPDOR), Multiple-Quantum Magic Angle Spinning (MQMAS) and Off-Resonance quadrupolar Nutation to

characterize these catalysts more precisely. These techniques revealed that the most part of P is in close contact with alumina with predominant formation of $AlPO_4$ which possesses a monolayered structure with a slightly higher degree of ordering than the amorphous ones. Formation of stacked phosphate layers and bulk phosphates are excluded.

The objectives of the present study are to give a detailed identification of the states and environments of Al and P on the Mo-P-Alumina based sol-gel catalysts by using solid state ^{27}Al or ^{31}P MAS-NMR and 2-dimensional ^{27}Al MQMAS NMR. Theories and principles of the MQMAS-NMR technique are not discussed here as they were already given elsewhere (19-21).

2.2.3.2. Experimental Section

Catalyst Preparation

The details of the preparation procedure of Mo-P-Alumina based sol-gel catalysts, the list of catalysts and their main characteristics (atomic composition, specific surface area) were already described (2). Two series of catalysts with expected Mo loadings of 20 and 30 wt% on the Mo element basis (actually, their contents were ~17 and ~26 wt% Mo, respectively) and a wide range of P content (from 1 to 13 wt% P) were prepared from hydrolysis of aluminium sec-butylate (ABS) in the presence of ammonium heptamolybdate and/or a phosphorus precursor. Orthophosphoric acid (H_3PO_4) and phosphorus pentoxide (P_2O_5) were selected as P precursors to investigate their effect. The Mo-P (MP) catalysts obtained at each stage are noted as MPD(X-Y)H, MPC(X-Y)P where « MPD » or « MPC » means a dried « D » or a calcined « C » sample with X wt% of Mo and Y wt% of P, respectively (contents expected from the preparation procedure). H or P refers to the nature of P precursor such as H_3PO_4 or P_2O_5, respectively.

NMR measurements

Conventional solid state ^{27}Al MAS-NMR spectra were obtained from a Bruker ASX400 spectrometer operating at a resonance frequency of 104.26 MHz with a recycling time of 3 s and a short pulse time of 1 µs. The spinning frequency was ~15 kHz and $Al(H_2O)_6^{3+}$ was taken as a reference. ^{31}P MAS-NMR spectra were obtained from a Bruker ASX100 spectrometer operating at a resonance frequency of 40.53 MHz with a recycling time of 40 s and a pulse time of 2 µs. The spinning frequency was ~7 kHz and H_3PO_4 was taken as a reference.

Liquid state ^{31}P NMR spectra were also recorded to identify the nature of the P species present in the preparation solution. They were obtained on a Bruker ASX300 spectrometer operating at a resonance frequency of 121.50 MHz with a

recycling time of 1 s and a pulse time of 2 μs. H_3PO_4 was taken as a reference. The H_3PO_4 and P_2O_5 precursors were dissolved in 2-butanol with a concentration corresponding to the preparation of MPC(0-11)H or MPC(0-12)P catalyst (Mo and ASB were not introduced in these measurements).

The details of the experimental procedures for the 2D ^{27}Al MQMAS-NMR measurements were already described (19-21). The spectra were obtained with the Z filtering method (22) from a Bruker ASX400 spectrometer working at 104.3 MHz. Samples were spun at ~13 kHz using a slightly off-setting of the magic angle in order to eliminate spinning sidebands from unsymmetrical transitions. The recycling time was 1 s. The pulse lengths and RF fields were 2 and 0.8 μs with 250 kHz and 8.3 μs with 10 kHz, for the two first hard pulses and the selective 90 ° pulse, respectively. Decoupling for protons was applied systematically. 1024 points were acquired in both dimensions. For the 3Q MAS measurement, 6-phase cycling was combined with an overhall classical cyclops 4-phase cycle in order to minimize phase and amplitude mis-settings of the receiver. The minimum number of accumulations to be realized was thus 24 for each t_1 step. In this study, only the trends in the variations of the chemical shifts will be discussed. No quantitative data for quadrupolar interaction will be reported since the quantitative analysis of 2D-^{27}Al MQMAS NMR may be somehow delicate due to spectral broadening and overlapping.

2.2.3.3. Results and Discussion

2.2.3.3.1 ^{27}Al MAS-NMR

(a) Samples obtained with H_3PO_4 as a P precursor

Figure 1 shows the ^{27}Al MAS-NMR spectra of the dried sol-gel catalysts obtained with H_3PO_4 as a P precursor. Table 1 also shows the list of chemical shifts and their assignments obtained in reference compounds. Within the measurement conditions, side bands cannot be theoretically observed in this region. Although it is somehow difficult to correctly differentiate all the contributions of spectra mainly due to peak broadening, it is still possible to identify some species on the catalysts. Pure alumina MPD(0-0) (fig.1a) has a single broad signal at 7 ppm which can be assigned to octahedral aluminum Al_{octa} sites (15). Signal broadening might be partly attributed to the presence of different chemical compounds of aluminum such as $Al(OH_2)_p(OC_2H_4CH(OH)CH_3)_m(OCH(CH_3)C_2H_5)_n$ (where p+n+m=6) (15). The organic ligands come from the alkoxide precursor and from the alcohol solvents used in the synthesis.

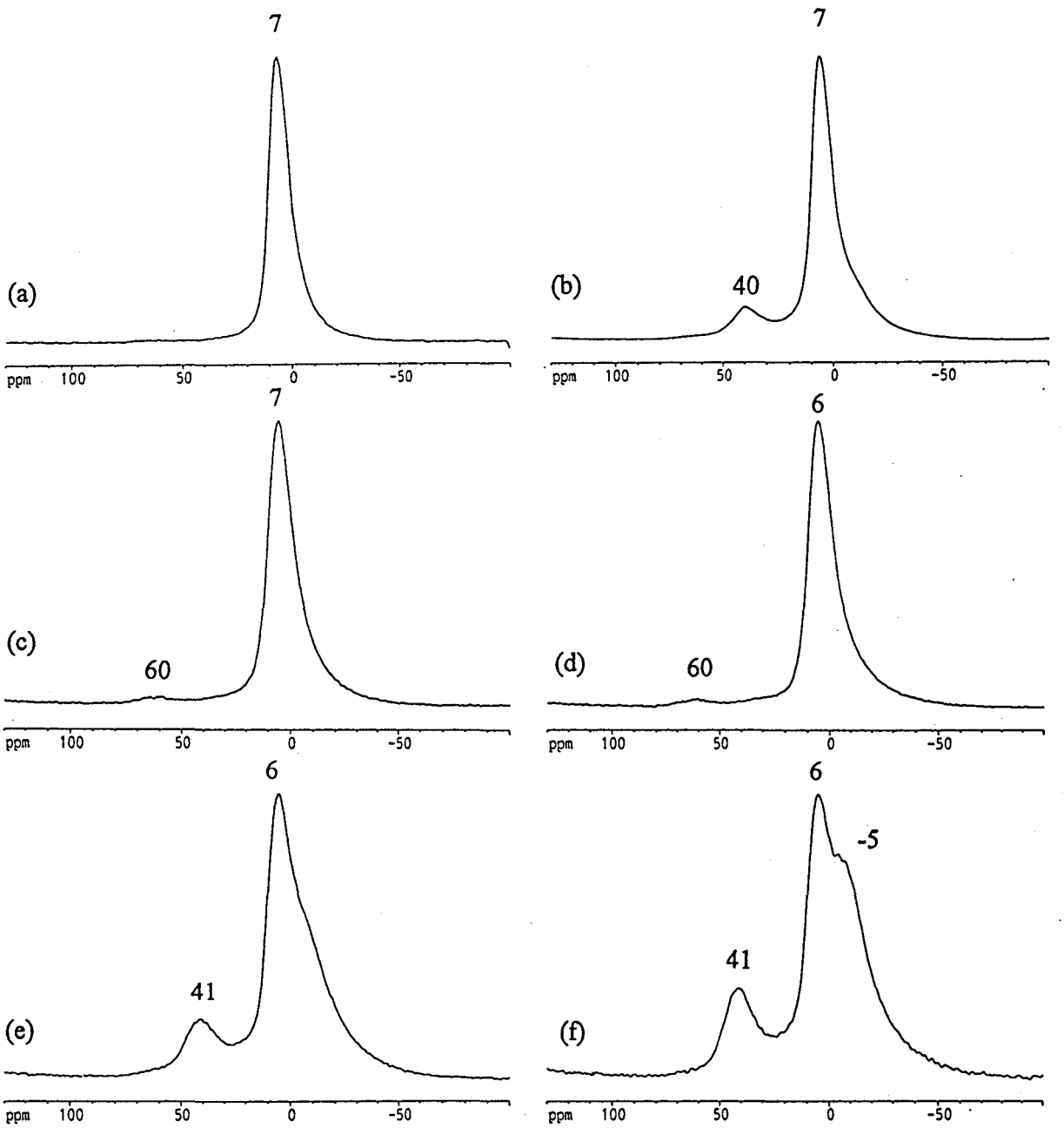

Fig.1. ^{27}Al MAS-NMR spectra of Mo-P-Alumina based sol-gel catalysts obtained after the drying stage at 100 °C. The P containing catalysts were prepared with H_3PO_4 as a P precursor. (a) MPD(0-0), (b) MPD(0-11)H, (c) MPD(20-0), (d) MPD(30-0), (e) MPD(20-11)H and (f) MPD(30-11)H.

Table 1. List of chemical shifts and their assignments of ^{27}Al MAS-NMR for Mo-P-Alumina sol-gel catalysts.

δ ppm	Al species	Reference compounds or environments	ref.
~-15	Al_{octa}-O-Mo	$Al_2(MoO_4)_3$	11
-5 to -30	Al_{octa}-O-P	$Al(H_2O)_n(OP)_{6-n}$	23
0 to 10 *	Al_{octa}	γ-Alumina $Al(H_2O)_n(OR)_{6-n}$	15
10	Al_{octa}-O-R	unreacted alkoxide	26
13	-	$[Al(OH)_n(H_2O)_{6-n}]_n(MoO_4)(n=1,2)$	10
14	Al_{penta}-O-P	$Al(H_2O)_n(OP)_{5-n}$	28
~30	Al_{penta}	distorted γ-Alumina	16
~40	Al_{tetra}-O-P	$AlPO_4$	8
53 to 75*	Al_{tetra}	γ-Alumina	15

* The chemical shift value depends on the degree of alumina condensation.

In catalysts containing Mo [MPD(20-0) and MPD(30-0)], P [MPD(0-11)H] or both elements [MPD(20-11)H and MPD(30-11)H], a shoulder in the spectra between 0 and ~-30 ppm is observed (Fig.1(b) to (f)). For the last sample, a distinct shoulder at ~-5 ppm is also detected. The tail contribution in the spectra increases with increasing the amount of P and Mo. The tail could be due to the presence of new Al octahedral sites, noted Al_{octa}-O-Mo and Al_{octa}-O-P, where molybdenum or phosphorus are located in second coordination shell of aluminium (23), or to strongly distorted Al_{octa} sites which could exhibit large second order quadrupolar interactions. MPC(20-0) (fig.1(c)) and MPC(30-0) (fig.1(d)) also show a signal at ~60 ppm which can be assigned to Al_{tetra} (15). In addition, phosphorus containing catalysts show a new signal at ~40 ppm which can be assigned to Al in $AlPO_4$ or more generally to tetrahedral Al sites noted Al_{tetra}-O-P (8). The global amount of interaction between P and Al tends to increase in the presence of Mo as the intensity of the signal at ~40 ppm is stronger in the Mo containing MPD(20-11)H and MPD(30-11)H catalysts (fig.1(e) and (f)) than that in the Mo-free MPD(0-11)H catalyst (fig.1(b)).

Figure 2 shows the ^{27}Al MAS-NMR spectra of the sol-gel catalysts obtained from H_3PO_4 as a P precursor after calcination at 500 °C. Clearly, important modifications are detected by comparison to the dried samples (fig.1). The MPC(0-0) catalyst (fig.2(a)) has Al_{octa} (the main peak) and tetrahedral aluminum Al_{tetra} sites at ~65 ppm (15). Furthermore, a weak and broad component at about 30 ppm is also observed between the two main peaks.

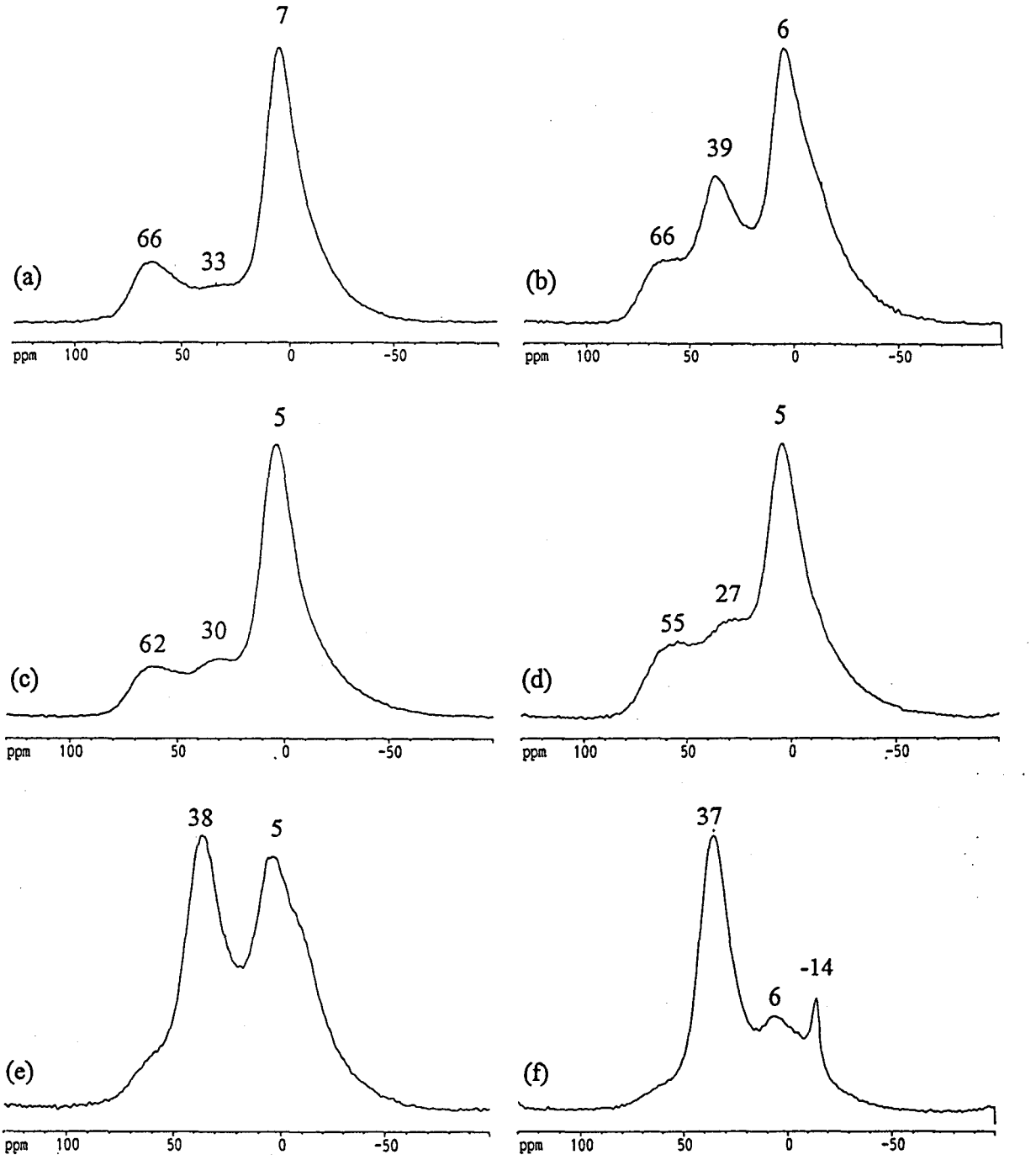

Fig.2. ^{27}Al MAS-NMR spectra of Mo-P-Alumina based sol-gel catalysts obtained after calcination in air at 500 °C. The P containing catalysts were prepared with H_3PO_4 as a P precursor. (a) MPC(0-0), (b) MPC(0-11)H, (c) MPC(20-0), (d) MPC(30-0), (e) MPC(20-11)H, (f) MPC(30-11)H.

This third signal is more clearly detected in the Mo-Alumina catalysts such as MPC(20-0) or MPC(30-0) (fig.2(c) and (d)). It might be assigned to penta coordinated aluminium Al_{penta} sites (16). However, the possibility to build surface tetrahedral Al_{tetra}-O-Mo sites cannot be excluded as intensity of this peak increases with increasing amount of molybdenum. The MPC(0-11)H sample (fig. 2(b)) exhibits three distinct signals at 66, 39 and 6 ppm assigned to Al_{tetra}, Al_{tetra}-O-P and Al_{octa} sites, respectively. Though $AlPO_4$ is already present in the dried state, the intensity of the peak corresponding to the Al_{tetra}-O-P sites clearly increases with calcination. This means that the formation of $AlPO_4$ mainly occurs during calcination, which strengthens the Al-P interactions through the formation of Al-O-P bridges. The calcined Mo-P-Alumina catalysts such as MPC(20-11)H and MPC(30-11)H (fig.2(e) and (f)) have also Al_{tetra}, Al_{octa} sites and Al in $AlPO_4$ (Al_{tetra}-O-P) whose NMR characteristics are ~60, 6 and 37 ppm, respectively. However, their relative populations are strongly dependent on the sample composition. Especially, the catalyst MPC(30-11)H gives the highest relative amount of $AlPO_4$. It is considered that high loadings of Mo and P facilitate the destruction of γ-Alumina and the formation of Al-O-P bridges or the $AlPO_4$ phase on the catalysts as evidenced by XRD measurements (2). Moreover, a sharp peak at ~-14 ppm is also obtained in MPC(30-11)H (fig.2(f)); it corresponds to the presence of $Al_2(MoO_4)_3$ (11). This compound is supposed to be derived from the reaction between bulk MoO_3 and the alumina surface because it is always observed when bulk MoO_3 is present on the alumina (2, 24, 25). Schematically, one can write :

$$3\ MoO_3(bulk) + Al_2O_3(surface) \rightarrow Al_2(MoO_4)_3$$

However, a weak shoulder (~-14 ppm) or a tail with negative chemical shifts is essentially observed in all the Mo and/or P containing calcined samples as in the case of the dried catalysts. This has been attributed to the effect of Mo or P in the second coordinative shell of the Al sites or to strongly distorted Al_{octa} sites which could exhibit large second order quadrupolar interactions.

Concerning the resonance evolution, the top peak positions of Al_{octa}, Al_{penta} and Al_{tetra} tend to decrease (in ppm) with increasing the Mo loading. This might be caused by an increase of the alumina framework distortions which increase the quadrupole interactions and hence this quadrupolar induces the shifts. It can be also due to a decrease of the Al condensation degree in the gel caused by the presence of Mo (26).

Although ^{27}Al MAS-NMR gives useful information on the state of Al in Mo-P-Alumina based hydrotreating catalysts, it remains difficult to completely describe the Al sites. These results will be examined again with those obtained by 2D-^{27}Al MQMAS-NMR.

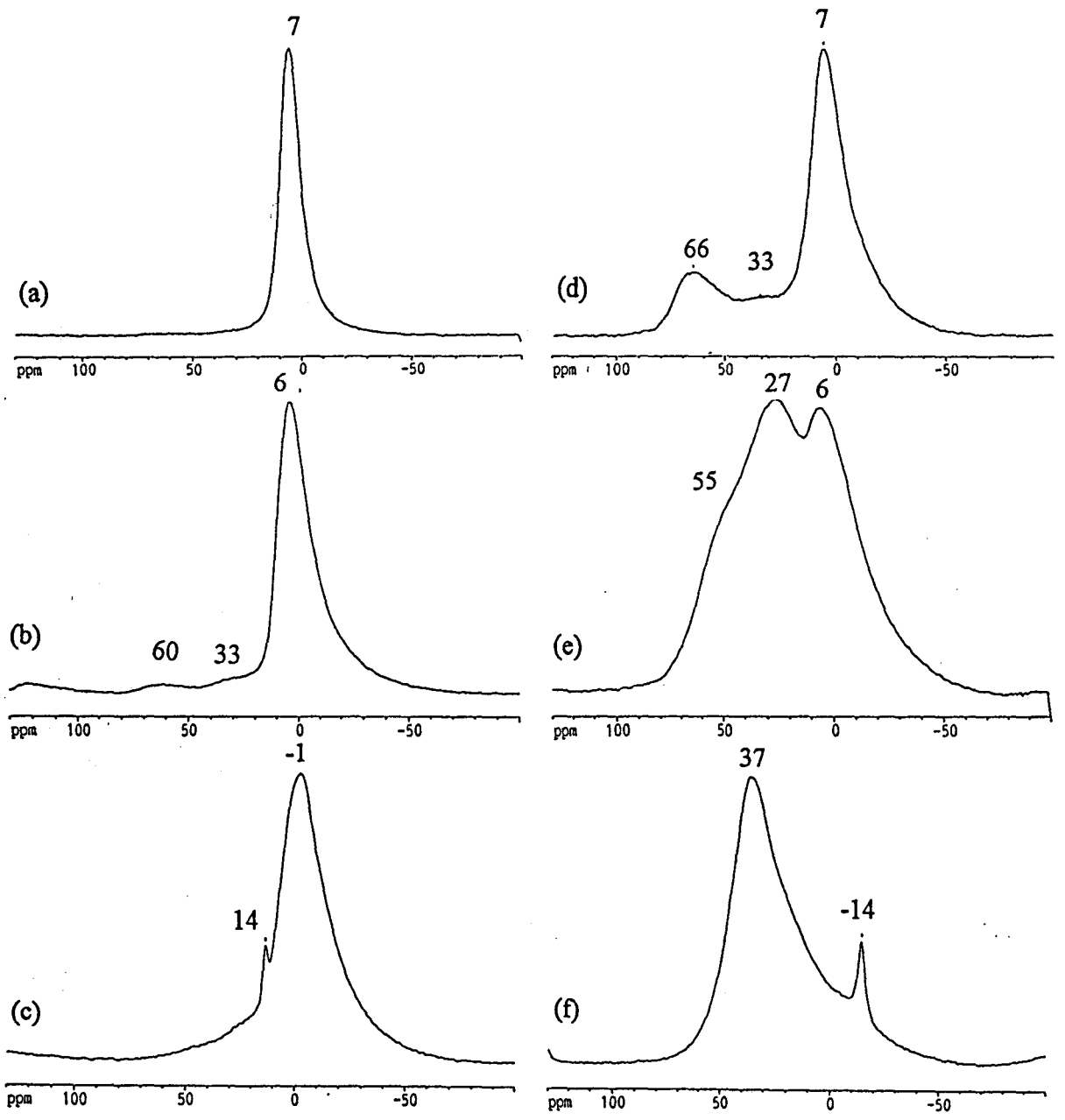

Fig. 3. ^{27}Al MAS-NMR spectra of dried and calcined Mo-P-Alumina based sol-gel catalysts prepared with P_2O_5 as a P precursor. Catalysts obtained after the drying stage at 100°C : (a) MPD(0-0), (b) MPD(0-12)P, (c) MPD(30-13)P. Catalysts obtained after calcination at 500°C : (d)MPC(0-0), (e) MPC(0-12)P, (f) MPC(30-13)P.

(b) Samples obtained with P_2O_5 as a P precursor

Figure 3 shows the ^{27}Al MAS-NMR spectra of sol-gel catalysts (dried and calcined) obtained with P_2O_5 as a P precursor. For comparison purposes, the spectra of pure alumina [MPD(0-0) and MPC(0-0)] are also reported (fig.3(a) and (d)). These spectra are quite different from those obtained with H_3PO_4 as a P precursor. For the dried MPD(0-12)P catalyst (fig.3(b)), two weak features at ~60 and ~33 ppm with an intense peak at 5 ppm are observed. They are corresponding to Al_{tetra}, Al_{penta} and Al_{octa} sites respectively. For sample MPD(30-13)P (fig.3(c)), an intense and broad signal at -1 ppm is present with a less intense sharp peak at 14 ppm. As already mentioned, the former signal can be assigned to Al_{octa} sites in the gel with a lower degree of condensation (15). This result suggests that the presence of P_2O_5 in the sample preparation has a detrimental effect on the hydrolysis and condensation steps of the Al sec-butylate. Zaharescu et al. (27) also reported that the degree of hydrolysis and condensation of alkoxide is strongly influenced by PO(OR)x complexes in the system of phosphorus-TEOS (tetraethoxysilane $Si(OEt)_4$). The second peak at 14 ppm might be assigned to unreacted alkoxide, to $[Al(OH)_n(H_2O)_{6-n}]_n(MoO_4)$ (with n=1 or 2) or to Al_{penta}-O-P (26, 10, 28).

The calcined MPC(0-12)P sample (fig.3(e)) shows three strong signals at 55, 27 and 6 ppm. They can be assigned to Al_{tetra}, Al_{penta} and Al_{octa} sites as for the dried MPD(0-12)P catalyst. However, their proportion are considerably different. Especially, the peak intensity of the Al_{penta} site is extremely strong for the calcined sample. This suggests that the structure of MPC(0-12)P is highly distorted. It is also remarkable that a signal attributed to $AlPO_4$, which should be observed at ~40 ppm, can not be detected in sample MPC(0-12)P in contrast to the previous MPC(0-11)H sample (fig.2(b)) prepared from H_3PO_4 as a P precursor. This means that the formation of $AlPO_4$ is considerably prevented in the P-Alumina catalysts prepared from P_2O_5 as a P precursor in the absence of Mo. However, the Mo-P containing catalyst MPC(30-13)P (fig.3(f)) gives an intense and broad signal at 37 ppm and a smaller sharp signal at -14 ppm which are assigned to $AlPO_4$ and $Al_2(MoO_4)_3$, respectively. It is inferred again that the presence of Mo leads to the predominant formation of $AlPO_4$ in the series of catalysts prepared from P_2O_5 as a P precursor, as in the case of the previous series prepared from H_3PO_4.

2.2.3.3.2 ^{31}P MAS-NMR

(a) Samples obtained with H_3PO_4 as a P precursor

Figure 4 shows the ^{31}P-NMR spectra of the dried and calcined sol-gel catalysts obtained with H_3PO_4 as a P precursor. In the dried MPD(0-11)H catalyst (fig.4(a)), considering the asymmetric line shape, the broad signal can be decomposed into two overlapping peaks at ~-8 and ~-21 ppm which are assigned to monomeric phosphate and polymeric phosphorus oxo-species, respectively (8). However, Mo-P-Alumina catalysts such as MPD(20-11)H, MPD(30-5)H and MPD(30-11)H (fig.4(b) to (d)) show another characteristic peak at ~ -15 ppm. This signal could be assigned to less polymerized P oxo-species. The presence of molybdenum might be effective for dispersing phosphorus oxo-species on the alumina support.

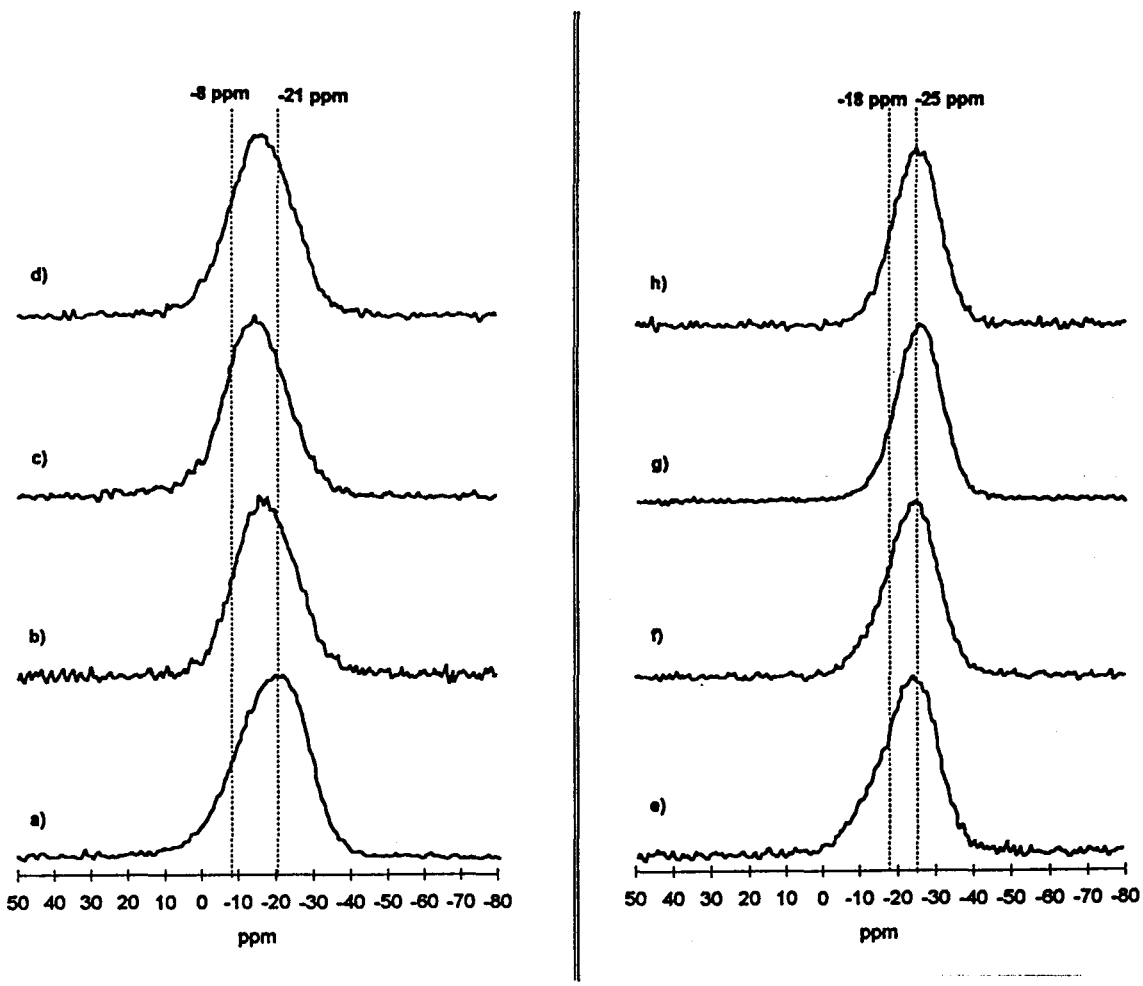

Fig. 4. ^{31}P MAS-NMR spectra of dried and calcined Mo-P-Alumina based sol-gel catalysts prepared with H_3PO_4 as a P precursor. Catalysts obtained after the drying stage at 100°C : (a) MPD(0-11)H, (b) MPD(20-11)H, (c) MPD(30-5)H, (d) MPD(30-11)H. Catalysts obtained after calcination at 500°C : (e) MPC(0-11)H, (f) MPC(20-11)H, (g) MPC(30-5)H, (h) MPC(30-11)H.

All the calcined catalysts show broad signals (fig.4(e) to (h)) which can be decomposed into peaks at ~-18 and ~-25 ppm and assigned to polyphosphate and $AlPO_4$, respectively (7-8). The Mo containing catalysts such as MPC(30-5)H and MPC(30-11)H (fig.4(g) and (h)) show less polyphosphate and then relatively more $AlPO_4$ than the Mo-free MPC(0-11)H (fig.4(e)).

(b) Samples obtained with P_2O_5 as a P precursor

Figure 5 shows the ^{31}P-NMR spectra of selected sol-gel catalysts (dried and calcined) obtained with P_2O_5 as a P precursor.

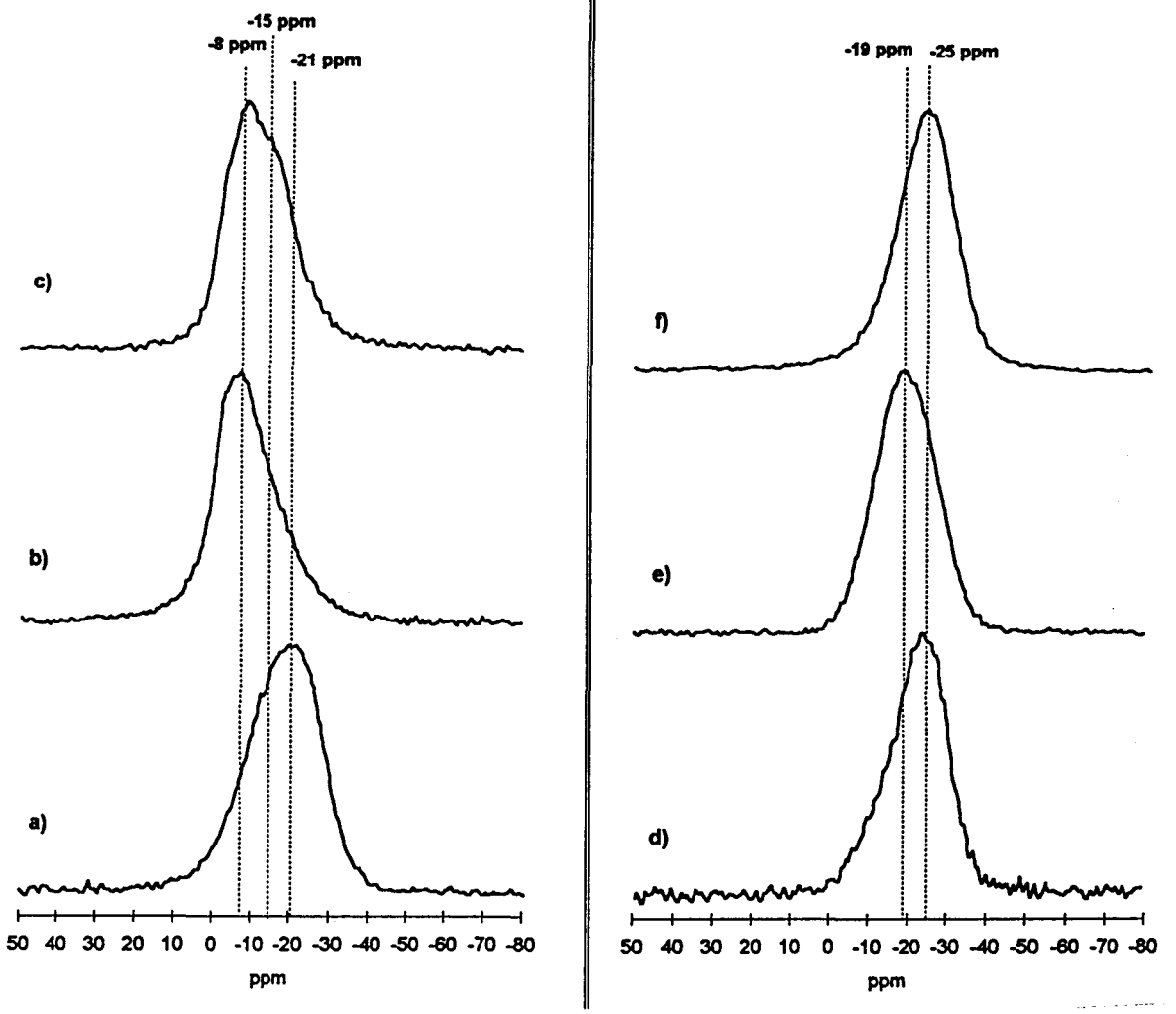

Fig. 5. Comparison of ^{31}P MAS-NMR spectra of dried and calcined Mo-P-Alumina based sol-gel catalysts prepared from P_2O_5 and H_3PO_4 as P precursors. Catalysts obtained after the drying stage at 100°C : (a) MPD(0-11)H, (b) MPD(0-12)P, (c) MPD(30-13)P. Catalysts obtained after calcination at 500°C : (d) MPC(0-11)H, (e) MPC(0-12)P, (f) MPC(30-13)P.

For comparison purposes, the spectra of P-Alumina catalysts obtained with H_3PO_4 as a P precursor are also reported. MPD(0-12)P (fig.5(b)) gives a broad spectrum with an apparent maximum at ~-8 ppm which is mainly assigned to monomeric phosphate species while MPD(0-11)H (fig.5(a)) mainly gave the spectra for polymeric phosphate at -21 ppm, respectively. In the presence of Mo and P (fig. 5(c)), a spectra at ~-15 ppm can be also detected.

After calcination, the MPC(0-12)P catalyst has mainly polymeric P oxo-species identified by a peak at ~-19 ppm (fig.5(e)). However, the signal for $AlPO_4$ at ~-24 ppm, which is a predominant species in the MPC(0-11)H sample obtained from H_3PO_4 precursor (fig. 5(d)), is hardly detected; this is in agreement with the results of ^{27}Al MAS-NMR which did not reveal the presence of such a phase. On the other hand, Mo and P containing MPC(30-13)P (fig. 5(f)) mainly forms $AlPO_4$ as in the case of MPC(0-11)H.

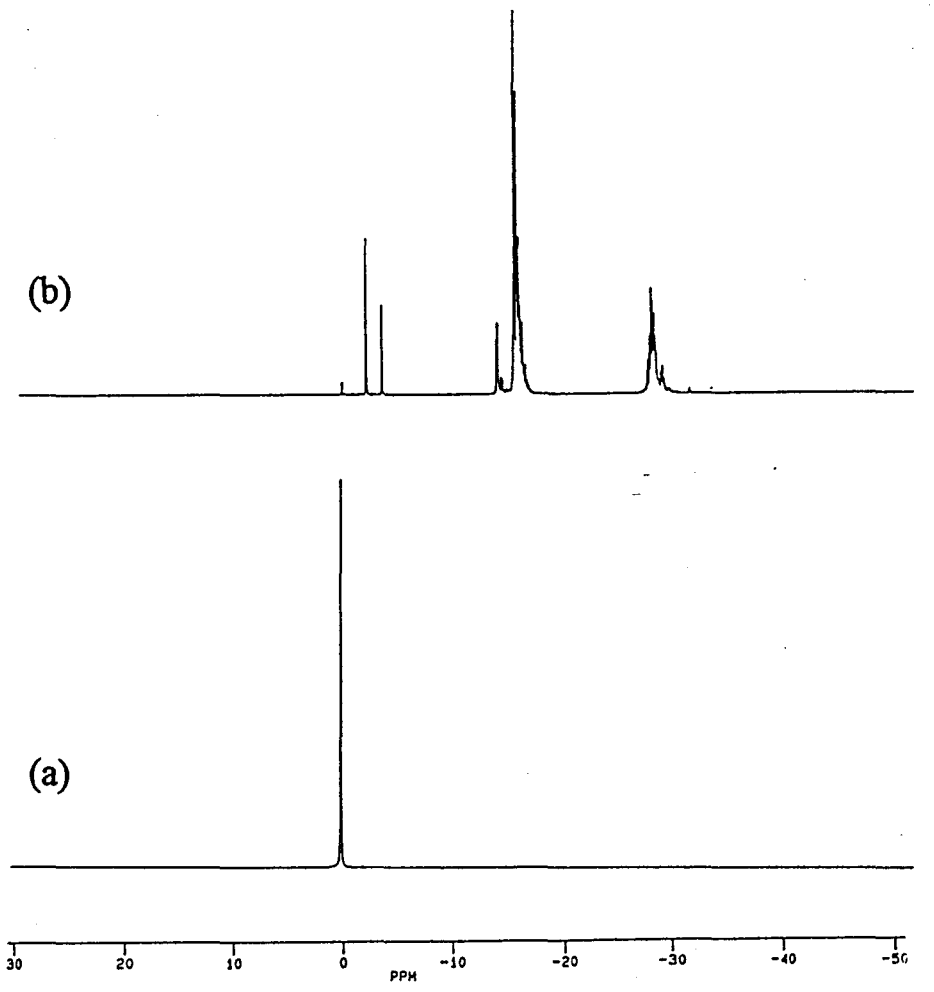

Fig. 6. Liquid ^{31}P NMR spectra of the solutions with the P precursors used to prepare the sol-gel catalysts. (a) H_3PO_4 dissolved in 2-butanol, (b) P_2O_5 dissolved in 2-butanol.

To investigate the influence of the nature of the P precursor, liquid ^{31}P NMR spectra of solutions of H_3PO_4 or P_2O_5 in 2-butanol are reported in Figure 6. In the H_3PO_4-butanol solution, only the PO_4^{3-} ions are detected at ~1 ppm which indicates a weak solvent effect on the phosphate ions. On the other hand, in the P_2O_5-butanol solution, a lot of sharp peaks around -15 and -27 ppm which might be attributed to different P alcoholate compounds such as $PO(OH)(OBut)_2$ or $PO(OBut)(OH)_2$ were observed. It is suggested that the H_3PO_4 precursor as phosphate ions can easily interact with the alumina framework and lead to form $AlPO_4$ species but steric hindrance around phosphorus in P alcoholates should inhibit their interaction with the alumina framework in the P_2O_5 precursor.

In dried Mo containing MPD(30-13)P catalyst (fig.5(c)) gives another signal at -15 ppm which is also observed in MPD(30-11)H. Since the spectra at -15 ppm is always detected in the presence of Mo, this signal might be also assigned to Mo-P heteropoly compounds. The calcined MPC(30-13)P catalyst shows mainly a signal at ~-25 ppm (fig.5(f)) which is attributed to $AlPO_4$ species.

From the conventional ^{31}P and ^{27}Al MAS-NMR spectra, it can be concluded that the affinity of phosphorus with the alumina framework to form $AlPO_4$ depends strongly on the nature of phosphorus precursor used to prepare the catalysts and also on the presence of Mo.

2.2.3.3.3 2D ^{27}Al MQMAS-NMR

Figure 7 presents the 2D-^{27}Al MQMAS-NMR maps of selected sol-gel catalysts prepared with H_3PO_4 as a P precursor, either after the drying stage or after calcination. The values at the peak maximum are also listed in Table 2. The scales of these sheared spectra have been described in ref. (21).

Table 2. Peak maximum obtained by 2D-^{27}Al MQMAS NMR on selected Mo-P-Alumina based sol-gel catalysts.

catalysts	Chemical shift (ppm)				
MPD(0-0)				11	
MPD(0-11)H		45		11	-5
MPD(30-0)				11	
MPD(30-11)H		47		11	-5
MPC(0-0)	77		38	10	
MPC(0-11)H	77	(42)	(39)	12	
MPC(30-0)	73		40	11	
MPC(30-11)H		42		12	

( ) ; The peak top value of spectra is not clearly identified.

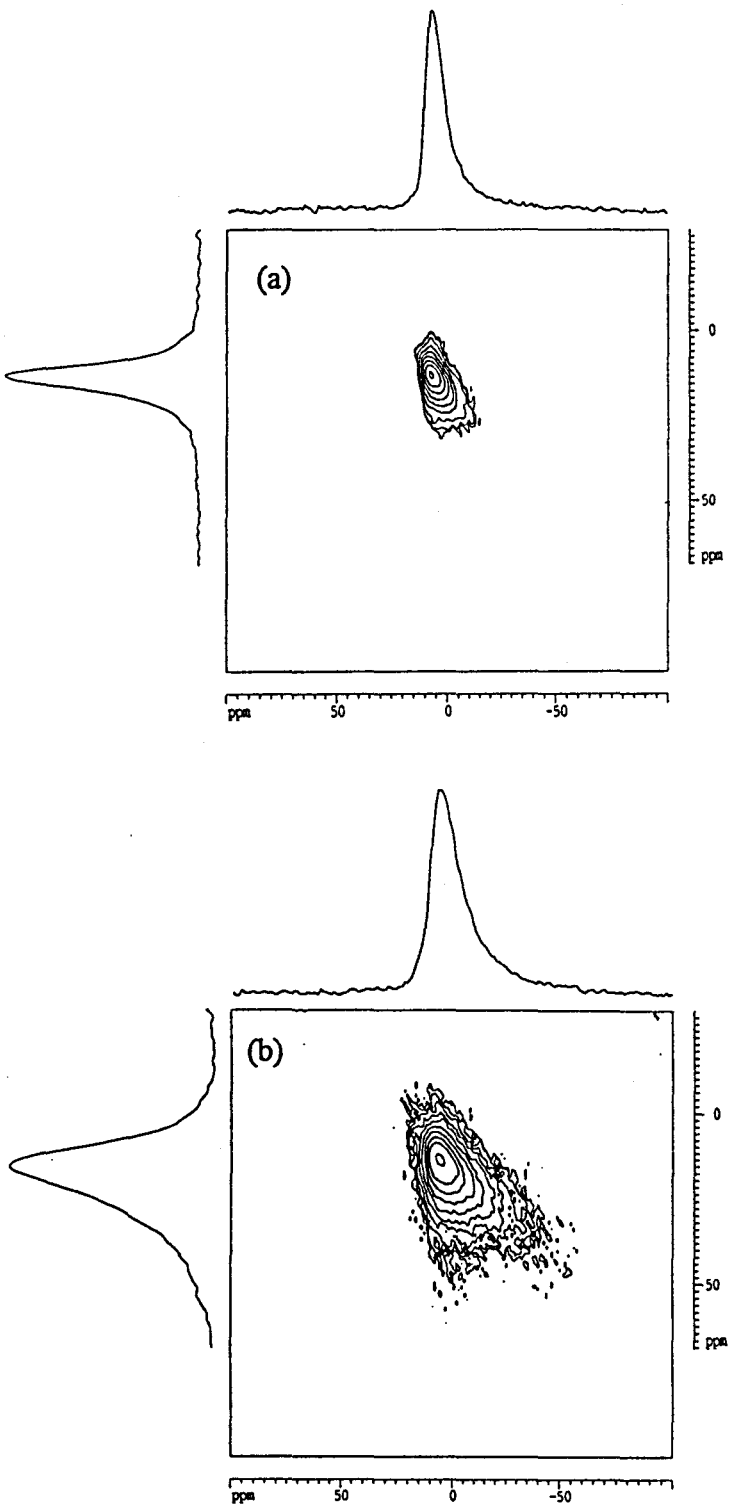

Fig.7. 2D-^{27}Al MQMAS-NMR spectra of Mo-P-Alumina based sol-gel catalysts. The P containing catalysts were prepared with H_3PO_4 as a P precursor. Catalysts obtained after the drying stage at 100°C : (a) MPD(0-0), (b) MPD(30-0), (c) MPD(0-11)H, (d) MPD(30-11)H. Catalysts obtained after calcination at 500°C : (e) MPC(0-0), (f) MPC(30-0), (g) MPC(0-11)H, (h) MPC(30-11)H

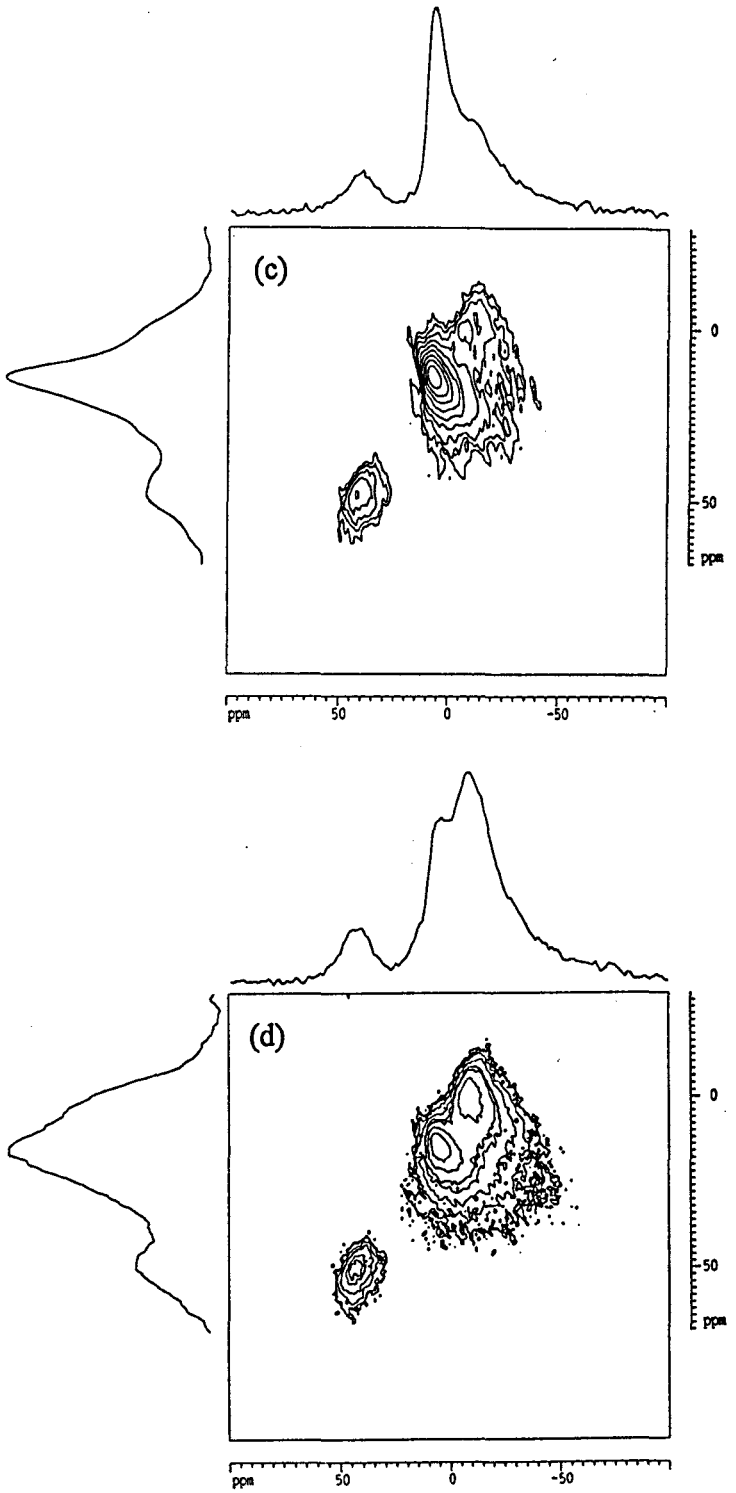

Fig.7. 2D-^{27}Al MQMAS-NMR spectra of Mo-P-Alumina based sol-gel catalysts. The P containing catalysts were prepared with H_3PO_4 as a P precursor (continued).

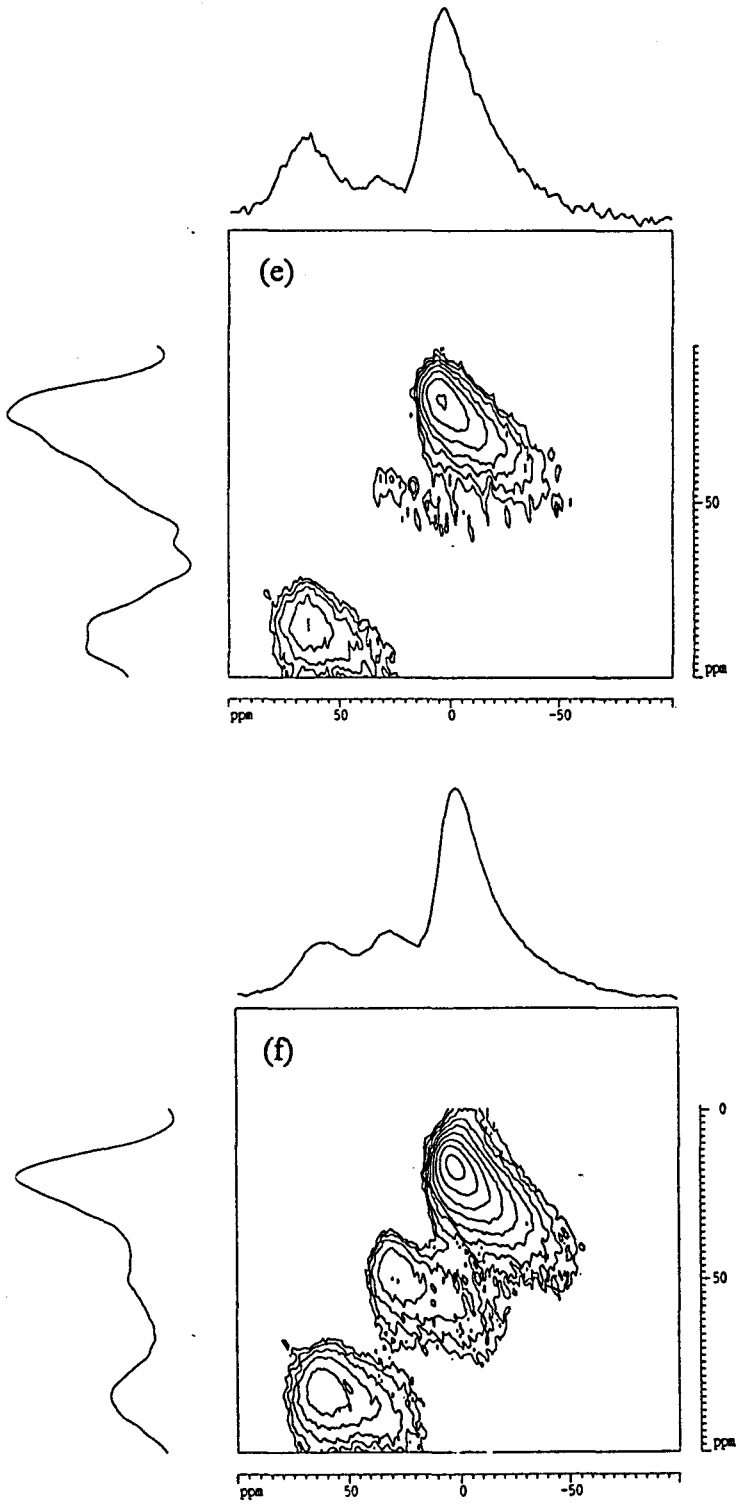

Fig.7. 2D-^{27}Al MQMAS-NMR spectra of Mo-P-Alumina based sol-gel catalysts. The P containing catalysts were prepared with H_3PO_4 as a P precursor (continued).

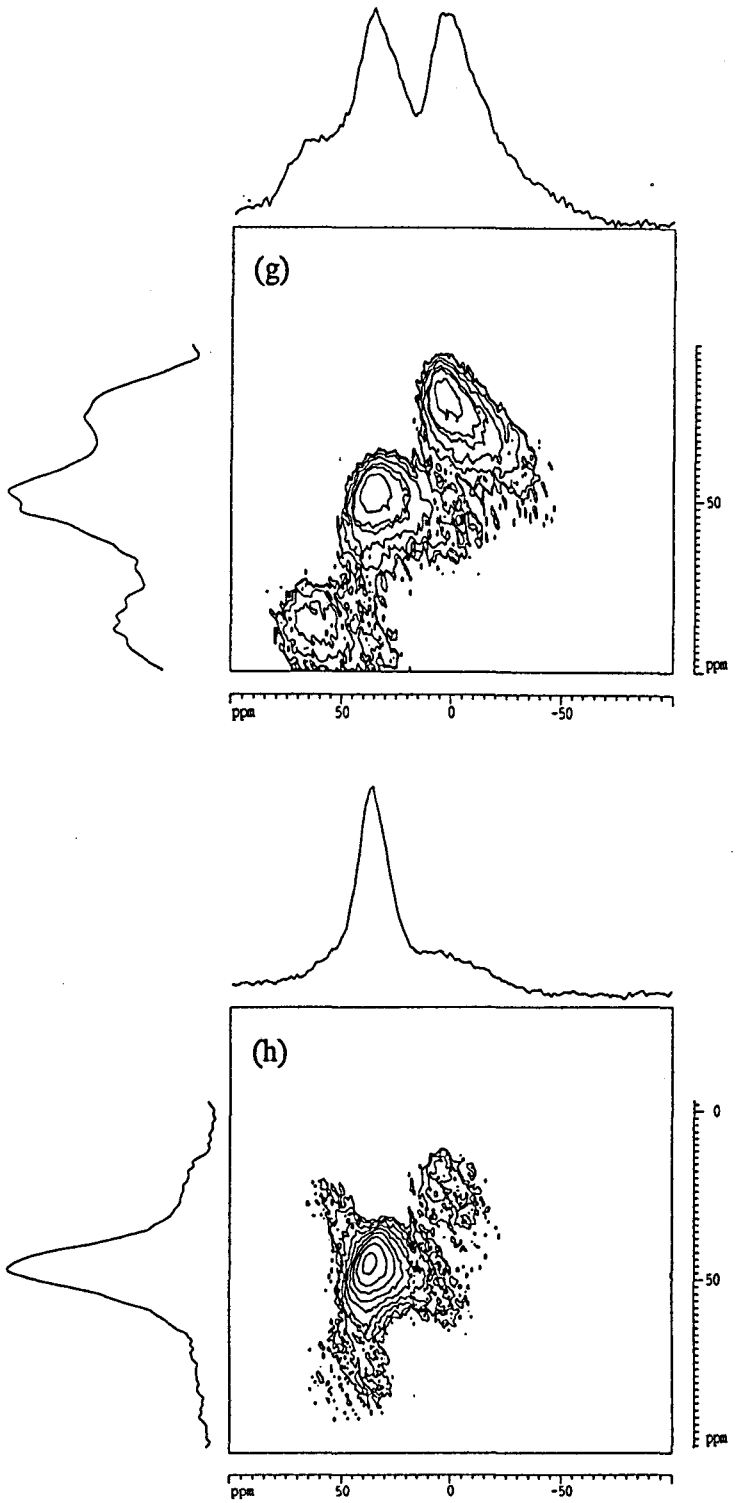

Fig.7. 2D-^{27}Al MQMAS-NMR spectra of Mo-P-Alumina based sol-gel catalysts. The P containing catalysts were prepared with H_3PO_4 as a P precursor (end).

The dried alumina sample MPD(0-0) shows (fig.7(a)) a single state at ~11 ppm corresponding to Al_{octa} sites . This result is in excellent agreement with the ^{27}Al MAS-NMR investigation. In the P-containing catalysts such as MPD(0-11)H (fig.7(c)) and MPD(30-11)H (fig.7(d)), a new aluminium site towards lower frequencies can be easily identified at ~-5 ppm. This clearly indicates that the tail of ^{27}Al MAS-NMR spectra between 0 and ~-30 ppm observed in the dried MPD(0-11)H and MPD(30-11)H (fig.1(b) and (f)) is attributed to an Al environment such as Al_{octa}-O-P. In addition, a small amount of Al_{tetra}-O-P sites is also observed at ~45 ppm in these catalysts. On the other hand, the dried Mo-Alumina MPD(30-0) catalyst (fig.7(b)) possesses only one type of Al_{octa} site as in the MPD(0-0) sample and no spectra attributed to Al_{octa}-O-Mo is observed. However, the distortion of the Al_{octa} sites seems to be much more pronounced than the ones present in pure alumina as MPD(0-0).

After calcination, the pure alumina sample MPC(0-0) (fig.7(e)) presents mainly Al_{octa} and Al_{tetra} sites (10 and 77 ppm respectively) with a very small amount of Al_{penta} sites at 38 ppm. This also quite agrees with the result of ^{27}Al MAS-NMR. The Mo containing MPC(30-0) catalyst (fig.7(f)) has three components at ~73, 40 and 11 ppm and assigned to Al_{tetra}, Al_{penta} and Al_{octa} sites, respectively. The presence of Mo introduces a large distortion into the alumina framework as a significant intensity increase of Al_{penta} feature is observed by comparison with the MPC(0-0) catalyst. The 2D map of sample MPC(0-11)H is closely similar to the one of the MPC(30-0) catalyst. The two peak maximum at 77, and 12 ppm can be also assigned to Al_{tetra} and Al_{octa} sites, respectively. However, considering the results of ^{27}Al MAS-NMR and that the spectra projection around 40 ppm to the left hand shows small doublets, the MPC(0-11)H sample (and also the MPC(30-11)H sample) must contain two different species around ~40 ppm which can be decomposed into Al_{penta} and Al_{tetra}-O-P sites, respectively. In addition, the P containing calcined catalysts MPC(0-11)H and MPC(30-11)H (fig. 7 (g) and (h)) do not show a spectra around -5 ppm as it was clearly observed in the corresponding dried catalysts. Therefore, the shoulder around -14 ppm observed in the ^{27}Al MAS-NMR measurement of calcined catalysts (fig.2) can be considered as highly distorted Al_{octa} sites while those in the dried catalysts are attributed to the Al_{octa}-O-P sites. In the MPC(30-11)H catalyst, one strong peak at 42 ppm is mainly observed. The other Al_{octa}, Al_{penta} and Al_{tetra} sites are very weak. This confirms that large loadings of Mo and P tend to destroy the structure of γ-Alumina and facilitate the formation of the $AlPO_4$ phases. The spectra for $Al_2(MoO_4)_3$ is not observed in MPC(30-11)H around -15 ppm in 2D-MQMAS NMR. It might be difficult to detect such a sharp and rather weak peak in these experimental conditions.

Considering the 2D-maps presented in figure 7, it is obvious that 2D-^{27}Al MQMAS-NMR gives interesting information on the state of Al in highly divided alumina-based catalysts due to its extraordinary high resolution and the results complete those obtained by conventional ^{27}Al MAS-NMR.

2.2.3.4. Conclusion

Molybdenum oxide-phosphorus oxide-Alumina sol-gel catalysts with a wide range of P loading (from 0 to 11 wt% of P) were prepared to elucidate the effect of phosphorus on the states of Al and P. The amount of phosphorus and the nature of the P precursors (H_3PO_4 or P_2O_5) affect them significantly. Aluminium mainly exists in octahedral, tetrahedral and penta-coordinated environments. P containing catalysts also possesses mainly Al_{octa}-O-P sites after the drying stage and Al_{tetra}-O-P sites after calcination, respectively. The use of P_2O_5 strongly prevents hydrolysis and condensation of the Aluminium sec-butylate. In dried catalysts, P is supported as monomeric or polymeric P oxo-species when using H_3PO_4, while P is supported as organic monomeric P oxo-species when using P_2O_5. In calcined samples, the H_3PO_4 precursor favors the formation of $AlPO_4$ (Al_{tetra}-O-P surface species) while the P_2O_5 precursor leads to form polymeric P oxo-species in the absence of Mo. In any cases, the interaction of phosphorus with alumina is favored by the presence of Mo.

It is concluded that the combination of conventional ^{27}Al and ^{31}P MAS-NMR with 2D-^{27}Al MQMAS-NMR is extremely useful to elucidate the precise state of Al and P species in Mo-P-Al based hydrotreating catalysts.

2.2.3.5. References

1. Le Bihan, L ; Mauchaussé, C. ; Duhamel, L. ; GrimbLot, J. ; Payen, E.,J. Sol-gel Sci. Tech., **1994**, 2, 837.
2. Iwamoto, R. ;Grimblot, J. Stud. Surf. Sci. Catal., **1997**, 106, 195.
3. Eijsbouts, S.; Van Gestel, J.; van Veen, J. A. R.; de Beer, V. H. J. ; Prins, R., J.Catal., **1991**, 131, 412.
4. Lewis, J. M. ; Kydd, R. A., J. Catal., **1992**, 136, 478.
5. Jian, M. ; Prins, R., Catal. Lett., **1995**, 35, 193.
6. Poulet, O. ; Hubaut, R. ; Kasztelan, S. ; Grimblot, J., Bull. Soc. Chim. Belg., 100, 857.
7. Han, O. H. ; Lin, C. Y. ; Haller, G. L., Catal. Lett., **1992**, 14, 1.
8. DeCanio, E. C. ; Edwards, J. C. ; Scalzo, T. R., Storm, D. A. ; Bruno, J. W., J. Catal., **1991**, 132, 498.
9. Cheng, W. C. ; Luthra, N. P., J. Catal., **1988**, 109, 163.

10.Edwards, J. C. ; DeCanio, E. C., Catal. Lett., **1993**, 19, 121.
11.Cho, H. ; Park, S. B. ; Kwak, J. H., J. Mol. Catal., **1996**, 104, A, 285.
12.Kraus, H. ; Prins, R., J.Catal., **1996**, 164, 251.
13.Kraus, H., Thesis, ETH 11620, **1996**.
14.Kraus, H. ; Prins, R., J.Catal., **1997**, 170, 20.
15.Kurokawa, Y.; Kobayashi, Y.; Nakata, S., Hetero. Chem. Rev., **1994**, 1, 309.
16.Risbud, S. H. ; Kirkpatrick, R. J. ; Taglialavore, A. P. ; Montez, B., J. Am. Ceram. Soc., **1987**, 70(1), C10.
17.van Eck, E. R. H. ; Kentgens, A. P. M. ; Kraus, H. ; Prins, R., J. Phys. Chem., **1995**, 99, 16080.
18.Kraus, H. ; Prins, R. ; Kentgens, A. P. H., J. Phys. Chem., **1996**, 100 (40), 16336.
19.Fernandez, C.; Amoureux, J. P.; Chezeau, J. M.; Delmotte, L.; Kesseler, H., Microporous Mater., **1996**, 6, 331.
20.Fernandez, C. ; Amoureux, J. P., Chem. Phys. Lett., **1995**, 242, 449.
21.Amoureux, J.P., Fernandez, C., Solid-State NMR, in press.
22.Amoureux, J.P., Fernandez, C., Steuernagel, S., J. Magn. Reson. **1996**, A123, 116.
23.Bautista, F. M. ; Campelo, J. M. ; Garcia, A. ; Luna, D. ; Marina, J. M. ; Romero, A. A. , Appl. Catal., **1993**, 96, 175.
24.Ramirez, J. ; Castano, V. M., Leclercq, C. ; Agudo, A. L., Appl. Catal., A, **1992**, 83, 251.
25.López Cordero, R. ; López Guerra, S.; Fierro, J. L. G. ; López Agudo, A., J. Catal., **1990**, 126, 8.
26.Rezgui, S. ; Gates, B. C., Chem. Mater., **1994**, 6, 2386.
27.Zaharescu, M. ; Vasilescu, A. , Badescu. V. ; Radu, M., J. Sol-gel Sci. Tech., **1997**, 8, 59.
28.Brow, R. K. ; Kirkpatrick, R. J. ; Turner, G. L. , J. Am. Ceram. Soc., **1990**, 73(8), 2293.

2.3 Le système Ni-P-Alumine : Genèse, structure et propriétés catalytiques du système Ni-P-Alumine préparé par voie sol-gel. (Genesis, Characterizations and Activities of Ni-P-Alumina Based Hydrotreating Catalysts Prepared by a Sol-Gel Method)

Abstract

Nickel oxide - P oxide - Alumina catalysts with different Ni loadings (mainly ~7 and ~18 wt% as a element) and a wide range of P loading (0-16 wt% as a element) were prepared by a sol-gel method to elucidate the role of phosphorous on the genesis, structural and catalytic properties. Three kinds of Ni precursors (nickel nitrate, nickel carbonate and nickel acetate) were examined. The textural and structural properties of dried and calcined forms were studied by means of various characterization techniques. Specific surface area (SSA) of catalysts did not change significantly at low P loading while it decreased from ~500 to 200 m^2/g at higher P loading. X-ray powder diffraction (XRD) measurements revealed that high loading of Ni and P within the alumina framework provokes aggregation of bulk NiO. In addition, IR measurements suggested that Ni interacts with the alumina in a different way from Mo and P species. ^{27}Al and ^{31}P-NMR measurements revealed that the presence of P suppresses the formation of $NiAl_2O_4$ and predominantly forms the $AlPO_4$ phase (Al_{tetra}-O-P surface species) after calcination. Thiophene HDS activity was promoted significantly by the P addition mainly due to less formation of stable nickel aluminate species, although high amount of P loading decreased the HDS activity due to the segregation of Ni component into bulk NiO.

2.3.1. Introduction

The active phase of hydrotreating catalysts generally consists of nickel-molybdenum or cobalt-molybdenum sulphide deposited on γ-alumina. To achieve higher activity by improving the catalysts, it is useful to investigate the effect of P on the physicochemical properties and catalytic activity of Ni species supported on alumina. In general, the alumina support is usually prepared from calcination of an aluminium hydroxide precursor. The Ni and P precursors are usually introduced on the alumina support by dry or wet impregnation methods. In the previous chapter, preparations of Mo-P-Alumina catalysts based on a sol-gel method were examined. In this sol-gel method, alumina is obtained by hydrolysis of aluminium alkoxide. Metal components are incorporated homogeneously with the alumina precursor during the support preparation. In case of Mo-Alumina catalysts, this advanced method can give at least 20 wt% of well dispersed Mo up to ~ 10 wt% P and also 30 wt% of well dispersed Mo up to 4 wt% P.

Furthermore, it was proved that the sol-gel preparation method has a great advantage for their characterization by surface science technique because of their extremely high SSA and high metal loadings. Therefore, it seems to be quite interesting to investigate the effect of P on the genesis, structural and catalytic properties of Ni-Alumina hydrotreating catalysts based on sol-gel method.

The role of P on the conventional Ni based hydrotreating catalysts has been already widely studied. López-Agudo et al. (1) reported that addition of P increases gas oil HDS and pyridine HDN due to the formation of acidic $AlPO_4$. Morales et al. (2) suggested that the addition of P increases the amount of octahedral Ni^{2+} sites which are assumed to be responsible for the HDS reaction. Andreev et al. (3) proposed that formation of highly dispersed $NiPS_3$ plays an important role for promoting alumina based hydrotreating catalysts. On the other hand, Robinson et al. (4) concluded that the $NiPS_3$ phase is not stable under the hydrotreating conditions while the formation of Ni_2P phase is responsible for the improvement of activity. Therefore, the precise effect of P has been not well understood yet.

In this work, we wished to elucidate the role of P on the genesis, textural, structural and catalytic activities of Ni-P-Alumina based hydrotreating catalysts prepared by the sol-gel method. Their main structural properties and thiophene HDS activity will be compared.

2.3.2. Experimental

Catalyst Preparation

Ni-P-Alumina catalysts based on a sol-gel method were prepared according to the procedure summarized in Figure 1. The alumina was prepared by the hydrolysis of aluminium sec-butylate (ASB) dissolved in 2-butanol (2BN). Nickel and P components were incorporated with the alumina precursor before the hydrolysis of ASB. 99% of ortho-phosphoric acid (H_3PO_4) and the nickel precursor were dissolved in 1,3-butanediol, simultaneously. H_3PO_4 has been chosen as a P precursor as it showed higher HDS activity and acid property than P_2O_5 as shown in paragraphs 2.2.1 and 2.2.2. To investigate the effect of Ni precursor, three kinds of Ni salts such as nickel nitrate ($Ni(NO_3)_2{\cdot}6H_2O$), nickel acetate ($Ni(C_2H_3O_2)_2$) and nickel carbonate basic hydrate ($NiCO_3{\cdot}2Ni(OH)_2$) were used for catalyst preparation. The catalysts obtained at each stage are noted as, for example, NPD(X-Y)n, NPC(X-Y)a and NPC(X-Y)c where NPD or NPC means dried or calcined samples, X or Y means the expected loading in wt% of Ni or P as elements, respectively. In addition, n, a, and c are sometimes noted at the end of the catalyst name to distinguish the nature of Ni precursor such as nitrate, acetate and carbonate, respectively.

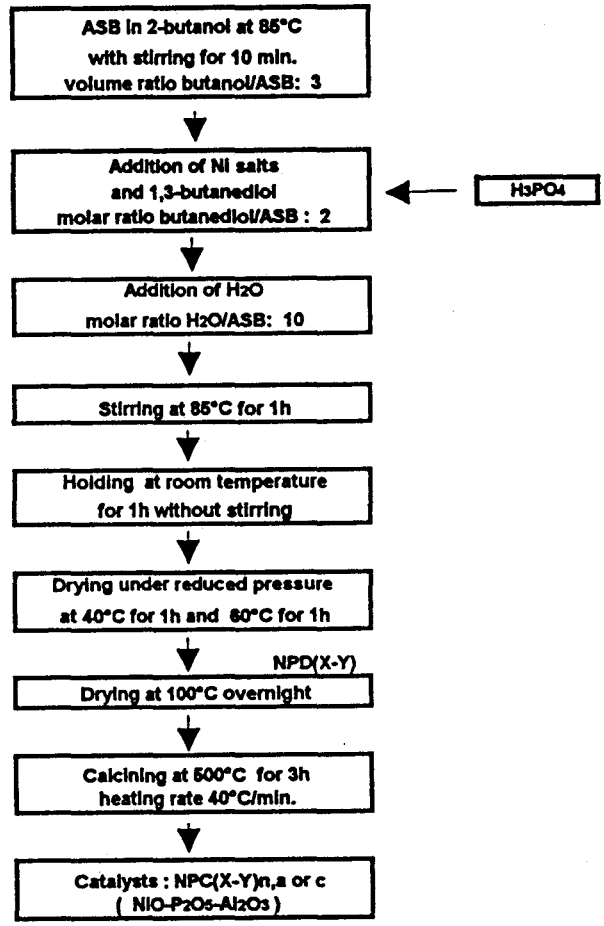

Fig.1. Procedure for preparation of Ni-P-Alumina sol-gel catalysts.

Catalysts characterization

The chemical compositions were provided by the "Service Central d'analyses du CNRS" (Vernaison, France). BET specific surface area (QUANTASORB Jr., Quantachrome) was measured after a pretreatment at 200 °C for 30 min., X-ray diffraction (Siemens D5000 Diffractometer equipped with a goniometer, a monochromator and a Cu X-ray tube), FT-IR (Nicollet 510 Spectrometer ; samples pelleted with KBr), ^{27}Al-NMR (ASX400 BRUKER ; resonance frequency 104.26 MHz, recycling time 3 sec., pulse time 1 µsec., spinning frequency 15 kHz and $Al(H_2O)_6^{3+}$ as a reference) and ^{31}P-NMR (ASX100 BRUKER ; resonance frequency 40.53 MHz, recycling time 40 sec., pulse time 2 µsec., spinning frequency 7 kHz and H_3PO_4 as a reference) were also used to characterize the obtained samples mainly after the calcination step.

Catalytic activity

Hydrodesulfurization of thiophene was carried out at atmospheric pressure in a flow type reactor packed with 0.2 g of catalyst. The catalysts was sulphided at 400 °C for 2 h with a H_2/H_2S (90/10) gas mixture at a flow rate of 50 $ml.min^{-1}$. After presulphidation, thiophene, purified by vacuum distillation, was introduced in the reactor at 400 °C and at constant pressure (50 torr) with a flow of dried hydrogen (10 $ml.min^{-1}$). The conversion of thiophene were determined by gas chromatography, at the steady state, 3 h after the thiophene introduction.

2.3.3. Results and Discussion

Specific surface area (SSA) and chemical composition

Table 1 shows chemical composition and specific surface area per gram of catalyst (SSA) for all the calcined samples. The amount of residual carbon remaining after calcination is less than 1.5 wt% and tends to decrease with the P loading.

Table 1 Chemical composition and specific surface area of calcined Ni-P-Alumina sol-gel catalysts

Catalysts	Ni precursor	Ni (wt%)	P (wt%)	Carbon (wt%)	SSA (m^2/g)
NPC(0-0)	-	0	0	0.5	503
NPC(0-11)	-	0	10.6	0.3	474
NPC(6-0)n	$Ni(NO_3)_2$	7.5	0	1.4	595
NPC(6-3)n	$Ni(NO_3)_2$	7.2	2.7	1.4	606
NPC(6-4)n	$Ni(NO_3)_2$	6.3	4.4	1.1	595
NPC(6-7)n	$Ni(NO_3)_2$	6.6	6.5	0.7	573
NPC(6-12)n	$Ni(NO_3)_2$	7.4	12.1	0.9	330
NPC(18-0)n	$Ni(NO_3)_2$	18 .0	0	1.4	499
NPC(18-2)n	$Ni(NO_3)_2$	17.2	2.2	1.0	502
NPC(18-5)n	$Ni(NO_3)_2$	18.0	4.7	0.9	442
NPC(18-6)n	$Ni(NO_3)_2$	16.8	5.9	0.9	404
NPC(18-9)n	$Ni(NO_3)_2$	18.0	8.9	0.5	335
NPC(18-13)n	$Ni(NO_3)_2$	16.1	12.6	0.4	302
NPC(18-16)n	$Ni(NO_3)_2$	16.3	16.4	0.5	194
NPC(24-0)n	$Ni(NO_3)_2$	23.0	0	0.8	374
NPC(18-11)a	$Ni(C_2H_3O_2)_2$	16.7	10.6	0.4	243
NPC(18-11)c	$NiCO_3$	14.9	10.6	0.4	477

The SSA of bare alumina and Ni-Alumina catalysts such as the NPC(0-0),

NPC(6-0)n and NPC(18-0)n are higher than 490 m^2/g. The SSA does not change pronouncedly up to 5 wt% P while it decreases at higher P loading (~200 m^2/g in the series of 18 wt% Ni). The NPC(18-11)a which was prepared from nickel acetate as the Ni precursor has almost same SSA as that of the nickel nitrate series at the equivalent P level, although the SSA of NPC(18-11)c prepared from the nickel carbonate precursor is higher than that of nickel nitrate. This suggests that the nature of Ni precursor affects significantly on the hydrolysis step of ASB.

X-ray powder diffraction (XRD)

Fig. 2 shows the X-ray powder diffraction patterns of selected sol-gel catalysts prepared from nickel nitrate as the Ni precursor. The bare alumina NPC(0-0) (Fig. 2a) can be identified as poorly crystalline γ-Alumina. For the P-free Ni-Alumina NPC(18-0) catalyst (Fig. 2b), a small shift of the peak positions indicates the formation of spinel $NiAl_2O_4$ instead of γ-alumina. It is noteworthy that the formation of $NiAl_2O_4$ is clearly suppressed by the addition of P (Fig. 2c and 2d). The well dispersed state of nickel oxide is kept up to 13 wt% (Fig. 2d) since no crystalline phase was detected. However, bulk NiO is identified at 15 wt% P in the series of 18 wt% Ni (Fig. 2e). This result indicates that a large amount of P prevents the interaction between Ni oxide and alumina framework as in the case of Mo-Alumina (see paragraph 2.2.1 Fig. 2e and 2f).

The XRD patterns of NPC(18-11)a and NPC(18-11)c catalysts prepared from different Ni precursors were also investigated (the figures are not shown here). The catalyst prepared from nickel carbonate as the Ni precursor shows a considerable segregation of bulk NiO already at 11 wt% P loading. It is suggested that the nickel carbonate precursor has less interaction with the aluminium precursor due to its lower solubility in water or alcoholic solvents. The catalyst prepared form nickel acetate as the Ni precursor also gives a small amount of NiO formation at 11 wt% P loading. Therefore, the nickel nitrate appears the most suitable precursor among the three to obtain the higher dispersion of Ni on alumina.

Infrared spectroscopy

Fig. 3 show infrared spectra of selected calcined catalysts prepared from nickel nitrate as the Ni precursor. For comparison purposes, the IR spectrum of Mo-Alumina based MPC(30-0) catalyst is also reported (the information on this catalyst was presented in paragraph 2.2.1).

In bare alumina (NPC(0-0)), one strong band at 770 cm^{-1} assigned to the stretching vibration of Al-O-Al and three bands between 1425 to 1630 cm^{-1} attributed to physically or coordinately adsorbed H_2O are observed (5,6).

attributed to physically or coordinately adsorbed H_2O are observed (5,6).

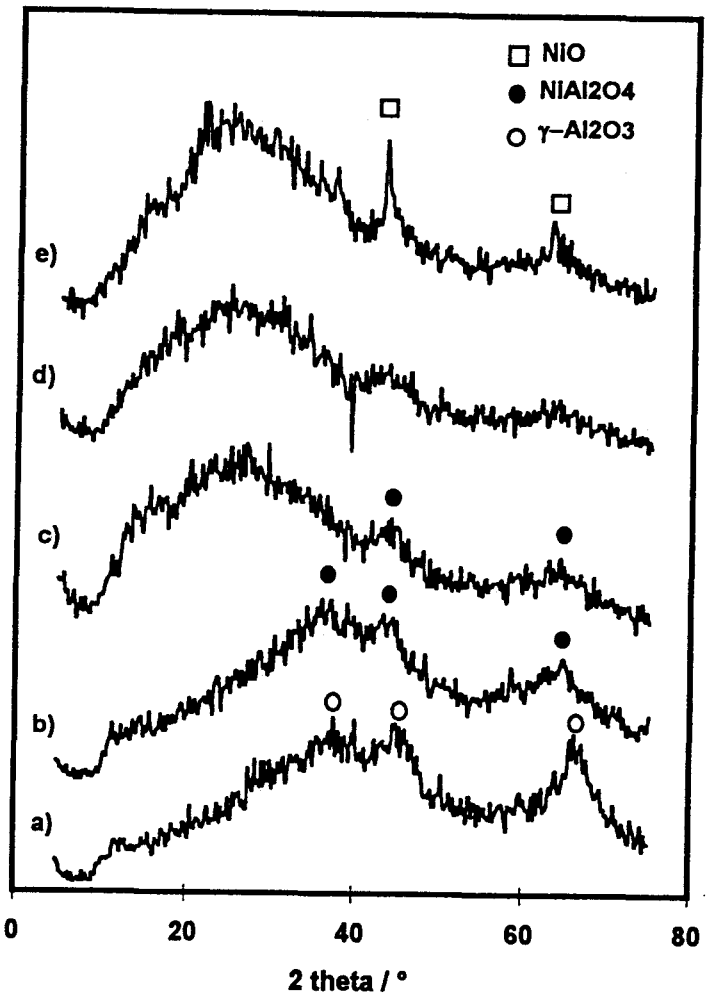

Fig. 2 X-ray diffraction patterns of Ni-P-Alumina sol-gel catalysts prepared from nickel nitrate as a Ni precursor. a) NPC(0-0), b) NPC(18-0), c) NPC(18-9) d) NPC(18-13) e) NPC(18-16).

In P loaded samples (NPC(0-11) or NPC(6-12)), two bands also appear at ~ 1125 and 1090 cm^{-1} which are assigned to the stretching vibration of $P{=}O_t$ and P-O, respectively (7-9). In case of Mo-P-Alumina (MPC(30-0)), P-Alumina (NPC(0-11)) and Ni-P-Alumina (NPC(6-12)) catalysts, the bands at 1503, 1425cm^{-1} disappear by introducing Mo or P. This suggests that Mo and P are interacting or modifying sites of alumina which have the capability to adsorb H_2O. In case of P-free Ni-Alumina (NPC(6-0)) catalysts, however, the characteristic three bands remain as in the case of bare alumina. Therefore, Ni species interacts with alumina sites in a different way from the one for Mo and P species.

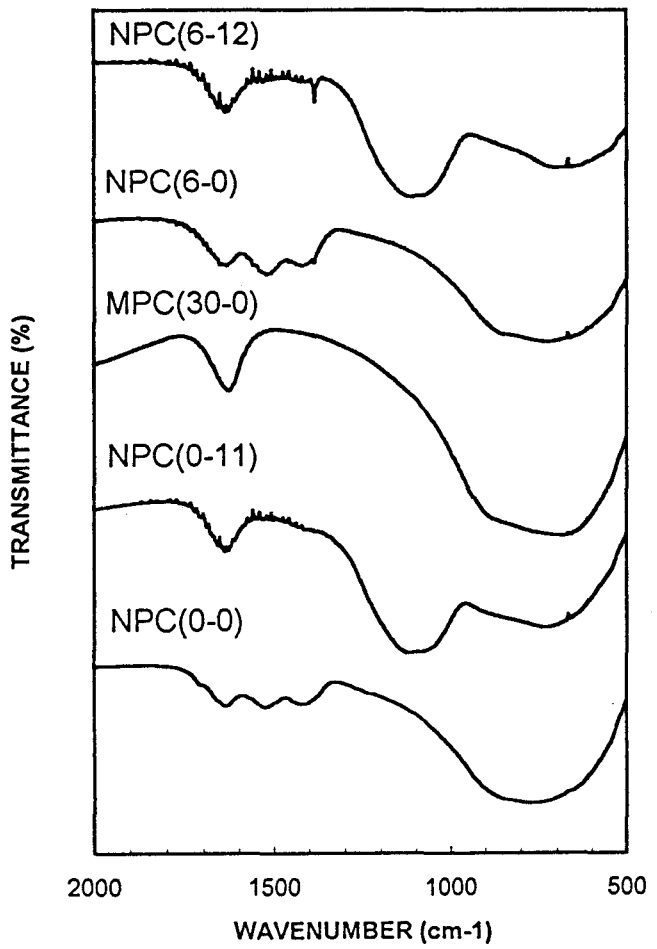

Fig. 3 IR spectra of Ni-P-Alumina sol-gel catalysts prepared from nickel nitrate as a Ni precursor.

Solid state ^{27}Al NMR

Fig. 4 shows solid state ^{27}Al NMR spectra of sol-gel catalysts obtained from $Ni(NO_3)_2$ as the Ni precursor after the drying stage. Within the measurement conditions, side bands are not theoretically observed in this region. In the dried sample, the bare alumina precursor (NPD(0-0), Fig. 4a) has only a single broad signal at ~7 ppm which is assigned to octahedral aluminium site (6). With addition of Ni (Fig. 4b, 4c and 4d) , a weak spectra assigned to tetrahedral Al (Al_{tetra}) is observed at ~65 ppm. At higher Ni loading, a spectra for penta-coordinated alumina (Al_{penta}) (6) or $NiAl_2O_4$ is also observed at ~30 ppm (Fig. 4c). The results indicate that even in the drying stage, presence of Ni induces modification of alumina precursor framework. However, by comparison with spectra on the calcined samples, it is suggested that the interaction between Ni^{2+} paramagnetic ions and the Al_2O_3 is still weak as less broadening is observed in

dried sample with high Ni loading. With addition of large amounts of P, an additional signal for $AlPO_4$ is also detected at ~40 ppm (Fig. 4f). The top peak position of Al_{octa} spectra shifts and broadens toward lower frequency. This might be in part attributed to decreases of alumina density (6,10) or to the formation of Al_{octa}-O-P sites considering the results of 2D ^{27}Al MQMAS NMR (see paragraph 2.2.2 Fig. 7d).

Fig. 5 shows solid state ^{27}Al NMR spectra of calcined sol-gel catalysts obtained from $Ni(NO_3)_2$ as the Ni precursor. On the bare alumina (Fig. 5a), signals attributed to the Al_{octa}, Al_{tetra} and Al_{penta} sites are observed at ~7, 60 and 33 ppm, respectively (6,11). The Ni-Alumina catalysts show a significant broadening of spectra after calcination due to the existence of a strong interaction between the Ni^{2+} paramagnetic ions and alumina centers, especially above ~ 20 wt% of Ni (Fig. 5d and 5c). This interaction reveals the presence of bridges Ni^{2+}-O-Al as shown in the $NiAl_2O_4$ spinel. Such an observation is in well agreement with the XRD results. However, the intensity of the signal around ~30 ppm decreases significantly with the P content as is obvious in the NPC(18-5) (Fig. 5e) and NPC(18-16) (Fig. 5f). Clearly, the amount of $NiAl_2O_4$ has considerably decreased by P introduction. In these P containing calcined catalysts, the spectra for $AlPO_4$ phase (Al_{tetra}-O-P surface species) was mainly observed at ~38ppm but Al_{octa} and Al_{tetra} are hardly detected. It is considered that the strong affinity of P and Ni with the alumina framework favors the destruction of γ-Alumina structure.

Solid state ^{31}P NMR

Fig. 6 shows solid state ^{31}P NMR spectra of dried and calcined sol-gel catalysts obtained from nickel nitrate as the Ni precursor. Although the spectra are broader and the chemical shifts are smaller than those for the ^{27}Al NMR, it is still possible to identify several species on the catalysts. A broad signal obtained from the dried NPD(0-11) (Fig. 6a) could be decomposed into 2 signals at ~-10 and -21 ppm. They are assigned to monomeric and polymeric P oxo-species, respectively (12). On the other hand, the Ni-P-Alumina catalysts such as NPD(18-5) (Fig. 6b), NPD(18-9) (Fig. 6c) and NPD(18-16) (Fig. 6d) give an other characteristic signal at about ~-16 ppm while it disappears by calcination. This signal might be assigned to less polymerized polymeric phosphate or some Ni-P species but the presence of Ni phosphate is not proved. Anyway, the presence of Ni seems to affect significantly the state of phosphorus.

All the calcined samples show polymeric P oxo-species and $AlPO_4$ at about ~-18 and -25 ppm, respectively. However, The Ni-P-Alumina catalysts (Fig. 6f to 6h) seems to have less polymeric P oxo-species than P-Alumina catalyst (Fig. 6e) as the symmetry of signal at ~-25 ppm tend to increase by the P addition.

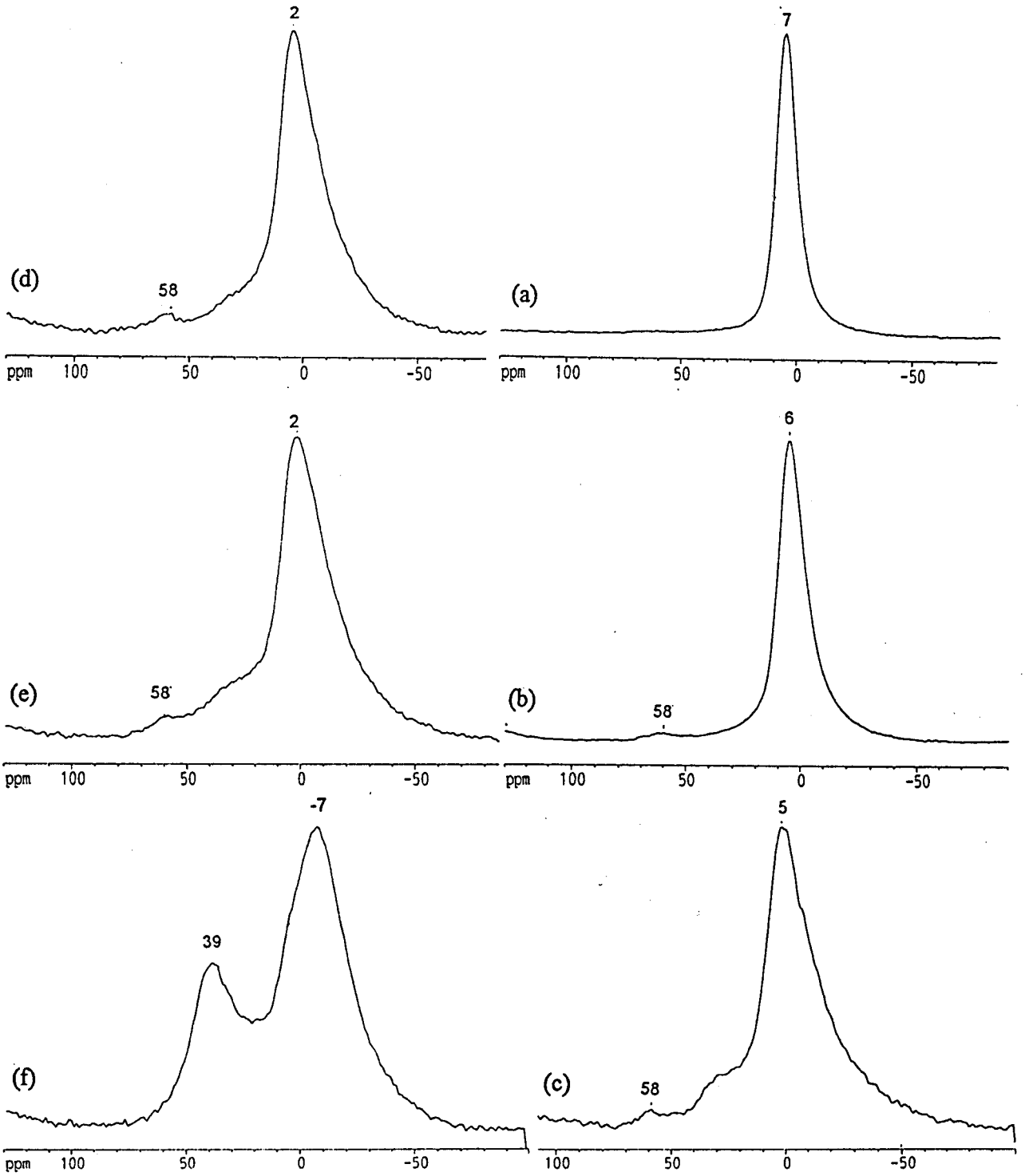

Fig. 4. Solid state ^{27}Al-NMR spectra of dried Ni-P-Alumina sol-gel catalysts. (a)NPD(0-0),(b)NPD(6-0),(c)NPD(24-0),(d)NPD(18-0),(e)NPD(18-5), f)NPD(18-16).

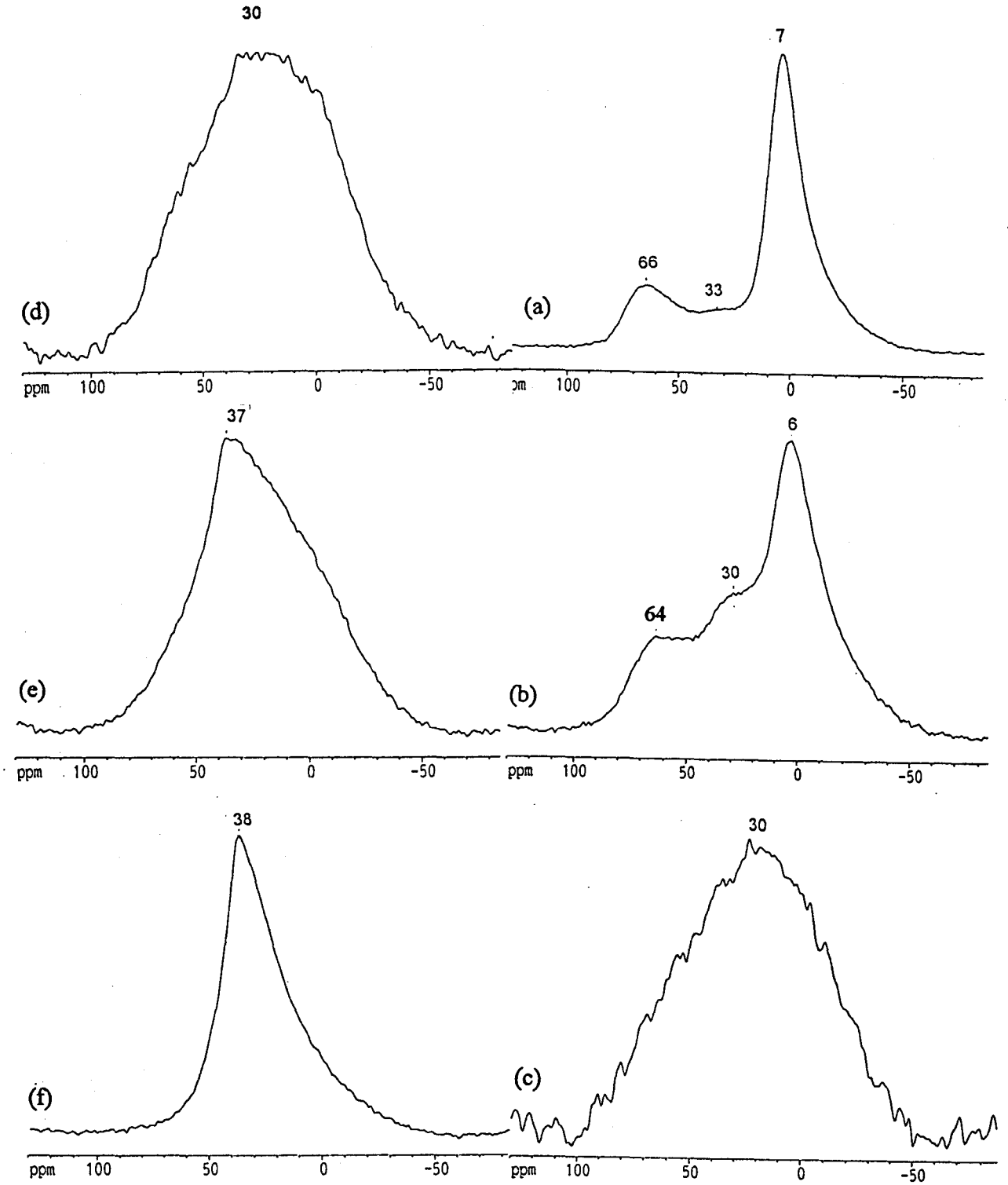

Fig. 5. Solid state ^{27}Al-NMR spectra of calcined Ni-P-Alumina sol-gel catalysts. (a)NPC(0-0),(b)NPC(6-0),(c)NPC(24-0),(d)NPC(18-0),(e)NPC(18-5), (f)NPC(18-16).

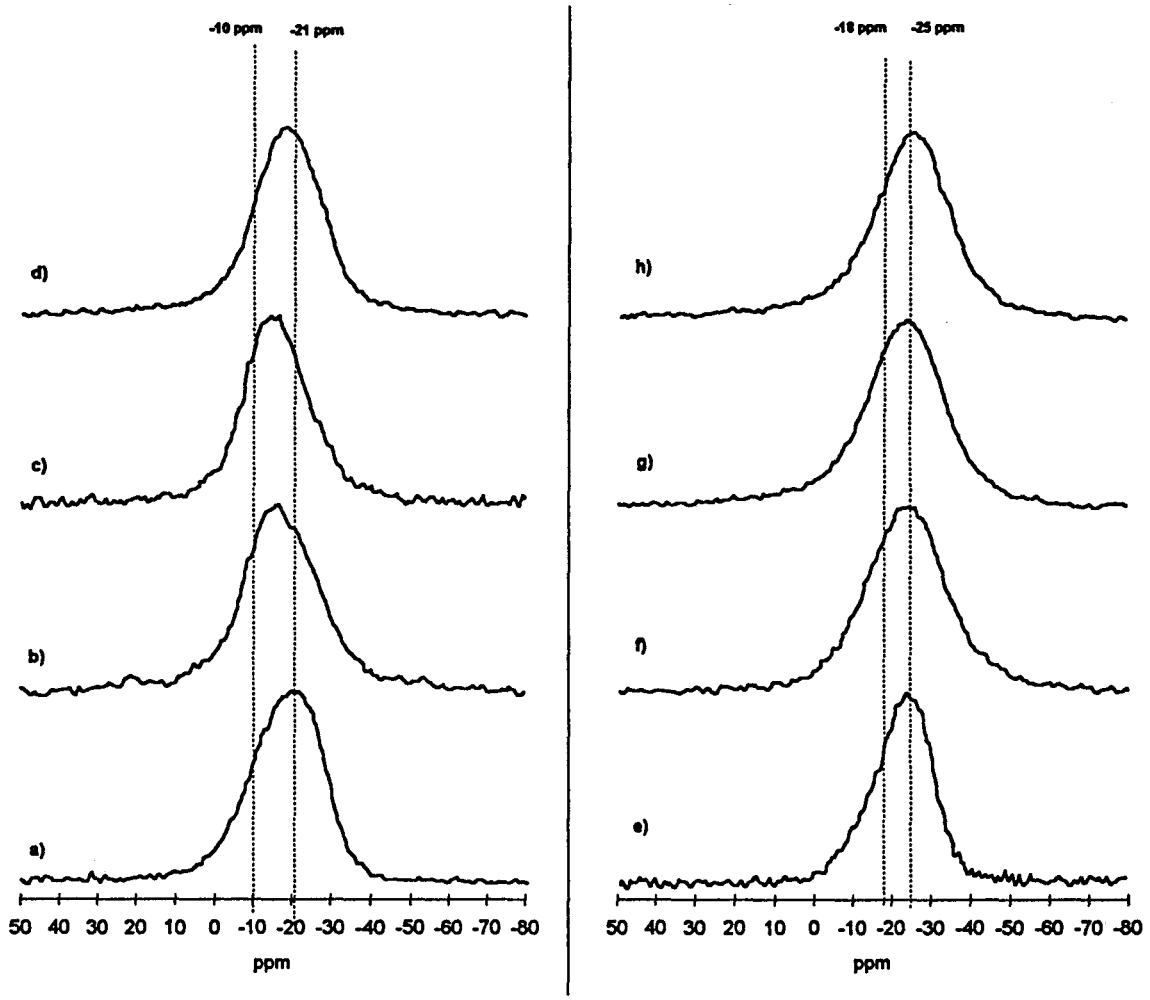

Fig. 6. Solid state ^{31}P-NMR spectra of Ni-P-Alumina sol-gel catalysts. Catalysts obtained after the drying stage at 100 °C. (a)NPD(0-11), (b)NPD(18-4), (c)NPD(18-9) (d)NPD(18-16) ; Catalysts obtained after the calcination stage at 500 °C (e)NPC(0-11),(f)NPC(18-4),(g)NPC(18-9), (h)NPC(18-16).

Thiophene HDS activity

Fig. 7 shows the thiophene HDS activity over the Ni-P-Alumina sol-gel catalysts as a function of the P content. The HDS activity increases with increasing of P content up to 12 wt% P in the series of 6 wt% Ni catalyst. The HDS activity in the series of 18 wt% Ni also increases up to 13 wt% P and slightly decreases at 16 wt% P. This decrease in the HDS activity could be attributed to the formation of bulk NiO considering the XRD results.

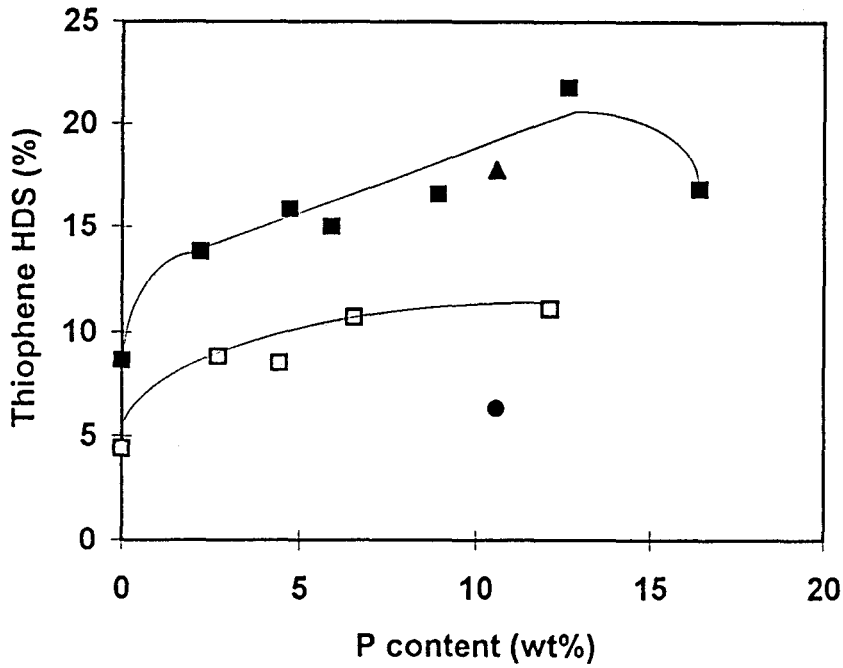

Fig. 7 Thiophene HDS activity over the Ni-P-Alumina sol-gel catalysts. Square denotes the catalysts prepared from nickel nitrate as the Ni precursor (opened : 6 wt% Ni, closed : 18 wt% Ni). ● : catalysts prepared from nickel carbonate as a Ni precursor, ▲ : catalysts prepared from nickel acetate as a Ni precursor.

The catalyst prepared from nickel acetate as a Ni precursor shows almost the same HDS activity as the nickel nitrate series at the equivalent P loading. On the other hand, the catalyst prepared from nickel carbonate as a Ni precursor gives very low HDS activity even with its higher SSA. Therefore, it is inferred that the HDS activity is mainly attributed to the amount of active sites and the dispersion of Ni species as estimated by the XRD measurements. Duchet and co-workers (13) also proposed that well dispersed Co sulphide on carbon have high activity for HDS. In the case of P-free Ni-Alumina, the strong interaction between Ni and alumina forms stable $NiAl_2O_4$ species. Consequently, not all the Ni are participating in the reaction. On the other hand, in the Ni-P-Alumina catalysts, decrease in the interaction between Ni and Al leads to the increase the formation of active Ni sulphide phase. In fact, XPS study revealed that the sulphidability of Ni species increases in the presence of P (see paragraph 2.4.2).

Fig. 8 shows the selectivity for saturated C_4 products (butane) in thiophene HDS reaction over Ni-P-Alumina catalyst. The hydrogenation selectivity of Ni-P-

Alumina is quite lower than that of Mo-P-Alumina catalysts. It reaches an almost steady value, irrespective of the P content. It is therefore suggested as expected that active sites of nickel sulphides are quite different from those in MoS_{2-x}.

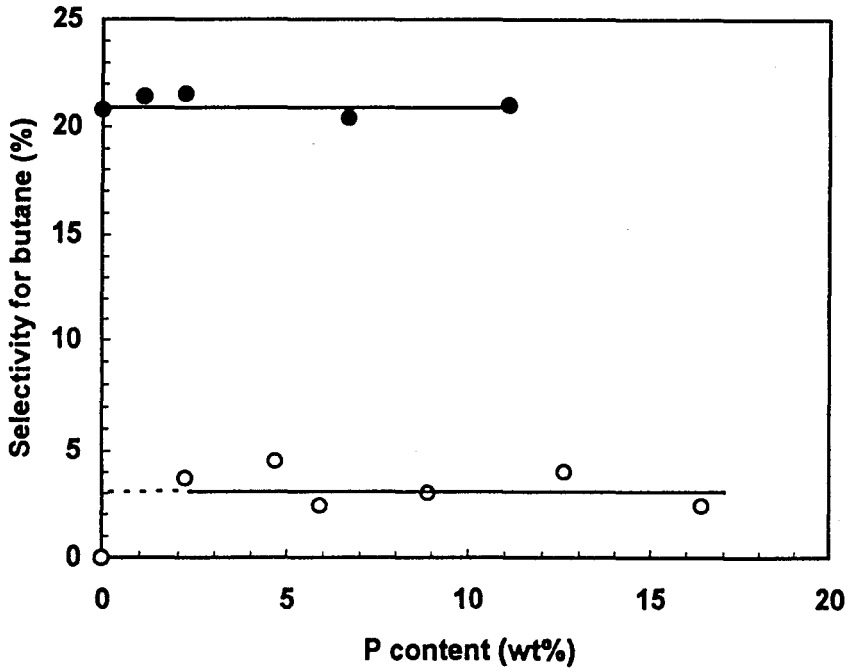

Fig. 8 The selectivity for saturated C_4 product in thiophene HDS reaction over the sol-gel catalysts. O : Ni-P-Alumina (~18 wt% of Ni), ● : Mo-P-Alumina catalysts (~18 wt% of Mo), respectively. The reaction were carried out at 400 °C for the Ni-P-Alumina and 300 °C for the Mo-P-Alumina catalysts.

2.3.4. Conclusion

The Ni- P-Alumina catalysts with a wide range of P loading were prepared by a sol-gel method to elucidate the role of phosphorous on the textural, structural and catalytic properties of Ni-Alumina based catalysts. It was found that amount of P and nature of Ni precursors affect significantly on the physicochemical and catalytic properties of obtained catalysts. Large amount of P decreases specific surface area and favors the segregation of bulk NiO species. The presence of P also decreases the formation of nickel aluminate ($NiAl_2O_4$) and provokes the formation of $AlPO_4$ (Al_{tetra}-O-P surface species).

The moderate loading of P improves thiophene HDS activity considerably by increasing the amount of active Ni sulphide, while large amount of P decreased it due to the formation of bulk NiO. The active sites of Ni-Alumina

Alumina is quite lower than that of Mo-P-Alumina catalysts. It reaches an almost steady value, irrespective of the P content. It is therefore suggested as expected that active sites of nickel sulphides are quite different from those in MoS_{2-x}.

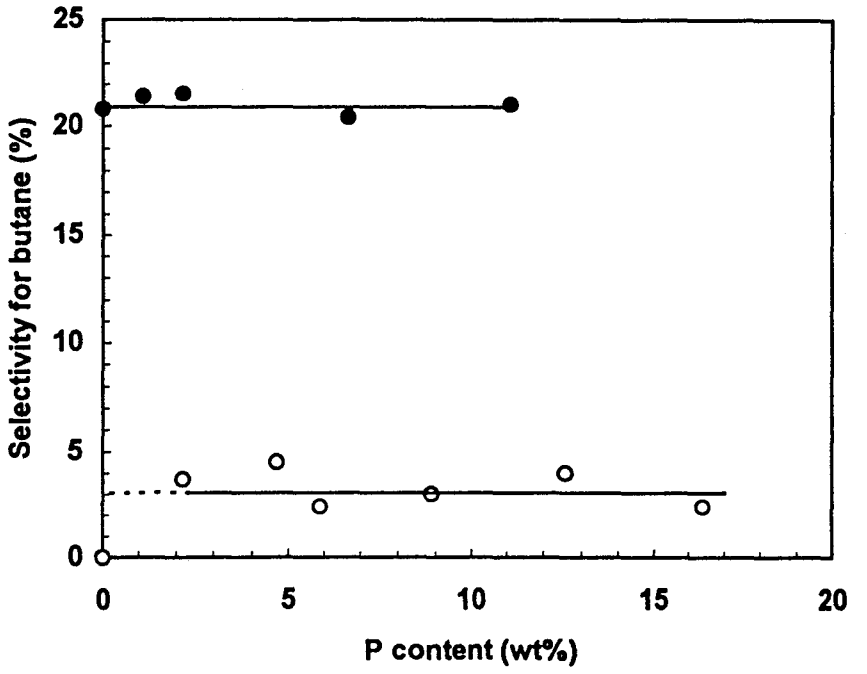

Fig. 8 The selectivity for saturated C_4 product in thiophene HDS reaction over the sol-gel catalysts. O : Ni-P-Alumina (~18 wt% of Ni), ● : Mo-P-Alumina catalysts (~18 wt% of Mo), respectively. The reaction were carried out at 400 °C for the Ni-P-Alumina and 300 °C for the Mo-P-Alumina catalysts.

2.3.4. Conclusion

The Ni- P-Alumina catalysts with a wide range of P loading were prepared by a sol-gel method to elucidate the role of phosphorous on the textural, structural and catalytic properties of Ni-Alumina based catalysts. It was found that amount of P and nature of Ni precursors affect significantly on the physicochemical and catalytic properties of obtained catalysts. Large amount of P decreases specific surface area and favors the segregation of bulk NiO species. The presence of P also decreases the formation of nickel aluminate ($NiAl_2O_4$) and provokes the formation of $AlPO_4$.

The moderate loading of P improves thiophene HDS activity considerably by increasing the amount of active Ni sulphide, while large amount of P decreased it due to the formation of bulk NiO. The active sites of Ni-Alumina

based catalysts might be different from that in the MoS_2 structure since the Ni-Alumina shows the considerably lower hydrogenation activity than Mo-Alumina based catalysts. If CUS are considered to be the main active sites, the nature of the metal center (Mo or Ni) and its electronic properties could effectivly affect both activity and selectivity. Fig. 9 gives a brief description of the possible location of Ni in Ni-P-Alumina catalysts after calcination.

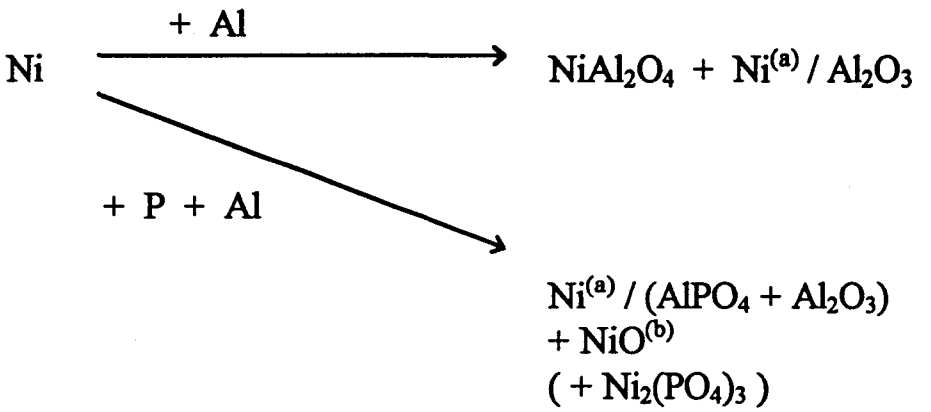

(a) The dispersed Ni species which are probably responsible for the HDS reaction after sulphidation.
(b) NiO is only formed at high Ni loading.

Fig. 9 Schematic description of Ni location in Ni-P-Alumina catalysts after calcination.

2.3.5. Reference

(1) López-Agudo, A., Cordero, R. L., Palacios, J. M., and Fierro, J. L., Bull. Soc. Chem. Belg., **104**, 237 (1995)
(2) Molales, A., Ramirez, M. M., and Agudelo, M.M.R., Appl. Catal., **23**, 23 (1986)
(3) Andreev, A., Vladov, Ch., Petrov, L., and Atanasova, P., Appl. Catal. **108** (A), L97 (1994)
(4) Robinson, W.R.A.M., van Gestel, J.N.M., Korányi, T.I., Eijsbouts, S., van kraan, A.M., van Veen, J.A.R., and de Beer, V.H.J., J. Catal., **161**, 539 (1996)
(5) Boorman, P.M., Kydd, R.A., Sorensen, T.S., Chong, K., Lewis, J.M., and Bell, W.S., Feul, **71**, 87 (1992)

(6) Kurokawa, Y., Kobayashi, Y., and Nakata, S., Heterogeneous. Chem. Rev., **1**, 309 (1994)
(7) Lewis, J.M., and Kydd, R.A., J. Catal., **132**,465 (1991)
(8) Spojakima, A., and Damyanova, S., React. Kinet. Catal., **53**, 2, 405 (1994)
(9) Morterra, C., Magnacca, G., and de Maestri, P.P., J. catal., 152, 384 (1995)
(10) Bautista, F.M., Miller, J.M., and Zajac, G.W., Appl. Catal., **62**, 205 (1990)
(11) Risbud, S. H., Kirkpatrick, R. J., Taglialavore, A. P., and Nintez, B., J. Am. Ceram. Soc., **70 (1)**, C10 (1987)
(12) Decanio, E.C., Edward, J. C., Scalzo, T. R., Storm, D. A., and Bruno, J. W., J. Catal., **132**, 498, (1991)
(13) Duchet, J.C., van Oers, E.M., de Beer, V.H.J., and Prins, R., J.Catal, **80**, 386 (1983)

2.4 Le système Ni-Mo-P-Alumine : Comparaison avec les systèmes Mo-P et Ni-P-Alumine.

2.4.1 Genèse, structure et propriétés catalytiques du système Ni-Mo-P-Alumine préparé par voie sol-gel
(Genesis, Structural and Catalytic Properties of Ni-Mo-P-Alumina based Hydrotreating Catalysts Prepared by a Sol-Gel Method)

Abstract

Nickel oxide - Molybdenum oxide - P oxide - Alumina catalysts with a wide range of P loading were prepared by a sol-gel method to elucidate the role of phosphorous on the genesis, structural and catalytic properties of Ni -Mo based hydrotreating catalysts whose loading are expected to be ~ 6.5 wt% for Ni and ~20 wt% for Mo. The amount of P introduced in the catalyst formulation varied from 0 to ~10 wt%. The textural and structural properties of dried and calcined solids were studied by means of various characterization techniques. Specific surface area (SSA) of catalysts decreased gradually in proportion to the P loading. X-ray powder diffraction (XRD) revealed that both small and large amount of P within the alumina framework provoke aggregation of bulk MoO_3. ^{27}Al-NMR indicated that a part of octahedral aluminium sites is highly distorted in the presence of Ni, Mo and P. From ^{31}P-NMR measurements, predominant formation of polymeric P oxo-species and $AlPO_4$ were observed after calcination steps. The thiophene hydrodesulphurization (HDS) activity gave a maximum at 2 wt% of P loading due to an increase in Mo dispersion. Large amount of P loading (~ 10 wt% P) was negative effect on HDS activity due to the formation of bulk MoO_3. The selectivity in butane formation seems also to indicate the presence of another Ni sulphide phase which has a poor hydrogenation ability.

2.4.1.1. Introduction

In the previous parts, we have been investigated the effect of P on the Mo-P and Ni-P-Alumina catalysts prepared by sol-gel method. Although the addition of P in the catalyst formulation tends to decrease the dispersion of the active components, it has been shown that Mo can be incorporated in the Mo-P-Alumina system with a well dispersed state up to ~ 10 wt% of P at ~20 wt% of Mo. Similarly on the Ni-P-Alumina system, Ni can be well dispersed as well up to ~ 13 wt% of P at ~ 20 wt% of Ni. P addition increased the acid property of Mo-P-Alumina while it depends strongly on the nature of the P precursors used to

prepared the catalysts. The presence of P also increased thiophene HDS activity over Ni-P-Alumina. To achieve higher HDS activity by sol-gel made catalysts, it is quite interesting to investigate the effect of P on the genesis, structural and catalytic properties of promoted Ni-Mo based alumina sol-gel catalysts because it is the same as some conventional hydrotreating catalysts formulations.

The role of P on HDS activity over promoted Mo-Alumina based hydrotreating catalysts has already been largely studied. Muralidhar et al. (1) reported that thiophene HDS activity over Co-Mo-P-Alumina catalysts does not change at 0.5 wt% P loading while the activity decreases at 5 wt% P loading. Eijsbouts et al. (2,3) concluded that thiophene HDS over Ni-Mo Alumina catalysts is not promoted by P addition while the selectivity for unsaturated hydrocarbons slightly increases. On the other hand, Atanasova et al. (4) found that P gives maximum activity for thiophene HDS at ~2 wt% P_2O_5 over Ni-Mo-P-Alumina catalyst. Walendziewski (5) also observed a small maximum for thiophene HDS over a Co-Mo-P-Alumina catalyst containing 1.3 wt% P while selectivity for hydrogenated product was lower than for a P-free catalyst. Chadwick et al. (6) also revealed that thiophene HDS over Ni-Mo-Alumina catalyst shows a broad maximum at ~1 wt% P. Lewis et al. (10) observed positive effects of P on thiophene and quinoline spiked gas oil HDS at ~1 wt% P over Ni-Mo-P-Alumina catalysts. Kemp et al. (8) reported that Ni-Mo-P-Alumina and Co-Mo-P-Alumina catalysts prepared by hydrogel method shows the higher HDS activity for cracked heavy gas oil (CCHGO) than commercial catalyst. Jones et al. (9) found that gas oil HDS activity increases up to 3 wt% P. Chen et al. (10) also reported that HDS of atmospheric residue over Co-Mo-P-Alumina catalyst shows maximum activity at 5.4 wt% P.

Therefore, the precise effect of P on HDS activity over promoted Mo-P-Alumina catalysts has been not well understood yet and required more studies. In this work, the role of P on the genesis, textural, structural and catalytic activities of Ni-Mo-P-Alumina based hydrotreating catalysts prepared by a sol-gel method with a wide range of P loading were examined. Their main structural properties were compared with thiophene HDS activity.

2.4.1.2. Experimental

Catalyst Preparation

The Ni-Mo-P-Alumina oxide precursors based on a sol-gel method, were prepared according to the procedure summarized in Figure 1.

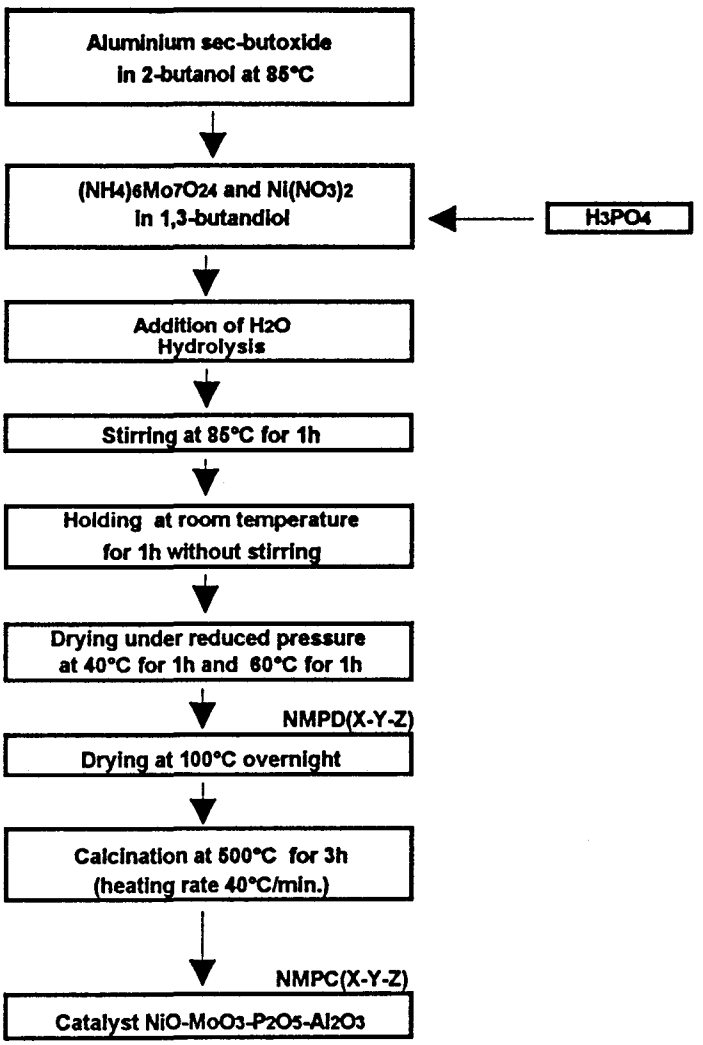

Figure 1. Procedure for preparation of Ni-Mo-P-Alumina sol-gel catalysts

Alumina was prepared by the hydrolysis of aluminium sec-butylate (ASB) dissolved in 2-butanol (2BN). Nickel, molybdenum and phosphorus were incorporated with the alumina precursor during the gel preparation. 99% of ortho-phosphoric acid (H_3PO_4), ammonium heptamolybdate (AHM) and nickel nitrate [$Ni(NO_3)_2 \cdot 6H_2O$] were mixed in 1,3-butanediol, simultaneously. H_3PO_4 and nickel nitrate have been chosen as P and Ni precursors of catalyst preparation because they were shown to be better for obtaining higher thiophene HDS activity in the Mo-P and Ni-P-Alumina systems. Ni/Mo atomic ratio was adjusted to 0.5 since it is considered to give the highest promoting effect in conventional HDS catalysts. The catalysts obtained are noted as, for example, MPD(Y-Z), NPC(X-Z), NMPD(X-Y-Z), NMPC(X-Y-Z) where D or C means dried or

calcined samples ; MP, NP or NMP mean Mo-P, Ni-P or Ni-Mo-P-Alumina based catalysts ; X, Y or Z means the expected loading in wt% of the elemental Ni, Mo or P from the preparation procedure, respectively.

Catalysts characterization

The chemical compositions were provided by the "Service Central d' analyses du CNRS" (Vernaison, France). The calcined samples, obtained as powders, were characterized by BET specific surface area (QUANTASORB Jr., Quantachrome) after a preheating at 200 °C for 30 min. Average pore diameter and pore volume are measured by N_2 adsorption (Belsorp 2S, Bell Japan Inc.) after a preheating at 200 °C for 3 h. X-ray diffraction (Siemens D5000 Diffractometer equipped with a goniometer, a monochrometor and a Cu X-ray tube), ^{27}Al-NMR (ASX400 BRUKER ; resonance frequency 104.26 MHz, recycling time 3 sec., pulse time 1 µsec., spinning frequency 15 kHz and $Al(H_2O)_6^{3+}$ as a reference) and ^{31}P-NMR (ASX100 BRUKER ; resonance frequency 40.53 MHz, recycling time 40 sec., pulse time 2 µsec., spinning frequency 7 kHz and H_3PO_4 as a reference) were also used to characterize the prepared samples, mainly after the calcination step.

Catalytic activity

Thiophene HDS reaction was carried out with the same procedure as already described in Mo-P-Alumina system. 0.2 g of catalyst was sulphided at 400 °C for 2 h with a H_2/H_2S (90/10) gas mixture at a flow rate of 50 ml/min and after cooling down to 300 °C, thiophene, purified by vacuum distillation, was introduced in the reactor at constant pressure (50 torr) with a flow of dried hydrogen (10 ml/min.) at atmospheric pressure. The reaction products (butane and butenes) were analyzed by gas chromatography.

2.4.1.3. Results and Discussion

Chemical composition and pore structure

Table 1 shows chemical composition and specific surface area per gram of catalyst (SSA) of selected calcined samples. The amount of residual carbon remaining in calcined samples is less than 0.5 wt% for all the Ni-Mo-P-Alumina catalysts. SSA decreases in proportion to the P content, although it remains as high as 400 m^2/g even with both high metal loadings (19.5 wt% of Mo and 6.3 wt% of Ni, respectively) and high P content (6.3 wt%) (sample NMPC(6-20-6)).

Table 1 Composition and SSA of calcined Ni-Mo-P-Alumina sol-gel Catalysts

Catalysts [a]	Mo (wt%)	Ni (wt%)	P (wt%)	Carbon (wt%)	SSA[b] (m^2/g)
MPC(0-0)	0	0	0	0.5	503
MPC(0-11)	0	0	10.6	0.3	474
NMPC(6-20-0)	20.8	6.5	0	0.3	609
NMPC(6-20-1)	19.3	7.2	1.3	0.5	526
NMPC(6-20-2)	21.6	6.8	2.4	0.4	461
NMPC(6-20-4)	20.4	5.8	3.8	0.3	451
NMPC(6-20-6)	19.5	6.3	6.3	0.5	400
NMPC(6-20-10)	20.3	5.8	9.7	0.3	263

(a) X, Y and Z in MPC(Y-Z) and NMPC(X-Y-Z) mean expected loading of Ni, Mo and P, respectively. (b) Specific surface area.

Average pore diameter (PD) and pore volume (PV) of selected sol-gel catalysts, measured by N_2 adsorption, are shown in Table 2. As a general tendency, the addition of Mo and P increases PD and PV while that of Ni decreases them. It is inferred that the addition of Ni and Mo affects the hydrolysis step of alumina gel. In another way, it is also considered that negatively charged Mo oxo-anions leads to the repulsion of negative charged alumina particles and positive charged Ni cations favors the attraction of alumina particles. The addition of P give fairly broad pore size distribution up to ~300 Å (figure is not shown here). In spite of its extremely high SSA, its PD are not considerably small like in carbon support. This means that sol-gel catalysts possess a highly porous texture compared with conventional hydrogel-derived alumina.

Table 2. Pore diameter (PD) and pore volume (PV) of selected sol-gel catalysts.

Catalysts	PD (Å)	PV (cc/g)
MPC(0-0)	68	0.89
MPC(30-0)	102	0.95
MPC(30-11)	160	0.86
NPC(6-0)	50	0.65
NPC(6-9)	116	0.88
NMPC(6-20-0)	96	0.62
NMPC(6-20-4)	176	0.71

X-ray powder diffraction (XRD)

Fig. 2 shows the X-ray powder diffraction patterns of the Ni-Mo-P-Alumina sol-gel catalysts. In the P-free NMPC(6-20-0) catalyst (Fig. 2a), the formation of bulk MoO_3 phase is identified. The addition of 2 to 4 wt% P into catalyst formulation prevents the formation of bulk MoO_3 as its relevant diffraction peaks are hardly detected (Fig. 2b and 2c). However, bulk MoO_3 appears again above 6 wt% P (Fig. 2d and 2e).

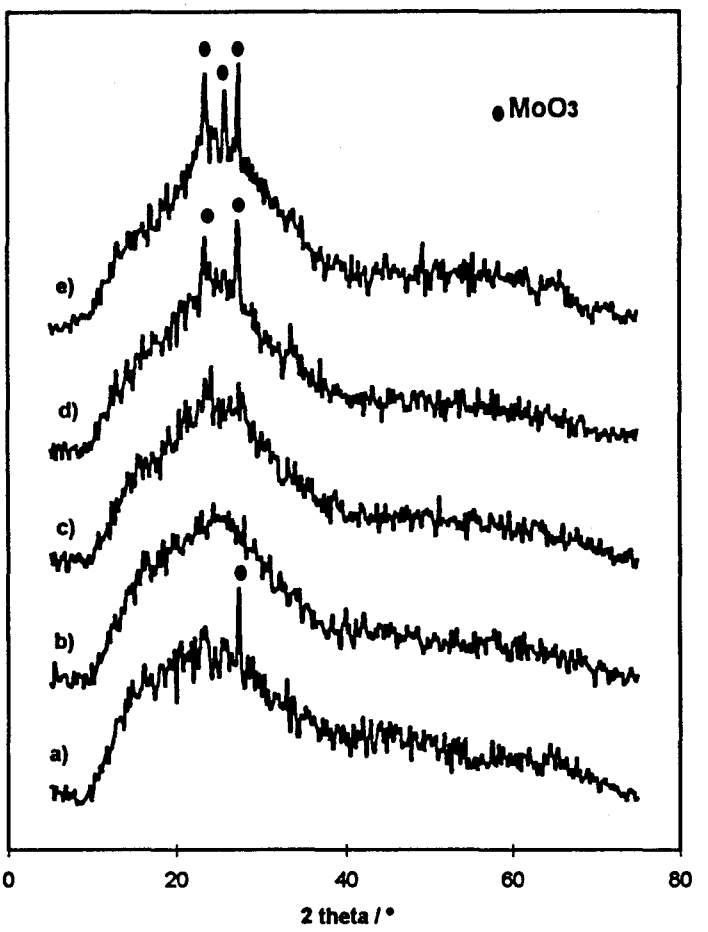

Fig. 2. X-ray diffraction patterns of Ni-Mo-P-Alumina sol-gel catalysts. a)NMPC(6-20-0), b)NMPC(6-20-2), c)NMPC(6-20-4), d)NMPC(6-20-6) and e)NMPC(6-20-10)

This result indicates that a moderate amount of P increases the dispersion of Mo but smaller or larger amount of P is detrimental for optimal Mo dispersion. It can be considered that the presence of P helps to increase the stability of Ni-

Mo complexes which could be formed in the preparation solution, though larger amount of P then impedes the interaction between the Mo oxo-species and alumina as already seen in the Mo-P-Alumina system. Since no bulk NiO nor $NiAl_2O_4$ is observed even at high P loading, Ni may be predominantly associated or in close interaction with Mo species rather than with the Al surface.

Solid state ^{27}Al-NMR

Fig. 3 shows solid state ^{27}Al-NMR spectra of dried and calcined Ni-Mo-P-Alumina based sol-gel catalysts and of the bare alumina reference. Within the measurement conditions, side bands are not theoretically observed in this region. Although it is somehow difficult to correctly differentiate all the contributions of spectra mainly due to peak broadening, it is still possible to identify some species on the catalysts.

In the drying state of samples, bare alumina (MPD (0-0), Fig. 3a) shows a single broad signal assigned to octahedral aluminium site (Al_{octa}) at 7 ppm (11). With addition of Ni and Mo (NMPD(6-20-0), Fig. 3b), a peak of weak intensity attributed to tetrahedral aluminium sites (Al_{tetra}) appears at ~60 ppm. With addition of large amounts of P (NMPD(6-20-10) Fig. 3d), the formation of $AlPO_4$ (more generally, Al_{tetra}-O-P sites) are also observed at ~ 40 ppm. In addition, broadness of Al_{octa} spectra toward lower frequency may indicates the formation of Al_{octa}-O-P sites considered from previous 2D ^{27}Al-MQMAS NMR studies for dried Mo-P-Alumina sample (paragraph 2.2.2 Fig. 7d).

In the calcined state, signals attributed to Al_{octa}, Al_{tetra} and 5-fold coordinated aluminium sites are observed at 7, 66 and 30 ppm (11,12) in the bare alumina (Fig. 3e). The P-free Ni-Mo-Alumina catalyst (NMPC(6-20-0), Fig. 3f) shows a spectrum almost similar to those of the bare alumina while the intensity of Al_{tetra} is relatively weak. The formation of nickel aluminate is not pronouncedly observed at ~25 ppm in NMPC(6-20-0) in contrast with that in Mo-free Ni-Alumina catalyst NPC(6-0) (see paragraph 2.3 Fig. 5b). This indicates again that Ni species preferably associates with Mo species rather than with the alumina support in the Ni-Mo-Alumina catalyst. This interaction between Ni and Mo in oxide form may transform into a commonly accepted Ni-Mo-S phase after sulphidation (13-15). In the presence of P, the characteristic spectra for $AlPO_4$ (Al_{tetra}-O-P surface species) are also observed at ~36 ppm (Fig. 3h). The top peak position of Al_{octa} around 5 ppm shifts toward lower values and tends to be broader with P and Mo loading. This suggests that distortion of Al becomes more pronounced in the presence of P, Ni and Mo.

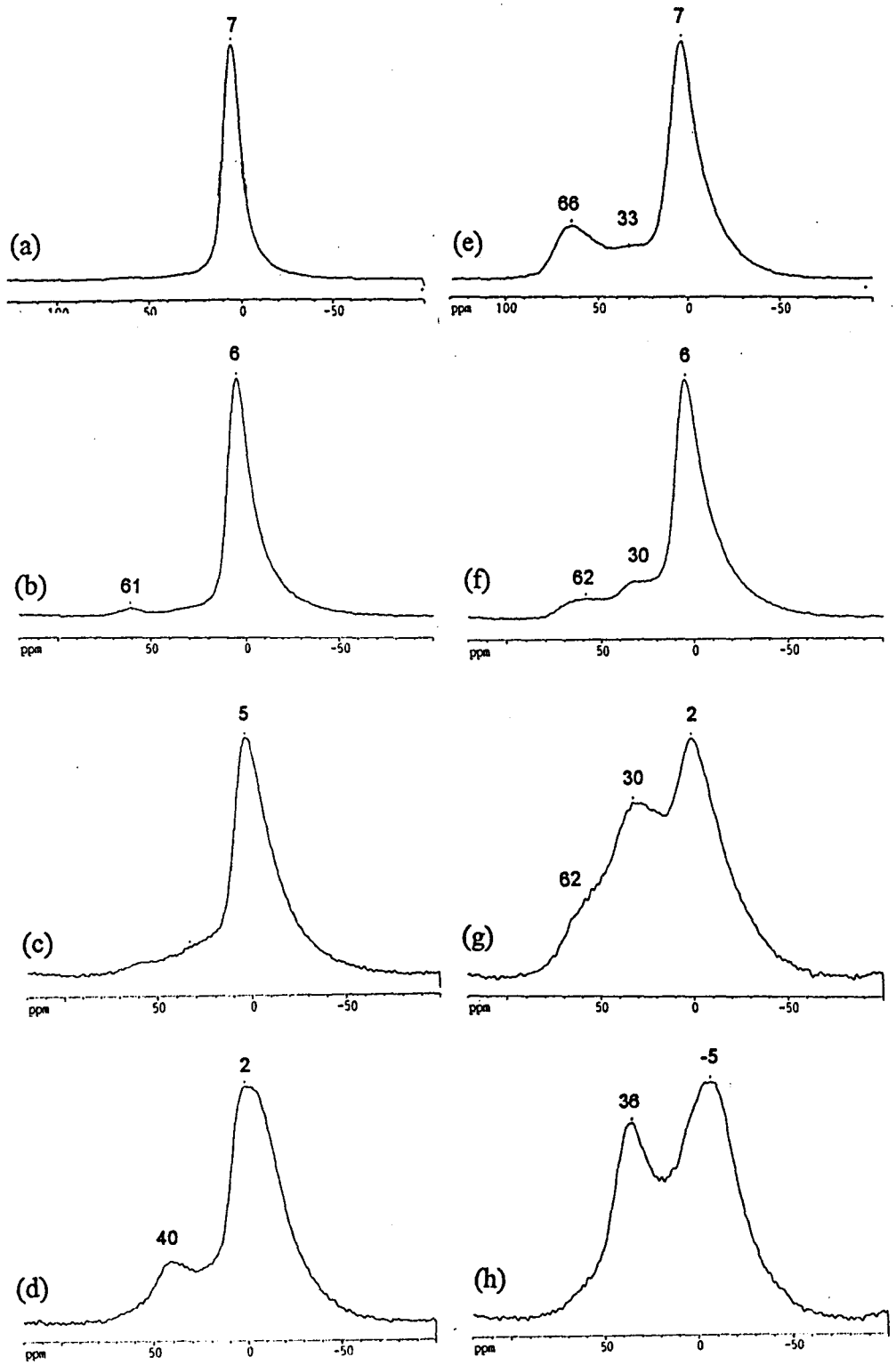

Fig. 3. Solid state ^{27}Al-NMR spectra of Ni-Mo-P-Alumina sol-gel catalysts. A :Catalysts obtained after drying stage at 100 °C (a)MPD(0-0),(b)NMPD(6-20-0),(c)NMPD(6-20-4),(d)NMPD(6-20-10) ; B :Catalysts obtained after calcination stage at 500 °C (e)MPC(0-0),(f)NMPC(6-20-0),(g)NMPC(6-20-4),(h)NMPC(6-20-10).

Moreover, in the NMPC(6-20-10) catalyst (Fig. 3h), the formation of $Al_2(MoO_4)_3$ is not observed while bulk MoO_3 is detected by XRD. This is not the same as the case of Mo-P-Alumina catalysts (paragraph 2.2.2 Fig. 2f). Although Ni seems to be preferably associated with Mo species, at least a part of Ni supported on alumina make weaker the interaction between the Al and Mo-oxo species to conduct after calcination to aluminium molybdate.

Solid state ^{31}P-NMR

Fig. 4 shows solid state ^{31}P-NMR spectra of dried and calcined Ni-Mo-P-Alumina sol-gel catalysts and of P-Alumina reference.

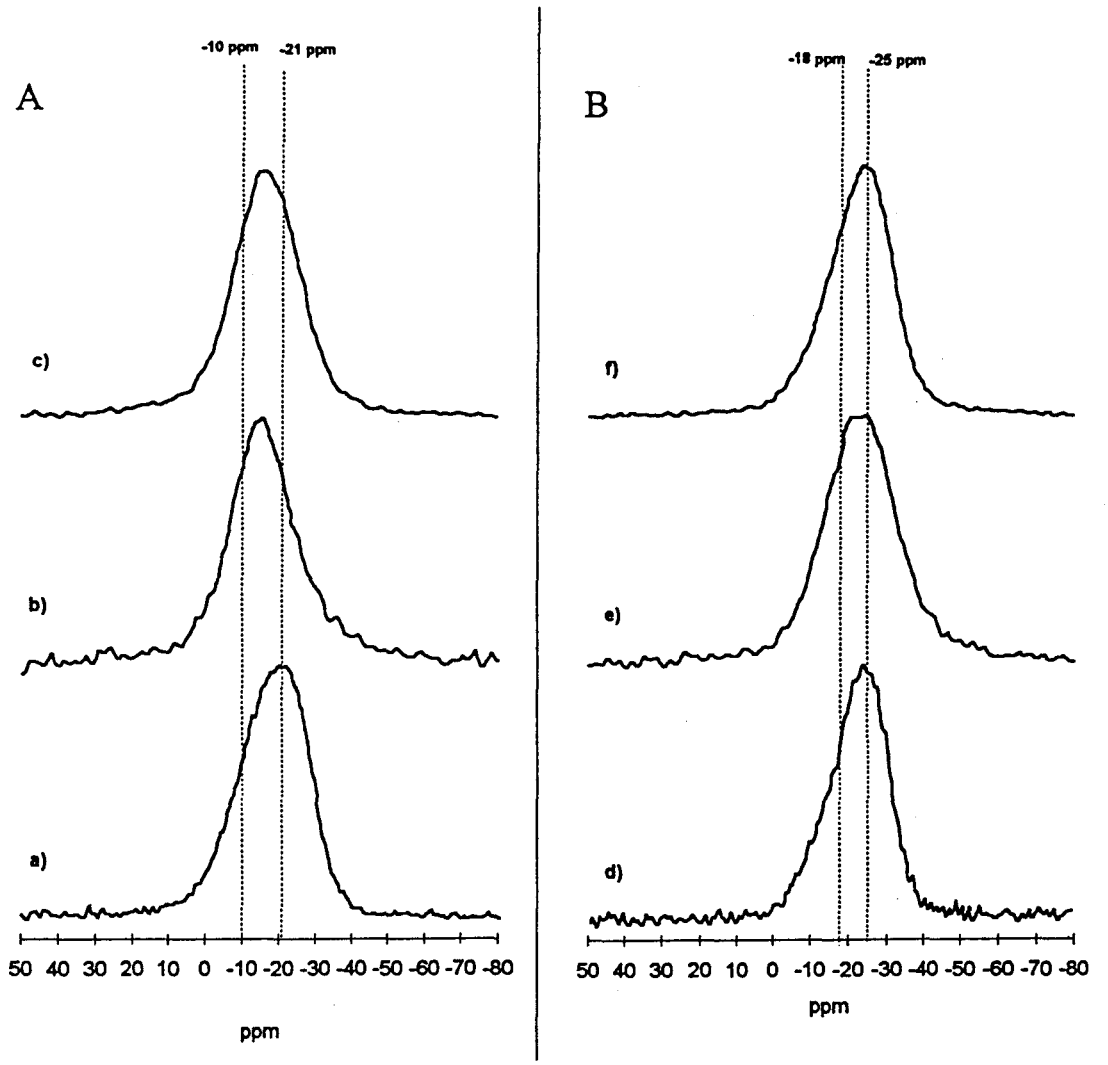

Fig. 4. Solid state ^{31}P-NMR spectra of Ni-Mo-P-Alumina sol-gel catalysts.
A :Catalysts obtained after drying stage at 100 °C (a)MPD(0-11),(b)NMPD(6-20-4),(c)NMPD(6-20-10) ; B :Catalysts obtained after calcination stage at 500 °C (d)MPC(0-11),(e)NMPC(6-20-4),(f)NMPC(6-20-10).

In dried samples, the P-Alumina catalyst (MPD(0-11), Fig. 4a) gives monomeric and polymeric P oxo-species at ~ -10 and -21 ppm, respectively (16). On the other hand, the Ni, Mo and P containing catalysts such as NMPD(6-20-4) (Fig. 4b) and NMPD(6-20-10) (Fig. 4c) give another characteristic signal at about ~-15 ppm as well as the Ni-P-Alumina and Mo-P-Alumina catalysts (see paragraph 2.3 Fig.6 and paragraph 2.2.3 Fig.4, respectively). This signal could be assigned to the formation of less polymerized P oxo-species or to the formation of some Ni-Mo-P mixed oxo-species.

The effect of P addition on the ^{31}P-NMR spectra of calcined samples is not so pronounced. All the calcined catalysts show polymeric P oxo-species and $AlPO_4$ at about -18 and -25 ppm, respectively.

Thiophene HDS activity

Fig. 5 shows the thiophene HDS evolution of Ni-Mo-P-Alumina sol-gel catalysts as a function of the P content. For a comparison basis, the results of Mo-P-Alumina [sample MPC(20-7)] and Ni-P-Alumina [sample NPC(18-9)] measured at same reaction conditions are also indicated in this figure. Concerning the trend for the Ni-Mo-P-Alumina catalysts, a initial HDS activity increases up to around 2 wt% P and then a smooth decrease. The initial HDS activity increase up to 2 wt% P is probably due to a better Mo dispersion as revealed by XRD measurements since samples NMPC(6-20-2) and NMPC(6-20-4) do not indicate the presence of bulk MoO_3 (Fig.2). In the same way, the smooth HDS activity decrease at higher P loading could be correlated to the formation of bulk MoO_3. The HDS conversion level between ~ 30 to 38 % for P loading ranging from 2 to 10 wt% is considerably higher than the sum of the activity of Mo-P-Alumina and Ni-P-Alumina catalysts which does not exceed 10 wt%. Clearly, a large part of Mo in the sulphided state is promoted by the Ni species like in the classical Ni-Mo catalysts. In this way, Fig. 5 gives a clear indication of the promotor hierarchy for thiophene HDS : Ni is the effective promotor of the active MoS_2 phase while the further addition of 2 to 4 wt% of P make the catalysts still more efficient. The combination effects could also be due to the contribution of P to stabilize the Ni-Mo complexes present in the preparation solution.

The results of butane selectivity during thiophene HDS presented in Fig. 6 complement those of Fig.5. The results obtained on the series Ni-P-Alumina and Mo-P-Alumina with a comparable metal (Mo or Ni) loading are also presented in Fig. 6 for comparison basis.

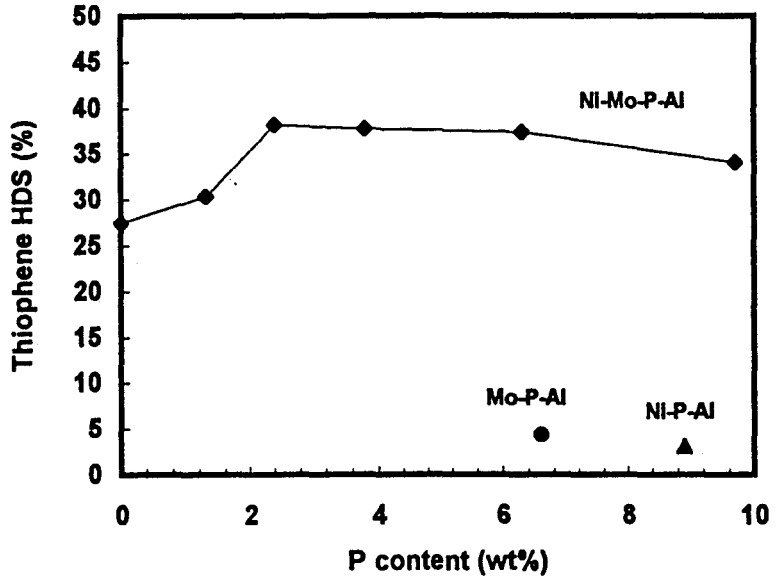

Fig. 5. Thiophene HDS activity of Ni-Mo-P-Alumina sol-gel catalysts. Mo-P-Alumina and Ni-P-Alumina are also indicated for comparison reason (Reaction temperature 300 °C).

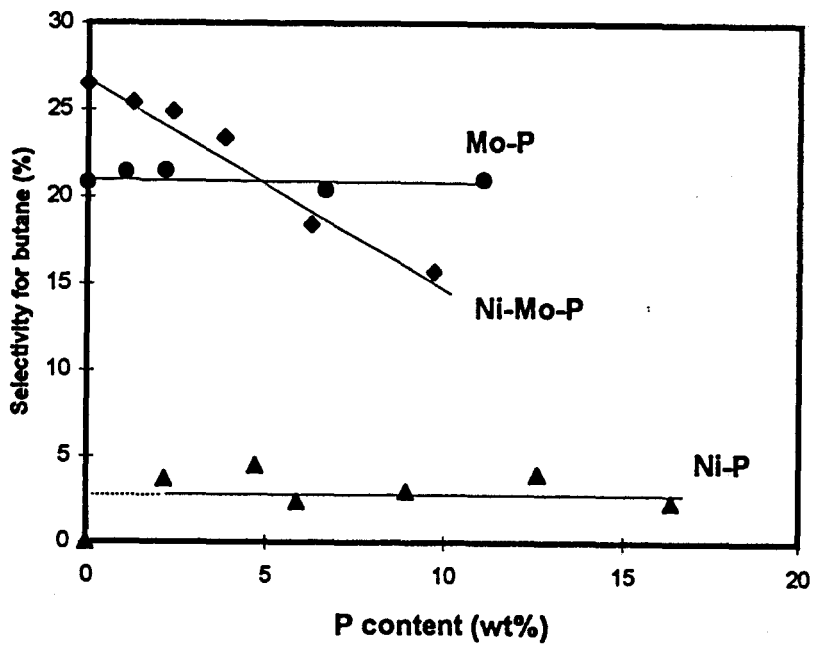

Fig. 6. Selectivity for hydrogenation of C_4 products in thiophene HDS over Ni-Mo-P-Alumina sol-gel catalysts (Reaction temperature : Mo-P and Ni-Mo-P 300 °C, Ni-P 400 °C)

It is shown that the hydrogenation selectivity for saturated C_4 production (butane) decreases quite linearly with the P content in the Ni-Mo-P-Alumina catalysts. The P loading has no influence on C_4 selectivity of Mo-P nor Ni-P-Alumina catalysts with however a higher butane selectivity for Mo-P than Ni-P-Alumina system. The P-free Ni-Mo catalysts has a further higher hydrogenation selectivity than that of Mo-P-Alumina catalysts. This indicates that presence of Ni promotes both HDS and HYD activities. However, the decrease of butane selectivity with increasing P loading to reach the level of Ni-P-Alumina catalyst by extrapolation suggests that a part of Ni species dissociates from Mo species in the presence of P and gives an isolated Ni sulphide with very poor hydrogenation capacity as shown in the Ni-P-Alumina system. If this hypothesis is correct, it is highly probable that a part of Ni species is not acting as a promotor and MoS_2 is not totally promoted in the presence of P. Therefore, it is considered that higher Ni/Mo ratio could more improve the HDS activity in the presence of P.

2.4.1.4. Conclusion

The Ni-Mo-P-Alumina catalysts with a wide range of P loading were prepared by a sol-gel method to elucidate the role of phosphorous on the textural, structural and catalytic properties of Ni-Mo based hydrotreating catalysts. The amount of P affects significantly on the physicochemical and catalytic properties of obtained catalysts. Large amount of P decreases the specific surface area. A moderate amount of P increases the Mo dispersion due to the stabilizing Ni-Mo complex in a preparation solution. The HDS activity is considerably improved by the P addition up to 2 wt% due to Mo dispersion increase. However, dissociation of Ni from Mo species may occur by the addition of P considering the hydrogenation selectivity decreases.

2.4.1.5. Reference

(1) G.Muralidhar, F.E.Massoth and J.Shabtai, J. Catal., 50, 3, 237 (1989)
(2) S. Eijsbouts, L.N.M.van Gestel, J.A.R.van Veen and V.H.J. de Beer, J. Catal., 131, 412 (1992)
(3) S. Eijsbouts, L.V.Gruijthuijsen, J.Volmer, V.H.J.de Beer and R. Prins, Ad. Hydrotreating Catal., 79 (1989)
(4) P. Atanasova, and T. Halachev, Appl. Catal., 38, 235 (1988)
(5) J. Wanlendziewski, React. Kinet. Catal., 43, 1, 107 (1991)
(6) D.Chadwick, D.W.Aitchison, R.Ohlbaum and L.Josefsson, Stud. Surf. Sci. Catal., 16, 323 (1983)
(7) J.M.Lewis, R.A.Kydd, P.M.Boorman and P.H.van Rhyn, Appl. Catal., 84,103 (1992)
(8) R.A.Kemp and C.T.Adams, Appl. Catal., 134, A, 299 (1996)
(9) J.M.Jones, R.A.Kydd, P.M.Boorman and P.H.van Rhyn, Fuel, 74(12), 1985 (1995)
(10) Y.W.Chen, W.C.Hsu, C.S.Lin, B.C.Kang, S.T.Wu, L.J.Leu and J.C.Wu, Ind. Eng. Chem. Res., 29, 1830 (1990)
(11) Y. Kurokawa,Y. Kobayashi and S. Nakata, Hetero. Chem. Rev., 1, 309 (1994)
(12) S. H. Risbud, R. J. Kirkpatrick, A. P. Taglialavore and B. Nintez, J. Am. Ceram. Soc., 70, 1, C10 (1987)
(13) H. Topsøe, B.S.Clausen, R.Candia, C.Wivel and S.Mørup, J.Catal., 68, 433 (1981)
(14) R.Candia, N-Y. Topsøe, B.S.Clausen and H.Topsøe, Bull. Soc. Chim. Belg., 93, 783 (1984)
(15) J.A.R.van Veen, E.Gerkema, A.M.Van der Kraan, P.A.J.M.Hendriks and H.Beens, J.Catal., 133, 122 (1992)
(16) E.C.Decanio, J. C. Edward, T. R. Scalzo, D. A. Storm and J. W. Bruno, J. Catal., 132, 498, (1991)

2.4.2 Effet du phosphore sur la sulfuration des catalyseurs à base d'alumine préparés par voie sol-gel
(Effect of P on the Sulphidability of Alumina Based Hydrotreating Catalysts Prepared by a Sol-Gel Method)

Abstract

A set of Mo-(P)-Al, Ni-(P)-Al and Ni-Mo-(P)-Alumina based hydrotreating catalysts were prepared by a sol-gel method to elucidate the role of phosphorus on sulphidability of Mo and Ni species. In Mo-P-Alumina catalyst, the sulphidability of Mo species strongly depended on the Mo and P content. At low Mo loading (17 wt% of Mo), the addition of P did not affect the Mo sulphidability which was estimated by measurement of bulk S/Mo atomic ratio after thiophene HDS reaction. On the other hand, it decreased the S/Mo ratio from 2 to 1 at higher Mo loading (26 wt% of Mo). XPS O 1s binding energies (BE) and full width of half maximum (FWHM) of high Mo loading catalysts suggested that a part of P is associated with Mo species through oxygen atoms. It was suggested that strong P-O-Mo bond may prevent exchanging oxygen by S atom during the sulphidation procedure. On the other hand, in Ni-P-Alumina catalyst, the addition of P increased the sulphidability of Ni species from 78 to 93 %. In Ni-Mo-P-Alumina catalyst, the sulphidability of Mo also decreased with P addition as in the case of Mo-P-Alumina catalyst. Large FWHM of XPS Mo 3d and O 1s spectra suggested that strong interaction between Ni, Mo, O and P also exists in Ni-Mo-P-Alumina catalyst. However, the sulphidability of Ni was higher (100%) than that of Mo-free Ni-Alumina catalyst and depends less on the P addition, since the Ni species are predominantly associated with Mo species.

2.4.2.1. Introduction

As already described in paragraph 2.3.1, the addition of P into Ni-Mo-Alumina sol-gel catalysts improved pronouncedly its thiophene HDS activity. Since hydrotreating catalysts are almost always used under H_2 or H_2S, it must be very important to understand the effect of P on sulphidability of both supported molybdenum and promotors.

The sulphidability of Ni-Mo-P-Alumina based hydrotreating catalysts has been already largely studied. Mangnus et al. (1) showed by TPS that P/Al and $AlPO_4$ are chemically unreactive with H_2S up to 723 °C. Chadwick et al. (2) also found no evidence of sulphided P formation from XPS measurements. These results indicate that P oxo-species does not transform to phosphorus sulphides or phosphorus oxy-sulphides during the classical conditions of the hydrotreating reactions. Sajkowski et al. (3) reported that P presence does not affect the

sulphiding behavior of Mo/Al catalysts. Mangnus et al. (1) also found that the S/Mo ratio in the MoP/Al catalysts after TPS measurements is independent of its P content and always shows a steady value of 2. Concerning solid state reactions, MoS_2 does not react with $AlPO_4$ to form MoP_x species (where x=1,2) below 1000 °C due to thermodynamic limitations (1). However, Poulet et al. (4) reported that P decreases the S/Mo ratio of a MoP/Al catalyst after sulphidation or after a subsequent hydrogen treatment. Sulphidation procedure of Co-Alumina or Ni-Alumina catalysts generally leads to the formation of Co_9S_8 or Ni_3S_2. López-Agudo et al. (5) reported that the sulphidability of Ni measured by XPS is not influenced by the P addition. However, Mangnus et al. (1) reported that the temperature of complete sulphidation of Co-P/Al increases with increasing the P content. The S/Co atomic ratio after sulphidation at 1000 °C decreases from 1.3 to 0.39 with P addition due to the formation of not sulphided compounds like cobalt phosphides . In sulphided Co-Mo-Alumina or Ni-Mo-Alumina catalysts, the formation of CoMoS or NiMoS structure has been commonly accepted as well as individual Mo, Co or Ni sulphide species. Andrev et al. (6) suggested the formation of the $NiPS_3$ compound after the sulphidation of NiMoP/Al. However, Robinson et al. (7) revealed that $NiPS_3$ decomposed to Ni_2P under the hydrotreating conditions, even in the presence of H_2S.

In spite of large amounts of investigations as described above, the effects of P on the sulphidability of P-containing alumina based hydrotreating catalysts has not been well understood yet. In this work, therefore, the effects of P on the sulphidability of alumina based sol-gel catalysts was investigated mainly by using XPS surface analysis. The sol-gel catalysts might be quite suitable for this kind of studies since they has extremely high specific surface area and high metal loading.

2.4.2.2. Experimental

Catalyst preparation and sulphidation

A set of Mo-Alumina, Mo-P-Alumina, Ni-Alumina, Ni-P-Alumina, Ni-Mo-Alumina and Ni-Mo-P-Alumina catalysts were prepared based on a sol-gel method. The detail preparation procedures of each catalysts were already described in paragraph 2.2.1, 2.3 and 2.4.1. Alumina precursor was prepared by a hydrolysis of aluminium sec-butylate (ASB). $(NH_4)_6Mo_7O_{24}$, $Ni(NO_3)_2 \cdot 6H_2O$ and 99% of ortho-phosphoric acid (H_3PO_4) were used as Mo, Ni and P precursors. They were incorporated with ASB before the hydrolysis. Phosphoric acid and nickel nitrate have been selected to prepare catalysts as they were revealed to show higher catalytic performance. The name of catalysts obtained were noted on the same manner as the previous reports. MPC(Y-Z), NPC(X-Z), NMPC(X-Y-Z)

means Ni, Mo or P containing catalyst where X, Y or Z mean the amount of Ni, Mo or P loading in wt% as a element, respectively.

Sulphidation of catalysts was carried out in situ by passing a gas mixture containing 10 vol% H_2S in H_2 at 400 °C for 2 h at a flow rate of 50 ml/min. Bulk S/Mo atomic ratio of Mo-P-Alumina catalysts was measured by chemical analysis (provided by Service Central d'analyses du CNRS; Vernaison, France) after thiophene HDS reaction at 300 °C for 3 h. The details of the reaction conditions have been already described in paragraph 2.2.1.

XPS measurements

XPS spectra were obtained by using a AEI ES 200 B spectrometer equipped with an Al X-ray source working at 300 W and 1486.6 eV. Binding energies (BE) were referenced against the Al 2p peak at 74.8 eV. The measurements of all the sulphided samples were always carried out without air exposure to avoid surface oxidation. The sulphided sample kept in a reactor was took out in a glove box attached to the spectrometer. Then, the sample powder was pressed on an indium foil mounted on the sample probe which can be introduced directly into the spectrometer.

The degree of Mo sulphidation was calculated after decomposition the Mo 3d complex spectra into three doublets, relevant respectively to the presence of Mo(VI), Mo(V) and Mo(IV) species (11). The Mo $3d_{5/2}$ and Mo $3d_{3/2}$ peak separation was assumed to be constant (3.1 eV) and with a relative proportion equal to 1.5/1. The degree of Ni sulphidability was calculated by a procedure already described in ref.(12) which do not require complete spectra decomposition as the satellite structures of the different Ni species are quite complicate. The procedure uses only the contribution of the half area of Ni 2p sulphide spectra in the lower BE side (A_h) which is not affected by that of oxide species. The degree of Ni sulphidation is then given by

$A_h / (0.29A_t)$ (where A_t means the total area of Ni $2p_{3/2}$)

Ni 2p and P 2p XPS spectra of bulk Ni_2P were also measured after the same sulphidation procedure and were referenced to C 1s (BE= 285 eV) for comparison reason.

2.4.2.3.Results and Discussion

Mo-Alumina and Mo-P-Alumina catalysts

Fig. 1 shows the relation between P content and bulk S/Mo atomic ratio measured after thiophene HDS reaction. The sulphidability of molybdenum strongly depends on the P and Mo content. The presence of P does not affect the

sulphidability of Mo oxo-species (bulk S/Mo value) at a low Mo content (~17 wt%). On the other hand, it decreases considerably from ~2 to ~1 with P loading at higher Mo loading (~26 wt% of Mo).

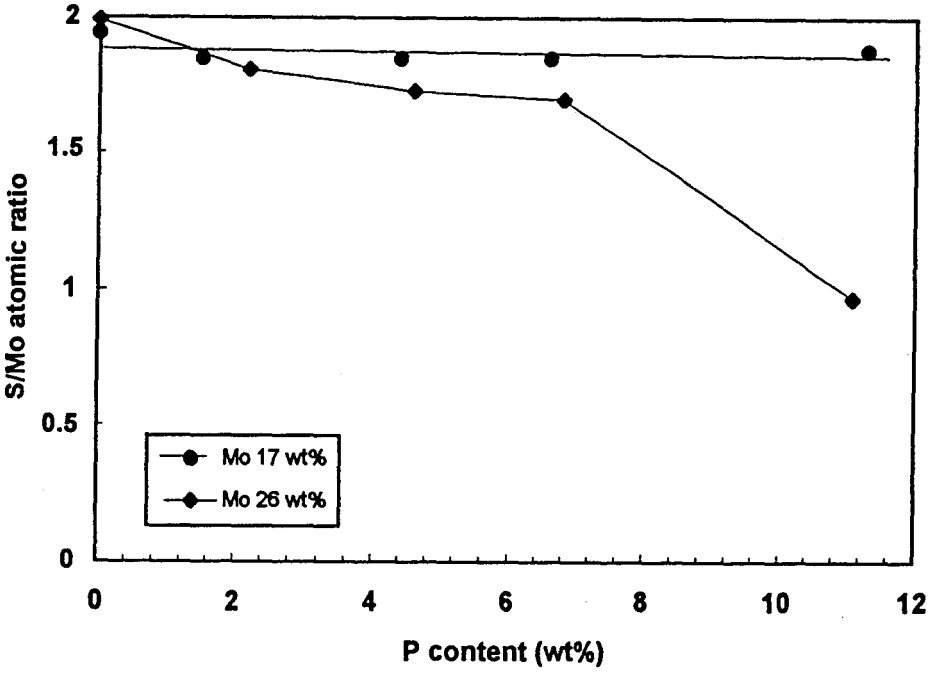

Fig. 1. Variation of the atomic S/Mo ratio measured after thiophene HDS as a function of P loading for Mo-P-Alumina catalysts.

Results of XPS measurements of Mo-Alumina and Mo-P-Alumina catalysts before and after *in situ* sulphidation are shown in Table 1. Before sulphidation, Mo is completely present as Mo(VI) species in oxidic environment. The addition of P does not apparently affect the state of Mo species.

After catalyst sulphidation, however, 90 % of Mo(VI) oxide is transformed into Mo(IV) in MoS_2 and into an intermediate state which can be attributed to Mo (V) oxy-sulphide in the P-free MPC(30-0) catalyst. It is suggested that strong chemical bonding between the Mo oxo-species and the alumina surface (Mo-O-Al bridges) prevents complete sulphidation because O of the bridged are not easily exchanged by S atoms. The addition of P further decreases the sulphidability of Mo(VI) into Mo(V) and Mo(IV) from 90 to ~ 85 %. (The S/Mo ratio obtained from bulk analysis is higher than that from XPS measurement. Since the bulk S/Mo ratio was measured after thiophene HDS reaction, sulphur

might be added onto Mo species during HDS reaction). In addition, the FWHM of O 1s increase pronouncedly by the addition of P, especially after sulphidation. The BE of O 1s in the P -containing MPC(30-5) also increases after sulphidation. These results suggest that a strong interaction between P and Mo species exists through the bridged oxygen bonding.

However, the sulphidability does not change in the series of low Mo loading catalyst. It is suggested that Mo and P oxo-species may have no interaction each others in the low P loading region. Since there are still abundant OH groups reactive with P and Mo on the alumina surface in the low Mo loading, Mo and P species may be supported on the alumina individually. With increasing P and Mo loading, however, P oxo-species should start to interact with Mo oxo-species by sharing their oxygen bonds. The strong chemical P-O bonds in mixed Mo-O-P species make the bridged oxygen atoms not easily exchangeable by S atoms and therefore may prevent sulphidation of the Mo oxo-species. These results could explain in part the discrepancies reported in the literature on P effect on the sulphidability of Mo-Alumina based hydrotreating catalysts. In addition, XRD measurement revealed that the addition of P decrease Mo dispersion especially above 6 wt% of P in the series of high Mo loading catalyst (see paragraph 2.2.1 Fig. 2). Therefore, the sulphidability decrease above 6 wt% P in the series with 26 wt% Mo may be also attributed to the Mo dispersion decrease.

The dispersion of P species in MPC(30-4) seems to be not affected by sulphidation as the intensities of I(P)/I(Al) are almost constant as shown in Table 1.

Ni-Alumina and Ni-P-Alumina

Results of XPS measurements of Ni-Alumina and Ni-P-Alumina sol-gel catalysts before and after *in situ* sulphidation are also shown in Table 1. Before sulphidation, all the Ni species exists as Ni^{2+} ions in an oxide environment.

After catalysts sulphidation, 78 % of Ni^{2+} ions transform into Ni species in a sulphided environment in NPC(18-0). The presence of P increases the sulphidability of Ni from 78 to 93 % (NPC(18-9)). It is considered that the strong interaction between P oxo-species and alumina (i.e. the formation of $AlPO_4$) prevent the formation of stable nickel aluminate. P may also interact with Ni to create new phases like Ni_2P during the sulphidation step. However, the formation of Ni_2P is not clearly confirmed in the sulfided NPC(18-10) catalyst as the characteristic P 2p spectra at ~130 eV attributed to the reference Ni_2P compounds is not observed in NPC(18-9). Therefore, Ni_2P would be minor species in this Ni-P-Alumina system because its formation needs rather higher temperature than 1000 °C (1).

The intensity of I(Ni) / I(Al) slightly increase after sulphidation of NPC(18-0) which would suggest a better dispersion of Ni or a diffusion from the bulk to surface. On the contrary, sulphidation of NPC(18-9) does not significantly affect the I(Ni) / I(Al) ratio.

Ni-Mo-Alumina and Ni-Mo-P-Alumina

Results of XPS measurements of Ni-Mo-Alumina and Ni-Mo-P-Alumina sol-gel catalysts before and after sulphidation are also shown in Table 1. Before sulphidation, all Ni and Mo exist as Ni^{2+} ions and Mo(VI) species in an oxide environment, respectively. The FWHM of Mo 3d spectra in NMPC(6-20-4) catalyst increases slightly by the addition of P. Such broadening is not observed in Ni-free Mo-P-Alumina catalysts (MPC(30-5)). Considering that the FWHM of O 1s also increases by the P addition, the formation of mixed phases with different Mo and O environment could be the most reasonable explanation for this spectra broadening.

After catalyst sulphidation at 400 °C, the Mo species in P-free NMPC(6-20-0) catalyst are not completely transformed into Mo(IV) species in a MoS_2 environment. 10 % of Mo(VI) and 22 % of intermediate oxy-sulphide Mo (V) are still present. The presence of Ni decreases slightly the sulphidability of Mo into MoS_2 from 73 to 68 % from the comparison of MPC(30-0) and NMPC(6-20-0). On the other hand, the addition of P further decreases the sulphidability of Mo oxo-species from 68 to 57 % (NMPC(6-20-4)). Therefore, the sulphidability of Mo(VI) into Mo(IV) in Ni-Mo-P-Alumina is lower than that of the Mo-P-Alumina catalyst (MPC(30-5)) (61%). Especially, it is important to note that the amount of oxy-sulphide significantly increases by addition of P in NMP(6-20-4) (from 22 to 36 %). Relatively larger FWHM of Mo 3d in Mo(VI) and Mo(V) also suggests that a strong interaction between Ni, Mo and P through remaining oxygen is still maintained even after sulphidation.

The sulphidability of Ni species in Ni-Mo-Alumina NMP(6-20-0) catalysts is considerably higher than that of Mo-free and P-free NPC(18-0). The Ni^{2+} ion in the catalysts is completely sulphided. The addition of P does not affect the Ni sulphidability in the NMPC(6-20-4) catalyst. It is again considered that the main part of Ni species are predominantly associated with Mo species which favors the sulphidation of Ni species in Ni-Mo-Alumina based catalysts. This interaction between Ni and Mo in oxide form may transform into a commonly accepted Ni-Mo-S phase after sulphidation (13-15). Because the formation of stable $NiAl_2O_4$ is not predominant in the Ni-Mo-Alumina system, the addition of P may not affect pronouncedly the Ni sulphidability.

Table 1 Results of XPS measurements of Sol-Gel catalysts

Catalysts	pretreatment	B.E. (eV) Mo 3d 5/2		FWHM	Ni 2p 3/2		FWHM	O 1s	FWHM	S 2p	FWHM	P 2p	FWHM	Intensity I(Mo)/I(Al)	I(Ni)/I(Al)	I(P)/I(Al)
MPC(30-0)	Calcination	Mo(VI)	233.5 (100%)	2,4				531,8	2,7					3,6		
	sulphidation	Mo(VI)/oxide	233.4 (11%)	2,2				532,2	2,8	162,8	2,6			3,1		
		Mo(V)	231.9 (17%)	2,0												
		Mo(IV)/MoS2	229.4 (73%)	1,8												
MPC(30-5)	Calcination	Mo(VI)	233.3 (100%)	2,4				532,1	3,2			134,9	2,7	4,3		0,7
	sulphidation	Mo(VI)/oxide	233.7 (14%)	2,3				532,8	3,7	162,4	2,9	135,1	3,3	4,0		0,6
		Mo(V)	231.8 (22%)	2,0												
		Mo(IV)/MoS2	229.7 (61%)	2,0												
NPC(18-0)	Calcination				Ni2+(oxide)	857.4 (100%)	3,8	532,2	3,3						2,1	
	sulphidation				Ni2+(oxide)	856.4 (22%)	3,8	531,8	2,9	162,4	3,0				2,6	
					Ni (sulphide)	854.3 (78%)	2,6									
NPC(18-9)	Calcination				Ni2+(oxide)	857.2 (100%)	3,8	532,2	3,0			134,4	2,8		1,4	1,2
	sulphidation				Ni2+(oxide)	856.8 (7%)		532,4	2,5	162,1	3,0	134,0	2,5		1,2	1,3
					Ni (sulphide)	853.8 (93%)	2,6									
NMPC(6-20-0)	Calcination	Mo(VI)	233.2 (100%)	2,2	Ni2+(oxide)	856,6 (100%)	3,8	531,5	2,6					3,8	2,4	
	sulphidation	Mo(VI)/oxide	233,1 (10%)	2,4	Ni2+(oxide)			531,5	2,8	162,2	2,5			3,5	1,6	
		Mo(V)	230,6 (22%)	2,3	Ni (sulphide)	853,5 (100%)	3,8									
		Mo(IV)/MoS2	229,1 (68%)	1,5												
NMPC(6-20-4)	Calcination	Mo(VI)	232.8 (100%)	2,6	Ni2+(oxide)	856.8 (100%)	3,8	532,0	3,1			134,4	2,7	2,6	1,2	1,0
	sulphidation	Mo(VI)/oxide	233,1 (7%)	3,5	Ni2+(oxide)			532,1	2,8	161,9	2,6	134,5	2,5	2,4	1,4	1,0
		Mo(V)	230,9 (36%)	2,5	Ni2+(sulphide)	853,7 (100%)	3,8									
		Mo(IV)/MoS2	228,9 (57%)	1,8												

2.4.2.4. Conclusion

The Ni-Mo-P-Alumina based hydrotreating catalysts were prepared by a sol-gel method to elucidate the role of phosphorus on the sulphidability of Mo and Ni species. In Mo-P-Alumina catalyst, effect of P on the sulphidability strongly depends on the Mo and P content. P does not affect the sulphidability of Mo oxo-species at low Mo loading while it decreases with the addition of P at higher Mo loading. On the other hand, in Ni-P-Alumina catalyst, the addition of P increases the sulphidability of Ni species by preventing the formation of $NiAlO_4$. In Ni-Mo-P-Alumina catalyst, the sulphidability of Mo species also decreases by the addition of P while that of Ni species is less affected by the P addition since Ni is predominantly associated with Mo species rather than with the alumina support. It is concluded that strong P-O chemical bonds in (Ni)-Mo-O-P mixing species prevents the exchange of oxygen by sulphur atom during sulphidation of (Ni)-Mo-P-Alumina catalysts.

2.4.2.5. Reference

(1) R.J.Mangnus, A.D.van Langeveld, V.H.J.de Beer and R.Prins, Appl. Catal., 68, 161 (1991)

(2) D.Chadwick, D.W.Aitchison, R.Ohlbaum and L.Josefsson, Surf. Stud. Sci. Catal., 16, 323 (1983)

(3) D.J.Sajkowski, J.T.Miller and G.W.Zaiac, Appl. Catal., 62, 205 (1990)

(4) O.Poulet, R.Hubaut, S.Kasztelan and J.Grimblot, Bull. Soc. Chim. Belg., 100, 857 (1991)

(5) A.López-Agudo, R.L.Cordero, J.M.Palacios and J.L.Fierro, Bull.Soc ;Chim.Belg., 104, 237 (1995)

(6) H. Topsøe, B.S.Clausen, R.Candia, C.Wivel and S.Mørup, J.Catal., 68, 433 (1981)

(7) R.Candia, N-Y. Topsøe, B.S.Clausen and H.Topsøe, Bull. Soc. Chim. Belg., 93, 783 (1984)

(8) J.A.R.van Veen, E.Gerkema, A.M.Van der Kraan, P.A.J.M.Hendriks and H.Beens, J.Catal., 133, 122 (1992)

(9) A.Andreev, Ch.Vladov, L.Prahov and P.Atanasova, Appl. Catal. 108, A, L97 (1994)

(10)W.R.A.M.Robinson, J.N.M. van Gestel, T.I.Korányi, S.Eijsbouts, A.M. van der kraan, J.A.R. van Veen and V.H.J. de Beer, J.Catal., 161, 539 (1996)

(11) A.Galtayries, S. Wisniewski and J.Grimblot, J.Electron Spectrosc. Related Phenom., in press

(12)S. Houssenbay, S. Kasztelan, H.Toulhoat, J.P.Bonnelle and J.Grimblot, J. Phys. Chem., 93, 7176 (1989)

2.4.3 Effet du phosphore sur les propriétés acides des catalyseurs à base d'alumine préparés par voie sol-gel.

(Effect of P on the Acid Property of Ni-Mo-Alumina Based Hydrotreating Catalysts Prepared by a Sol-Gel Method)

Abstract

A series of Mo-P, Ni-P and Ni-Mo-P-Alumina based catalysts with a wide range of P loading (0 to 10 wt%) were prepared by a sol-gel method to elucidate the role of phosphorous on the acid property of alumina based hydrotreating catalysts. The addition of P increases acid property of sol-gel catalysts in the order : P-Al = Ni-P-Al < Mo-P-Al < Ni-Mo-P-Al as evidenced by the cyclopropane (CP) cracking conversion. Their product distributions strongly depends on the nature of catalysts. Ni-P-Alumina catalysts gave only propene as well as P-Alumina. Mo-P-Alumina catalysts gave both propene and propane. Moreover, Ni-Mo-P-Alumina catalysts gave propene, propane (ring opening products) and also C_1, C_2, C_4 molecules (cracking of C_3 and their oligomerization products). The variation of selectivity suggested that P creates at least two kinds of acid sites both on alumina and on the MoS_2 slabs. The later acid sites due to Mo-P-OH species are more stronger than the former attributed to $AlPO_4$. The presence of Ni makes the later acid strength more stronger. It addition, the later stronger acid sites might possess hydrogenation activity due to their strong hydrogen donor character.

2.4.3.1. Introduction

The effect of P on acid property of hydrotreating catalysts has been widely studied as already described in part I, paragraph 1.2.5.3. However, its precise role is not well understood yet. In paragraph 2.2.3, it has been found that the acidity of Mo-Alumina based sol-gel catalysts increases with P loading. This study suggested that the acidity is in part attributed to the interaction between P and the alumina support since the catalysts prepared from P_2O_5 as a P precursor, which gives less $AlPO_4$ formation, showed less CP cracking. Moreover, it was suggested that the interaction between P and Mo also creates stronger acid sites. In this paragraph, the effect of P on the acid property of alumina-based sol-gel hydrotreating catalysts such as Ni-P, Mo-P, and Ni-Mo-P-Alumina will be investigated in more detail by CP cracking reaction.

2.4.3.2. Experimental

Catalysts

A set of Ni-P, Mo-P and Ni-Mo-P-Alumina sol-gel catalysts used in this study were MPC(30-Z)H, NPC(6-Z)n and NMPC(6-20-Z), respectively. MP, NP or NMP mean Mo-P, Ni-P or Ni-Mo-P based alumina catalysts which had the expected loading of 30 wt% Mo for Mo-P-Alumina, 6 wt% Ni for Ni-P-Alumina, and 6 wt% of Ni and 20wt% of Mo for Ni-Mo-P-Alumina, respectively. Z means expected amount of P loading and it varied from 0 to ~10 wt%. H and n means phosphoric acid and nickel nitrate as P and Ni precursors used for preparation of catalysts, respectively. These precursors have been selected as they have been shown better for obtaining higher thiophene HDS activity or CP cracking. The other properties were already described in the previous chapters.

CP cracking (Acid property)

To estimate the acid properties of the prepared catalysts, cracking of cyclopropane (CP) was carried out at atmospheric pressure with the same procedure as already described in paragraph 2.2.2 but the reaction temperature was changed to 280 °C for comparison reason. 0.2 g of catalyst was sulphided at 400 °C for 2 h with a H_2/H_2S (90/10) gas mixture at a flow rate of 50 ml/min. Then, the reaction temperature was kept at 280 °C for 2 h in a CP/He/H_2 (2.5/47.5/50) gas mixture at a flow rate of 10 ml/min.. The reaction products (mainly propene and propane with small amount of C_1, C_2 and C_4 hydrocarbons) were analyzed by gas chromatography.

2.4.3.3. Results and Discussion

CP cracking activities over Mo-P-Alumina, Ni-P-Alumina and Ni-Mo-P-Alumina sol-gel catalysts are shown in Fig. 1. Pure alumina shows no CP cracking activity. The order of CP cracking activity is described as Ni-P-Al = P-Al <Mo-P-Al <Ni-Mo-P-Alumina catalysts. These results mean that the Ni-Mo-P-Alumina catalysts possess stronger acidity than the Ni-P-Alumina and Mo-P-Alumina catalysts. The CP conversion over the Ni-Mo-P-Alumina catalysts almost levels off at ~4 wt% P while those over Mo-P-Alumina and Ni-P-Alumina catalysts increase in proportion to the P content.

In this reaction, several reaction products are identified such as propane, propene (ring opening products) and C_1, C_2, C_4 (cracking of C_3 and following oligomerization products ; hereinafter referred as products X) depending on the catalyst formulations. The reaction mechanism is schematically shown in Fig. 2. It is considered that the formation of products X needs stronger acidity than that of ring opening products.

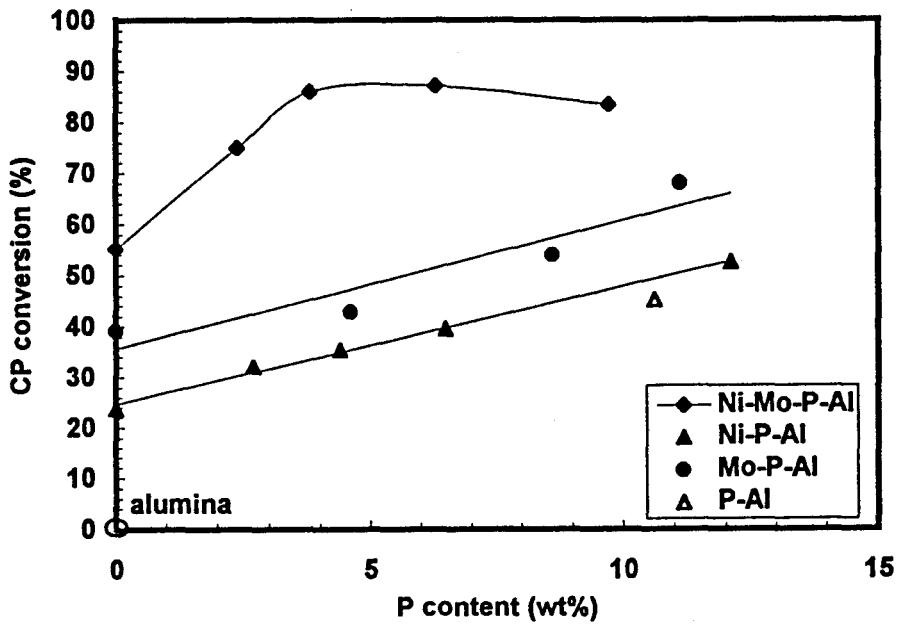

Fig.1. CP conversion over sol-gel catalysts

Variation of product selectivity in the function of P content over P-Alumina, Ni-P-Al, Mo-P-Alumina and Ni-Mo-P-Alumina catalysts are shown in Fig. 3. Indeed, their distributions strongly depends on the nature of catalysts. In the P-Alumina and Ni-P-Alumina catalysts, only propene was obtained as a product (Fig. 3a). Since they show almost the same conversion and selectivity at the same P loading level, it is inferred that the increase in acidity of Ni-P-Alumina catalysts is mainly attributed to the $AlPO_4$ phase formed on the alumina support. Ni seems to have no influence for such reaction with the range of proposed formulation.

The Ni free Mo-P-Alumina catalysts give both propene and propane (Fig. 3b). The selectivity of propane increases from 9 to 25 % with increasing P loading. In the previous study, it was appeared that the acidity of Mo-P-Alumina catalysts increase in the presence of hydrogen (paragraph 2.2.3 Fig. 3). However, those of Mo-free P-Alumina catalysts does not increase in the presence of hydrogen (results is not shown in figure). This strongly indicates that the acidity increase in the presence of H_2 is not related to the formation of new P-OH groups from P=O bonds on the alumina but to the dissociation of hydrogen on Mo species.

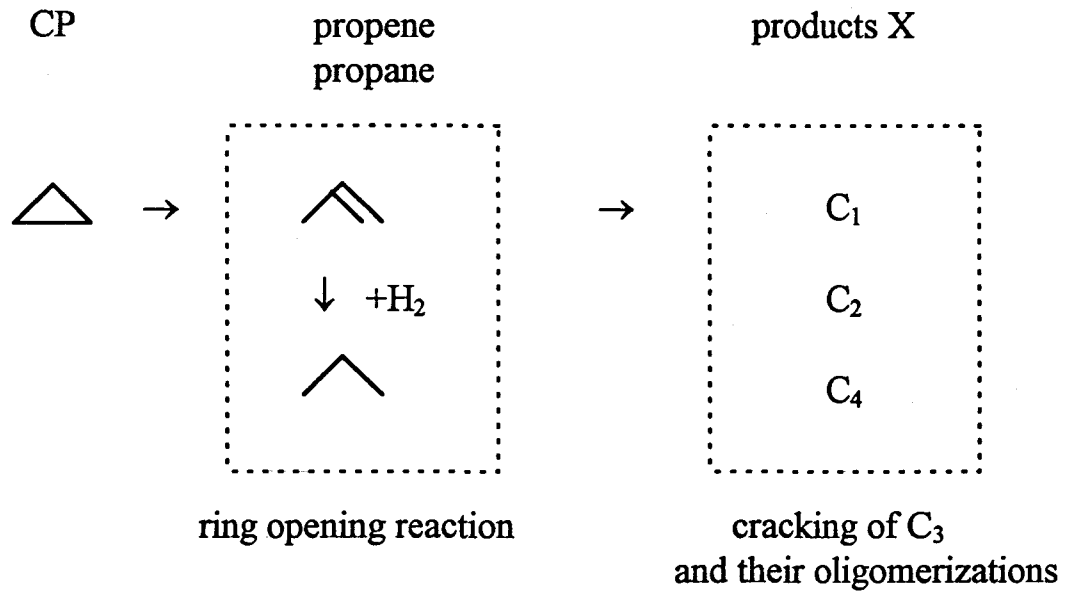

Fig. 2. Schematic reaction mechanism of cyclopropane cracking

In Ni-Mo-P-Alumina catalysts, higher yield of propane than the Mo-P-Alumina catalysts are observed and it increases with P content up to 6 wt% P (Fig. 3c). In addition, the Ni-Mo-P-Alumina catalysts give considerable yield of products X. These results mean that the presence of both Ni and P enhance significantly the acidity and hydrogenation activity of Mo-Alumina catalyst. It is suggested that two different kinds of acid sites attributed to the $AlPO_4$ and Ni-Mo-species may also exist in the Ni-Mo-P-Alumina catalysts as well as Mo-P-Alumina system. The acid strength of sites associated with the Ni-Mo structure might be extremely stronger than that attributed to the $AlPO_4$ or Ni-free Mo species considering the noticeable formation of products X. Regarding from XPS results in the paragraph 2.4.2, the stronger acid site could be also attributed to remaining oxygen in MoS_2 slab due to the worse sulphidation. The effect of promotor Ni is to modify the electronic charge density of MoS_2 slab or to increases more OH groups in MoS_2 (decrease the sulphidability).

However, strong acidity and high hydrogenation selectivity (propane) could be also explained by the formation of Ni-Mo-S like phase (1). To confirm the effect of Ni and P on the acidity increase, the selectivity for hydrogenated product in thiophene HDS (butane) and CP cracking (propane) over Ni-Mo-P-Alumina catalysts were compared. As already shown in the paragraph 3.4.1, Fig. 6, the formation of butane in the thiophene HDS reaction over Ni-Mo-P-Alumina decreases with its P loading.

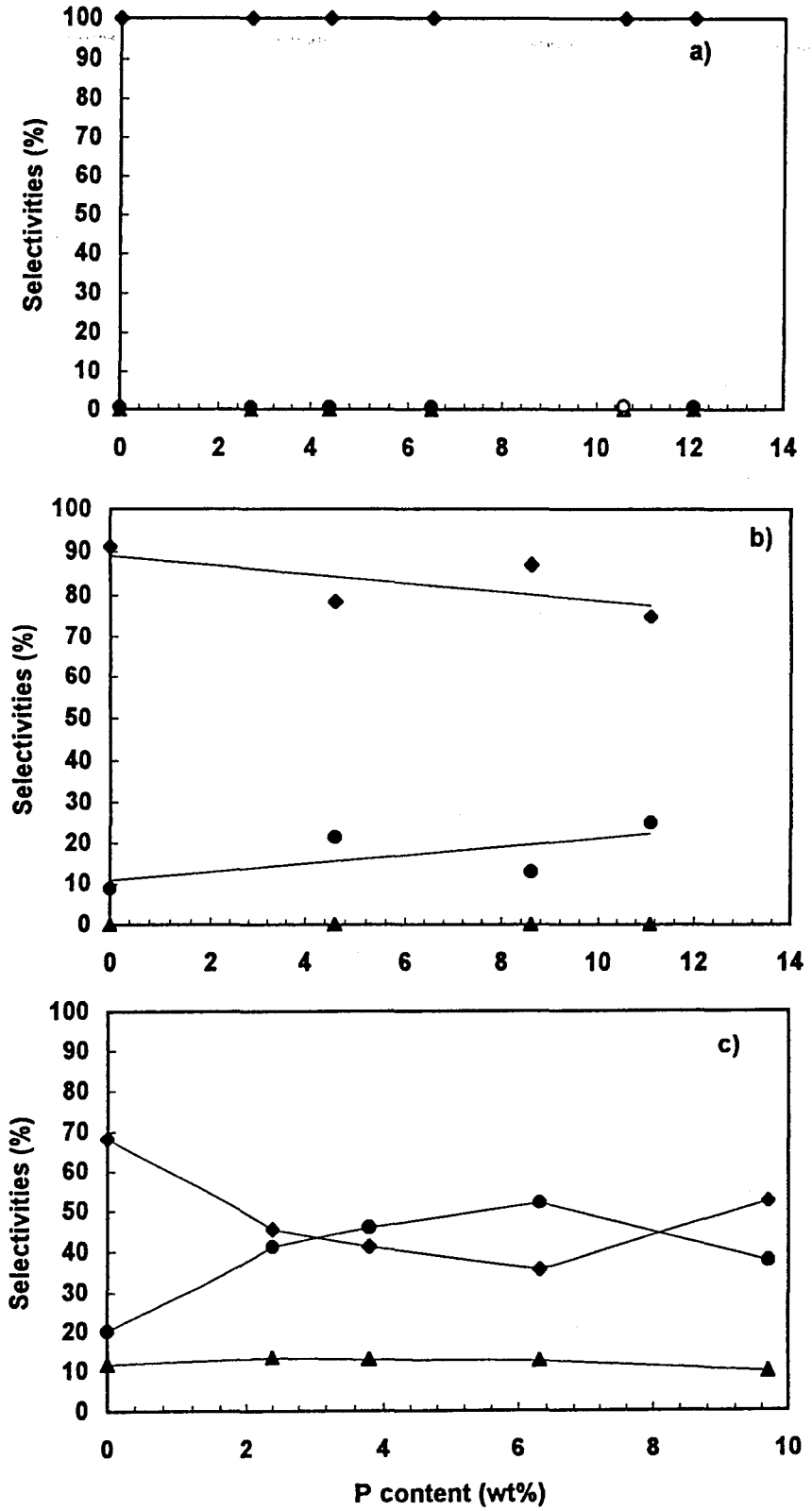

Fig. 3 Product selectivity in CP conversion over sol-gel catalysts.
a)Ni-P-Alumina and P-Alumina (open symbol), b) Mo-P-Alumina, c) Ni-Mo-P-Alumina, ◆ : propene, ● : propane, ▲ : product X.

On the other hand, yield of propane in CP cracking over the Ni-Mo-P-Alumina increases with P content (Fig. 3c). These results mean that hydrogenation reactions (HYD) followed by thiophene HDS and CP cracking proceed on completely different active sites. It is suggested therefore that the increase in CP cracking and propene HYD activities in the presence of P does not relates to the Ni-Mo-S phase, but probably to the formation of Ni-Mo-P-OH mixing sites in Ni-MoS_2 slab due to the low sulphidability.

In a previous study, it was revealed that the yield of propane from CP cracking over the Mo-P-Alumina catalysts correlates with that of the products X formation at 350 °C (see paragraph 2.2.3). In this study, higher yield of propane is also well correlated with that of products X since both shows a maximum around 4 to 6 wt% of P while selectivity of products X in Fig. 3c is almost unchanged with P addition. It is inferred that the strong acid sites might act as HYD sites as they can give hydrogen to the reactants more easily due to its stronger hydrogen donor character. Kanai et al. (2) also reported that strong acid sites works simultaneously as a hydrogenation sites. In terms of reactions involving hydrogen, HYD and acid reactions could be considered the same but the difference between them is whether the hydrogen remains on the catalyst or is incorporated to molecules at end of reactions. If the hydrogen on the Brönsted acid sites can be consumed by the reactants and compensated by spillover hydrogen immediately, acid sites could act as hydrogenation sites.

2.4.3.4. Conclusion

A series of Mo-P, Ni-P and Ni-Mo-P-Alumina sol-gel catalysts were prepared to elucidate the role of phosphorous on the acid property of alumina based hydrotreating catalysts. The addition of P increases pronouncedly the acidity measured by cyclopropane cracking in the order : Ni-Mo-P-Al > Mo-P-Al > Ni-P-Al = P-Alumina catalysts. However, the distribution of products selectivity strongly depended on the catalysts formulations. The addition of P may creates at least two kinds of acid sites associated with $AlPO_4$ and with MoS_2 slab (Mo-P-OH mixing species). The later acid sites related to Mo-P-OH are more stronger than the former attributed to $AlPO_4$. The presence of Ni makes the later acid strength more stronger. In addition, the later stronger acid sites might also show some HYD activity.

2.4.3.5. Reference

(1) H.Topsøe, B.S.Clausen and F.E.Massoth (Ed. J.R.Anderson and M.Boudart), Catalysis vol. 11,
(2) J.Kanai, J.A.Martens, P.A.Jacobs, J.Catal., 133, 527 (1992)

2.5 Conclusion

Nous avons mis au point un protocole expérimental dérivant de la méthode de préparation de solides par voie sol-gel qui a permis d'évaluer les effets induits par le phosphore sur les propriétés texturales et structurales et sur les performances réactionnelles de catalyseurs d'hydrotraitement à base de Ni, Mo et alumine. Par l'utilisation combinée de diverses méthodes de caractérisation et de tests catalytiques à pression atmosphérique sur molécules modèles, les effets tant positifs que négatifs du phosphore ont été évalués et discutés.

Même si, en général, l'addition de P provoque une diminution de l'aire spécifique et la dispersion des phases oxydes supportées, une quantité modérée peut préserver de grandes aires spécifiques, supérieures à 400 $m^2.g^{-1}$ avec des teneurs en Mo de l'ordre de 20% en poids. Les caractérisations par RMN (^{27}Al et ^{31}P) ont montré que P conduit à la formation prédominante de $AlPO_4$ ou d'espèces poly-oxophosphates après calcination. En particulier, l'utilisation de P_2O_5 dans la synthèse produit cette dernière espèce en grande quantité, en l'absence de Mo. L'hydrodésulfuration du thiophène n'est pas notablement améliorée par addition de P dans les systèmes Mo-P alors qu'elle l'est pour la série Ni-P. Dans ce cas, la présence de P empêche la formation de $NiAl_2O_4$ trop stable pour se sulfurer. P, en quantité modérée, améliore l'activité HDS des catalyseurs Ni-Mo-P par une meilleure dispersion du Mo (phase MoS_2) et aussi par une augmentation des espèces de Ni actives. Les propriétés acides, mises en évidence par le craquage du cyclopropane, sont aussi accentuées par la présence de P dans les catalyseurs Mo-P, Ni-P et surtout Ni-Mo-P-alumine. Les résultats suggèrent qu'au moins deux sites acides différents sont présents sur les catalyseurs Mo-P et Ni-Mo-P associés respectivement à $AlPO_4$ et à l'interaction Mo-P alors que sur la série Ni-P, l'acidité est due à la présence de $AlPO_4$. L'acidité attribuée aux espèces Mo est

plus marquée que celle de $AlPO_4$. La forte interaction Mo-O-P fait aussi diminuer la sulfuration du Mo qui engendre alors des groupes OH, très acides, liés à la phase MoS_2. Il est aussi possible que ces sites acides contribuent à l'amélioration de la fonction hydrogénante, dans certaines conditions.

Un modèle décrivant localisation du phosphore dans les catalyseurs sulfurés Mo-P-Alumine et Ni-Mo-P-Alumine est proposé dans la figure 1.

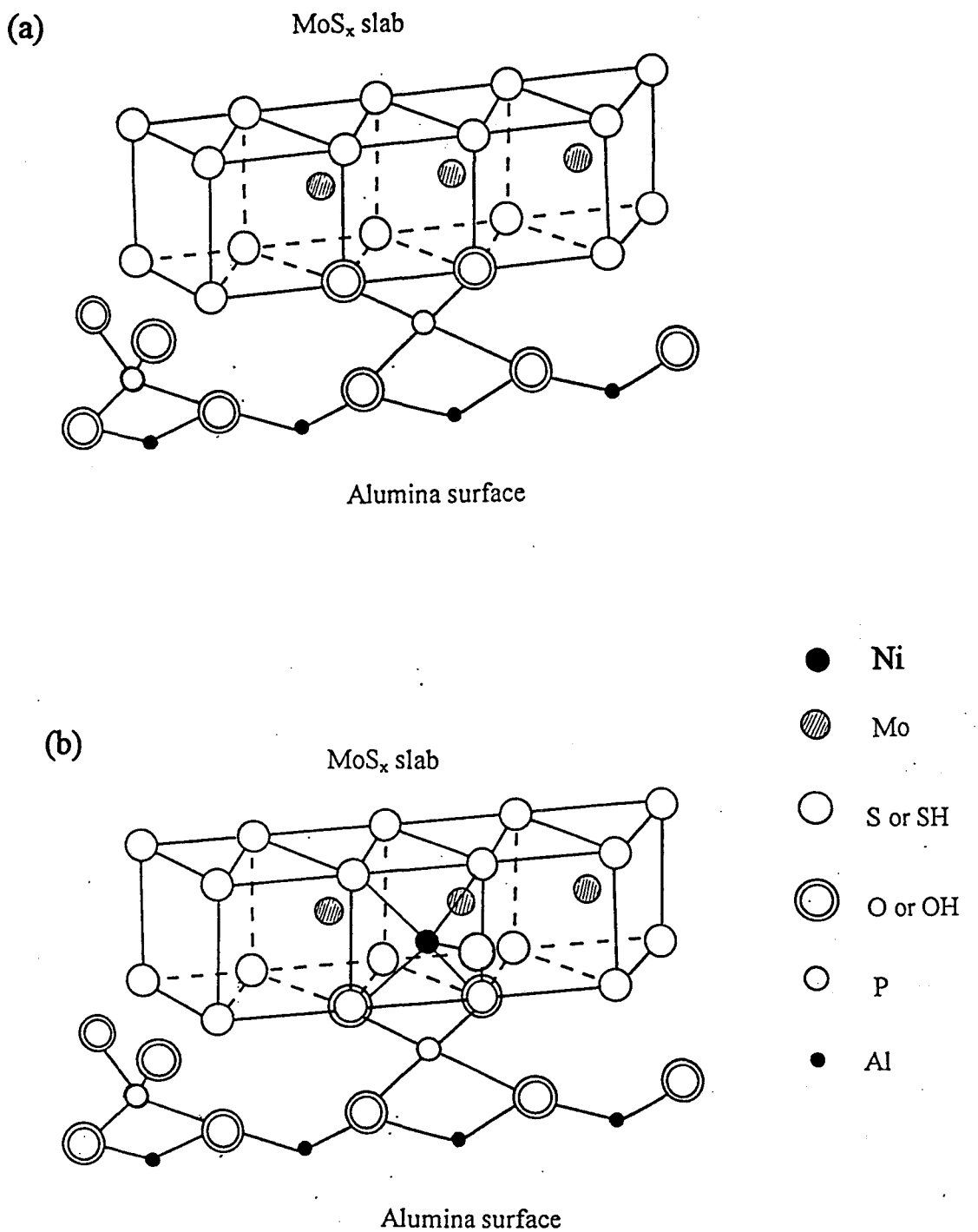

Fig. 1 Localisation du phosphore dans les catalyseurs sulfurés (a) Mo-P-Alumine et (b) Ni-Mo-P-Alumine.

Conclusion générale

Les deux parties présentées dans ce travail confirment que l'addition du phosphore dans les formulations des catalyseurs d'hydrotraitement à base d'alumine induit des modifications complexes, et parfois contradictoires. La raison principale repose probablement sur la richesse de la chimie du phosphore qui, combinée à celle du molybdène, entraîne une grande diversité de phases et de sites à la surface de l'alumine. La notion de réactivité compétitive doit aussi être soulignée dans cette conclusion.

L'examen bibliographique exposé en première partie a révélé la richesse de la chimie du phosphore dans le contexte des solides et conditions impliqués dans les réactions d'hydrotraitement. Il a clairement montré du doigt les contradictions reportées dans la littérature. Néanmoins, des idées convergentes ont pu être établies. Par exemple, P joue un rôle important sur la texture, sur la dispersion du Mo et sa répartition dans la particule de catalyseur. D'autre, il apparaît que P agit sur les propriétés acides des catalyseurs et améliore les performances en HDN et HYD des cycles aromatiques. Son effet sur l'HDS est plus contrasté. L'ensemble des résultats expérimentaux reportés dans la deuxième partie permet de mieux cerner les effets induits par l'addition de P dans les catalyseurs d'hydrotraitement de type Ni-Mo-alumine, même si l'étude n'a porté que sur des séries préparées selon un protocole sol-gel. Nous avons pu montré que:

1. P améliore la dispersion des phases actives aux fortes teneurs, surtout pour le système Ni-Mo,
2. P évite la formation d'aluminate de nickel et permet une meilleure disponibilité du Ni pour former les phases sulfures,
3. P provoque la formation de la phase acide $AlPO_4$,

4. P induit une diminution de la sulfuration du Mo et permet de développer de nouveaux sites acides et
5. ces sites acides semblent aussi contribuer à améliorer les performances hydrogénantes.

Certains de ces effets ont déjà été signalés dans la première partie bibliographique. Cependant, des travaux sont encore nécessaires afin d'apporter d'autres améliorations et de permettre une véritable optimisation de ces catalyseurs. Il nous apparaît, en effet, que des mesures catalytiques dans des conditions plus proches de celles rencontrées dans la réalité devraient conforter nos résultats, notamment en ce qui concerne l'acidité et l'aptitude au craquage d'hydrocarbures. L'examen des solides (par RMN en particulier) des solides après sulfuration et après tests catalytiques devraient permettre une description plus réaliste des différentes phases présentes.